Université de Montréal

Development and plasticity of locomotor circuits in the zebrafish spinal cord

par

LAURA D. KNOGLER

Département de pathologie et biologie cellulaire

Faculté de médecine

Thèse présentée à la Faculté de médecine
en vue de l'obtention du grade de doctorat (Ph.D.)
en pathologie et biologie cellulaire

Novembre, 2014

© Laura Knogler, 2014

Université de Montréal

Faculté des études supérieures et postdoctorales

Cette thèse de doctorat intitulée :

« Development and plasticity of locomotor circuits in the zebrafish spinal cord »

Présentée par:

LAURA D. KNOGLER

a été évaluée par un jury composé des personnes suivantes:

Guy Doucet, Ph.D.

Président-rapporteur

Pierre Drapeau, Ph.D.

Directeur de recherche

Roberto Araya, Ph.D.

Membre du jury

Paul De Koninck, Ph.D.

Examinateur externe

Louis-Eric Trudeau, Ph.D.

Représentant du doyen de la FES

RÉSUMÉ

Un objectif important en neurobiologie est de comprendre le développement et l'organisation des circuits neuronaux qui entrainent les comportements. Chez l'embryon, la première activité motrice est une lente contraction spontanée qui est entrainée par l'activité intrinsèque des circuits spinaux. Ensuite, les embryons deviennent sensibles aux stimulations sensorielles et ils peuvent éventuellement nager, comportements qui sont façonnées par l'intégration de l'activité intrinsèque et le rétrocontrôle sensoriel. Pour cette thèse, j'ai utilisé un modèle vertébré simple, le poisson zèbre, afin d'étudier en trois temps comment les réseaux spinaux se développent et contrôlent les comportements locomoteurs embryonnaires.

Pour la première partie de cette thèse j'ai caractérisé la transition rapide de la moelle épinière d'un circuit entièrement électrique à un réseau hybride qui utilise à la fois des synapses chimiques et électriques. Nos expériences ont révélé un comportement embryonnaire transitoire qui précède la natation et qu'on appelle « double coiling ». J'ai démontré que les motoneurones spinaux présentaient une activité dépendante du glutamate corrélée avec le « double coiling » comme l'a fait une population d'interneurones glutamatergiques ipsilatéraux qui innervent les motoneurones à cet âge. Ce travail (Knogler et al., *Journal of Neuroscience*, 2014) suggère que le « double coiling » est une étape distincte dans la transition du réseau moteur à partir d'un circuit électrique très simple à un réseau spinal entrainé par la neurotransmission chimique pour générer des comportements plus complexes.

Pour la seconde partie de ma thèse, j'ai étudié comment les réseaux spinaux filtrent l'information sensorielle de mouvements auto-générés. Chez l'embryon, les neurones sensoriels mécanosensibles sont activés par un léger toucher et ils excitent en aval des interneurones sensoriels pour produire une réponse de flexion. Par contre, les contractions spontanées ne déclenchent pas ce réflexe même si les neurones sensoriels sont toujours activés. J'ai démontré que les interneurones sensoriels reçoivent des entrées glycinergiques pendant les contractions spontanées fictives qui les empêchaient de générer des potentiels d'action. L'inhibition glycinergique de ces interneurones, mais pas des autres neurones spinaux, est due à l'expression d'un sous-type de récepteur glycinergique unique qui augmente

le courant inhibiteur. Ce travail (Knogler & Drapeau, *Frontiers in Neural Circuits*, 2014) suggère que la signalisation glycinergique chez les interneurones sensoriels agit comme un signal de décharge corolaire pour l'inhibition des réflexes pendant les mouvements auto-générés.

Dans la dernière partie de ma thèse, je décris le travail commencé à la maîtrise et terminé au doctorat qui montre comment la plasticité homéostatique est exprimée *in vivo* aux synapses centrales à la suite des changements chroniques de l'activité du réseau. J'ai démontré que l'efficacité synaptique excitatrice de neurones moteurs spinaux est augmentée à la suite d'une diminution de l'activité du réseau, en accord avec des études *in vitro* précédentes. Par contre, au niveau du réseau j'ai démontré que la plasticité homéostatique n'était pas nécessaire pour maintenir la rythmicité des circuits spinaux qui entrainent les comportements embryonnaires. Cette étude (Knogler et al., *Journal of Neuroscience*, 2010) a révélé pour la première fois que l'organisation du circuit est moins plastique que l'efficacité synaptique au cours du développement chez l'embryon.

En conclusion, les résultats présentés dans cette thèse contribuent à notre compréhension des circuits neuronaux de la moelle épinière qui sous-tendent les comportements moteurs simples de l'embryon.

Mots clés: les circuits de la moelle épinière, générateur central de motifs, décharge corollaire, plasticité homéostatique, comportement locomoteur, poisson zèbre embryonnaire, neurobiologie développementale

SUMMARY

A fundamental goal in neurobiology is to understand the development and organization of neural circuits that drive behavior. In the embryonic spinal cord, the first motor activity is a slow coiling of the trunk that is sensory-independent and therefore appears to be centrally driven. Embryos later become responsive to sensory stimuli and eventually locomote, behaviors that are shaped by the integration of central patterns and sensory feedback. In this thesis I used a simple vertebrate model, the zebrafish, to investigate in three manners how developing spinal networks control these earliest locomotor behaviors.

For the first part of this thesis, I characterized the rapid transition of the spinal cord from a purely electrical circuit to a hybrid network that relies on both chemical and electrical synapses. Using genetics, lesions and pharmacology we identified a transient embryonic behavior preceding swimming, termed double coiling. I used electrophysiology to reveal that spinal motoneurons had glutamate-dependent activity patterns that correlated with double coiling as did a population of descending ipsilateral glutamatergic interneurons that also innervated motoneurons at this time. This work (Knogler et al., *Journal of Neuroscience*, 2014) suggests that double coiling is a discrete step in the transition of the motor network from an electrically coupled circuit that can only produce simple coils to a spinal network driven by descending chemical neurotransmission that can generate more complex behaviors.

In the second part of my thesis, I studied how spinal networks filter sensory information during self-generated movement. In the zebrafish embryo, mechanosensitive sensory neurons fire in response to light touch and excite downstream commissural glutamatergic interneurons to produce a flexion response, but spontaneous coiling does not trigger this reflex. I performed electrophysiological recordings to show that these interneurons received glycinergic inputs during spontaneous fictive coiling that prevented them from firing action potentials. Glycinergic inhibition specifically of these interneurons and not other spinal neurons was due to the expression of a unique glycine receptor subtype that enhanced the inhibitory current. This work (Knogler & Drapeau, *Frontiers in Neural Circuits*, 2014) suggests that glycinergic signaling onto sensory interneurons acts as a corollary discharge signal for reflex inhibition during movement.

In the final part of my thesis I describe work begun during my masters and completed during my doctoral degree studying how homeostatic plasticity is expressed *in vivo* at central synapses following chronic changes in network activity. I performed whole-cell recordings from spinal motoneurons to show that excitatory synaptic strength scaled up in response to decreased network activity, in accordance with previous *in vitro* studies. At the network level, I showed that homeostatic plasticity mechanisms were not necessary to maintain the timing of spinal circuits driving behavior, which appeared to be hardwired in the developing zebrafish. This study (Knogler et al., *Journal of Neuroscience*, 2010) provided for the first time important *in vivo* results showing that synaptic patterning is less plastic than synaptic strength during development in the intact animal.

In conclusion, the findings presented in this thesis contribute widely to our understanding of the neural circuits underlying simple motor behaviors in the vertebrate spinal cord.

Keywords: spinal cord circuitry, central pattern generator, corollary discharge, homeostatic plasticity, locomotor behavior, embryonic zebrafish, developmental neurobiology

LAY SUMMARY

The spinal cord is an important part of our nervous system and drives motor movements. If the normal function of the spinal cord is disrupted, for example due to developmental defects or to injury or disease, then motor movements are compromised or lost entirely (paralysis). Although we know a great deal about the different kinds of neurons and connections present in the spinal cord there still remains much to understand about how the circuit functions as a whole. My research uses a simple vertebrate, the zebrafish, to study the neural circuits within the spinal cord that contribute to spontaneous and sensory-evoked behaviors early in development. By using techniques that allow me to record the activity of individual neurons in combination with microscopy and behavioral studies I can examine the development, function and plasticity of connections between different types of neurons and how this activity relates to motor movements. My research has revealed three key findings about spinal cord circuits.

First, my colleagues and I identified a novel developmental behavior that precedes mature swimming in the zebrafish. This behavior occurs spontaneously and is driven by a small group of neurons in the spinal cord that initially send only electrical signals to each other, unlike the mature nervous system that uses chemical neurotransmitters. We showed that a population of excitatory spinal interneurons is active during this behavior and that these neurons first begin to develop chemical connections using the neurotransmitter glutamate at this developmental stage. These findings help explain how the earliest development proceeds in the zebrafish spinal cord and will help us understand these processes in terrestrial vertebrates, including mammals.

Second, I described a simple mechanism by which the zebrafish avoids being startled by somatosensation (touch) resulting from its own movement. During motor movements, the spinal cord sends a signal to inhibit a sensory interneuron that is usually responsible for conveying information about light touch. As a result, a touch stimulus resulting from the fish's own movement does not cause a reflexive startle response whereas any touch stimulus coming from the external environment (e.g. a predator) efficiently evokes a response. These findings may be important for understanding how animals filter out self-generated sensory

stimuli and may have implications for human diseases such as schizophrenia where filtering may be abnormal or absent.

Finally, in the last study I describe how the spinal circuits that are responsible for producing swimming behavior can be adjusted in response to changes in the environment. By experimentally reducing the activity of neurons throughout the fish, I found that neurons could use homeostatic mechanisms to change their synapse properties in order to maintain normal activity levels. This work also showed that despite these experimental treatments to globally reduce the activity of neurons, swimming behavior was mostly unaffected. These results help us understand how genetics combine with environmental factors (nature *versus* nurture) to generate a functional spinal cord circuit that produces swimming.

TABLE OF CONTENTS

LIST OF FIGURES AND TABLES

CHAPTER 1

CHAPTER 2

CHAPTER 3

CHAPTER 4

LIST OF ABBREVIATIONS

α-Btx	alpha-bungarotoxin
AMPA	α-Amino-3-hydroxy-5-methyl-4-isoxazolepropionic acid
APV	(2R)-amino-5-phosphonovaleric acid
dlc	dorsolateral commissural
CiA	circumferential ascending
CiD	circumferential descending
CNQX	6-cyano-7-nitroquinoxaline-2,3-dione
CoBL	commissural bifurcating longitudinal
CoLo	commissural local
CoPA	commissural primary ascending
CoSA	commissural secondary ascending
CPG	central pattern generator
CTZ	cyclothiazide
DLR	diencephalic locomotor region
DNA	deoxyribonucleic acid
dpf	days post-fertilization
DRG	dorsal root ganglion
EPSC	excitatory post-synaptic current
ER	estrogen receptor
GABA	gamma-aminobutyric acid
GCaMP	genetically encoded calcium indicator
GFP	green fluorescent protein
hpf	hours post-fertilization
IC	ipsilateral caudal
IN	interneuron
KCl	potassium chloride
LTD	long-term depression
LTP	long-term potentiation

MLR	mesencephalic locomotor region
MN	motoneuron
mPSC	miniature post-synaptic current
mRNA	messenger ribonucleic acid
NMDA	N-Methyl-D-aspartate
PhTX	philanthotoxin
PIC	periodic inward current
RB	Rohon-Beard
SB	synaptic burst
SBEM	serial blockface scanning electron microscope
syp	synaptophysin
TNFα	tumor necrosis factor-alpha
TTX	tetrodotoxin
UAS	upstream activating sequence
VeLD	ventral lateral descending

ACKNOWLEDGEMENTS

First and foremost I would like to thank my supervisor Dr. Pierre Drapeau for his mentorship during my graduate studies. He has been an endless source of optimism and information not to mention hilarious anecdotes throughout my time in the lab. I appreciate how supportive Pierre has been of my research ideas. He has encouraged me to participate in numerous courses and conferences which have allowed me to thrive independently. I am very grateful for his invaluable guidance during my studies and in my future research plans.

I would also like to acknowledge the numerous contributions of Dr. Louis Saint-Amant to my graduate studies. Particularly in the early stages of my project, Louis generously offered his time and expertise for experimental troubleshooting. He also encouraged me to think more critically about my work and offered many valuable insights.

I appreciate the many useful and entertaining discussions with zebrafish colleagues past and present including Dr. Gary Armstrong, Dr. Kessen Patten, Dr. Sean Low, Sébastien Côte and Alexandra Lissouba. I am grateful to our laboratory technician Meijiang Liao for her molecular biology expertise as well as her cheerful help in general lab matters. Thanks as well to Guy Laliberté and Marina Drits for zebrafish care. Many thanks to my other friends and fellow graduate students in the department especially Dr. Ariel Wilson who was a major source of inspiration and moral support throughout my studies.

Many thanks to my thesis jury members Dr. Guy Doucet, Dr. Paul De Koninck and Dr. Roberto Araya for their important contributions at this final stage of my doctorate as well as to my doctoral committee members Dr. Graziella di Cristo and Dr. Karl Fernandez for their support and feedback over the course of my studies. I would also like to thank Dr. Kerry Delaney at UVic for his scientific mentorship at the earliest stage of my research career.

I was fortunate to have participated in the excellent Neurobiology course at the Marine Biological Laboratory run by Dr. Grae Davis and Dr. Tim Ryan. This was an extremely inspiring and rewarding scientific experience unlike anything else. I am thankful to have had this opportunity and I hope to return to Woods Hole many times over the course of my career.

Last but not least, I am tremendously grateful to my partner Joel Ryan for his unwavering support during my PhD. I could not have done this without him. Vielen Dank!

CHAPTER 1

I. GENERAL INTRODUCTION

I.1. THE DEVELOPMENT OF MOTOR BEHAVIORS

In order to survive, animals of all species must quickly develop motor behaviors that allow them to perform essential tasks such as prey capture and predator evasion. Motor movements first appear during embryonic stages as neural circuits of the spinal cord begin to develop. In general, the earliest movements are driven by the spontaneous activation of spinal circuits but are later triggered by external stimuli in the environment or modified by sensory feedback as additional neurons are born and integrated into the network. As a result, a series of transient motor behaviors is produced during development that reflects the ongoing maturation of the underlying circuitry. These behaviors exhibit remarkable similarity across species, from which we can identify key aspects of vertebrate development. Understanding their cellular bases remains an important challenge for modern research.

I.1.1. Historical studies of embryonic behavior

Embryology has fascinated biologists for centuries as a means to understand how animals, including humans, develop in the natural world. The morphology of the embryo initially attracted scientists interested in comparative anatomy, however interest rapidly shifted towards the physiology of the embryo and particularly the behaviors that were produced during development. Studies dating back to the 17th century report the earliest movements of mussels and oysters (Leeuwenhoek, 1695) as well as *in ovo* movements of the chick embryo (Harvey, 1651). However, it was due to the work of two scientists centuries later, the physiologist W. Preyer and the anatomist G. E. Coghill, that the development of animal behavior truly established itself as a field of study. Their work stimulated a great deal of interest in researching developmental physiology that continues to this day.

In his 1885 book "Specielle Physiologie des Embryo," Preyer described his detailed observations of embryonic movement in a variety of vertebrates including the frog and chick embryo. He concluded from his novel findings and previous research that the earliest movements occurred at a time when embryos were not yet responsive to sensory stimuli, which was in clear contrast to the widely held belief that these behaviors were purely reflexive. Coghill's approach was to correlate the stages of behavioral development with cellular anatomy in order to begin the process of unravelling the underlying causes of

behavior. He focused on the salamander *amblystoma*, for which he characterized discrete, sequential spontaneous and sensory-evoked embryonic behaviors that corresponded to the appearance of different classes of neurons and the connections between them. Coghill also performed lesion experiments to observe the effects of severing these connections on behavior. In his book "Anatomy and the Problem of Behavior," published in 1929, he summarized his findings and encouraged thinking about the development of behaviors in parallel with corresponding changes in the nervous system. Despite the organized, scientific approach that Preyer and Coghill brought to the study of embryonic behavior, the scientific community at the time was mainly composed of "reflexologists" who believed that local reflexes responding to sensory stimulation were the "primary units of embryonic behavior" (Hamburger, 1989) and became linked together to create more complex movements. The reflexologists therefore did not accept the idea that early embryonic behaviors could arise spontaneously (e.g. without sensory stimulation) and these opposing ideas created a controversy in the field that remained deadlocked with little advance in research.

A turning point in the field came decades later with the research of V. Hamburger, in particular his classic 1963 paper titled "Some aspects of the embryology of behavior." This article summarized key observations and experiments relating to motor behaviors in the vertebrate embryo across species including fish, amphibians, birds and mammals and included several important new findings from his own work in the chick embryo. From this survey of fundamental studies he presented a cohesive argument for "spontaneous and reflexogenic motility...as two independent basic constituents of embryonic behavior. The former is considered to be the primary component...". This work prompted an explosion of studies in the field and an increasing interest in comparative physiology that led to our current understanding of embryonic vertebrate behavior.

In the following sections I will provide a brief overview of the research from lower vertebrates and mammals that have significantly contributed to our progress in understanding the development of motor behaviors.

I.1.2. Embryonic motor behaviors in lower vertebrates

As described above, Coghill observed early amphibian behavior in *amblystoma*, a simple vertebrate. He described five stages of behavior, beginning with the non-motile stage and followed by progressively more complex movements as the embryo began to move spontaneously and in response to touch with stereotyped flexures, coils, "S-bends," and swimming (Coghill, 1929). From these observations, he made many astute predictions about the role of individual neurons in these behaviors. For example, he proposed that some neurons in the motor system might have intrinsic rhythmic activity, that commissural connections were important for the left-right alternations of swimming and that the trunk of the animal might contain all of the necessary elements for producing locomotion. His work provided new insight into how animal behaviors could be studied in parallel with cellular anatomy in order to decipher how the nervous system produces behavior. Although spontaneous and sensory-evoked behaviors seem to arise simultaneously in *amblystoma*, this work nonetheless profoundly changed the way biologists regarded behavioral physiology and certainly laid the foundation for future studies of the development of behavior and the nervous system in other vertebrates.

Around this same time, many researchers were also investigating motor behaviors in fish with a similar aim to understand how the rhythmic locomotor activity of swimming is produced. Amongst cartilaginous and bony (teleost) fish, spontaneous movements are observed during development that progress from single to alternating flexions as movements mature into swimming behaviors guided by sensory feedback (reviewed by Hooker, 1952). In one teleost fish, the toadfish, embryos begin moving spontaneously at 9 days post-fertilization (dpf) while still in the egg and do not begin to respond to touch until 27 dpf, only after hatching has occurred (22 dpf) and swimming activity has already begun (25 dpf) (Tracy, 1926). The particularly long latency between the onset of spontaneous and sensory-evoked behaviors in the toadfish provided strong evidence that the basic circuits for locomotion can develop prior to sensory feedback and that they can be activated spontaneously. Furthermore, these results lent support to the idea that intrinsic rhythmic activity could drive behaviors during early development.

Finally, the work of Hamburger in the chick embryo greatly advanced our understanding of behavioral development. In the chick embryo, which hatches at 20 dpf, spontaneous flexions of the head and undulating contractions of the trunk ("S-waves") first appear at 3.5 dpf but a response to tactile stimulation cannot be elicited until 7 dpf (Hamburger & Hamilton, 1951). From 7 dpf onward, embryonic movements are uncoordinated and no longer resemble the spontaneous motor patterns of *amblystoma*, suggesting that embryonic behaviors might share a generalized vertebrate pattern from which certain specializations arise. A careful quantification of early movements showed that the frequency of spontaneous activity continually increased with age up to a peak at 13 dpf then decreased sharply by 19 dpf (Hamburger et al., 1951). During the stage of decreasing frequency of spontaneous movements the duration of the motor activity became longer, hinting at an important transition towards sustained locomotor movements. Another important experiment around this time demonstrated that the spontaneous motor activity in the chick embryo was as the result of neurogenic and not myogenic activity and used anatomical investigations to show that the onset of motility correlated with innervation of the muscle fibres by neurons (Visintini and Levi-Montalcini, 1939). Hamburger and Balaban (1963) performed lesion experiments in the spinal cord that resulted in the autonomous production of rhythmic activity in the embryo above and below the lesions. Together, these findings suggested that spontaneous activity was generated by intrinsic rhythmic activity from spinal neurons and so it was declared that "spontaneous, self-generated motility is the major issue in the development of behavior" (Hamburger, 1963).

I.1.3. Embryonic motor behaviors in mammals

Compared to lower vertebrates, mammals begin to show spontaneous movements at later stages of body development, particularly in the human fetus where the earliest movements begin at approximately five weeks of age (Felt et al., 2011). Well over a century of research has been devoted to understanding the development of human fetal movements (reviewed by Hooker, 1952; Lacquaniti et al., 2012) but here I will focus on key observations and experiments from model organisms.

From early studies in several species including rats, guinea pigs, cats and sheep, it appeared that spontaneous and reflexive movements develop nearly simultaneously in mammals (reviewed by Hamburger, 1963). In the embryonic cat, spontaneous movements of the neck begin at 24 dpf and responses to touch appear just days later, at 28 dpf (Windle & Griffin, 1931). The authors noted that these early movements strongly resembled the flexions seen in *amblystoma* and appeared "fish-like," hinting at a highly conserved sequence of motor development across vertebrates. However, the majority of early studies in mammalian embryos were focused on reflex development and failed to describe spontaneous activity in adequate detail.

In an effort to relate the results of his earlier studies in the chick to mammalian development, Hamburger and colleagues began a thorough examination of spontaneous and sensory-evoked embryonic motor development in the rat (Narayanan et al., 1971). They found that periodic spontaneous motor activity in the rat embryo began at 16 dpf then underwent a similar progression where activity rates peaked early then decreased in frequency in much the same pattern as in the chick (Hamburger et al., 1951) and cat (Windle & Griffin, 1931; Windle et al., 1933). These spontaneous movements in the rat embryo were described as undulations of the trunk that strongly resembled previous observations in the chick and also persisted in the isolated trunk. However, they saw that rat embryos already responded to tactile stimuli at 16 dpf, showing that relative to the chick and other lower vertebrates, spontaneous activity starts relatively late in the rat and tactile inputs are sensed early (Narayanan et al., 1971). Furthermore, they observed that movements were not jerky and disorganized as seen in later stages of spontaneous motor activity in the chick but remained smooth and integrated throughout maturation. This may be related to the delayed onset of spontaneous motor activity in mammals that appears late in limb development after joints are formed (Narayanan et al., 1971).

The reason that the time course of development of spontaneous and sensory-evoked movement in the spinal cord is different in mammals may arise from the fact that they have long gestation periods where the embryo is protected to a great extent from the external environment. From these and subsequent studies in mammals it became clear that although

the timeline of the development of motor behaviors may be slightly different from lower vertebrates it nonetheless follows a highly conserved sequence of developmental stages.

I.1.4. Summary of behavioral studies

Comparative studies across vertebrate species reveal that spontaneous motor activity is a conserved feature of embryonic development. These periodic movements do not require sensory input, suggesting that at theses early stages rhythmicity must be provided by the nervous system itself. While spontaneous, centrally generated motor activity can account for the earliest embryonic behaviors, sensory feedback and reflexes also contribute and indeed these behaviors strongly resemble one another. As the nervous system continues to mature, spontaneous and touch-evoked movements develop from slow, single flexions to repeated, alternating fast contractions in a stereotyped sequence. These common features of embryonic behavior suggest that the underlying organization of motor circuits is very similar across vertebrates. As tools became available to study developmental physiology at the cellular level, researchers were eager to investigate how the activity of individual cells of the nervous system contributed to these well-characterized motor behaviors.

I.2. THE NEURAL CONTROL OF LOCOMOTION

As far back as the 18th and 19th centuries, experiments on spinalized animals revealed that circuits residing in the spinal cord were sufficient to produce a basic pattern of locomotion (Clarac 2008; Guertin, 2009). The general interpretation of these results was that reflexes activated by local, peripheral feedback acted on central spinal circuits to produce patterned locomotor behaviors (Sherrington, 1910). It was not until the early 20th century that T.G. Brown showed that activity must originate from central patterns in the spinal cord because it persisted under doses of anaesthesia that abolished peripheral reflexes in cats, rabbits and guinea pigs (Brown, 1911, 1914). Subsequent studies of the isolated nervous system of invertebrates including the crayfish (Hughes & Wiersma, 1960) and the locust (Wilson, 1961) showed that rhythmic motor patterns could be produced in the isolated nerve cord that resembled motor activity in the intact animal. This work led to the idea that "… central patterning is the necessary and often the sufficient condition for determining the main

characteristic features of almost all actions" (Bullock, 1961) and thus the term "central pattern generator" (CPG) was established to refer to the basic spinal circuits that drive patterned motor output without sensory feedback. This work was happening at the same time as the behavioral observations of Hamburger and colleagues and thus the connection was quickly made between the concept of central pattern generators and the centrally generated nature of spontaneous motor behavior in the chick embryo. Additional pathways carrying sensory information could then be integrated into this existing CPG circuit during development in order to initiate and control motor patterns. Here, I will summarize the essential components of the CPG and sensory feedback circuits in order to describe our current understanding of how the developing nervous system controls motor behaviors.

I.2.1. Central pattern generators driving locomotion

The CPG has been a subject of extensive research since the 1980s and several important principles have emerged regarding the components and organization of the spinal CPG of vertebrates. The spinal cord is a bilaterally symmetrical network of neurons whose output controls movements on each side of the body independently. The spinal CPG consists of core groups of neurons on each side of the spinal cord that activate muscles as well as connections between the two sides to coordinate out of phase activity (Goulding, 2009). In terrestrial mammals such as mice, each limb is controlled by a CPG network at the corresponding level of the spinal cord consisting of several interconnected modules that control individual joints (Kiehn, 2006; Goulding, 2009), while in swimming vertebrates such as lamprey or zebrafish, the components of the CPG network are more evenly distributed along the length of the spinal cord to control trunk musculature (Grillner, 2006; Wiggin et al., 2012).

Decades of experimental evidence from the lamprey (Grillner, 2003, 2006) and *xenopus* tadpole (Roberts et al., 1998) have produced a basic wiring diagram for the vertebrate swim CPG consisting of four functional classes of neurons (Figure 1). First, each segment contains a group of motoneurons, known as a motor pool, that each activates a single adjacent muscle. The recruitment and activation of these motoneurons depends on the synaptic activity of both excitatory and inhibitory interneurons within the CPG (Figure 1).

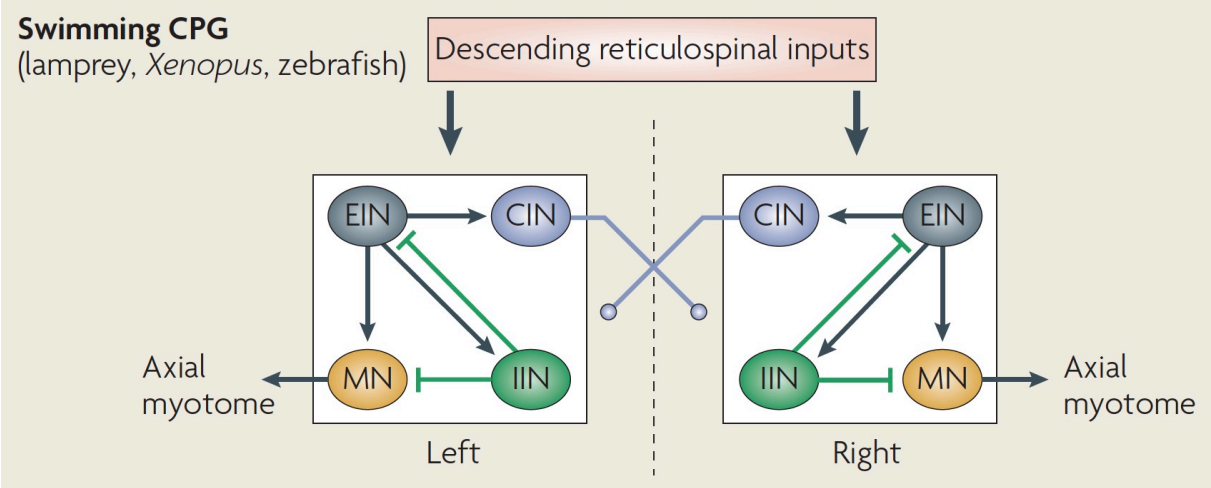

Figure 1. The locomotor central pattern generator (CPG) in swimming vertebrates.

The swimming CPG is composed of four functional classes of spinal neurons that are connected in such a way that they generate a rhythmic patterned locomotor output. Excitatory glutamatergic interneurons (EINs, grey cells) are rhythmically active and excite all three other CPG neuron cell types during swimming. Commissural glycinergic interneurons (CINs, blue cells) project across the spinal cord to provide the mid-cycle inhibition needed for left-right coordination. Ipsilateral glycinergic interneurons (IINs, green cells) provide inhibition to the CPG that may limit motorneuron (MN, yellow cell) activation in order to increase the frequency of swimming. MNs are the output neuron of the spinal cord and excite adjacent muscle fibers to produce movement. Source: adapted from Goulding, Nature Reviews Neuroscience, 2009.

Excitatory CPG interneurons are rhythmically active and release glutamate to drive on-cycle rhythmic firing in downstream motorneurons (as well as other spinal interneurons) during swimming (Buchanan and Grillner, 1987; Buchanan et al., 1989; Li et al., 2006). Excitation of motoneurons is driven by the activation of both N-Methyl-D-aspartate (NMDA) and α-Amino-3-hydroxy-5-methyl-4-isoxazolepropionic acid (AMPA) glutamate receptors that produce slow and fast excitatory post-synaptic potentials (EPSPs) (Dale & Grillner, 1986; Li et al., 2003) and blocking these receptors prevents slow and fast swimming, respectively (Grillner et al., 1991). Excitatory premotor interneurons have descending axons so that the initial activation of rostral CPGs is conveyed along the spinal cord and locomotion proceeds in a rostral to caudal direction (Figure 1).

Additional neurons contribute to the coordination of the left and right halves of the spinal cord so that activity alternates between the two sides of the body to produce forward locomotion such as swimming or walking (Figure 1). A group of commissural inhibitory interneurons use glycine to provide mid-cycle inhibition to the contralateral spinal cord to ensure that bilateral muscles are contracting out of phase with each other (Buchanan, 1982; Dale, 1995). Finally, ipsilateral glycinergic interneurons provide local inhibition within the CPG including direct synapses onto motoneurons (Rovainen, 1974, 1982; Buchanan, 1982; Buchanan & Grillner, 1987). The organization of the CPG for both walking and swimming thus ensures two important features of locomotion: excitatory interneurons drive rhythm generation in the network *via* motoneurons while commissural inhibitory interneurons pattern left-right coordination.

Rhythm generation in the embryonic spinal CPG in some species is driven not by glutamate but instead by passive depolarization that spreads between cells *via* gap junctions. Gap junctions are channels composed of connexin proteins that allow the bidirectional passage of electrical currents as well as small signaling molecules such as cyclic AMP (reviewed by Pereda, 2014). Gap junctions appear to be prevalent in embyronic vertebrate motor circuits between many types of neurons including motorneurons and the premotor interneurons that are crucial for generating rhythmicity in the CPG (reviewed by Kiehn & Tresch, 2002). Furthermore, there is accumulating evidence to suggest that some CPG neurons, including motoneurons, may have instrinsic pacemaker properties that contribute to

the generation of rhythmic activity (Li, 2011). These findings suggest that rhythm generation can be produced by intrinsic oscillations and electrical coupling of neurons in the network prior to the development of chemical synapses and is supported by biologically realistic CPG modeling studies (Kepler et al, 1990; Loewenstein et al., 2001; Horn et al., 2012). It is thought that as chemical synaptogenesis proceeds the overall contribution of gap junctions decreases but they nonetheless continue to play a role in some aspects of mature nervous system function such as lateral inhibition or activity synchronization (Kiehn & Tresch, 2002).

I.2.2. Descending control and sensory feedback modulate locomotion

The locomotor CPG can be driven at the earliest stages by intrinsic pacemaker activity or by the application of pharmacological agents such as NMDA (Cohen & Wallen, 1980; Brodin et al., 1985) but once the network is more developed the CPG is activated to produce locomotion mainly by descending inputs from higher brain regions with additional modulation from sensory feedback in the spinal cord (Figure 2). In the mature vertebrate nervous system, output neurons in subcortical pathways are linked *via* the basal ganglia to the tectum (superior colliculus), the mesencephalic (MLR) and diencephalic (DLR) locomotor command regions, or other brainstem motor centres where signals then activate reticulospinal neurons that will project to the spinal cord (Grillner et al., 2013). Studies from a number of species have identified descending excitatory inputs from the brainstem that activate certain CPG modules and thus produce a specific motor behavior (Buchanan & Grillner, 1987; Deliagina et al., 2002; Jordan, 1998; Kimura et al., 2013; Severi et al., 2014). For example, hindbrain reticulospinal Mauthner cells present in fish and amphibians send descending projections into the spinal cord that trigger fast escape behaviors (Korn & Faber, 2005).

Sensory pathways may also activate and modulate the spinal CPG directly through local sensory neurons and interneurons as shown by the simple touch reflex in *xenopus* (Li et al., 2003). The sense of light touch is mediated by sensory neurons located all over the body, therefore our skin can in fact be considered as the largest sense organ (Gallace & Spence, 2010). Sensory feedback from local pathways plays an important role to ensure continuing adaptation of ongoing locomotor behaviors in a changing environment (Rossignol et al., 2006).

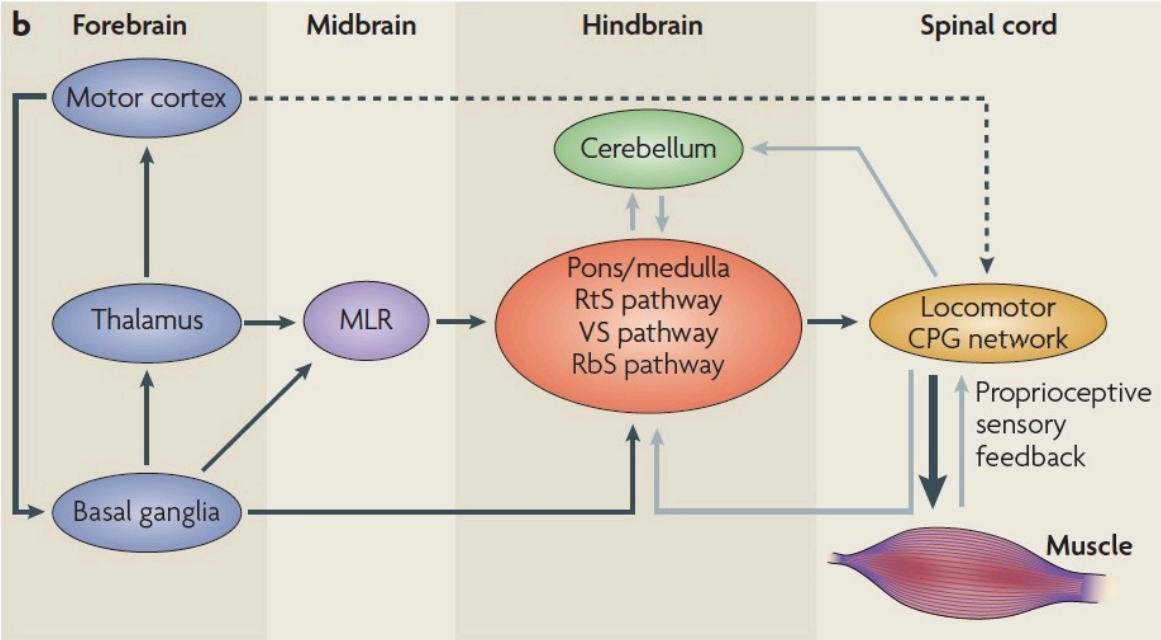

Figure 2. Organization of the locomotor system in vertebrates.

Motor pathways in aquatic and terrestrial vertebrates share a similar neuroanatomical structure. Local control of muscle movements is regulated by pools of motor neurons in the spinal cord that are part of a dispersed locomotor central pattern generator (CPG) network. Spinal motor centres are modulated by proprioceptive sensory feedback through sensory afferents. Descending reticulospinal (RtS), rubrospinal (RbS) and vestibulospinal (VS) pathways control the locomotor network in the spinal cord, although the reticulospinal pathway is the primary pathway for initiating locomotion. The reticulospinal pathway can be activated by the mesencephalic locomotor region (MLR), which has inputs from the basal ganglia and the thalamus. The cerebellum coordinates motor behaviors by mediating sensory and internal feedback and optimizing the motor pattern to the task at hand. It also coordinates spinal motor actions via supraspinal motor pathways. Connections from the motor cortex refine and initiate motor actions (dotted arrow). The black arrows indicate direct command pathways, the grey arrows indicate feedback pathways. Source: adapted from Goulding, Nature Reviews Neuroscience, 2009.

Neuromodulatory inputs are also known to modify the function of CPG networks (Harris-Warrick, 2011). Evidence from both invertebrates and vertebrates suggest that neuromodulators such as serotonin or dopamine may be essential for normal CPG function by either being connected within the circuit itself or by "priming" or modulating the network in a functional state, for example by regulating the excitability of CPG components (Katz, 1995).

Finally, in the developing embryo spinal or hindbrain neurons with intrinsic pacemaker properties may activate CPG networks prior to the maturation of sensory and neuromodulatory pathways (Broch et al., 2002; Tong & McDearmid, 2012) and there is evidence for continuing pacemaker activity in adults as well (Li, 2011; Smith et al., 2000). A complex combination of intrinsic and/or extrinsic neuromodulatory and synaptic interactions in addition to the pacemaker properties of neurons must therefore be considered when studying the generation of locomotion by spinal CPG networks.

I.2.3. Activity-dependent plasticity in spinal circuits

The function and dynamics of the network can also be modified as a result of plasticity mechanisms that alter the intrinsic properties of neurons or their synaptic connections. The best-studied type of plasticity is Hebbian plasticity, which consists of positive-feedback mechanisms that either strengthen strong synapses (*via* long-term potentiation, LTP) or weaken weak synapses (*via* long-term depression, LTD). LTP is thought to be a ubiquitous plasticity mechanism at excitatory synapses and particularly important in the experience-dependent refinement of neural circuits (reviewed by Malenka & Bear, 2004). Given the high degree of spontaneous activity in the developing zebrafish locomotor network, it is highly possible that Hebbian plasticity plays a role in fine-tuning spinal synapses during development. In counterbalance to Hebbian plasticity, which operates over short timescales (minutes) and small spatial distances (< 10 μm), homeostatic plasticity is thought to integrate neuronal activity over hours and days to rebalance network activity *via* negative-feedback mechanisms that seek to maintain stability in the network (Turrigiano & Nelson, 2004). Homeostatic plasticity may include extrinsic mechanisms such as the multiplicative scaling up or down of synapse strengths (synaptic scaling) or the addition or removal of synapses and

intrinsic mechanisms such as the redistribution of ion channels within a neuron (reviewed by Turrigiano, 2012).

Homeostatic plasticity mechanisms are thought to be crucial for compensating for changes in network activity such as during development or disease (Turrigiano, 2008). These mechanisms could be particular important in sensory and motor circuits, which are important for survival behaviors. Decades ago, researchers had observed that the amplitude of EPSPs onto motoneurons scaled up following experimentally-induced decreases in activity in cats and rats with lesions or pharmacological disruptions of activity (Gallego et al., 1979; Manabe et al., 1989; Webb & Cope, 1992), but it was not clear how to interpret these findings in light of their apparent contradiction to the known principles of Hebbian plasticity. Since this time, the field of homeostatic plasticity has exploded and many other *in vivo* studies have confirmed that these compensatory mechanisms are engaged at the cellular level following a reduction of activity in sensory (Deeg & Aizenman, 2011; Desai et al., 2002; Kaneko et al., 2008; Whiting et al., 2009) or motor pathways (Gonzales-Islas & Wenner, 2006; Wilhelm et al., 2009).

In order to show that these compensatory mechanisms are truly homeostatic it is crucial to also examine the consequences of this type of plasticity on the function of neural networks and the rhythmic behaviors they produce such as walking or swimming. For example, the escape swimming CPG network of the mollusc functionally recovers within a day following the lesion of commissural projections through the reversal of a key synaptic connection from inhibitory to excitatory (Sakurai & Katz, 2009). Furthermore, spontaneous activity in the chick embryo recovers just hours after chronic exposure to glutamatergic and cholinergic receptor antagonists (Chub & O'Donovan, 1998). The mechanism for this recovery is thought to involve an upregulation of glycine/GABA signaling that could recover initial activity rates because these neurotransmitters are depolarizing in the embryo. Beyond these studies however, little work has been done to study the homeostatic regulation of locomotor circuits controlling behavior despite an abundance of pharmacological and genetic tools available with which to manipulate and measure network activity in an intact animal.

I.3. THE EMBRYONIC ZEBRAFISH AS A SIMPLE VERTEBRATE MODEL

In order to understand the fundamental organization of the nervous system it is advantageous to study neural circuits in a model organism with relatively few neurons and thus a reduced complexity compared to higher vertebrates such as mammals. Over the past decades, neurobiology has benefited greatly from the use of simple vertebrate models such as *xenopus* and lamprey. The recent availability of genetic tools in the zebrafish has made it a powerful and increasingly popular model organism for studying questions in modern neuroscience including the neural control of locomotion. Despite the obvious differences in movement between the swimming of aquatic vertebrates such as fish and the walking of terrestrial vertebrates such as humans, the primary functional classes of spinal neurons and thus the organization of the CPG and associated sensory and neuromodulatory circuits, appear to be highly conserved (Jessell, 2000; Goulding, 2009; Figure 3).

Studying the embryonic zebrafish offers several experimental advantages. The embryonic spinal cord consists of only eight classes of interneurons (INs) with only a few types of each in any somite (trunk segment) and a known, limited number of sensory and motoneurons (MNs) that assemble into simple circuits, simplifying the identification and description of individual neurons. The intrinsic and synaptic properties of spinal neurons and muscle fibres such as morphology, resting membrane potential and mEPSC amplitude and frequency are well-documented for comparative purposes (Nguyen et al., 1999, Ali et al., 2000a). In spite of their simplicity, embryonic spinal circuits are already functional as evidenced by the presence of robust, stereotyped embryonic behaviors in zebrafish that begin within the first 24 hours of development (see below). We can therefore investigate the function and plasticity of developing locomotor circuits in the zebrafish from synapse to behavior at stages in development that would be very difficult to study in prenatal mammals.

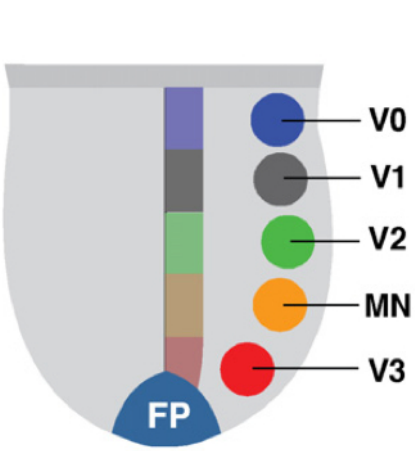

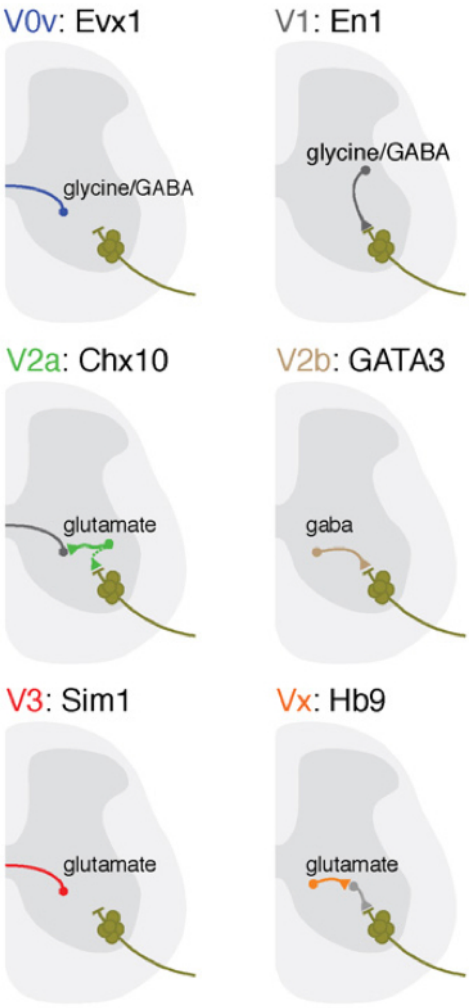

Jawless fish (lamprey)	Bony fish (zebrafish)	Amphibian (*Xenopus*)	Mammal (mouse)
Inhibitory CINs	CoBL neurons	CINs	dI6 neurons (Lbx1$^+$)
	CoSA neurons		$V0_D$ neurons (Dbx1$^+$, Evx1/2$^-$)
Excitatory CINs	MCoD neurons	Undetermined	$V0_V$ neurons (Evx1/2$^+$)
	UCoD neurons	Undetermined	$V3_V$ neurons (Sim1$^+$)
EINs	CiD neurons	dINs	V2a neurons (Chx10$^+$)
	VeMe neurons*		V3 neurons (Sim1$^+$)
			Hb9$^+$ neurons
L-interneurons	CiA neurons	aINs	V1 neurons (En1$^+$)
	eLD neurons		V2b neurons (Gata3$^+$)

* VeMe cells also have descending axons that may cross the ventral midline and are excitatory.

Figure 3. Functional neuron classes in the vertebrate spinal cord.

Upper left, distinct dorsoventral domains in the developing spinal cord give rise to motoneurons (MNs) and four cardinal interneuron populations (V0 - V3). Right, many of these interneuron subtypes can be identified based on their expression of postmitotic transcription factors, axonal morphology and neurotransmitter identity. Source: Grillner & Jessell, Current Opinion in Neurobiology, 2009. Lower table, the proposed homology of spinal neurons from different vertebrate species including zebrafish. Source: Goulding, Nature Reviews Neuroscience, 2009.

I.3.1. Timeline of locomotor behaviors in the developing zebrafish

The development of the zebrafish spinal cord CPG is rapid following fertilization (Figure 4). Beginning at 17 hours post-fertilization (hpf), the zebrafish embryo begins to produce slow, large amplitude 1 Hz spontaneous contractions of the trunk (Saint-Amant & Drapeau, 1998). This behavior, known as coiling, peaks in frequency at 19 hpf then rapidly declines to below 0.1 Hz by 26 hpf (Saint-Amant & Drapeau, 1998). By 21 hpf embryos develop a glutamate-dependent response to touch consisting of one to three alternating contractions of the tail (Saint-Amant & Drapeau, 1998; Downes and Granato, 2006; Pietri et al., 2009). Neither the response to touch nor spontaneous coiling depends on supraspinal inputs (Saint-Amant & Drapeau, 1998; Pietri et al., 2009).

From 29 hpf onward, embryonic zebrafish no longer produce coils but instead swim in response to touch or, to a lesser degree, spontaneously (Saint-Amant, 2006). Swimming behavior is driven by chemical glutamatergic and glycinergic neurotransmission and initially appears as a long burst of low-amplitude 10 Hz contractions (Kimmel et al., 1995) that develops following hatching into mature, 40 Hz "beat and glide" swimming by 4 dpf (Buss and Drapeau, 2001). Swimming activity recovers in the isolated spinal cord (Downes and Granato, 2006; Pietri et al., 2009) and can develop in the absence of descending inputs in the presence of NMDA (Chong and Drapeau, 2007), demonstrating that the neural circuitry within the spinal cord is sufficient to produce all of these earliest motor behaviors.

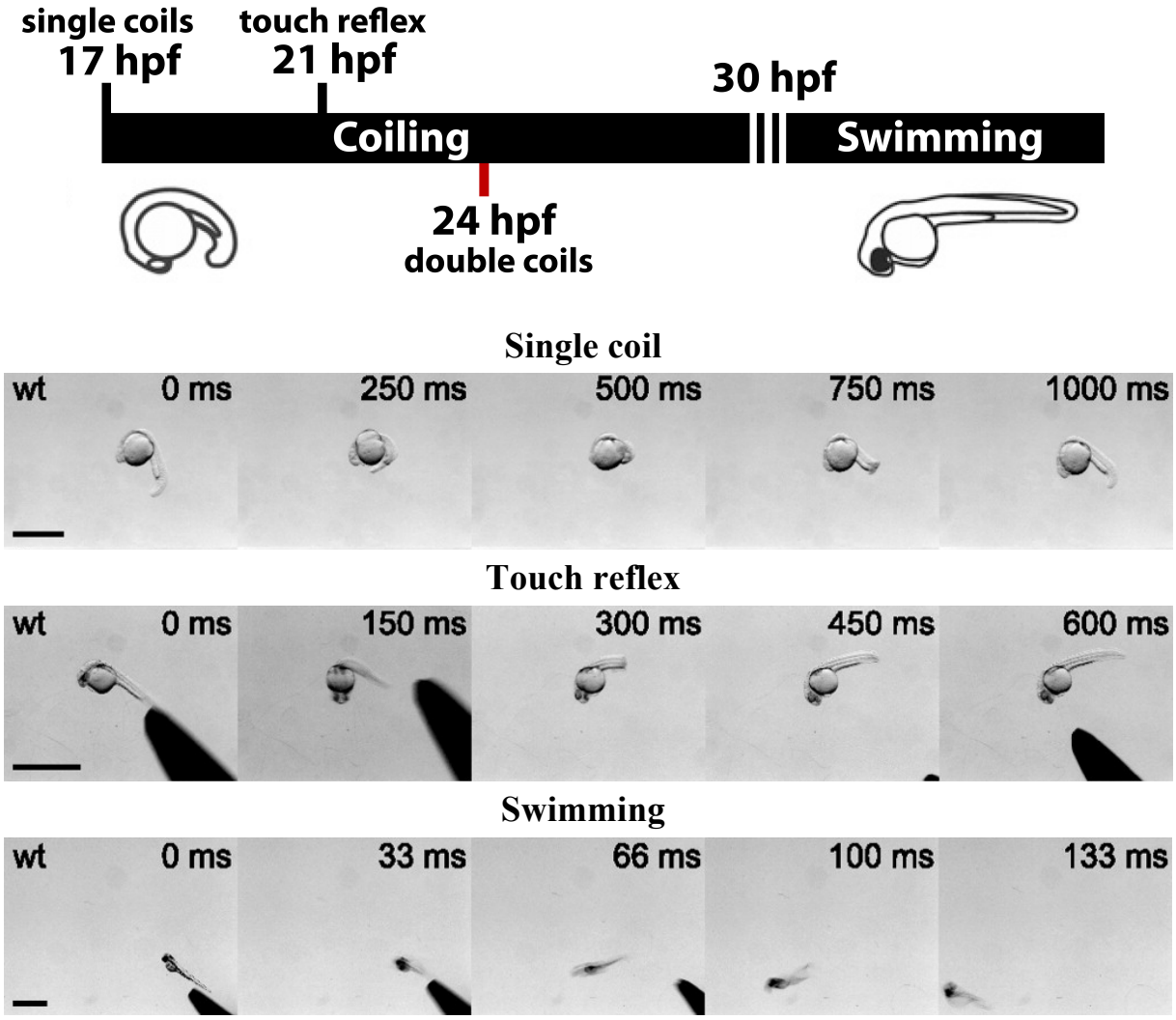

Figure 4. Overview of embryonic zebrafish behaviors.

Upper figure, developmental timeline in hours post-fertilization (hpf) of embryonic zebrafish motor behaviors. Single coils are spontaneous contractions that appear at 17 hpf. The touch reflex appears at 21 hpf in response to somatosensory stimuli. Double coils are spontaneous, alternating contractions that appear at 24 hpf. Around 30 hpf, both spontaneous and touch-evoked coiling transitions to swimming behavior. Lower panels, time-lapse images of a spontaneous single coil (20 hpf embryo; scale bar, 1 mm), the touch reflex (26 hpf embryo; scale bar 500 μm) and swimming (48 hpf; scale bar, 1 mm). Source: lower panels adapted from Low et al., Journal of Neurophysiology, 2012.

I.3.2. Classification of spinal sensory and CPG neurons in the early embryo

A great deal of knowledge of the embryonic zebrafish spinal cord is built on work from previous anatomical and behavioral studies with the *xenopus* tadpole and lamprey (Figure 5). In particular, several key studies describing the morphology and order of appearance of the earliest zebrafish spinal neurons and their projections was invaluable for comparative studies of the organization of spinal circuits (Mendelson, 1986; Myers et al, 1986; Bernhardt et al., 1990; Hale et al., 2001; Downes et al., 2002).

Proposed functional classes were initially assigned based on the anatomical features of neurons including the dorsoventral position of their soma, dendritic morphology and axonal projection, as these features would determine to a large extent the synaptic inputs and outputs of the neurons. Electrophysiological recordings of cellular activity further refined these categories by providing the intrinsic and synaptic properties of different neuronal classes as well as the contribution of different cell types to particular behaviors (Liao & Fetcho, 2008). The embryonic spinal cord is a particularly tractable circuit not only because there are fewer neurons present at this time but also because at these early stages it is thought that neuron classes have a primitive function that has yet to undergo further diversification and specialization (Goulding et al., 2002; Goulding & Pfaff, 2005; Kimura et al., 2006).

Neurotransmitter identity is another key feature of neurons that defines their role within the network, with glutamate and glycine being the major chemical neurotransmitters driving behavior in the zebrafish, as in other lower vertebrates (Grillner et al., 1991). A thorough classification of the neurotransmitter properties of spinal neurons in zebrafish embryos and larvae has been an important tool for predicting the function of neuronal classes (Higashijima et al., 2004b). Finally, with the increasing availability of genetic tools many neuronal classes are now defined by a combinatorial “code” of transcription factors that is conserved across vertebrates and provides a means to target different neuron types for experimental manipulations (Jessell, 2000).

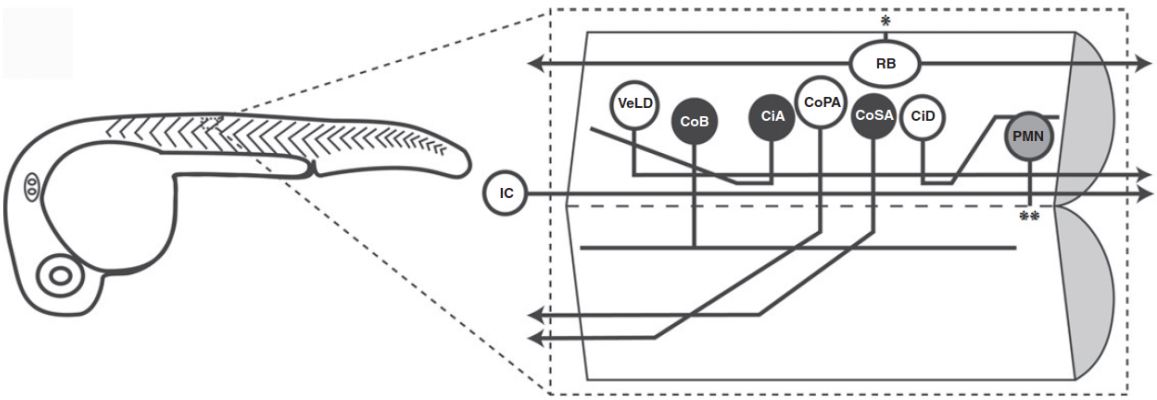

Figure 5. Neurons of the embryonic zebrafish spinal cord.

In the 26 hpf, fewer than twenty neurons with axons are present per segment of the spinal cord and they can be grouped in nine distinct cell types based on morphology. One spinal segment is shown in an open book configuration as if cut along the midline in a sagittal section. Glycinergic neurons are shown in black, cholinergic motoneurons in gray and glutamatergic neurons in white with the exception of the VeLD (which are GABAergic) and the IC cell (whose neurotransmitter identity is unknown). The asterisks denote points of exit from the spinal cord, * to the skin, ** to the ventral root. Please see the text for detailed descriptions of the cell types. Source: Saint-Amant, Progress in Brain Research, 2010.

As described above, the vertebrate locomotor CPG consists of four key components: motoneurons, descending excitatory interneurons and commissural and ascending inhibitory interneurons. In zebrafish embryos, three primary motoneurons are present per spinal hemisegment that innervate the adjacent muscles of either the dorsal, medial or ventral trunk (Myers et al., 1986; Figure 5). In addition to their distinctive axonal morphology, primary motoneurons are identified by their large, ventral soma, cholinergic identity and the expression of transcription factors from the Islet and Mnx family (Seredick et al., 2012). Secondary motoneurons do not begin growing out their axons until 26 hpf and likely contribute to the subsequent maturation of swimming behaviors (Drapeau et al., 2002). Motoneurons and their innervation of muscle fibres at the neuromuscular junction has been a well-studied field. Thus the focus of my work in this thesis is on the sensory and CPG circuits that generate motor patterns rather than the output of the motoneurons themselves.

It should be noted that the earliest activation of the zebrafish spinal cord (coiling) precedes central chemical neurotransmission and is driven entirely by electrical activity (Saint-Amant & Drapeau, 2001). A rostral pacemaker neuron, the ipsilateral caudal (IC) cell, projects a descending axon that periodically excites large groups of ipsilateral neurons through gap junctions, leading to the earliest motor behavior (Tong & McDearmid, 2012; Fig. 5). Just hours later, chemical neurotransmission has developed extensively and appears to shape the majority of activity in the spinal cord (Buss & Drapeau, 2001), although at some synapses electrical coupling persists in the larva and adult (Fetcho, 1992; Kimura et al., 2006). The presence of the purely electrical circuit is very transient and likely contributes to chemical synaptogenesis and the development of a mature locomotor network. In the following sections, I will outline the major classes of glycinergic and glutamatergic interneurons that have been shown to play a role in the earliest embryonic behaviors.

I.3.3. Glycinergic spinal interneurons

The earliest chemical synapses to form in the zebrafish spinal cord are glycinergic, starting at 20 hpf, followed a few hours later by glutamatergic synapses (Saint-Amant & Drapeau, 2000). The role of glycinergic interneurons in embryonic locomotor circuits is complicated by the fact that both GABA and glycine are depolarizing in the vertebrate

nervous system at early stages (Ben-Ari, 2002). Glycinergic inputs are depolarizing at all developmental stages of zebrafish discussed in this thesis (< 5 dpf) and the exact timing of the transition to a mature, hyperpolarizing response is not known. Depolarization occurs because the intracellular chloride concentration is high in immature neurons therefore the opening of GABA and glycine receptors causes chloride ions to flow out and depolarize the cell. However, depolarizing GABA and glycine can nonetheless be either excitatory or inhibitory depending on the resting membrane potential and threshold for action potential firing (Jean-Xavier et al., 2007). It has been postulated that depolarizing glycinergic signaling in early development provides an advantage in that it provides low levels of excitation in an immature circuit that activate voltage-gated calcium channels to promote maturation without causing overexcitation (Ben-Ari, 2002).

The population of neurons responsible for the earliest glycinergic activity in the zebrafish spinal cord is currently unknown but a recent study has identified glycine immunoreactive neurons in the hindbrain and rostral somite of the spinal cord at 20 hpf whose appearance coincides with the arrival of glycinergic inputs to spinal neurons (Moly et al., 2014). Indeed, lesion experiments suggest the presence of descending glycinergic inputs from the rostral spinal cord that synapse onto motoneurons and other spinal neurons at these early stages (Saint-Amant & Drapeau, 2000; Pietri et al., 2009). Much more is known about the identity of glycinergic spinal neurons in the later, larval zebrafish and their activity during locomotor behaviors.

The main classes of commissural glycinergic interneurons in the embryonic spinal cord are commissural secondary ascending (CoSA) and commissural bifurcating longitudinal (CoBL) interneurons (Bernhardt et al., 1990; Fig. 5). These neurons have extended axons by 24 hpf and express the transcription factor evx1 (Suster et al., 2009), although the CoSAs in fact appear to be a heterogeneous class of neurons that may include both glycinergic and glutamatergic neurons (Higashijima et al., 2004b). There is evidence to suggest that glutamatergic CoSAs appear first, followed by glycinergic CoSAs at later stages (> 36 hpf) (Satou et al., 2012), therefore interpreting the role of this class of neurons is aided by specific markers of neurotransmitter identity. Studies of the activity of glycinergic spinal zebrafish neurons during larval behaviors using the expression of GFP driven by the glycine transporter

promoter have shown that both CoSAs and CoBLs are rhythmically active during swimming, struggling and escape behaviors in the 3 dpf larva (Liao & Fetcho, 2008), but their role in embryonic behaviors in unknown. CoBLs in particular resemble the glycinergic interneurons with bifurcating axons that are the main source of mid-cycle inhibition for coordinating left-right alternation in the *xenopus* embryo (cINs; Dale, 1985), suggesting a homologous role in the zebrafish locomotor CPG.

Only one type of glycinergic neuron with an ipsilateral axonal projection has been identified in the embyronic and larval spinal cord, the circumferential ascending (CiA) interneuron (Bernhardt et al., 1990; Fig. 5). CiAs strongly resemble the glycinergic ascending interneurons (aINs) identified in *xenopus* as being crucial for providing inhibition during swimming (Li et al., 2002). Subsequent studies confirmed this homology by showing that both CiAs and aINs express the transcription factor engrailed (Higashijima et al., 2004a; Li et al., 2004) as well as premotor glycinergic interneurons of the mammalian spinal cord (Sapir et al., 2004). CiAs have been shown to inhibit spinal neurons (including motoneurons) during larval swimming in the > 4 dpf zebrafish (Higashijima et al., 2004a) and the homologous neurons contribute to producing fast locomotor rhythms in the embryonic mouse (Gosgnach et al., 2006). However, CiA axons do not begin to extend until around 26 hpf (Bernhardt et al., 1990) and they have little electrical coupling in the network (Saint-Amant & Drapeau, 2000) and therefore they do not contribute to early coiling behavior but may be important in shaping mature swimming.

Finally, a population of GABAergic neurons appears in the developing spinal cord between 24 - 28 hpf, the ventrolateral descending (VeLD) interneurons (Bernhardt et al., 1990; Fig. 5). VeLDs are thought to have extensive electrical coupling to motoneurons and excitatory interneurons in the embryo spinal network (Saint-Amant & Drapeau, 2000) while pharmacological blockade of GABA does not seem to alter the activity of developing locomotor circuits (Saint-Amant & Drapeau, 2000; Buss and Drapeau, 2001). The current consensus is that glycinergic and not GABAergic interneurons are the main inhibitory components of zebrafish locomotor circuits, as in other lower vertebrates, but future studies are still needed to characterize glycinergic signaling pathways and determine how these

depolarizing inputs cause functional excitation or inhibition in different cell types of the spinal CPG or sensory circuits.

I.3.4. Glutamatergic spinal interneurons

Although glycinergic inputs can depolarize immature neurons, glutamatergic neurotransmission is the classical excitatory neurotransmitter in the spinal cord and is crucial for producing rhythmic motor patterns. Circumferential descending (CiD) interneurons are the major class of glutamatergic interneurons that provide rhythmic, excitatory drive to primary and secondary motoneurons during locomotor behaviors in the larval zebrafish and thus thought to be the key excitatory component of the spinal CPG network (Kimura et al., 2006; McLean et al., 2008; Fig. 5). CiDs are also predicted to provide drive to motoneurons for embryonic coiling behaviors but this has not been demonstrated directly. CiDs are homologous to the descending excitatory interneurons (dINs) of *xenopus* that have been shown through extensive experimentation and modeling to be the source of excitatory drive for embyronic swimming (Roberts et al., 2010). This class of cells is defined genetically by the expression of the transcription factor chx10 (Kimura et al., 2006). At 3 dpf the majority of CiDs contact motoneurons though mixed synapses that provide excitation via both glutamatergic and electrical neurotransmission (Kimura et al., 2006). In the adult zebrafish, the activity of spinals CiDs is necessary for locomotion and sufficient to trigger swimming as revealed by ablation and optogenetic studies (Eklöf-Ljunggren et al., 2012). Neurons that express the transcription factor chx10 in mice are of a similar morphology to CiDs (Thaler et al., 1999) and are also rhythmically active during locomotion (Dougherty & Kiehn, 2010; Zhong et al., 2010), although their precise function in the locomotor CPG is less clear than in zebrafish.

In addition to excitation coming from the spinal CPG circuit, descending inputs from a small number of reticulospinal neurons of the hindbrain have reached the rostral spinal cord by 20 – 24 hpf (Mendelson, 1986) and excitation from these inputs appear to be crucial for the proper development of the spinal locomotor CPG including rhythm generation (Chong & Drapeau, 2007). In larval zebrafish, the optogenetic activation of hindbrain CiDs is sufficient to initiate swimming while hyperpolarizing these cells stops ongoing swimming activity

(Kimura et al., 2013). At early stages, these descending neurons may form a continuum with the spinal excitatory CPG components prior to the specialization of hindbrain nuclei as command centers (Soffe et al., 2009). Descending excitation from glutamatergic neurons may provide an important source of depolarization to set general levels of spinal activity in the embryo and to trigger spinal CPG development (Chong & Drapeau, 2007). In contrast, mutant zebrafish lacking sensory-evoked activation of the locomotor CPG during development show only slight modifications in motor patterns and no loss of rhythmicity (Low et al., 2010).

Although sensory inputs do not appear to be developmentally instructive, they are nonetheless crucial for survival behaviors such as escape. Two classes of glutamatergic spinal neurons play an important role in relaying somatosensory information to the locomotor CPG in the zebrafish embryo. Dorsal Rohon-Beard (RB) neurons are located bilaterally along the length of the trunk and have extensive mechanosensitive neurites that innervate the skin (Bernhardt et al., 1990; Fig. 5). By 21 hpf, sensory pathways have been established and light touch causes RBs to fire and excite many sensory interneurons through *en passant* synapses formed by longitudinal axons running rostrally and caudally (Saint-Amant & Drapeau, 1998; Easley-Neal et al., 2013). These postsynaptic partners are the glutamatergic commissural ascending primary (CoPA) interneurons (Fig. 5). The full complement of CoPAs is already present in the zebrafish spinal cord by 17-18 hpf, several hours before the onset of the touch response (Bernhardt et al., 1990). CoPAs have large, dorsal, triangular soma with horizontal dendrites and a long axon that crosses the midline and projects rostrally, often reaching the hindbrain (Bernhardt et al., 1990). It is the commissural axon of the CoPA that carries activation across the spinal cord so that a contralateral flexion response is produced following a touch stimulus. Many CiD soma are contacted by the ascending axons of CoPAs and may thus form part of a common path to amplify and relay excitation towards the MN during evoked responses (Pietri et al., 2009).

I.3.5. Experimental methods to study locomotor circuits

In addition to its reduced complexity and quantifiable behaviors, the zebrafish is amenable to physiological, optical and genetic analyses, making it an ideal model for studying neural circuits (Friedrich et al., 2010). Unlike mammals, zebrafish embryos develop

externally following fertilization and are optically transparent and thus well suited to experimental observation or manipulations at the earliest stages. At the one-cell stage, genetic material such as mRNA or DNA plasmids can be injected to introduce transgenes including fluorescent markers of neuron anatomy or activity. Alternatively, tools such as CRISPRs (clustered regularly interspaced short palindromic repeats) or antisense morpholinos can be injected to modify the sequence or expression, respectively, of endogenous genes (Asakawa et al., 2008; Blackburn et al., 2013).

The spinal cord in particular develops quickly and is easily accessible for whole-cell electrophysiological recordings (Downes, 2002; Hale et al., 2001; Saint-Amant & Drapeau, 1998). As described above, spinal neurons can be easily identified based on their morphology, neurotransmitter type and/or genetic markers such as transcription factors, which allow for relatively easy genetic manipulations such as the development of transgenic fish with GFP-labeled neuronal subtypes (Suster et al., 2009). Noninvasive techniques are also becoming widely available in the zebrafish to optically record and manipulate neuronal activity. Genetically encoded calcium indicators such as GCaMP can be used to reveal activity patterns across the entire zebrafish brain at single-cell resolution (Ahrens et al., 2012; Portugues et al., 2013). Optogenetic drivers of neuronal spiking such as channelrhodopsin can be used to test the sufficiency of neurons to produce a certain behavior while others, such as halorhodopsin or archaeorhodopsin, can silence spiking and thus provide tools to investigate the necessity of different neuronal classes (Portugues et al., 2013). Modern studies in zebrafish combining these powerful techniques are adding substantially to our fundamental knowledge of the neural circuits that control locomotion in the developing vertebrate (El Manira & Grillner, 2014).

I.3.6. Specific aims of the dissertation

Decades of research studying the locomotor CPG have greatly increased our knowledge of the neural circuits that control behavior but many fundamental questions remain. In this thesis, I explore the development of vertebrate locomotor circuits in the embryonic zebrafish with a focus on linking the specialized features of neurons and synapses to behaviors in the intact animal. For these studies, I utilized a multidisciplinary experimental

approach that included quantitative behavioral and electrophysiological analyses, genetic, pharmacological and surgical manipulations, as well as anatomical studies using *in vivo* fluorescent imaging.

My objectives were as follows: 1) To study how early CPG circuits driven by electrical activity become integrated with and eventually dominated by chemical neurotransmission during maturation, 2) To examine how the activity of spinal neurons in the somatosensory pathway modifies the activity of the CPG, and 3) To assess how the CPG develops following chronic increases or decreases in network activity. The following three chapters will address each of these objectives in turn.

CHAPTER 2

II. ARTICLE: "A HYBRID ELECTRICAL AND CHEMICAL CIRCUIT IN THE SPINAL CORD GENERATES A TRANSIENT NOVEL EMBRYONIC MOTOR BEHAVIOR"

The Journal of Neuroscience (2014) 34(29): 9644 –55.

LINKER STATEMENT

The following study was designed to examine the developmental stage (23 - 29 hpf) over which zebrafish embryos show a rapid transition from coiling to swimming, a significant change in behavior that we hypothesized reflects a maturation of the underlying neural circuitry. This important embryonic stage had not been previously studied in detail at the behavioral or cellular level. Here, we describe a novel transient behavior that appears in this brief time window and that correlates with the appearance of glutamatergic synapses and glutamate-dependent activity patterns. This study builds on previous work from the authors and significantly advances our understanding of developing locomotor circuits.

Section: Behavioral/Systems/Cognitive

A hybrid electrical/chemical circuit in the spinal cord generates a transient embryonic motor behavior

Laura D. Knogler*[1,2], Joel Ryan*[1], Louis Saint-Amant[1], and Pierre Drapeau[1,2#]
*Co-authors

Departments of Pathology and Cell Biology[1] and of Neuroscience[2], CRCHUM and GRSNC, Université de Montréal, Montréal, Québec, H3T 1J4, Canada

Abbreviated title: Hybrid double coil circuit in the zebrafish embryo

#Corresponding author: Pierre Drapeau, Ph.D.
Department of Neuroscience
Université de Montréal
2900, boulevard Édouard-Montpetit
Montréal, Québec H3T 1J4 Canada

Acknowledgements: This work was supported by fellowships from the NSERC and FRQS to L. Knogler, a studentship from the GRSNC (U. Montréal) to J. Ryan and grants from the CIHR and NSERC to L. Saint-Amant and P. Drapeau. Thanks to Shin-ichi Higashijima and Martin Meyer for sharing fish lines and reagents.

Conflict of interest: The authors declare no competing financial interests.

II.1. ABSTRACT

Spontaneous network activity is a highly stereotyped early feature of developing circuits throughout the nervous system including in the spinal cord. Spinal locomotor circuits produce a series of behaviors during development prior to locomotion that reflect the continual integration of spinal neurons into a functional network, but how the circuitry is reconfigured is not understood. The first behavior of the zebrafish embryo (spontaneous coiling) is mediated by an electrical circuit that subsequently generates mature locomotion (swimming) as chemical neurotransmission develops. We describe here a new spontaneous behavior, double coiling, that consists of two alternating contractions of the tail in rapid succession. Double coiling was glutamate-dependent and required descending hindbrain excitation, similar to but preceding swimming, making it a discrete intermediary developmental behavior. At the cellular level, motoneurons had a distinctive glutamate-dependent activity pattern that correlated with double coiling. Two glutamatergic interneurons, CoPAs and CiDs, had different activity profiles during this novel behavior. CoPA neurons failed to show changes in activity patterns during the period in which double coiling appears, while CiD neurons developed a glutamate-dependent activity pattern that correlated with double coiling and they innervated motoneurons at that time. Additionally, double coils were modified following pharmacological reduction of glycinergic neurotransmission such that embryos produced three or more rapidly alternating coils. We propose that double coiling behavior represents an important transition of the motor network from an electrically coupled spinal cord circuit that produces simple periodic coils to a spinal network driven by descending chemical neurotransmission which generates more complex behaviors.

II.2. INTRODUCTION

Spontaneous network activity is a highly stereotyped feature of developing circuits throughout the nervous system including the spinal cord (Blankenship & Feller, 2010; Feller, 1999). Spinal locomotor circuits produce a series of behaviors during development that reflect the continual integration of spinal neurons into a functional network. In the embryonic spinal cord, the first motor activity is a slow coiling of the trunk that is sensory-independent and therefore appears to be centrally driven (Corner, 1978; Hamburger, 1963; Narayanan et al., 1971). Embryos later become responsive to sensory stimuli and eventually locomote, behaviors that are shaped by the integration of central patterns and sensory feedback (Dale, 1995; van Mier et al., 1989). Our understanding of locomotor development has been greatly increased by studies in simple vertebrates, since the network complexity is reduced to a smaller number of neuronal classes, yet the functional organization of spinal circuits remains conserved across vertebrates (Grillner & Jessell, 2009). The zebrafish (*Danio rerio*) is a valuable model in which to study motor development due to its amenability to genetic, pharmacological and physiological analyses at embryonic stages with well-characterized immature behaviors (Saint-Amant, 2006).

The zebrafish embryo shows several motor behaviors. The earliest consists of transient slow, large amplitude repeating 1 Hz spontaneous coils of the trunk, occurring as early as 17 hours post-fertilization (hpf), soon after muscle innervation, but disappearing by 28 hpf (Saint-Amant & Drapeau, 1998). Coiling behavior is driven not by chemical neurotransmission but by pacemaker ipsilateral caudal (IC) neurons in the rostral spinal cord that initiate regular periodic depolarizations in spinal neurons (including motoneurons) via gap-junction coupling, leading to an ipsilateral contraction of the trunk (Saint-Amant & Drapeau, 2000, 2001; Tong & McDearmid, 2012). By 21 hpf embryos develop a glutamate-dependent response to touch consisting of one to three alternating contractions of the tail (Downes & Granato, 2006; Pietri et al., 2009; Saint-Amant & Drapeau, 1998). Neither the response to touch nor coiling depends on supraspinal inputs (Pietri et al., 2009; Saint-Amant & Drapeau, 1998). From 28 hpf onward, embryonic zebrafish show a swimming behavior driven by chemical glutamatergic and glycinergic neurotransmission and consisting of episodes of successive low-amplitude higher frequency (10 Hz) contractions in hatched (52

hpf) larvae (Kimmel et al., 1995) that gradually increase to 40 Hz (Buss & Drapeau, 2001). Swimming activity recovers in the isolated spinal cord (Downes & Granato, 2006; Pietri et al., 2009) and can develop in the absence of descending inputs in the presence of NMDA (Chong & Drapeau, 2007), demonstrating that the neural circuitry within the spinal cord is sufficient to produce all of these earliest motor behaviors.

However, much remains to be understood about how early electrical coupling is integrated with and eventually dominated by chemical neurotransmission during network maturation. Here, we report the identification of a novel intermediate double coiling behavior that bridges the developmental gap between embryonic coiling and mature locomotion (swimming). Double coiling is dependent on both electrical and glutamatergic transmission and as such represents the output of a hybrid motor network.

II.3. MATERIALS AND METHODS

II.3.1. Fish maintenance

Tübingen wildtype, *touché* heterozygous mutant (Low et al., 2010) and transgenic *chx10:gal4* (Kimura et al., 2013) strains of adult zebrafish were maintained according to guidelines approved by the Animal Experimentation Ethics Committee, Université de Montréal. Staging of embryos of, at this stage, undetermined sex, was performed as previously described (Kimmel et al., 1995).

II.3.2. Drug applications

All reagents were obtained from Sigma-Aldrich, unless otherwise noted. Embryos were anesthetized in 0.02% Tricaine and immobilized in 0.75% low-melting point agarose. 3 mM 6-cyano-7-nitroquinoxaline-2,3-dione (CNQX), 5 mM (2R)-amino-5-phosphonovaleric acid (APV), 1 μM tetrodotoxin (TTX), or saline was co-injected with 0.1% Fast Green dye and 2% FITC cell-permeant fluorescent tracer dye, in Evans medium (134mM NaCl, 2.9mM KCl, 2.1mM CaCl2, 1.2 mM MgCl2, 10 mM glucose, 10 mM HEPES, pH 7.8 with NaOH; Drapeau et al., 1999). Glass needles were pulled and mounted on a pipette holder and 65ms injections at 40 psi were delivered using a Picospritzer III (Parker Hannifin). Drugs were

administered by bolus injections in the forebrain of the embryos (Knogler et al., 2010) as lesion studies have shown that this brain region is not involved in the production of embryonic motor behaviors (Saint-Amant & Drapeau, 1998). Drug and sham injected embryos were gently removed from agarose and allowed to recover for 30 minutes in Evans medium, before proceeding to video recording. In recordings with strychnine, the tip of the tail was removed and embryos were incubated in a solution of 0, 5, or 50 μM strychnine in Evans for one hour prior to recordings to allow for sufficient penetration of the drug without inducing the effects of chronic strychnine treatment on neural development (Côté & Drapeau, 2012; Downes & Granato, 2006; McDearmid & Drapeau, 2006).

II.3.3. Lesions

Full transections of the spinal cord were performed under a dissection microscope on anesthetized embryos with a fragment of a razor blade mounted to a plastic pipette tip in Evans medium containing 0.02% tricaine. Medium was replaced several times following the lesion and animals were allowed to recover for 30 minutes before video recordings were taken.

II.3.4. Behavioral analysis

Embryonic motor activity was recorded using a Point Grey Research Grasshopper and Flea2 digital video camera at 15 to 60 Hz, mounted on an Olympus dissection microscope (SZX7) fitted with epifluorescence. Embryos were kept at 28.5 °C between recordings. Images were captured using PGR Flycap software and were then analyzed offline using ImageJ (NIH) software, wherein x,y coordinates and timing for each contraction was recorded using the Manual Tracker plugin.

II.3.5. Electrophysiology

Zebrafish embryos were dechorionated and anesthetized in 0.02% tricaine dissolved in Evans solution and dissected according to previously described procedures (Drapeau et al., 1999). Briefly, spinal neurons in somites 5 –15 were selected for recording based on their soma size and position as visualized by oblique illumination (Olympus BX61W1). To record

spontaneous activity, 15 μM D-tubocurarine (Sigma) was added to the Evans solution to block neuromuscular transmission. Electrophysiological recordings were done in the presence of 1-5 μM strychnine to block glycinergic events, or in 10 μM CNQX to block glutamatergic events. Patch-clamp electrodes for spinal neuron recordings (6–14 MΩ) were pulled from borosilicate glass and were filled with the following intracellular solution (in mM): 105 D-gluconic acid, 16 KCl, 2 MgCl2, 10 HEPES, and 10 EGTA, adjusted to pH 7.2, 290 mOsm (Drapeau et al., 1999). Sulforhodamine B (0.1%; Sigma) was also included in the patch solution to label the cells and confirm their identity after a recording. Standard whole-cell recordings from 23-30 hpf larvae were obtained using an Axopatch 200B and a Molecular Devices CV 203BU headstage amplifier (Molecular Devices). Data were acquired at 40 kHz and low-pass filtered at 10 kHz. Cells were held near their resting potential at -60 mV under voltage clamp unless otherwise specified. A maximum of three neural recordings were obtained from each embryo. Electrophysiological analyses were performed offline using Clampex 10.2 and Clampfit 10.2 software (Molecular Devices). The recordings were not analyzed if the resting potential was more positive than -40 mV or if the input resistance was below 500 MΩ. Following each recording, a series of fluorescent images of the rhodamine-filled cell and its axonal projections as well as bright-field images were collected with a QImaging camera (model 1394, QImaging Corp. Canada) using Micro-Manager software (http://www.micro-manager.org/). Images were inverted and brightness/contrast was adjusted using Adobe Photoshop CS2 (Adobe Systems, Inc., San Jose, CA, USA).

II.3.6. DNA microinjection and confocal microscopy

A plasmid containing five repeats of the upstream activating sequence (UAS) driving synaptophysin-GFP and DsRed (Meyer and Smith, 2006) was injected at a concentration of 50 ng/μl into transgenic *chx10:Gal4* zebrafish (Kimura et al., 2013) at the one-cell stage using a fine glass electrode and Picospritzer III (General Valve). Embryos were transferred to E3 (5 mM NaCl, 0.17 mM KCL, 0.33 mM $CaCl_2$, 0.33 mM $MgSO_4$) and raised as usual. Prior to imaging, embryos were dechorionated and anaesthetized with E3 medium containing tricaine. Embryos were pinned on their side in a sylgard-coated dish with fine tungsten wire through the notochord.

Confocal imaging was performed on a Quorum WaveFX spinning disk system (Quorum Technologies Inc) based on a modified Yokogawa CSU-10 head (Yokogawa Electric) mounted on an upright Olympus BX61W1 fluorescence microscope and equipped with a Hamamatsu ORCA-ER camera. Embryos were imaged using an Olympus LUM Plan 10X (NA 0.30) or 40X (NA 0.80) water-dipping objective. A bright field image and a set of stacked Z-series images with 2x2 binning were collected sequentially in each channel Volocity software (Improvision). Step size for z-stacks ranged from 0.3-1 μm. Z-stack maximum projections were created in ImageJ and combined to make color composites.

II.3.7. Statistical analyses

SPSS 21 (IBM) was used to assess data for statistical significance. All data sets were initially assessed for normality with the Shapiro-Wilk Test. For independent data sets with only two groups we used the Students' T, and for data from multiple groups we used a one or two-way ANOVA with Bonferroni correction for post-hoc testing ($p < 0.05$). In data obtained from the same embryos in different conditions, the repeated-measures variation of ANOVA was used. Chi-squared test was used for nominal data. Statistical significance is represented in the graphs as *** for $p < 0.001$, ** for $p < 0.01$, and * for $p < 0.05$, and individual p-values and number of embryos per condition are provided in figure legends and the text. Error bars in bar graphs indicate the standard error and results are described as the mean ± standard error. Excel was used to create all graphs except the box plots, which were created online using the BoxPlotR application (http://boxplot.tyerslab.com/). In these plots, box limits indicate the 25th and 75th percentiles as determined by R software, center lines show the medians, whiskers extend 1.5 times the interquartile range from the 25th and 75th percentiles and outliers are represented by open circles.

II.4. RESULTS

II.4.1. Transitional appearance of double coiling

Zebrafish embryos show a developmental transition in motor behaviors. From 17 hpf onwards, they show repeating spontaneous contractions with a peak average frequency of one

contraction per second (1Hz) at 19 hpf that decreases to below 0.1 Hz by 26 hpf and eventually disappear (Saint-Amant & Drapeau, 1998). These periodic spontaneous contractions consist of large-amplitude coils of the trunk during which the tip of the tail comes in contact with the head of the embryo (Fig. 1A) and at early stages tend to alternate sides. Beginning at 21 hpf a coiling response is elicited by touch, whereas by 28 hpf embryos will swim in response to touch or, to a lesser degree, spontaneously (Saint-Amant, 2006). In contrast to the slow frequency of coiling, when swimming is first observed in dechorionated embryos at 28 hpf it consists of low-amplitude contractions occurring at a relatively high frequency of 10 Hz. Transitions in spontaneous behavior between slow coiling and swimming have not been reported.

We examined spontaneous contractions at a high temporal resolution in order to probe for subtle changes during behavioral maturation. High-speed videos of spontaneous coiling events in dechorionated embryos partially immobilized in agarose revealed that spontaneous motor activity (coiling) could in fact be classified into at least two groups: single coils and double coils. Single coiling consisted of a single contraction of the trunk, after which the tail returned to its resting position (Fig. 1A). Double coiling, by contrast, consisted of two contralateral contractions of the trunk within one second (Fig. 1B). Between these two contractions, the tail did not return to a resting position, but instead the second contraction began rostrally before the first contraction had finished at the caudal end, forming a transient S-shape. These two types of coiling were also observable in non-immobilized animals and so we performed analyses of freely moving embryos to quantify the frequency of these events. These double coils first appeared at 24 hpf, seven hours after the appearance of single slow coils and three hours after the appearance of tactile responses and with time increased in number relative to single coils, representing the majority of events by 27 hpf (Fig. 1C; repeated-measures ANOVA shows significant effect of age with $p < 0.001$). The peak frequency of double coiling, at 27 hpf, was 0.015 ± 0.003 Hz (Fig. 1C, inset). A small number of events (< 5%) were also seen in these recordings that consisted of three or more alternating coils (data not shown).

We hypothesized that the relative increase in double coiling may introduce a mild refractory period in the motor network, thus contributing to the overall decrease in

spontaneous activity over this period of time. When we measured the quiescent periods before and after each type of coil at 26 hpf we found that on average the latency preceding a single or double coil was similar (Fig. 1D; 17.7 ± 1.6 and 20.2 ± 2.8 s, respectively; $p > 0.20$), while the latency following a double coil was nearly twice as long as compared to a single coil (Fig. 1D; 14.8 ± 1.1 and 23.7 ± 2.8 s for single and double coils, respectively; $p < 0.005$), revealing that the presence of double coils did indeed depress the motor network for a short time interval. These results suggest that the appearance of double coils represents a discrete event in the stepwise maturation from a single coiling behavior to swimming.

II.4.2. Double coiling does not depend on mechanosensory transduction

The touch response first appears at 21 hpf and consists of several alternating contractions of the tail beginning on the side contralateral to the stimulus (Pietri et al., 2009; Saint-Amant & Drapeau, 1998). One hypothesis for the appearance of double coils at a time shortly after the touch response is that double coils occur when a spontaneous single coil triggers a contralateral tactile response. We tested this hypothesis in a mutant line that is deficient in mechanosensation. Embryos of the touché mutant are completely unresponsive to touch as a result of defective sensory transduction (Low et al., 2010). In touché embryos there should therefore be no possibility of self-triggering a touch reflex in response to spontaneous movement. High-speed videos of 26 hpf embryos revealed no change in overall contraction frequency between touch-responsive controls and mutants touché siblings (Fig. 1E; 0.11 ± 0.01 and 0.094 ± 0.01 Hz, respectively; $p > 0.20$). The percentage of double coiling was likewise not significantly different between control and mutant embryos (Fig. 1F; 30.5 ± 4.7 and 27.4 ± 8.2 %, respectively; $p > 0.20$). Thus, double coiling was unaffected by a defect in mechanosensation suggesting that it is a spontaneous behavior.

II.4.3. Glutamatergic neurotransmission is required for double coiling

Early spontaneous coiling in the embryonic zebrafish has been shown to rely on a central pattern generator with gap junction-mediated electrical synapses between spinal neurons and to be independent of chemical neurotransmission other than at the neuromuscular junction (Saint-Amant & Drapeau, 2000). To test the necessity of chemical neurotransmission

for double coiling, we exposed embryos to the glutamate receptor antagonists CNQX or APV, which block AMPA or NMDA receptors, respectively. As previously reported (Saint-Amant & Drapeau, 2000; Pietri et al., 2009), the average coiling frequency was not significantly different between conditions (Fig. 2A; $p > 0.20$). However, CNQX treatment dramatically decreased the percentage of double coils throughout the period of 24 - 29 hpf (grey bars in Fig. 2B) e.g. at 26 hpf percentage of double coils in controls was 29.3 ± 6.5 vs 2.0 ± 0.9 % in CNQX treatment ($p < 0.005$ from 25 – 29 hpf). APV had an intermediate effect and decreased double coiling to less than 50% of control levels (black bars in Fig 2B, e.g. at 26 hpf double coiling frequency in APV treatment was 9.0 ± 3.8%, $p < 0.05$ from 26 – 29 hpf). TTX treatment, which blocks voltage-gated sodium channels, completely abolished motor activity, as previously described (data not shown) (Saint-Amant & Drapeau, 2001; Tong & McDearmid, 2012). These pharmacological results suggest that although both single and double coils are mediated by electrical coupling, double coils are more akin to touch responses and swimming in their requirement of an additional component of glutamatergic neurotransmission.

II.4.4. Normal frequency of occurrence of double coiling requires a descending excitatory drive from the hindbrain

The results described above suggest that double coiling is a newly identified motor network output that can be clearly distinguished from both single coiling and the touch-evoked coiling response. To better understand how double coiling is generated, we probed for the minimal neural circuitry required to produce the behavior. It has been previously shown that the neural circuitry within the spinal cord is sufficient to produce single coiling and the touch response and therefore does not rely on descending input from the hindbrain (Downes & Granato, 2006; Pietri et al., 2009). The isolated 48 hpf spinal cord is also able to generate swimming behavior if given enough time (> 20 minutes) to recover from the transection (Downes & Granato, 2006) and swimming-related activity can develop in the absence of descending inputs in the presence of NMDA (Chong & Drapeau, 2007), suggesting that the spinal cord is capable of producing the motor activity responsible for all of the earliest behaviors. Descending inputs from a small number of reticulopsinal neurons of the hindbrain

have reached the rostral spinal cord by 20 – 24 hpf and the second wave of supraspinal inputs does not arrive until 30 – 34 hpf (Mendelson, 1986).

To test the circuit requirements for double coiling, we lesioned 26 hpf embryos at the rostral end of the spinal cord, effectively removing all supraspinal structures including the hindbrain (Fig. 3A). A touch response was still present following the lesion, confirming that the rostral spinal cord remained intact. As a control, embryos were lesioned at the level of the midbrain, leaving the hindbrain intact (Fig. 3A). The frequency of single coiling was similar between these two conditions (0.11 ± 0.02 vs 0.14 ± 0.02 Hz for control vs lesioned embryos; $p > 0.20$). The percentage of double coiling events was significantly reduced in embryos lacking supraspinal input compared to embryos receiving control lesions (Fig. 3B; 43.3 ± 4.4 vs 21.0 ± 4.6 % for control vs lesioned embryos; $p < 0.005$), suggesting that the lesions resulted in a specific loss of double coiling. As a consequence the overall contraction frequency decreased significantly in lesioned embryos (0.30 ± 0.03 vs 0.20 ± 0.02 Hz for control vs lesioned embryos; $p < 0.005$). In addition, 22 out of 41 lesioned embryos failed to produce any double coils compared to just 1 out of 32 control embryos ($p < 0.0001$). Interestingly, the proportion of double coils in lesioned embryos was rescued to control levels when the concentration of KCl in the media was doubled to increase circuit activity (Fig. 3B; 54.1 ± 6.8 vs 42.5 ± 6.8 % for control vs lesioned embryos; $p > 0.20$). Furthermore, in high KCl conditions 6 out of 25 lesioned embryos failed to produce double coils, compared with 3 out of 22 control embryos ($p > 0.10$), consistent with rescue of the behavior. The average contraction frequency was also comparable in the high KCl condition (0.18 ± 0.02 vs 0.18 ± 0.02 Hz for control vs lesioned embryos; $p > 0.20$). These findings suggest that the spinal cord has the minimal circuitry capable of generating double coils but that the hindbrain may provide the necessary descending excitation to fully drive this behavior.

II.4.5. Blockade of glycinergic neurotransmission promotes multiple coils

Due to a high intracellular chloride gradient, glycine is depolarizing at embryonic stages and may excite spinal neurons by producing suprathreshold post-synaptic potentials but also shunt subsequent excitation, thereby raising the threshold for firing action potentials (for review, see Ben-Ari 2002). Accumulation of glycine in the network in the zebrafish shocked

mutant leads to a loss of spontaneous coiling activity and response to touch in the embryo (Cui et al., 2004, 2005), suggesting that the regulation of glycinergic signaling is important in the production of early behaviors. Previous studies using strychnine, a glycine receptor antagonist that disrupts glycinergic signaling in the zebrafish embryo, have shown dose-dependent effects on motor behaviors. Low doses of strychnine (1 μM) do not appear to alter the average frequency of spontaneous coiling (Saint-Amant & Drapeau, 2000) while high doses (≥ 400 μM) significantly decrease spontaneous coiling frequency and can also disrupt the touch-evoked response and swimming (Downes & Granato, 2006). However, high concentrations of strychnine may lead to off-target effects, such as by blocking nicotinic acetylcholine receptors in muscles and neurons (García-Colunga & Miledi, 1999). We therefore chose to examine the role that glycine neurotransmission might play in double coiling using moderate doses of strychnine.

Embryos were bathed for one hour in embryo medium containing 0, 5, or 50 μM strychnine to allow for penetration of the drug and spontaneous coiling activity was subsequently analyzed at 24, 26 and 28 hpf. In the absence of strychnine, multiple (three or more) coils were rare and accounted for less than 2% of all events in control embryos (Fig. 4A-C). At all three ages examined, however, strychnine had a dose-dependent effect of increasing the proportion of multiple coils and correspondingly decreased the proportion of single coils (Fig. 4A-C). This result is particularly interesting considering that the blockade of glutamatergic signaling resulted in a large increase in the proportion of single coils at the expense of a loss of double coiling (Fig. 2B), the opposite of the outcome seen here. An age-dependent effect of strychnine was also seen, as 50 μM strychnine treatment only slightly increased the proportion of multiple coils in 24 hpf embryos (to less than 5% of all events), while by 26 hpf and 28 hpf the proportion of multiple-coil events was increased to 15-20% of all events, a much larger increase over control values (Fig. 4A-C).

Coiling events with three or more contractions had a tendency to be followed by long periods of inactivity. Data pooled across strychnine-treated 26 hpf embryos shows that multiple-coil events with three or more contractions were on average followed by a latency more than three times longer than the latency to the next event following a single-coil in control embryos (Fig. 4D, $p < 0.001$). Interestingly, the latencies following both single and

double coils were also significantly increased in embryos treated with strychnine as compared to single-event latencies in controls, but to a lesser extent than seen with multiple coil events (Fig 4D.; $p < 0.05$ and $p < 0.005$ for single and double coiling, respectively). This is likely due to an overall reduction in event frequency related to the depressive effect of the multiple coiling on the network.

These results suggest that, despite the fact that glycine is depolarizing at this developmental stage (Saint-Amant & Drapeau, 2000), glycinergic neurotransmission itself does not appear to drive double coiling. Instead, the role of glycinergic inputs during spontaneous coiling events may be to limit the contralateral activation of the spinal cord by shunting the membrane resistance and keeping the membrane potential below action potential threshold.

II.4.6. Double coiling-related activity recorded in primary motoneurons

In order to examine the physiological characteristics of double coiling at the cellular level, we recorded from identifiable primary motoneurons (MNs) of the spinal cord between 24 – 30 hpf. Current injections were always capable of inducing burst firing of action potentials in the MN that lasted the duration of the current pulse (Fig. 5A). Whole-cell voltage-clamp recordings in MNs showed a regular pattern of gap junction-driven periodic inward currents (PICs) (Fig. 5B, C, E) that underlie single coiling, as previously described (Saint-Amant & Drapeau, 2000). Also of note was the presence of distinct fast large peaks (≥ 15 pA) increasing in amplitude and frequency with age (compare Fig. 5C [black arrowheads] with D). These peaks were determined to be synaptic glutamatergic events following several observations. Unlike depolarizations due to electrical coupling, the fast peaks reversed at membrane potentials more positive than the cation reversal potential (approximately 0 mV) (Fig. 5D). Pharmacological experiments showed that these fast peaks were not blocked by strychnine (N = 9/9; Fig. 5D) but disappeared upon addition of 10 μM CNQX to the extracellular solution to block AMPA receptors (N = 5/5; Fig. 5E). The largest glutamatergic peaks coincided with the electrical inward currents and had amplitudes up to 300 pA although much smaller glutamatergic peaks resembling miniature excitatory post-synaptic currents with amplitudes of 5 - 10 pA were also seen in the interval between events (Fig. 5E, grey

arrowheads and inset). These small putative glutamatergic mEPSCs were also abolished by CNQX application.

In addition to electrical and glutamatergic currents, synaptic bursts (SBs) appearing as inward currents and corresponding to glycine-mediated chloride extrusion (Saint-Amant & Drapeau, 2000) were present at a similar frequency and duration as the periodic electrical currents (Fig. 5B). Glycinergic synaptic bursts onto MNs are thought to originate from commissural glycinergic interneurons and paired current-clamp recordings have shown that these glycinergic inputs arrive at a MN at the same time that a gap junction-driven inward current is depolarizing the contralateral MN (and its electrically-coupled neighbors) and driving a single coil on that side of the trunk (Saint-Amant & Drapeau, 2001). In agreement with previous studies (Saint-Amant & Drapeau, 2000, 2001), synaptic bursts were completely absent in recordings where the extracellular solution contained 5 μM strychnine to block glycine receptors (n = 11/11). Under current-clamp, both glycinergic post-synaptic potentials as well as gap junction-driven depolarizations were capable of driving action potentials in motoneurons in embryos ≥ 25 hpf (Fig. 5G) though to a far greater degree with electrical than glycinergic inputs.

Given our knowledge that gap junction-driven depolarizations of MNs drive single coiling (Saint-Amant & Drapeau, 2000), we therefore hypothesized that a double coil would be distinguishable from a single coil by the close succession (< 1 s) of a mixed event composed of electrical then glycinergic inputs in a MN, in either order, which would correlate to the closely-timed depolarization of an ipsilateral then contralateral MN and therefore an alternating double coil. It is important to note that the glycinergic synaptic burst itself is a correlate of contralateral electrical depolarization and is not thought to drive the coiling activity (Saint-Amant & Drapeau, 2001). Indeed, electrophysiological recordings from MNs clearly showed mixed electrical/glycinergic events (Fig. 5B, H, I) that we interpret as physiological correlates of double coiling. These mixed events were first observable in a minority of MN recordings from 23-24 hpf embryos but were present in all MN recordings from embryos aged 26 - 30 hpf, correlating well with the increasing proportion of double coils observed in the intact embryo at these ages (Fig. 2B) and thus providing a useful readout of fictive double coiling. Evidence of fictive multiple coils (≥ three coils) was also seen under

conditions where strychnine was present and synaptic bursts were no longer present (Fig. 5J). These results mimic our behavioral results in strychnine (Fig. 4) and suggest that glycine (and synaptic bursts) do not drive coiling behavior and in fact may act to limit excitation in the network under physiological conditions.

II.4.7. Blockade of glutamatergic neurotransmission abolishes mixed events in motoneurons

To confirm the requirement of glutamatergic neurotransmission for the mixed events which represent fictive double coils, we perfused CNQX into the bath and looked for an effect on MN activity patterns. Bath application of 10 μM CNQX blocked all glutamatergic synaptic events in our recordings and was sufficient to eliminate all mixed events without affecting the overall frequency of electrical or glycinergic synaptic burst events alone (Fig. 6A; N = 4) or the amplitudes of these currents (Fig. 6B; $p > 0.20$ for both PICs and SBs). The change in amplitudes of mixed events could not be analyzed since they were absent or extremely rare in the presence of CNQX. Subsequent washing out of CNQX showed that the mixed events recovered, confirming that their loss was not due to an artifact of the long recording (Fig. 6C, D). These results corroborate our behavioral findings and suggest that the mixed events recorded in MNs are physiological correlates of fictive double coiling behavior and that glutamatergic signaling is indeed necessary for double coiling.

II.4.8. Candidate glutamatergic interneurons in the early motor network

Having described novel glutamate-dependent double coiling by behavioral, pharmacological, electrophysiological, genetic and lesion analyses, we next sought to identify the key interneurons in the neural network underlying this motor activity. There are a limited number of classes of interneurons in each somite of the spinal cord at this age and these interneurons have been well characterized in terms of dorsoventral soma position, axonal morphology and neurotransmitter phenotype (Bernhardt et al., 1990; Hale et al., 2001; Higashijima et al., 2004). Electrophysiological recordings in the early embryo have shown that in addition to the primary MNs at least four classes of spinal interneurons are active at 24 hpf: ipsilateral caudally projecting (IC), ventral lateral descending (VeLD), circumferential

descending (CiD) and commissural primary ascending (CoPA) interneurons (Saint-Amant & Drapeau, 2001). IC cells have pacemaker properties and are thought to initiate spontaneous network activity in the embryonic spinal cord via electrical coupling, suggesting that at early stages these neurons do not connect to the network with chemical synapses (Tong & McDearmid, 2012). VeLDs are GABAergic (Batista et al., 2008) whereas both CoPA and CiD neurons are glutamatergic (Batista et al., 2008; Higashijima et al., 2004; Kimura et al., 2006). Therefore, the CoPA and CiD neurons are the most likely candidates to mediate the glutamatergic neurotransmission important for double coiling behavior at early stages and we recorded from each type.

By 26 hpf CoPA axons can span up to 12 somites (Bernhardt et al., 1990), suggesting that these neurons have developed extensive axonal projections by the onset of double coiling behavior. In embryos as young as 24 hpf, filled CoPAs had axons that crossed the midline and ascended dorsally and rostrally for several somites (Fig. 7B). CoPA neurons receive direct glutamatergic input from sensory Rohon-Beard (RB) cells and relay this excitation during evoked behaviors (Pietri et al., 2009). We therefore recorded from these cells in 24 – 29 hpf embryos to examine how their activity might contribute to double coiling. The only spontaneous activity seen in CoPAs was a long duration (more than one second), ~ 20 mV amplitude depolarization that was often sufficient to elicit a single action potential at the onset of the depolarizing plateau (Fig. 7A; N = 20/20). In the absence of sustained firing, these recordings suggest that CoPAs are not as important for spontaneous behaviors as they are for the touch response in their proposed role as a sensory interneuron (Pietri et al., 2009).

II.4.9. Glutamatergic CiD interneurons are active during spontaneous behaviors

CiD neurons express the transcription factor chx10 and are part of the V2a population of excitatory premotor interneurons in zebrafish as well as in other vertebrates (Kimura et al., 2006). Many CiD soma are contacted by the ascending axons of the CoPA sensory interneurons in the dorsal longitudinal fasciculus (DLF) and may thus form part of a common path to relay excitation towards the contralateral MN during evoked responses (Pietri et al., 2009). We recorded from CiD neurons in 24 – 30 hpf embryos to examine their intrinsic and synaptic properties during the period of spontaneous double coiling.

At 24 hpf, CiD neurons had ipsilateral axons projecting ventrally and caudally that were varied in length from one to several somites (Fig. 7C). Whole cell current-clamp recordings showed that CiDs responded to current injections with a maximum of one to three action potentials at earlier ages, but became capable of burst firing with large undershoots by 27 hpf onward (Fig. 7D). CiDs were spontaneously very active and there was clear evidence of electrical coupling to the network at all ages studied. Like MNs, CiDs receive gap junction-driven periodic inward currents that by 26 - 27 hpf that were sufficient to produce bursts of action potentials under current-clamp conditions (Fig. 7E, upper trace). Glutamatergic synaptic events could also be seen on top of the electrical currents (Fig. 7F) and became increasingly apparent in size and frequency with age. Additionally, CiDs received depolarizing glycinergic synaptic bursts that led to action potential firing by 27 hpf (Fig. 7E, lower trace). Finally, voltage-clamp recordings revealed mixed events in CiDs (Fig. 7G) that were very similar to those seen in MN recordings (Fig. 5H), suggesting that the activity of the CiD is very similar to that of the MN.

Paired current-clamp recordings of CiD cells and ipsilateral MNs in embryonic zebrafish spinal cord have shown that their gap junction-driven depolarizations are synchronous, suggesting that they are part of a local coordinated group of ipsilateral neurons that are electrically coupled (Saint-Amant & Drapeau, 2001). Simultaneous recording of a CiD in cell-attached mode and an ipsilateral MN under whole-cell voltage-clamp located two somites caudally showed that the CiD fired several action potentials during the electrical component and prior to the onset of but not during the glycinergic component in a mixed event in the MN (Fig. 6H). Furthermore, the CiD received glycinergic inputs in the form of a synaptic burst in synchrony with the MN (Fig. 6I), suggesting that in addition to being electrically coupled, these cells receive coordinated synaptic input from the same or similar unidentified contralateral glycinergic neurons.

These results show that the intrinsic and synaptic properties of CiD neurons are maturing at the time double coiling first appears. CiDs are spontaneously highly active, capable of firing several action potentials and show activity that is very similar to the mixed events seen in MNs that we propose underlie double coils. These data suggest that the CiD

plays an important role in propagating ipsilateral excitation in the early embryo via electrical and/or chemical neurotransmission.

II.4.10. CiD neurons contact ipsilateral MNs and other CiDs with putative glutamatergic synapses

The activity pattern of the CiD neuron suggested that it may provide important ipsilateral drive, therefore to investigate the development of synaptic properties of these cells for glutamatergic neurotransmission we used the Gal4/UAS system to drive mosaic expression of synaptophysin-GFP and DsRed (syp:GFP-DsR) (Meyer & Smith, 2006) in chx10:Gal4 transgenic fish (Kimura et al., 2013). Confocal imaging revealed that the majority of DsRed-labeled cells had a CiD morphology, as identified by a caudal axon projecting first ventrally and then proceeding dorsally and laterally. It has been previously reported that CiDs are found in the spinal cord by 22 - 23 hpf and begin to extend their axons shortly thereafter (Bernhardt et al., 1990). Prior to 24 hpf, cells expressing DsRed were clearly seen in the spinal cord, but their axons were very short and cell identity was ambiguous. By 24 hpf, coinciding with the onset of double coils, CiDs were clearly seen with axons spanning up to two caudal somites (Fig. 8A). Except for the most proximal part of the axon projecting from the soma, distinct synaptophysin-GFP puncta were visible along the entire length of the axon to the growth cone (Fig. 8A). CiDs with more dorsally located soma had the longest axons and the most synaptophysin-GFP puncta, which relates to the fact that these are the earliest-born CiDs (Kimura et al., 2006).

Older embryos had labeled CiDs with considerably longer axons and synaptic puncta (Fig. 8B, C). Axons of CiD neurons in 27 hpf embryos spanned up to six somites in length and contained as many as 40 putative synaptic puncta. Several embryos had more than one cell labeled by syp:GFP-DsR and in addition to CiDs primary MNs were also occasionally labeled (Fig. 8B, C), allowing for the identification of possible postsynaptic partners of CiD at these early ages. Synaptophysin-GFP puncta of CiD axons were seen to contact the soma of primary MNs as well as other, more caudal CiDs (Fig. 8B-D). These results show that at the onset of double coiling, CiDs are extending axons that contact MNs and CiDs with putative

glutamatergic synapses. Consequently, they are well suited to propagate ipsilateral excitation at early stages via glutamatergic neurotransmission.

II.5. DISCUSSION

II.5.1. Double coiling: A novel intermediate behavior

The novel double coiling behavior described here has several characteristics that underlie its role as a transient, intermediate behavior that bridges the developmental gap between early single coiling with the onset of the touch response and the later appearance of swimming. The response to touch, which only slightly precedes the onset of double coiling, is a strong contraction contralateral to the site of touch, followed by one or two alternating coils (Saint-Amant, 2006). The touch response is, by definition, sensory-evoked and is glutamate-dependent, beginning with the activation of dorsal glutamatergic RB sensory neurons (Saint-Amant, 2006; Pietri et al., 2009). However, RBs are not spontaneously active therefore likely do not contribute to double coiling (Saint-Amant & Drapeau, 2001), in agreement with our evidence showing that touché mutants lacking mechanosensitive RBs (Low et al., 2010) show regular double coiling behavior.

The requirement of supraspinal connections for normal double coiling behavior but not for the response to touch (Pietri et al., 2009) suggests that at least part of the drive required for double coiling originates outside and therefore rostral to the spinal cord. By the onset of double coiling, axons of reticulopsinal neurons have projected to the rostral spinal cord (Mendelson, 1986) and may act upon the motor network via glutamatergic signaling to produce double coils. Since an increased KCl concentration enhanced double coiling in lesioned embryos, we hypothesize that hindbrain inputs may provide tonic drive to the rostral spinal cord at this age. If this were the case, the spinal cord should contain the minimal circuitry to generate double coiling, but would require an external drive to bring the network to threshold to perform the behavior. The delayed onset of double coiling relative to the response to touch may simply be due to a gradual buildup of the excitatory drive that becomes sufficient to spontaneously activate the network by 24 hpf without the major touch-evoked release of glutamate from the RBs. Excitatory drive is likely to increase rapidly during

development as intrinsic and synaptic properties of neurons are undergoing maturation, contributing to the transiency of the double coil behavior.

Double coiling is similar to previously described S-flexures observed in the salamander and in the chick (Hamburger, 1963) and may thus reflect a common vertebrate behavior. Like in S-flexures, the contractions during a double coil overlap, such that the second contraction begins at the rostral end before the first contraction has terminated at the caudal end, implying a close interaction between the two sides of the spinal cord. This overlapping of contractions is also seen in swimming, therefore double coiling is a logical intermediate to precede the low-amplitude, high-frequency swimming behavior. Swimming can be easily evoked but is more rarely spontaneously occurring in the embryo, perhaps due to a higher initial requirement for activation of the network compared to double coiling. However, once the threshold for swimming is reached, an immature burst can last several seconds in duration (Buss & Drapeau, 2001). In addition to the formation of chemical synapses, a shift in the activity of pacemaker IC cells towards more sustained burst firing may be important for the prolonged network activation underlying swimming (Tong & McDearmid, 2012).

II.5.2. The integration of chemical neurotransmission into an existing electrical circuit

Electrical coupling of neurons via gap junctions has been shown to contribute to the earliest activity in the developing nervous system of many invertebrate and vertebrate species including mammals (Bennett & Zukin, 2004). The development of neurotransmission in the zebrafish spinal cord begins with an electrically coupled network solely driven by ipsilateral descending pacemaker activation from rostral spinal IC cells (Tong & McDearmid, 2012). For the circuit to be capable of mediating rapid double coiling, new chemical connections must be made that interconnect the two sides of the spinal cord to achieve alternating activation with greater control of timing and intensity than electrical coupling.

The earliest chemical synapses to form in the zebrafish spinal cord are glycinergic, starting at 20 hpf, followed a few hours later by glutamatergic synapses (Saint-Amant & Drapeau, 2000). GABA, the other major fast neurotransmitter, does not seem to play an important role in these circuits (Saint-Amant & Drapeau, 2000; Buss & Drapeau, 2001),

therefore glutamate and glycine appear to be the major chemical neurotransmitters driving behavior, as in other lower vertebrates (Grillner et al., 1991). Pharmacological blockade of glutamate receptors led to a significant reduction in double coiling behavior in the intact embryo as well as a loss of mixed events (correlates of double coiling) in MNs. In contrast, blockade of glycine receptors resulted in increased contralateral trunk contractions such that many double coils were transformed into triple and quadruple coils. These neurotransmitter systems may therefore play complementary roles whereby glutamate signaling drives the double coiling and glycinergic signaling acts to modulate the resulting excitation so as to prevent extended periods of quiescence due to circuit depression. Indeed, the latencies following these multiple-coil events were significantly longer than those following double coiling, suggesting that activity-dependent depression of network excitability occurs following coiling events of increasing strength and duration as seen in many developing vertebrate networks (O'Donovan, 1999).

II.5.3. Neural activity patterns generating double coiling

We propose that the physiological correlate of the double coiling behavior we are describing here for the first time corresponds at the cellular level to (in either order) a glycinergic synaptic burst (corresponding to a contralateral contraction) and gap junction-driven periodic inward current (corresponding to an ipsilateral contraction) occurring in close, subsecond succession in the MN. Glutamatergic events of increasing amplitudes become clearly integrated into the mixed event over the period of 24 - 29 hpf, suggesting the formation and/or maturation of glutamatergic synapses onto the MNs at this time. No other new patterns of activity appear in the MN during this time window until the onset of fictive swimming bursts at 28 hpf, therefore the mixed events are likely correlates of double coiling. Efficient contralateral activation of the spinal cord following an ipsilateral contraction could be achieved via excitatory interneurons that contact contralateral spinal MNs and premotor interneurons. During the period in which the circuit is capable of generating spontaneous single and double coils, however, the commissural glutamatergic CoPA neuron only fires a single action potential then remains depolarized at the approximate reversal potential for chloride (- 35 mV) for more than one second, which is likely to shunt the membrane

resistance and prevent further action potential firing. The CoPA is thought to be a sensory interneuron homologous to dorsolateral commissural (dlc) sensory interneurons of *xenopus* (Li et al., 2003; Roberts and Sillar, 1990; Saint-Amant, 2010) as they are both contacted by sensory RB neurons (Easley-Neal et al., 2013; Li et al., 2003; Pietri et al., 2009) and receive strong, shunting inhibition during evoked activity (Pietri et al., 2009; Sillar & Roberts, 1992). The role of the CoPA in spontaneous behavior is therefore likely in the response to inhibition rather than in triggering coils.

Our recordings of spontaneous activity in embryonic CiDs showed that, like MNs, these neurons receive synaptic glutamatergic activity at this time as well as electrical and glycinergic inputs that often reached threshold and resulted in the firing of several action potentials. Furthermore, CiDs showed activity patterns similar to mixed events in the ipsilateral MN and also fired action potentials during fictive double coiling, suggesting that they play an important role in this behavior. CiDs may be forming some of the earliest glutamatergic connections in the spinal cord. At 24 hpf, chx10+ cells (of which the CiD are the majority) are present at a density of 2 - 3 cells per hemisegment and virtually all of these cells are positive for vglut2 at 32 hpf, the earliest time point examined (Kimura et al., 2006). Our mosaic labeling of syp:GFP-DSR in chx10+ cells showed that CiDs may be forming functional glutamatergic synapses as early as 24 hpf onto MNs and other CiDs. Recent functional imaging studies using expression of a synaptophysin-GCaMP fusion protein have shown that calcium transients are seen at these puncta, suggesting that they are indeed functional presynaptic release sites (Menelaou et al., 2013; Nikolaou et al., 2012). These putative synaptic sites clearly colocalized with the soma of ipsilateral caudal MNs and CiDs and may be responsible for some of the glutamatergic synaptic events seen as early as 24 hpf in our voltage-clamp recordings from CiDs and MNs.

In summary, spontaneous coiling in the embryo starts in an environment in which only gap junctions are present, creating a network of electrically coupled neurons which can only propagate slow waves of activity. As the circuit matures, chemical synapses first add to the existing circuit without modifying the behavior too much, as we have shown with the transition from single to double coils. As development proceeds, the waning influence of gap junctions on circuit activity may lead to an opening for chemical synapses to finely sculpt

local motor circuitry into producing faster and more intricate motor behaviors such as swimming.

II.6. REFERENCES

Batista MF, Jacobstein J, Lewis KE (2008) Zebrafish V2 cells develop into excitatory CiD and Notch signalling dependent inhibitory VeLD interneurons. Dev Biol 322:263-275.

Ben-Ari Y(2002) Excitatory actions of gaba during development: the nature of the nurture. Nat Rev Neurosci 3:728–739.

Bennett MVL, Zukin RS (2004) Electrical coupling and neuronal synchronization in the mammalian brain. Neuron 41:495-511.

Bernhardt RR, Chitnis AB, Lindamer L, Kuwada JY (1990) Identification of spinal neurons in the embryonic and larval zebrafish. J Comp Neurol 302:603-616.

Blankenship AG, Feller MB (2010) Mechanisms underlying spontaneous patterned activity in developing neural circuits. Nat Rev Neurosci 11:18-29.

Buss RR, Drapeau P (2001) Synaptic drive to motoneurons during fictive swimming in the developing zebrafish. J Neurophysiol 86:197-210.

Chong M, Drapeau P (2007) Interaction between hindbrain and spinal networks during the development of locomotion in zebrafish. Dev Neurobiol 67:933-947.

Corner M (1978) Spontaneous motor rhythms in early life--phenomenological and neurophysiological aspects. Prog Brain Research 48:349-366.

Côté S, Drapeau P (2012) Regulation of spinal interneuron differentiation by the paracrine action of glycine. Dev Neurobiol 72:208-214.

Cui WW, Saint-Amant L, Kuwada JY (2004) shocked gene is required for the function of a premotor network in the zebrafish CNS. J Neurophysiol 92:2898 –2908.

Cui WW, Low SE, Hirata H, Saint-Amant L, Geisler R, Hume RI, Kuwada JY (2005) The zebrafish shocked gene encodes a glycine transporter and is essential for the function of early neural circuits in the CNS. J Neurosci 25:6610–6620.

Dale N (1995) Experimentally derived model for the locomotor pattern generator in the Xenopus embryo. J Physiol (Lond) 489:489 –510.

Downes GB, Granato M (2006) Supraspinal input is dispensable to generate glycine-mediated locomotive behaviors in the zebrafish embryo. J Neurobiol 66:437-451.

Drapeau P, Ali DW, Buss RR, Saint-Amant L (1999) In vivo recording from identifiable neurons of the locomotor network in the developing zebrafish. J Neurosci Methods 88:1-13.

Easley-Neal C, Fierro J, Buchanan J, Washbourne P (2013) Late recruitment of synapsin to nascent synapses is regulated by Cdk5. Cell Reports 3:1199-1212.

Feller MB (1999) Spontaneous correlated activity in developing neural circuits. Neuron 22:653-656.

García-Colunga J, Miledi R (1999) Modulation of nicotinic acetylcholine receptors by strychnine. Proc Natl Acad Sci USA 96:4113-4118.

Grillner S, Jessell TM (2009) Measured motion: searching for simplicity in spinal locomotor networks. Curr Opin Neurobiol 19:572-586.

Grillner S, Wallen P, Brodin L, Lansner A (1991) Neuronal network generating locomotor behavior in lamprey. Annu Rev Neurosci 14:169-199.

Hale ME, Ritter Da, Fetcho JR (2001) A confocal study of spinal interneurons in living larval zebrafish. J Comp Neurol 437:1-16.

Hamburger V (1963) Some aspects of the embryology of behavior. Quart Rev Biol 38:342-365.

Higashijima S-I, Schaefer M, Fetcho JR (2004) Neurotransmitter properties of spinal interneurons in embryonic and larval zebrafish. J Comp Neurol 480:19-37.

Kimmel CB, Ballard WW, Kimmel SR, Ullmann B, Schilling TF (1995) Stages of embryonic development of the zebrafish. Dev Dyn 203:253-310.

Kimura Y, Okamura Y, Higashijima S-I (2006) alx, a zebrafish homolog of Chx10, marks ipsilateral descending excitatory interneurons that participate in the regulation of spinal locomotor circuits. J Neurosci 26:5684-5697.

Kimura Y, Satou C, Fujioka S, Shoji W, Umeda K, Ishizuka T, Yawo H, Higashijima S-I (2013) Hindbrain V2a neurons in the excitation of spinal locomotor circuits during zebrafish swimming. Curr Biol 23:843-849.

Knogler LD, Liao M, Drapeau P (2010) Synaptic scaling and the development of a motor network. J Neurosci 30:8871-8881.

Li W-C, Soffe SR, Roberts A (2003) The spinal interneurons and properties of glutamatergic synapses in a primitive vertebrate cutaneous flexion reflex. J Neurosci 23:9068-9077.

Low SE, Ryan J, Sprague SM, Hirata H, Cui WW, Zhou W, Hume RI, Kuwada JY, Saint-Amant L (2010) touché Is required for touch-evoked generator potentials within vertebrate sensory neurons. J Neurosci 30:9359-9367.

McDearmid JR, Drapeau P (2006) Rhythmic motor activity evoked by NMDA in the spinal zebrafish larva. J Neurophysiol 95:401-417.

Menelaou E, VanDunk C, McLean DL (2013) Differences in spinal V2a neuron morphology reflect their recruitment order during swimming in larval zebrafish. J Comp Neurol 522: 1232-1248.

Meyer MP, Smith SJ (2006) Evidence from in vivo imaging that synaptogenesis guides the growth and branching of axonal arbors by two distinct mechanisms. J Neurosci 26:3604-3614.

Narayanan CH, Fox MW, Hamburger V (1971) Prenatal development of spontaneous and evoked activity in the rat (Rattus norvegicus albinus). Behavior 40:100-134.

Nikolaou N, Lowe AS, Walker AS, Abbas F, Hunter PR, Thompson ID, Meyer MP (2012) Parametric functional maps of visual inputs to the tectum. Neuron 76:317-324.

O'Donovan MJ (1999) The origin of spontaneous activity in developing networks of the vertebrate nervous system. Curr Opin Neurobiol 9:94-104.

Pietri T, Manalo E, Ryan J, Saint-Amant L, Washbourne P (2009) Glutamate drives the touch response through a rostral loop in the spinal cord of zebrafish embryos. Dev Neurobiol 69:780-795.

Roberts A, Sillar KT (1990) Characterization and function of spinal excitatory interneurons with commissural projections in *Xenopus laevis* embryos. Eur J Neurosci 2:1051-1062.

Saint-Amant L (2006) Development of motor networks in zebrafish embryos. Zebrafish 3:173-190.

Saint-Amant L (2010) Development of motor rhythms in zebrafish embryos. Prog Brain Res 187:47– 61.

Saint-Amant L, Drapeau P (1998) Time course of the development of motor behaviors in the zebrafish embryo. J Neurobiol 37:622-632.

Saint-Amant L, Drapeau P (2000) Motoneuron activity patterns related to the earliest behavior of the zebrafish embryo. J Neurosci 20:3964-3972.

Saint-Amant L, Drapeau P (2001) Synchronization of an embryonic network of identified spinal interneurons solely by electrical coupling. Neuron 31:1035-1046.

Sillar KT, Roberts A (1992) Phase-dependent modulation of a cutaneous sensory pathway by glycinergic inhibition from the locomotor rhythm generator in *Xenopus* embryos. Eur J Neurosci 4:1022-1034.

Tong H, McDearmid JR (2012) Pacemaker and plateau potentials shape output of a developing locomotor network. Curr Biol 22:2285-2293.

van Mier P, Armstrong J, Roberts A (1989) Development of early swimming in *Xenopus laevis* embryos: Myotomal musculature, its innervation and activation. Neuroscience 32:113-126.

II.7. FIGURES

FIGURE 1

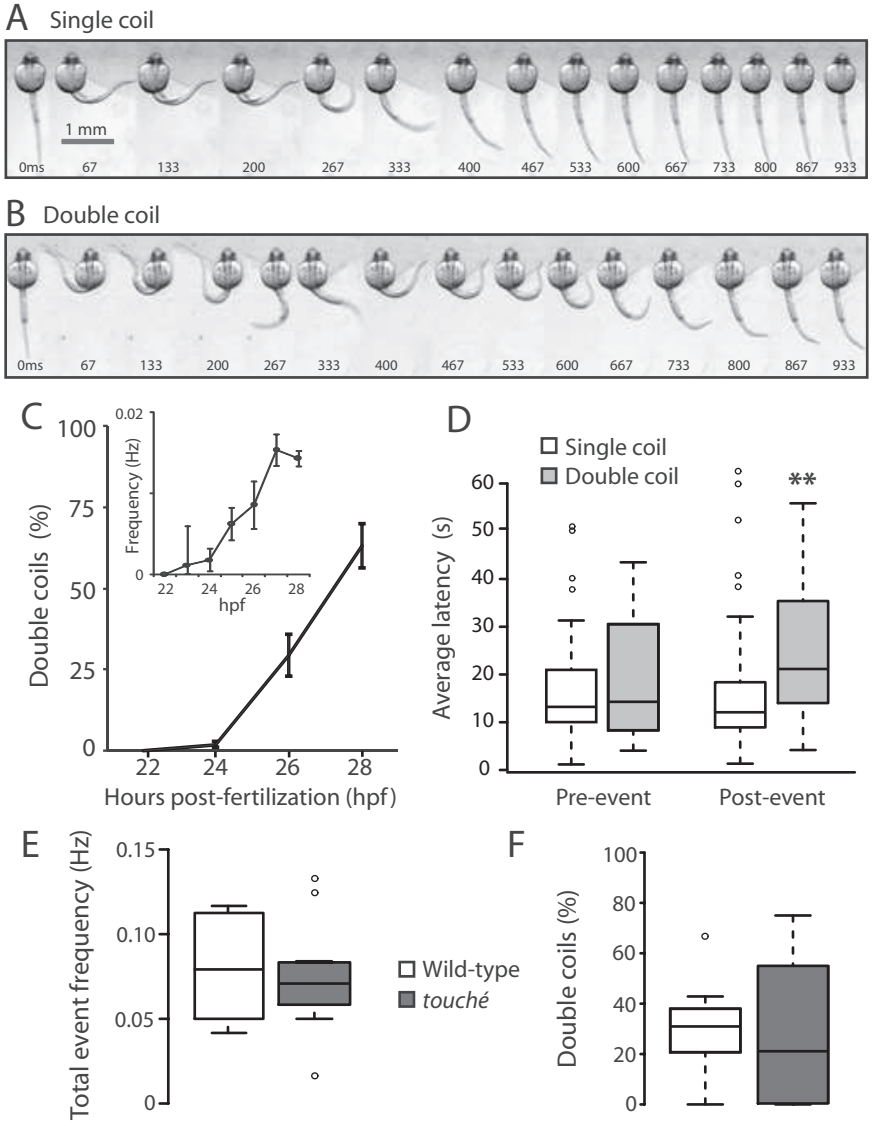

Figure 1. Double coiling appears during embryonic development and depresses network activity. A) Still images taken at 67 ms intervals from a video recording of an agarose-embedded 26 hpf embryo exhibiting a spontaneous single coil and B) a double coil. Due to the embedding medium surrounding the head, the tail does not come into direct contact with the head in these images as it would in a non-immobilized embryo. Scale bar in A is same as

for B. C) The relative percentage (%) of double coils in freely moving wild-type embryos at 22, 24, 26 and 28 hpf (N = 30); inset shows the mean frequency of double coiling over the same period of time. D) Average latency, or time inactive, for a single coil (open bars) and a double coil (grey bars) in 26 hpf embryos before (left, Pre-event) and after (right, Post-event) (N = 30). E) Box plot showing the total event frequency and F) the percentage of double coils at 26 hpf in touché mutants (dark grey bars) and wild-type siblings (white bars). $N_{ctrl} = 12$, $N_{touché} = 12$.

FIGURE 2

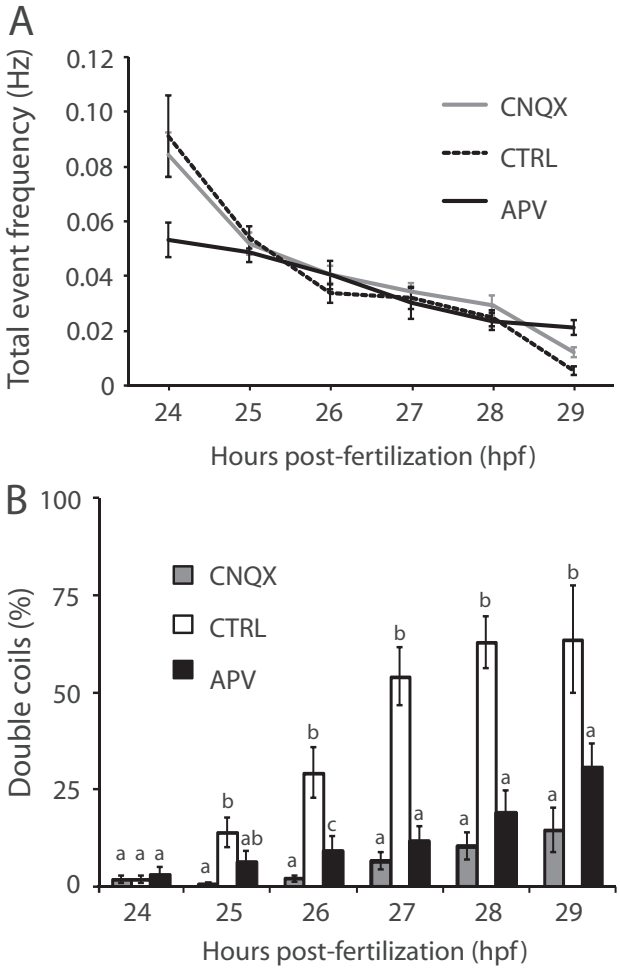

Figure 2. Glutamatergic neurotransmission is required for double coiling. A) Overall event frequency is unaffected by glutamate receptor antagonists. B) The relative proportion of double coils (%) is significantly decreased following CNQX (grey bars) or APV treatment (black bars). Means that are not sharing a letter are significantly different. Error bars represent SE. $N_{control} = 32$, $N_{CNQX} = 43$, $N_{APV} = 41$.

FIGURE 3

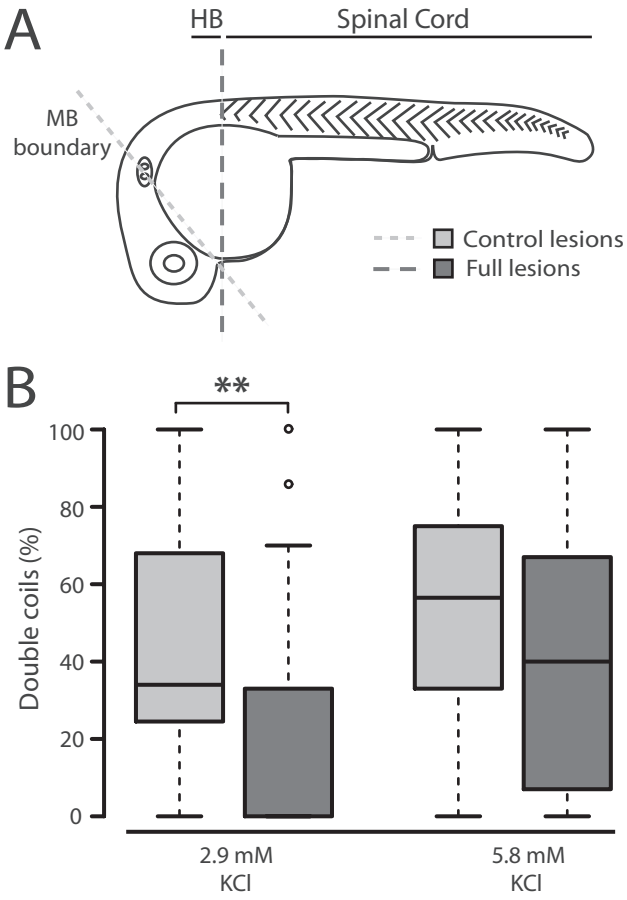

Figure 3. Double coils require a descending excitatory drive from the hindbrain. A) Diagram depicting the site of control lesions at the midbrain (MB) boundary to leave the hindbrain (HB) intact and full lesions at the caudal hindbrain to isolate the spinal cord. B) Box plot showing the proportion of double coils at 26 hpf in control (grey bars) and fully lesioned embryos (dark bars) in normal 2.9 mM KCl (left, $N_{ctrl} = 32$, $N_{lesion} = 41$) and elevated 5.8 mM KCl (right, $N_{ctrl} = 22$, $N_{lesion} = 25$).

FIGURE 4

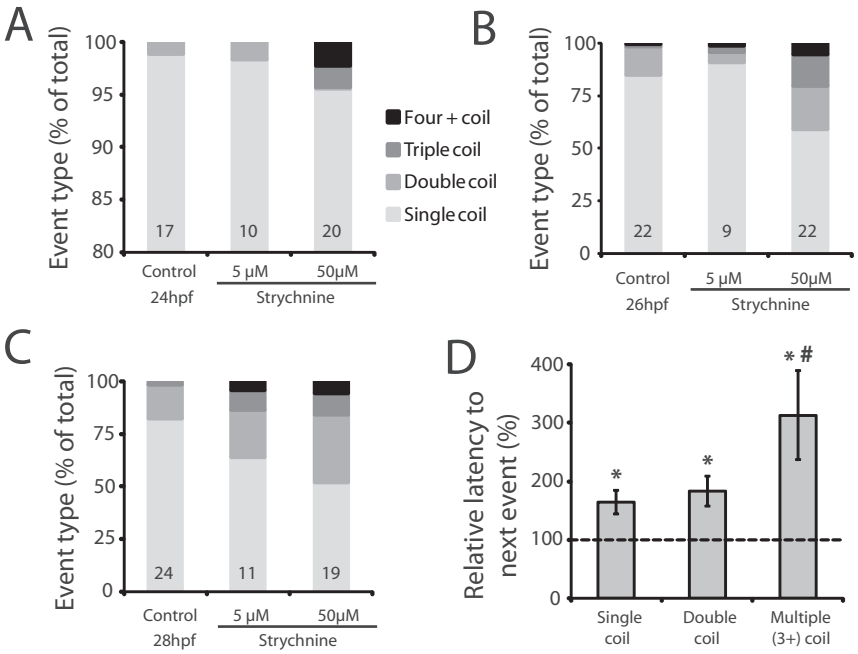

Figure 4. Decreased glycinergic signaling results in an increase in multiple coiling. Relative percentage of spontaneous events showing single, double, triple and four and more (four +) coils in embryos treated with strychnine and untreated controls at A) 24 hpf, B) 26 hpf and C) 28 hpf. Note the expanded Y-axis scale in A). Numbers at the base refer to the numbers of embryos in each condition. D) Average latencies in strychnine-treated 28 hpf embryos following a single, double, or multiple (three or more) coil as normalized to single coil latency in control embryos (dashed line). $N_{ctrl} = 22$, $N_{strychnine} = 31$; * $p < 0.05$ compared to control; # $p < 0.05$ within strychnine-treated embryos.

FIGURE 5

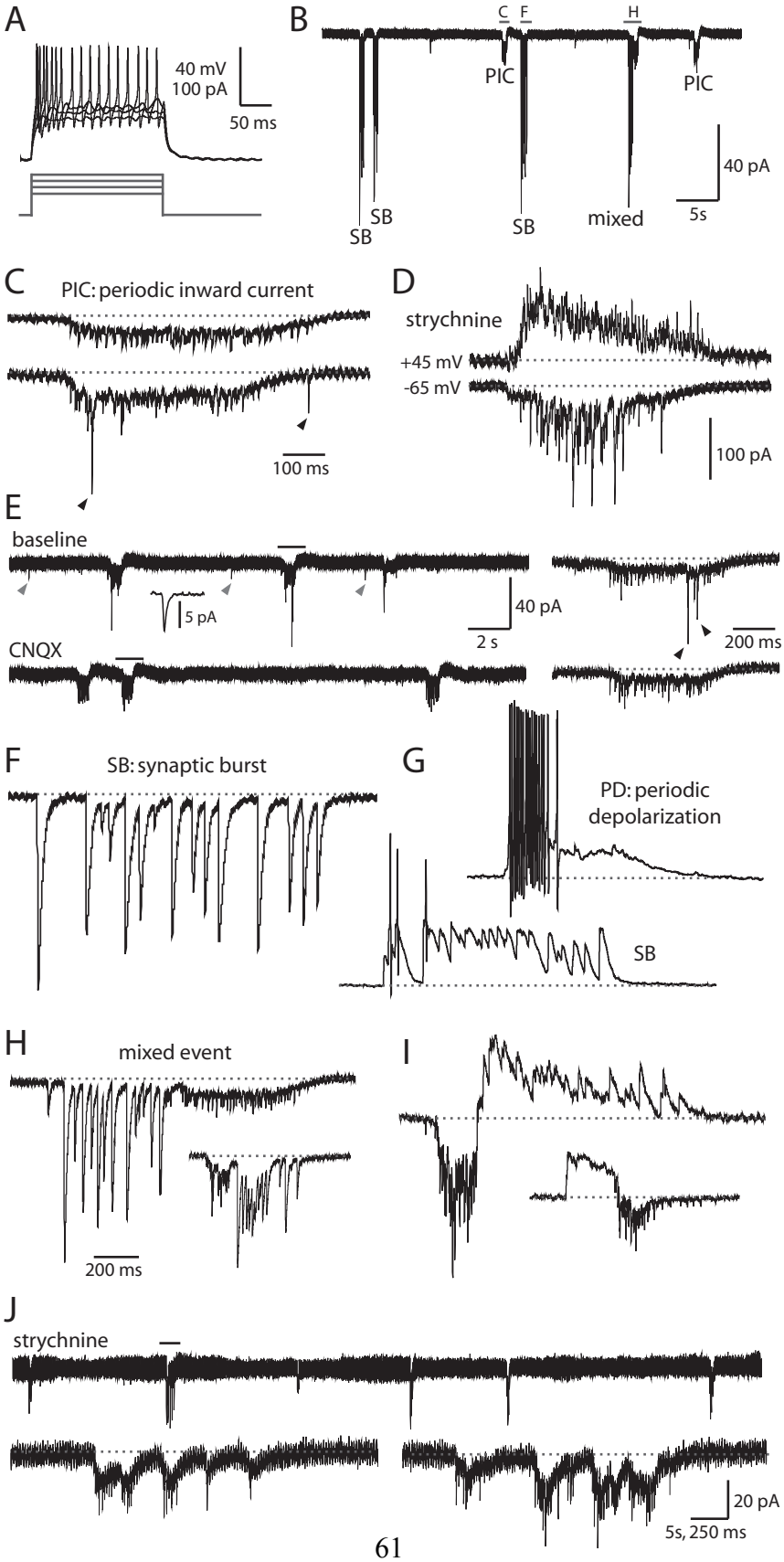
A
40 mV
100 pA
50 ms
B
C F
H
PIC
PIC
40 pA
5s
SB
SB
SB
mixed
C
PIC: periodic inward current
100 ms
D
strychnine
+45 mV
-65 mV
100 pA
E
baseline
5 pA
40 pA
2 s
200 ms
CNQX
F
SB: synaptic burst
G
PD: periodic
depolarization
SB
H
mixed event
200 ms
I
J
strychnine
20 pA
5s, 250 ms

Figure 5. Motoneurons show mixed electrical and synaptic events corresponding to glutamate-dependent fictive double coils. A) Representative current injections showing burst firing of action potentials in embryonic MNs. Upper panel, current-clamp recording from neurons, lower panel, current steps. B) Patterned activity in a 25 hpf embryo includes gap junction-driven periodic inward currents (PIC), synaptic bursts (SB) and mixed events. Holding potential in this trace and all others is -65 mV (unless otherwise indicated). Events in the indicated region are expanded in panels C, F and H. C) PICs are low amplitude inward currents produced by the electrical coupling of neurons that often coincide with synaptic glutamatergic events. Upper trace, a PIC (from region indicated in B) that shows no glutamatergic peaks. Lower trace, a PIC in the same MN that does show synaptic glutamatergic events (arrowheads). Baseline is shown as a dotted grey line for reference in this and subsequent figures. Vertical scale same as for B but note different time scale. D) Examples of PICs under voltage-clamp seen in an older embryo (27 hpf) with glutamatergic events of increased amplitude and frequency. These recordings were done in the presence of 5 μM strychnine. Some of the currents are reversed at a positive holding potential of +45 mV (upper trace) compared to a normal holding potential (-65 mV, lower trace), corresponding to purely glutamatergic events. Time scale same as in C but note difference vertical scale. E) Excerpt from a voltage-clamp recording in a 26 hpf embryo showing three examples of PICs at baseline (left, upper trace) and in the presence of 10 μM CNQX (left, lower trace). Small amplitude peaks occurring between events resembling glutamatergic mEPSCs are highlighted with grey arrowheads and an average of several peaks (n = 19) is shown in the inset at a hundred times expanded timescale. Regions indicated with a black bar are shown on a ten times expanded timescale at the right for each condition. Glutamatergic peaks occurring during a PIC are indicated with black arrowheads. F) Synaptic bursts (from region indicated in B) are strychnine-sensitive (see text) glycinergic currents of large amplitude with a similar duration to PICs. G) Representative whole-cell current-clamp recordings from a primary MN in a 26 hpf embryo. Resting membrane potential of the neuron is -60 mV, scale same as in C. Upper trace, a spontaneous periodic depolarization (PD) triggers burst firing of action potentials. Lower trace, a glycinergic synaptic burst (SB) can also trigger action potentials. H) Representative whole-cell voltage-clamp recordings of a mixed events (upper trace from

region indicated in B) during which a PIC (with or without glutamatergic peaks) and a SB occur in close (sub-second) succession in either order. Vertical scale for uppermost trace same as in B but note different time scale. Inset is scaled down by 50%. I) Examples of mixed events from the same MN as in G under voltage-clamp at an intermediate holding potential of -20 mV (more positive than the chloride reversal potential of approximately -35 mV) showing that glycinergic currents but not electrical and glutamatergic currents are reversed. Scale for upper trace and inset same as for H. J) Upper trace, a 100 second excerpt of a MN voltage-clamp recording in a 26 hpf embryo in the presence of 5 μM strychnine showing that glycinergic synaptic bursts are absent but gap junction-driven PICs remain. Lower trace, left, is expanded from the region indicated in the upper trace and is an example of an event with many PICs occurring closely together in time and resembling a fictive multiple coil. Lower trace, right, is an example from a different MN.

FIGURE 6

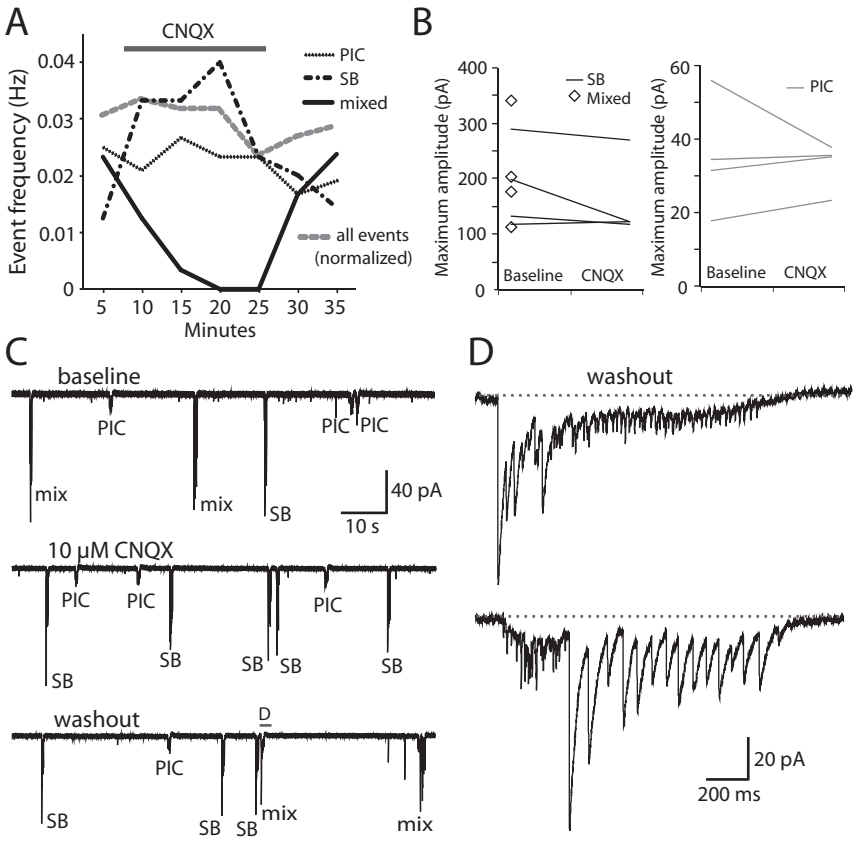

Figure 6. Blockade of glutamatergic neurotransmission abolishes mixed events in motoneurons but not SBs or PICs. A) Average frequency of each type of event as well as the total (normalized) event frequency during a representative whole-cell recording (N = 4) in which 10 µM of CNQX was washed into and out of the extracellular recording solution. B) The average maximum amplitudes of SBs and mixed events (left) and PICs (right) at baseline are not significantly changed by the presence of CNQX. Amplitude of mixed events is not given for the CNQX condition because these events were rare or absent. Maximum amplitude of PICs at baseline ignored glutamatergic peaks. C) Excerpts of voltage-clamp recordings from the experiment in A showing the presence of mixed events at baseline (upper trace), the selective loss of mixed events following the addition of CNQX (middle trace) and their subsequent recovery following CNQX washout (lower trace). D) Representative mixed events following CNQX washout. The upper trace is from the region indicated in the washout recording in C and the lower trace is from the same MN.

FIGURE 7

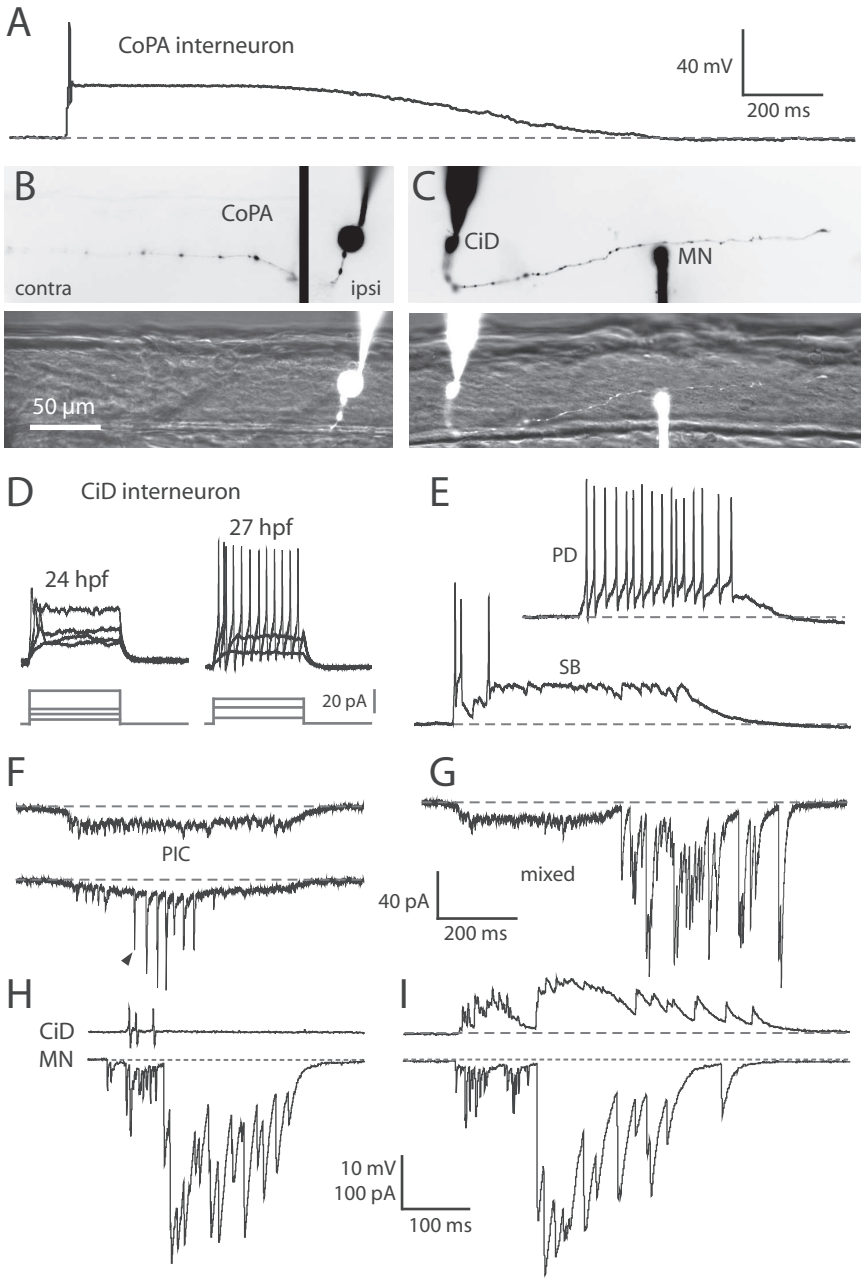

Figure 7. Glutamatergic CiD interneurons are highly active at early embryonic stages and in contrast to CoPAs fire bursts of action potentials during spontaneous behaviors. A) Representative whole-cell current-clamp recording from a CoPA neuron showing a long duration depolarizing plateau event that often triggers an action potential at the onset. Resting

membrane potential of the neuron is -60 mV. Baseline is shown as a dashed grey line for reference in all traces. B) Example of a filled CoPA following a whole-cell recording. The upper image shows the inverted fluorescent image of the rhodamine-filled ipsilateral cell body (right, ipsi) merged with the filled ascending contralateral axon (left, contra). The lower image shows the filled CoPA (ipsilateral plane only) in fluorescence against the spinal cord in brightfield. Rostral is to the left and dorsal is to the top (the same for all subsequent figures). C) Example of filled neurons from a simultaneous whole-cell recording of a CiD and ipsilateral MN. The upper image shows the inverted fluorescent image of rhodamine-filled cells and the descending ipsilateral CiD axon (the ventral MN axon is obscured by the recording electrode). The lower image shows the filled cell bodies in fluorescence against the spinal cord in brightfield. Scale bar same as in B. D) Representative current injections showing single versus burst firing of action potentials in CiD neurons at 24 hpf (left) and 27 hpf (right), respectively. In each set, upper traces are current-clamp recording from neurons and lower traces are current steps. Scale for upper traces same as in A. E) Representative whole-cell current-clamp recordings from a CiD neuron. Resting membrane potential of the neuron is -60 mV, scale same as in A. Upper trace, a spontaneous periodic depolarization (PD) triggers burst firing of action potentials in a 27 hpf embryo. Lower trace, a glycinergic synaptic burst (SB) can also trigger action potentials. F) Examples of PICs seen under voltage-clamp in a CiD. Upper trace, a PIC that shows no glutamatergic peaks. Lower trace, a PIC from the same CiD that does show synaptic glutamatergic events (arrowhead indicates the first of several). Holding potential is -65 mV, scale shown in G. G) Representative example of a mixed event seen under voltage-clamp in a CiD. H) Simultaneous recordings from a 28 hpf embryo of a CiD (cell-attached mode, top trace) and a MN (voltage-clamp, bottom trace) during fictive double coiling. I) Whole cell voltage-clamp recording from the same pair of neurons as in H to show the similar patterning of activity during fictive double coiling. Holding potential is +20 mV in the upper trace.

FIGURE 8

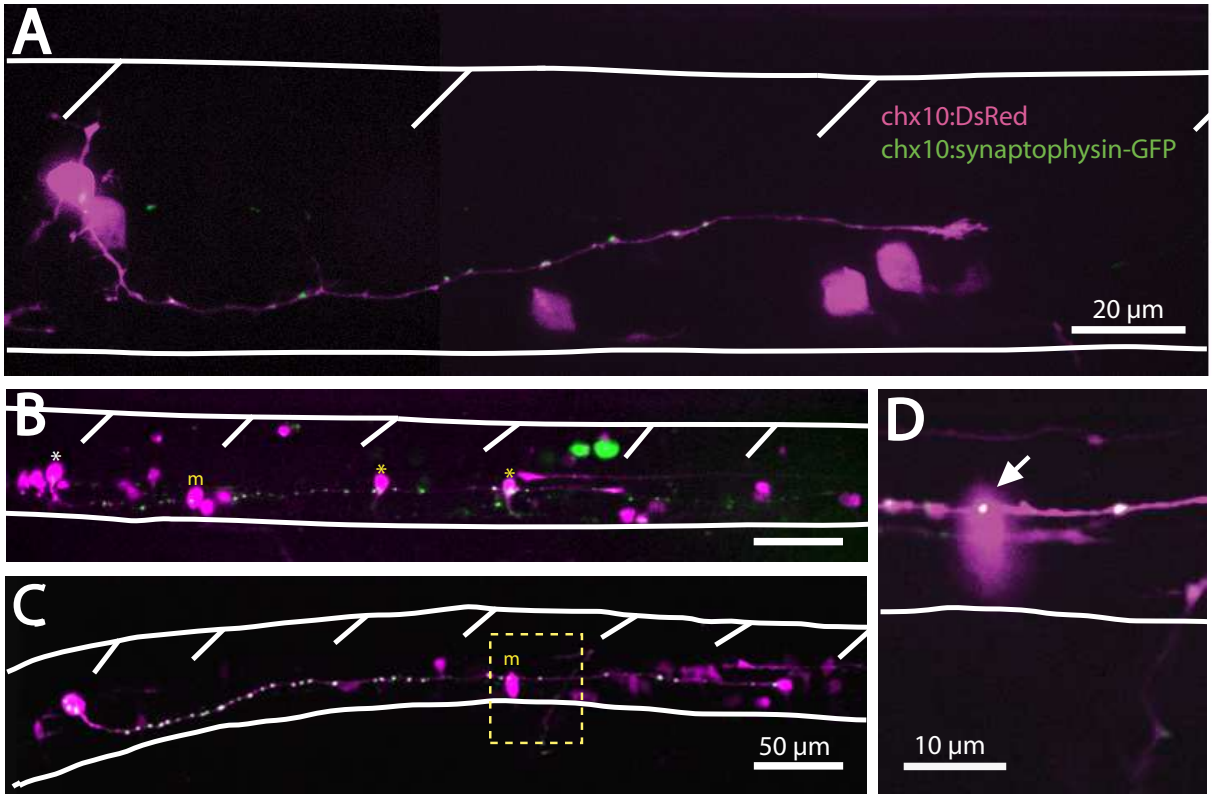

Figure 8. Embryonic spinal CiD neurons have putative synapses that contact caudal primary MNs and other CiDs. A) Representative example of a DsRed-expressing CiD neuron in a 24 hpf embryo with distinct synaptophysin-GFP puncta along the length of the axon. Spinal cord and somite boundaries are outlined in white. B) A CiD neuron (white asterisk) in a 27 hpf embryo has an axon spanning four somites and synaptophysin-GFP puncta that contact caudal CiDs (yellow asterisks) as well as a primary MN (yellow m). Scale bar same as for C. C) A rostral CiD neuron in a 28 hpf embryo has an axon spanning 5-6 somites and contacts a primary MN (arrow). D) High resolution single 1 µm confocal plane showing the putative synaptic contact (arrow) between the CiD and MN from the boxed area in C).

CHAPTER 3

III. ARTICLE: "SENSORY GATING OF AN EMBRYONIC ZEBRAFISH INTERNEURON DURING SPONTANEOUS MOTOR BEHAVIORS"

Frontiers in Neural Circuits (2014), 8:121.

LINKER STATEMENT

The following study sought to explain how zebrafish embryos avoid activating the touch reflex in response to their own spontaneous movements. Work from our previous study (Knogler et al., 2014) and others showed that embryos are highly spontaneously active, therefore we hypothesized that spinal circuits must be organized in such a way that neurons in the somatosensory pathway responded exclusively to external touch. Here, I performed whole-cell electrophysiological recordings from a sensory interneuron that receives excitatory inputs from sensory neurons carrying information about light touch. This study reveals a simple mechanism whereby activation of the locomotor CPG sends a corollary discharge signal to inhibit sensory interneurons during spontaneous and ongoing movement. This study provides important insight into how sensory feedback controls and is controlled by the locomotor CPG.

Sensory gating of an embryonic zebrafish interneuron during spontaneous motor behaviors

Laura D. Knogler and Pierre Drapeau*

Departments of Pathology and Cell Biology and of Neuroscience, CRCHUM and GRSNC, Université de Montréal, Montréal, Québec, H2X 0A9, Canada

Abbreviated title: Sensory gating during embryonic motor behaviors

*Corresponding author: Pierre Drapeau, Ph.D.
CRCHUM R09.482
900, rue Saint-Denis
Montréal QC, H2X 0A9 Canada

Acknowledgements:
This work was supported by a doctoral fellowship from the FRQS to L. Knogler and grants from the FRQS-GRSNC, CIHR and NSERC to P. Drapeau. Thanks to J. Ryan for helpful discussions and to J.C. Lacaille and D. Bowie for reagents.

Conflict of interest: The authors declare no competing financial interests.

III.1. ABSTRACT

In all but the simplest monosynaptic reflex arcs, sensory stimuli are encoded by sensory neurons that transmit a signal *via* sensory interneurons to downstream partners in order to elicit a response. In the embryonic zebrafish (*Danio rerio*), cutaneous Rohon-Beard (RB) sensory neurons fire in response to mechanical stimuli and excite downstream glutamatergic CoPA (commissural primary ascending) interneurons to produce a flexion response contralateral to the site of stimulus. In the absence of sensory stimuli, zebrafish spinal locomotor circuits are spontaneously active during development due to pacemaker activity resulting in repetitive coiling of the trunk. Self-generated movement must therefore be distinguishable from external stimuli in order to ensure the appropriate activation of touch reflexes. Here, we recorded from CoPAs during spontaneous and evoked fictive motor behaviors in order to examine how responses to self-movement are gated in sensory interneurons. During spontaneous coiling, CoPAs received glycinergic inputs coincident with contralateral flexions that shunted firing for the duration of the coiling event. Shunting inactivation of CoPAs was caused by a slowly deactivating chloride conductance that resulted in lowered membrane resistance and increased action potential threshold. During spontaneous burst swimming, which develops later, CoPAs received glycinergic inputs that arrived in phase with excitation to ipsilateral motoneurons and provided persistent shunting. During a touch stimulus, short latency glutamatergic inputs produced cationic currents through AMPA receptors that drove a single, large amplitude action potential in the CoPA before shunting inhibition began, providing a brief window for the activation of downstream neurons. We compared the properties of CoPAs to those of other spinal neurons and propose that glycinergic signalling onto CoPAs acts as a corollary discharge signal for reflex inhibition during movement.

Keywords: Sensory interneurons, zebrafish, spinal cord, spontaneous behavior, glycine receptors, AMPA receptors, corollary discharge, reflex inhibition

III.2. INTRODUCTION

Early embryonic circuits must be capable of responding to sensory stimuli in order to perform essential motor behaviors such as avoiding predation. Additionally, sensorimotor circuits must be organized in such a way that the animal's own movement is distinguishable from movement in the environment in order to make computations regarding expected and novel sensory feedback. One way in which the nervous system compensates for self-movement is to send corollary discharge signals from motor-related pathways to modulate activation of sensory pathways (reviewed by Crapse & Sommer, 2008). Corollary discharges may target different parts of the sensory pathway and use diverse mechanisms to alter sensory function depending on the species and the modality being studied. The embryonic vertebrate spinal cord provides a simplified neural network within which to study the modulation of sensory pathways that ensure the appropriate activation of sensorimotor behaviors.

A simple disynaptic spinal reflex arc has been described for a contralateral flexion response in hatchling *xenopus* (Li et al., 2003). Following a touch to the skin, one or more Rohon-Beard (RB) sensory neurons strongly activate glutamatergic dorsolateral commissural (dlc) sensory interneurons which in turn excite premotor interneurons and motoneurons, leading to a contraction of the contralateral trunk away from the stimulus followed by escape swimming. Immediately following dlc interneuron excitation, glycinergic corollary discharges arrive in phase with excitation to ipsilateral motoneurons to provide sustained inhibition to the dlc interneuron during swimming (Li et al., 2002; Li et al., 2004; Sillar & Roberts, 1988; Soffe, 1993). The relative abundance of AMPA and NMDA receptors in different neuronal classes within the circuit also contributes to the proper activation of this reflex pathway (Li et al., 2003).

In the zebrafish spinal cord, commissural primary ascending (CoPA) interneurons are one of the earliest born cells and extend long axons that span more than ten somites rostrally by 26 hours post-fertilization (hpf) (Bernhardt et al., 1990), prior to hatching on day two. CoPAs are thought to be homologous to *xenopus* dlc interneurons due to their similarly large dorsal soma, ascending commissural axonal projections and glutamatergic identities (Bernhardt et al., 1990; Higashijima et al., 2004a). In addition, embryonic CoPAs are contacted by RB sensory neurons (Easley-Neal et al., 2013) and following a response to touch

at 24 hpf receive short latency excitation followed by a long duration glycine-mediated conductance that is thought to inhibit activation (Pietri et al., 2009). Based on these results, zebrafish CoPAs are predicted to be sensory interneurons that carry the initial excitation to the contralateral spinal cord during evoked behaviors, as dlc interneurons do in *xenopus*. However, very little is known about the intrinsic and synaptic properties of CoPAs and their pattern of activation during spontaneous behaviors such as coiling and swimming.

We hypothesized that CoPAs must be selectively inhibited during early spontaneous coiling and later swimming behaviors in order to prevent the ongoing activation of the touch reflex during spontaneous movement. To test this idea, we targeted embryonic CoPA interneurons for electrophysiological recordings in order to investigate their intrinsic and synaptic properties in the context of spontaneous and touch-evoked behaviors. In particular, we looked for activation patterns and receptor properties of CoPAs that could contribute to their specialized role in gating somatosensory activation of a reflex pathway. We show that inhibitory corollary discharges onto CoPA interneurons combined with the presence of a rare glycine conductance with slow kinetics contribute to the inhibition of the somatosensory pathway during early spontaneous behaviors. These findings are compared to results from other vertebrates as well as invertebrates in order to determine general features of sensory gating in spinal circuits.

III.3. MATERIALS AND METHODS

III.3.1. Zebrafish maintenance

Tübingen wildtype strains of adult zebrafish were maintained according to guidelines approved by the Animal Experimentation Ethics Committee, Université de Montréal. Staging of embryos (of as yet undetermined sex) was performed as previously described (Kimmel et al., 1995).

III.3.2. Electrophysiology and pharmacology

Zebrafish embryos were dechorionated and anesthetized in 0.02% tricaine dissolved in Evans solution (134mM NaCl, 2.9mM KCl, 2.1mM CaCl2, 1.2 mM MgCl2, 10 mM glucose,

10 mM HEPES, pH 7.8 with NaOH) and dissected according to previously described procedures (Drapeau et al., 1999). Briefly, spinal neurons in somites 5 –15 were selected for recording based on their soma size and position as visualized by oblique illumination (Olympus BX61W1). To record spontaneous activity, 15 μM D-tubocurarine was added to the Evans solution to block neuromuscular transmission. To stimulate a touch response, a glass electrode connected to a picospritzer (Parker Hannifin, Fairfield, NJ) squirted bath solution near the tip of the tail at the desired pressure and duration (5-10 psi, 4-20 ms).

Electrophysiological recordings were done in the presence of 1-10 μM strychnine to block glycine receptors, in 7-10 μM 6-cyano-7-nitroquinoxaline-2,3-dione (CNQX) to block AMPA receptors, or in 50 μM (2R)-amino-5-phosphonovaleric acid (APV) to block NMDA receptors. 0.5-1 μM tetrodotoxin (TTX) was used to block evoked activity when recording miniature post-synaptic currents. Patch-clamp electrodes for spinal neuron recordings (6–14 MΩ) were pulled from borosilicate glass and were filled with the following intracellular solution (in mM): 105 D-gluconic acid, 16 KCl, 2 MgCl2, 10 HEPES and 10 EGTA, adjusted to pH 7.2, 290 mOsm (Drapeau et al., 1999). Sulforhodamine B (0.1%) was also included in the patch solution to label the cells and confirm their identity after a recording. Filled CoPAs had a triangular soma and distinctive dendrites that distinguished them from otherwise morphologically similar CoSAs. Recordings from cells whose identity was ambiguous were not included in subsequent analyses. 4 mM QX-314 was added to the intracellular solution in some experiments to block voltage-gated sodium channels. All drugs were obtained from Sigma (St. Louis).

Standard single and dual whole-cell recordings from 24 - 29 hpf larvae were obtained using an Axopatch 200B and a Molecular Devices CV 203BU headstage amplifier (Molecular Devices). Data were acquired at 40 kHz and low-pass filtered at 10 kHz. Cells were held near their resting potential at -65 mV under voltage clamp unless otherwise specified. A maximum of three neural recordings were obtained from each embryo. Electrophysiological analyses were performed offline using Clampex 10.2 and Clampfit 10.2 software (Molecular Devices). The recordings were not analyzed if the resting membrane potential was more positive than -40 mV or if the input resistance was below 500 MΩ. Following each recording, a series of fluorescent images of the rhodamine-filled cell and its axonal projections as well as bright-

field images were collected with a QImaging camera (model 1394, QImaging Corp. Canada) using Micro-Manager software (http://www.micro-manager.org/). Images were inverted and brightness/contrast was adjusted using Adobe Photoshop CS2 (Adobe Systems, Inc., San Jose, CA, USA).

III.3.3. Statistical analyses

SPSS 21 (IBM) was used to assess data for statistical significance. All data sets were initially assessed for normality with the Shapiro-Wilk Test. For independent data sets with only two groups we used the Students' T-test or Mann-Whitney U test and for data from multiple groups we used a one-way ANOVA with Tukey's post-hoc test to look for differences between conditions ($p < 0.05$). In data obtained from the same group under different conditions, the paired-samples T-test or repeated-measures variation of ANOVA was used. A Pearson statistic or Spearman rank rho was used to assess correlations for parametric or non-parametric data, respectively. Statistical significance is represented in the graphs as *** for $p < 0.001$, ** for $p < 0.01$ and * for $p < 0.05$ and individual p-values and numbers of embryos per condition are provided in figure legends and the text. Error bars in bar graphs indicate the standard error and results are described as the mean ± standard error. Excel was used to create all graphs except the box plots, which were created online using the BoxPlotR application (http://boxplot.tyerslab.com/). In these plots, box limits indicate the 25th and 75th percentiles as determined by R software, center lines show the medians, whiskers extend 1.5 times the interquartile range from the 25th and 75th percentiles and outliers are represented by open circles.

III.4. RESULTS

III.4.1. Intrinsic properties of embryonic CoPA interneurons are similar to other spinal neurons

We performed whole-cell patch clamp recordings in CoPA neurons in 24 - 29 hpf embryos under current clamp conditions in order to characterize their intrinsic spiking properties and input resistances over this period of development. At 24 - 25 hpf, depolarizing

current steps of increasing amplitude failed to elicit more than one action potential in the CoPA at the current onset (Fig. 1A, B; N = 5/5). However, in embryos ≥ 26 hpf, CoPAs produced sustained firing throughout the duration of the current step and less current was needed to bring the neuron to threshold (Fig. 1A; N = 9/9). A similar developmental maturation of firing has been shown in excitatory premotor spinal interneurons (Knogler et al., 2014). By 26 hpf, action potentials had large amplitudes and were always overshooting (Fig. 1A; N = 9). The instantaneous spiking frequency during depolarizing current steps (4 – 36 pA; steps of 4 pA) was calculated for CoPA neurons in 24 – 25 hpf embryos versus 26 – 28 hpf embryos to produce an F-I curve (Fig. 1B; N = 5, 9). All CoPAs ≤ 25 hpf fired singly with current injection whereas CoPAs from older embryos clearly increased their firing frequency with greater amounts of positive current. Though they were slightly less excitable at lower stimulus intensities, at higher stimulus intensities the response of CoPA neurons resembled that of CoSA neurons (Fig. 1B; N = 9), which also have commissural ascending axons and are highly active at this age (Bernhardt et al., 1990; see later). A 32 pA current injection resulted in burst firing in all CoPA and CoSA neurons as well as in primary motoneurons and was used to compare average instantaneous firing frequencies across cell type (Fig. 1C). The average firing frequencies for CoPAs, CoSAs and motoneurons were not significantly different (69.4 ± 2.8, 76.1 ± 2.3 and 79.0 ± 3.3 Hz, respectively; $p > 0.05$ for all pairwise comparisons; N = 9, 5, 9). Embryonic motoneurons typically have input resistances in the 1-2 GΩ range (Knogler et al., 2014; Saint-Amant & Drapeau 2000; Tong & McDearmid 2012) and our recordings showed input resistances averaging 2.0 ± 0.4 GΩ for primary motoneurons and 3.2 ± 0.4 and 3.1 ± 0.1 GΩ for CoPAs and CoSAs, respectively (Fig. 1D; $p > 0.05$ for all pairwise comparisons; N = 9, 7, 9).

These results show that CoPA interneurons are undergoing a maturation of intrinsic properties subsequent to the onset of the touch response at 21 hpf and preceding the onset of swimming at 29 hpf (Saint-Amant & Drapeau, 1998). By 26 hpf, the threshold for action potentials has lowered and CoPAs have switched to a sustained firing mode during current injection. The similarity of intrinsic membrane properties between different cell types at this embryonic stage suggests that this maturation may occurring in many classes of spinal neurons during this developmental period (Knogler et al., 2014).

III.4.2. Embryonic CoPAs show spontaneous long-lasting glycine-mediated depolarizations that shunts excitation

We have previously shown that CoPAs exhibit an activity pattern during the time window of spontaneous coiling behaviors that, unlike for premotor and motor neurons, is not modified during the transition from single to double coiling (Knogler et al., 2014). We examined the physiological properties of CoPAs in greater detail by single cell patch clamp recording. All current-clamp recordings from CoPA cells (N = 25/25) showed the presence of regular, spontaneous ~ 25 mV amplitude depolarizations that were often sufficient to elicit a single action potential at the onset of the depolarization (Fig. 2A and inset). In comparison to the spikes fired during current injection, this action potential had a smaller amplitude and was rarely overshooting (compare Fig. 2A *vs* Fig. 1A). Despite the ability of these cells at ages ≥ 26 hpf to produce sustained firing of action potentials in response to depolarizing current injections (Fig. 1A), multiple action potentials were never produced during spontaneous depolarizing events (Fig. 2A; N = 25/25). These spontaneous depolarizations lasted more than one second at 24 hpf and this duration was found to increase in correlation with age (Fig. 2B; e.g. average duration at 24 hpf = 1.11 ± 0.16 s, 27 hpf = 1.50 ± 0.06 s; Pearson's correlation coefficient $r = 0.49$, $p < 0.05$). These durations are more than twice as long as for spontaneous activity patterns in other spinal interneurons and motoneurons at this age (Knogler et al., 2014). Occasional events were seen in CoPAs with durations longer than two seconds that resembled two overlapping events (data not shown; these events were not included in calculating duration averages in Fig. 2B). Therefore, CoPAs showed what appeared to be unique, long-lasting shunting depolarization under physiological conditions.

We next investigated the nature of the CoPA depolarization. By 26 hpf, both glutamatergic and glycinergic signaling can be detected in the zebrafish spinal cord (Ali et al., 2000a; Saint-Amant & Drapeau, 2000; Saint-Amant & Drapeau, 2001; Pietri et al., 2009; Knogler et al., 2014) whereas GABAergic signaling does not play an important role (Buss and Drapeau, 2001; Saint-Amant & Drapeau, 2000). Glycine is depolarizing at this age due to a high intracellular chloride concentration (Saint-Amant & Drapeau, 2000) and can produce suprathreshold post-synaptic potentials depending on the reversal potential for chloride ions

relative to the threshold for action potentials (Jean-Xavier et al., 2007). Glycinergic currents can be isolated from depolarizing glutamatergic currents pharmacologically with receptor antagonists or by holding the cell at the reversal potential for cations (approximately 0 mV) and anions (approximately -35 mV) (Buss & Drapeau, 2001). Under voltage-clamp at resting membrane potentials (-65 mV), spontaneous currents in CoPAs were inward, whereas at less negative potentials (-20 mV), the direction of the currents reversed and when clamped at the chloride reversal potential there was no net flow of current (Fig. 2C, D; N = 4). These results suggested that the spontaneous depolarizations seen in the CoPA were due to the flow of chloride ions and therefore we examined the effect of glycine receptor blockade on this activity.

Our initial attempts to block these depolarizing events in CoPA interneurons with 1 μM strychnine failed to do so nor to significantly alter the duration or frequency of these events (Fig. 2E; $p > 0.05$; N = 3) despite the fact that this dose rapidly and effectively blocks the glycine-mediated depolarizations that are seen in motoneurons and other interneurons at this same age (Knogler et al., 2014; Saint-Amant & Drapeau, 2000; Saint-Amant & Drapeau, 2001). Previous studies have shown that different glycine receptor subunits may have different sensitivities to strychnine (Kuhse et al., 1990). We therefore tried a higher dose of 5 - 10 μM strychnine and saw that these depolarizing events were lost at this concentration (Fig. 2F, G; N = 5). We believe that the effect of strychnine to reduce CoPA activity was *via* direct blockade of glycine receptors on the cell rather than the blockade of presynaptic inputs in the circuit based on two observations. First, the amplitude (not frequency) of CoPA depolarization decreased progressively when 10 μM strychnine was introduced (Fig. 2F), suggestive of an increasing blockade of receptors. Secondly, as previously mentioned, 1 μM strychnine effectively blocks glycinergic currents in other cells whereas the glycine-mediated depolarizing events in CoPAs required a concentration of 10 μM strychnine for full blockade (Fig. 2G; $p < 0.001$ for 10 μM strychnine; N = 6), in keeping with a different sensitivity of their respective receptors to strychnine. No effect on spontaneous depolarizing events was seen with 10 μM bicuculine, a blocker of GABA receptors (N = 2), or with 10 μM CNQX, a blocker of AMPA receptors (N = 2), therefore these depolarizing events appeared to be mediated by chloride currents through glycine receptors.

Glycine receptor-mediated depolarizing conductance may shunt excitation and functionally inhibit immature neurons (Jean-Xavier et al., 2007). In order to further examine the effect of these glycinergic depolarizations on action potential firing, we injected positive current at short latencies following the onset of a spontaneous depolarization and measured the rate of action potential firing compared to the same amount of current injection at baseline. An injection of depolarizing current that was sufficient to produce sustained firing at resting membrane potentials was far less effective at driving action potentials when applied during the first second of a spontaneous depolarizing event (Fig. 2H, I; N = 11 events from 5 embryos), indicating that the CoPA is functionally inhibited by the depolarizing glycinergic conductance.

These results suggest that during the period of spontaneous behaviors, CoPAs receive glycinergic inputs that activate a chloride conductance leading to a long duration depolarizing event that is capable of shunting the membrane resistance and temporarily increasing the threshold for action potential firing. The long duration of spontaneous depolarizing events and lower sensitivity to strychnine compared to other interneurons and motoneurons at this age suggest that the CoPA may receive glycinergic inputs and/or express glycine receptors that are different from other spinal neurons.

III.4.3. Embryonic CoPAs have slow glycine-mediated synaptic currents

Developmental speeding of currents by subunit switching appears to be a general feature of vertebrate transmitter receptors, including those for glycine (reviewed by Takahashi, 2005). In order to examine the properties of glycine receptors in CoPA interneurons, we recorded miniature post-synaptic currents (mPSCs) in 26 - 29 hpf embryos. Recordings made in the presence of tetrodotoxin (TTX) to inhibit action potentials revealed the presence of depolarizing mPSCs with fast or slow rates of decay (category “s” and "f" events, respectively; Fig. 3A, B; N = 3 for both). To confirm this categorization, a frequency histogram plot of all mPSCs for a cell clearly showed a bimodal, non-overlapping distribution of decay time constants separating fast from slow currents (Fig. 3C). The mPSCs with slower kinetics were identified as glycinergic, as they were abolished by 10 μM strychnine (Fig. 3A, D; $p < 0.001$; N = 3). The mPSCs with faster kinetics were identified as glutamatergic, as they

were abolished by 5-10 μM CNQX (Fig. 3B, D; $p < 0.001$; N = 3). We further confirmed that the slow currents were chloride based (glycinergic) by measuring the I-V curve at holding potentials ranging from -80 mV to +80 mV in 20 mV steps. As expected, glycinergic mPSC amplitudes decreased as holding potentials moved from -80 mV towards -35 mV, the approximate chloride reversal potential and did not show rectification (Fig. 3E; N = 3). The frequency of both types of mPSCs was low (≤ 0.06 Hz; Fig. 3A, B, D) therefore since the two populations could be easily resolved based on kinetics alone, some recordings omitted CNQX in order to collect both fast and slow mPSCs.

Glycinergic mPSCs were recorded from CoPA interneurons, motoneurons and CoSA interneurons for comparison in 26 – 29 hpf embryos and their physiological properties are listed in Table 1. Glycinergic mPSCs in all cell types had similar amplitudes of approximately 30 pA (Fig. 3F; $p > 0.20$ for all pairwise comparisons) but were present at twice the frequency in CoPAs than in motoneurons (mPSC frequency was lower and could not be accurately determined in CoSA recordings). Rise times were significantly slower in CoPAs than in MNs or CoSAs ($p < 0.005$) but the most striking difference was the order of magnitude longer decay time constant (τ) of glycinergic mPSCs in CoPAs compared to MNs and CoSAs (Fig. 3F; $p < 0.001$). The decay time constant for CoPAs, nearly 100 ms, was similar to that observed for glycinergic mPSC and single channel kinetics in embryonic and adult Mauthner cells (Ali et al., 2000b; Hatta et al., 2001) and is within the range of values reported for rodent embryonic glycine receptors (Mangin et al., 2003). The decay time constants for CoSAs and motoneurons, in contrast, resembled the faster kinetics of glycinergic mPSCs in larvae and a subset of events in adult Mauthner cells (Ali et al., 2000b) as well as in P10-P20 rat motoneurons (Burzomato et al., 2004; Singer et al., 1998). The long decay time constant in CoPAs translated to a much larger charge transfer than in MNs and CoSAs ($p < 0.001$). No change in glycinergic mPSC parameters in CoPAs was seen with APV treatment (N = 4).

Table 1. Properties of glycinergic mPSCs in spinal neurons from 26-29 hpf embryos. #Student's t-test; *Tukey's post-hoc test. ND = not determined.

	CoPA	**MN**	**CoSA**
N	12	9	5
age (hpf)	27.5 ± 0.2	27.6 ± 0.4	27.5 ± 0.5
frequency (Hz)	0.043 ± 0.006###	0.020 ± 0.003	ND
amplitude (pA)	31.1 ± 4.6	30.2 ± 2.7	31.5 ± 4.5
10-90% rise time (ms)	1.31 ± 0.13**	0.80 ± 0.06	0.65 ± 0.08
decay time constant (ms)	90.5 ± 5.7***	7.56 ± 0.70	5.16 ± 0.52
charge transfer (nC)	2.70 ± 0.38***	0.25 ± 0.03	0.16 ± 0.02

Based on these mPSC properties and the low strychnine sensitivity of spontaneous currents, CoPAs appear to express different glycine receptors than CoSAs and motoneurons. The slow kinetics of glycine receptors in embryonic CoPA interneurons likely contribute to the long duration of their depolarizations following receptor activation and the resulting shunting of action potential firing.

III.4.4. CoPA interneurons express PhTX-insensitive AMPA receptors that mediate rectifying glutamatergic mEPSCs

Our recordings of miniature PSCs in CoPA in the presence of TTX and APV, an NMDA receptor antagonist, revealed the presence of fast, CNQX-sensitive AMPAergic currents that were easily distinguishable from slow glycinergic mPSCs (Fig. 3A, B). These fast currents were confirmed to be non-selective cationic (glutamatergic) by holding the membrane potential at the approximate reversal potentials for cations (0 mV; Fig. 3G). AMPAergic mEPSCs were rare at 24 hpf but increased rapidly in amplitude and frequency over development, therefore recordings were made in 26 - 29 hpf embryos to obtain a sufficient number of events. The properties of AMPAergic mEPSCs at this age are summarized in Table 2. (In both motoneurons and CoSAs at this age the frequency of mEPSCs was far lower, therefore we did not include these cells for comparison.) On average,

the amplitude and frequency of AMPAergic mEPSCs were similar to glycinergic mPSCs, but the kinetics of glutamatergic mEPSCs were far faster than those of glycinergic events in terms of both rise time and decay, leading to two orders of magnitude lower average transfer of charge per event (Fig. 3A, B). In addition, unlike glycinergic mPSCs whose properties were stable over the period of 26 - 29 hpf, the amplitude of AMPAergic mEPSCs increased over this short, four-hour window of time with a high and statistically significant correlation between amplitude and embryo age (Spearman rank rho = 0.76, $p < 0.05$; N = 9). AMPAergic mEPSCs also showed a trend towards increased frequency with embryo age although this correlation was not statistically significant (Pearson's correlation r = 0.51; p = 0.08; N = 9).

Table 2. Properties of AMPAergic mPSCs in CoPA interneurons from 26-29 hpf embryos.

	CoPA interneuron
N	9
age (hpf)	27.4 ± 0.3
frequency (Hz)	0.038 ± 0.010
amplitude (pA)	25.7 ± 5.5
10-90% rise time (ms)	0.41 ± 0.020
decay time constant (ms)	1.15 ± 0.040
charge transfer (nC)	0.040 ± .009

AMPAergic I-V curves were obtained by recording AMPAergic mEPSCs at holding potentials ranging from -80 mV to +80 mV in 20 mV steps in order to determine the degree of rectification. As expected, AMPAergic mEPSC amplitudes decreased as holding potentials moved from -80 mV towards 0 mV, the approximate cationic reversal potential (Fig. 3G; N = 3). However, no outward-going AMPAergic mEPSCs were seen beyond the cationic reversal potential, despite the large driving force present at +80 mV. Despite having a larger signal to noise ratio, evoked AMPAergic EPSCs onto CoPAs also failed to reverse at positive holding potentials (N = 3; data not shown), demonstrating a strong inward rectification of glutamatergic currents, consistent with the presence of calcium-permeable AMPARs that

should be sensitive to external polyamine block (Man, 2011). We examined the sensitivity of these receptors to external polyamine block by applying 10 μM philanthotoxin 343 (PhTX) to our recordings of AMPAergic mEPSCs from CoPAs. No consistent change in mEPSC amplitudes was seen following PhTX treatment (Fig. 3H; $N = 3$; $p > 0.20$). In order to ensure adequate receptor blockade, we applied 20 μM PhTX in combination with repeated activation of the receptors and saw that the amplitude of evoked glutamatergic events in CoPAs was significantly reduced by 23 ± 7 % (Fig. 3I; $N = 3$; $p < 0.05$).

These results suggest that glutamatergic inputs to CoPA interneurons are maturing rapidly over the period of development preceding swimming as evidenced by the increase in both amplitude and frequency of AMPAergic mEPSCs. Post-synaptic glutamatergic signaling in CoPAs appears to be mediated by strongly rectifying but mostly PhTX-insensitive AMPARs that may belong to a recently described functional class of AMPARs seen in the developing retina and hippocampus (see Discussion for details). Thus, both glutamatergic and glycinergic synaptic currents are atypical in the CoPA neurons and may be related to their unusual physiological properties.

III.4.5. Embryonic CoPAs are not part of the network driving ipsilateral coils and are shunted by glycinergic inhibition during contralateral coils

Having examined the properties of spontaneous synaptic inputs to CoPAs, we were next interested in looking at glycinergic and glutamatergic inputs to CoPAs in a behavioral context. The synaptic inputs to motoneurons during both spontaneous and evoked embryonic behaviors have been described in several studies (Saint-Amant & Drapeau, 2000; Saint-Amant & Drapeau, 2001; Pietri et al., 2009; Knogler et al., 2014). Briefly, spontaneous single coils are unilateral trunk contractions driven by electrically coupled ipsilateral cells generating low-amplitude depolarizing periodic inward currents (PICs) in motoneurons (Saint-Amant & Drapeau, 2000). During embryonic development, nascent glutamatergic inputs give rise to double coils, a transient developmental behavior that precedes swimming (Knogler et al., 2014). When the trunk is contracting in a coil, motoneurons contralateral to the coiling side receive large amplitude depolarizing glycinergic synaptic bursts (SBs), but these inputs do not drive the behavior itself (Saint-Amant & Drapeau, 2001). We can therefore interpret the

fictive behavior in the paralyzed animal electrical by knowing that electrical depolarizations in motoneurons drives ipsilateral coiling while glycinergic bursts are the physiological correlate of contralateral coiling (Knogler et al., 2014; Pietri et al., 2009; Saint-Amant & Drapeau, 2001).

We performed simultaneous whole-cell recordings from ipsilateral CoPAs and motoneurons in order to correlate activity in the CoPA with fictive spontaneous single and double coiling behavior (Fig. 4A; N = 3). Unlike the majority of other interneurons at this age, CoPAs were inactive during fictive ipsilateral single coils, as evidenced by a complete absence of activity during PICs (with or without coinciding glutamatergic events) in the motoneuron (Fig. 4B, F). Glycine-mediated depolarizations of CoPAs were, however, synchronized with glycinergic synaptic bursts in the ipsilateral motoneuron (Fig. 4C, F), indicative of a fictive contralateral coil. Interestingly, the duration of the depolarization in CoPAs far outlasted that of the inputs to motoneurons. Upon closer examination, the duration of the maximal depolarization in the CoPA appeared to overlap with the duration of the synaptic burst in the MN (Fig. 4C, dashed vertical line), suggesting that their glycinergic inputs may be similar but have distinct postsynaptic effects due to the far slower kinetics of CoPA glycine receptors. The occurrence of spontaneous fictive double coils as represented by mixed electrical (PIC) and glycinergic events (SB) in the motoneuron (Knogler et al., 2014) did not correlate with any new activity pattern in the CoPA (Fig. 4D, E). Once again, no activity was seen in the CoPA during the electrical component of the mixed event in the motoneuron (Fig. 4E, F).

These simultaneous recordings suggest that the glycinergic depolarizing events in the CoPA occur during a contralateral coiling event. Since the blockade of glycinergic signaling at this age does not block coiling behavior (Saint-Amant & Drapeau, 2000) and in fact may lead to multiple coils (Knogler et al., 2014), the CoPA is unlikely to be driving this spontaneous behavior. These results also demonstrate that the CoPA is not a part of the electrically coupled ipsilateral network, further suggesting that the CoPA does not play a key role in driving spontaneous single coils. Finally, the inputs onto the CoPA are not different during a double coil than during a single coil, supporting our previous hypothesis (Knogler et al., 2014) that this cell is not part of the circuit driving double coiling behavior.

III.4.6. Embryonic CoPAs receive brief glutamatergic excitation followed by long lasting, shunting glycinergic inputs in response to touch

Having shown that CoPAs are not likely to contribute to spontaneous coiling behaviors, we next examined their activity during touch-evoked coiling behavior. CoPAs are known to receive glutamatergic followed by glycinergic inputs in response to a touch stimulus at 24 hpf (Pietri et al., 2009). The depolarizing glycinergic inputs are presumed to inhibit activation of the CoPA but the effect of these currents on membrane potential and action potential firing has not been shown.

In order to characterize the spiking of CoPA interneurons following a touch stimulus, we performed electrophysiological recordings from CoPAs while squirting water onto the ipsilateral tail of the embryo to displace it slightly, evoking a touch response (Fig. 5A). In cell-attached mode, the stimulus robustly elicited one spike in the CoPA but otherwise no spikes were seen spontaneously in any recordings (Fig. 5B; N = 3). Under current-clamp conditions, the CoPA produced one or two action potentials then remained depolarized for one to two seconds following the stimulus (Fig. 5C lower trace and inset; N = 4 embryos). The response was very similar to that seen during spontaneous events occurring between stimuli except that in addition to the small amplitude action potential seen during both spontaneous and evoked events, the evoked response showed a short latency, overshooting action potential with a much larger amplitude (Fig. 5C and inset, D). The peak amplitude of the slow, long duration depolarization mediated by glycine was indistinguishable between evoked and spontaneous events (Fig. 5E).

We hypothesized that the first action potential seen in the CoPA following the stimulus was a fast suprathreshold response mediated by a strong glutamatergic input as Pietri et al., (2009) have shown that CoPAs receive short latency glutamate-driven cationic currents followed by large glycine-driven chloride currents following an ipsilateral touch stimulus. We confirmed that the short latency (< 20 ms) currents were cationic and remained inward at holding potentials up to-20 mV while the later arriving, larger currents were confirmed to be anionic currents as they disappeared at the chloride reversal potential (approximately -34 mV) and were reversed at -20 mV (Fig. 5F). Wash-in of 10 μM strychnine abolished the glycine-

driven chloride currents for evoked and spontaneous events while leaving evoked cationic currents unaffected (Fig. 5G; N = 2). The blockade of glycinergic signaling also revealed that CoPA interneurons often received multiple glutamatergic inputs following the stimulus that would normally be occluded by the large amplitude glycinergic chloride currents (Fig. 5G), suggesting that the arrival of shunting glycinergic inputs prevent sustained action potential firing even in the presence of multiple strong excitatory inputs. The additional glutamatergic EPSCs may be due to the activation of other RB neurons further away that contact the same CoPA.

These findings show that CoPAs fire a large, overshooting action potential triggered by short latency excitation from the glutamatergic RB in response to touch. Activation is followed quickly by the arrival of glycinergic inputs that produce a shunting response identical to that seen during a spontaneous coil, suggesting that CoPA is functionally inhibited in the same way during spontaneous and ongoing self-generated movement. These results further indicate that the response of the CoPA to glutamatergic inputs must be robust in order to produce this first, large amplitude action potential prior to the arrival of the shunting glycinergic inputs.

III.4.7. Other classes of embryonic spinal neurons show different activity patterns during spontaneous and touch-evoked activity

In order to better understand how the activity of CoPAs differs from that of other cells, we recorded the responses in other spinal neuron classes at rest and following a touch stimulus in 24 – 29 hpf embryos. Following an ipsilateral touch stimulus normally producing a contralateral trunk contraction, motoneurons received a burst of depolarizing glycinergic inputs with a latency of several tens of milliseconds, (Fig. 5H; N = 3) as previously shown at 24 hpf (Pietri et al., 2009). The glycinergic burst was capable of producing action potentials under current-clamp conditions (not shown) and was sometimes preceded by a small glutamatergic event (Fig. 5H, arrowhead) with a shorter latency, but these inputs were insufficient to drive an action potential. A single touch response sometimes elicited up to three fictive alternating coils, as indicated by the sub-second succession of a glycinergic burst (SB) followed by an electrical depolarization (PIC) then another SB in the motoneuron

recording (Fig. 5H, right). Spontaneously occurring events strongly resembled evoked responses except that the spontaneous events never showed short latency glutamatergic events preceding the glycinergic burst (Knogler et al., 2014).

As previously discussed, CoSA interneurons resemble CoPAs morphologically (see Fig. 1B) and it has been proposed that CoSAs may also play the role of sensory interneuron in the spinal cord (Hale et al., 2001; Liao & Fetcho, 2008). We recorded from embryonic CoSAs that were identified by their small, dorsal soma, ascending commissural axon and lack of dendrites at this age compared to CoPAs (Bernhardt et al., 1990). Although CoSAs are a heterogeneous class of neurons in terms of their neurotransmitter identity, only glutamatergic CoSAs have been shown to be present in the spinal cord at this early stage (Satou et al., 2012). Our recordings showed that CoSAs were highly active with spontaneous and evoked activity patterns resembling motoneurons (Fig. 5I) and also like motoneurons produced several spikes in cell-attached recordings both in response to touch stimuli and spontaneously (data not shown). A touch stimulus evoked a depolarizing glycinergic synaptic burst in ipsilateral CoSAs with a similar latency as in motoneurons and sometimes consisting of two or more additional fictive alternating coils (Fig. 5I; N = 5). These evoked events were also sometimes preceded by small, short latency glutamatergic peaks (Fig. 5I; arrowhead), which like in motoneurons were not sufficiently large to drive an action potential. Recordings (N = 7) of spontaneous activity from CoSAs showed activity patterns strongly resembling evoked responses (data not shown). These data suggest that CoSAs are part of the embryonic motor circuit active during spontaneous coiling behaviors but do not act as sensory interneurons at this age.

Finally, we also recorded from several embryonic CoBL neurons which at this stage are identifiable by their small dorsal soma and their unique bifurcating commissural axon that has both a major ascending and descending branch (Bernhardt et al., 1990). Our recordings failed to show any evidence of electrical depolarizations in CoBLs (N = 12). In fact, apart from two recordings in 28 – 29 hpf embryos, the majority of recordings (N = 10/12) also showed no evidence of synaptic glycinergic bursts and CoBLs never fired spontaneous action potentials. These findings indicated that CoBLs were not active during coiling behaviors and recordings during touch-evoked coiling supported these results (N = 2).

Our recordings from other commissural interneurons and motoneurons revealed two main patterns of activity. Spontaneous and evoked activity of motoneurons and CoSAs revealed depolarizing electrical as well as glycinergic events, demonstrating that these cell types participate in coiling behaviors. Both types of activity were capable of eliciting action potentials in these cells, particularly at later stages. In contrast, CoBLs did not fire action potentials during spontaneous or evoked activity, suggesting that despite having extended long axons by this age these cell types do not participate in coiling behaviors. These results suggest that CoSAs, the only other commissural interneuron class active at this age, participate in motor rather than sensory circuits and highlight the importance of the CoPA in relaying somatosensory input contralaterally during evoked embryonic behaviors.

III.4.8. CoPAs receive rhythmic inhibition in phase with excitation to ipsilateral MNs during burst swimming episodes

The latest-appearing embryonic zebrafish behavior is swimming, which begins around 28 hpf. Swimming can be elicited at this age by a touch stimulus to the tail, or, to a lesser degree, to the head and may also appear spontaneously (Saint-Amant & Drapeau, 1998). During immature burst swimming in zebrafish, motoneurons receive tonic depolarization composed of both chloride and cationic conductances in addition to rhythmic excitatory post-synaptic currents that are capable of driving action potentials in the motoneuron throughout the duration of the behavior (Buss & Drapeau, 2001). This motoneuron activity drives ipsilateral muscle contractions while the contralateral motoneurons receive excitation out of phase, thus driving alternating contractions of the trunk as seen during free swimming behavior (Masino & Fetcho, 2005; McDearmid & Drapeau, 2006).

We recorded from CoPAs in 28 - 29 hpf embryos in the absence of touch stimuli in order to observe their activity patterns during spontaneous bouts of fictive burst swimming. Occasionally, an activity pattern was seen that we interpreted to be an episode of fictive immature burst swimming due to the unusually long duration (> 3 seconds) of the activity (Fig. 6A; N = 3 events in 3 embryos). This activity strongly resembled a longer duration version of the glycine-mediated depolarization seen during a coiling event in the CoPA (compare Fig. 6A and Fig. 2A). Consistent with the activity pattern seen during coiling, no

more than one small action potential at the onset was ever produced and no fast EPSPs were seen on top of the depolarization, suggesting that no glutamatergic inputs arrived to CoPAs during the period of swimming or that these inputs were not visible due to shunting.

In order to confirm that these observations of CoPA activity were indeed correlated with swimming activity, we obtained a simultaneous whole-cell recording from a CoPA interneuron and ipsilateral motoneuron in a 29 hpf embryo during which a bout of spontaneous fictive swimming occurred (Fig. 6B). The CoPA showed a long duration depolarization that peaked at the chloride reversal potential and resembled the long duration events recorded in individual CoPAs (Fig. 6A). The CoPA activity persisted for the duration of the excitatory inputs to the motoneuron and distinct peaks could be seen during the depolarization that were in phase with excitatory inputs to the ipsilateral motoneuron (Fig. 6C). In this recording the peaks in the CoPA depolarization consistently followed the peaks in the MN excitation by on average 3.3 ± 0.2 ms (Fig. 6D), a small fraction of the 30-100 ms interval between peaks. Due to the rarity of these spontaneous swimming events we were unable to confirm the identity of the currents by changing the reversal potential or with pharmacological receptor antagonists but the depolarization in the CoPA clamped the membrane potential near the chloride reversal potential and had slow decay kinetics, strongly suggesting that these were mediated by chloride and not cationic currents.

These results show that CoPAs receive rhythmic glycinergic inputs in phase with excitation to the ipsilateral motoneuron during swimming. The activity patterns in CoPAs during coiling and swimming are very similar apart from their durations, suggesting that the same type of presynaptic glycinergic neurons might mediate functional inhibition for these different behaviors. These findings support the hypothesis that CoPAs are actively inhibited by corollary discharge during different types of self-generated movement in the embryo.

III.5. DISCUSSION

The goal of this study was to examine the intrinsic and synaptic properties of sensory CoPA interneurons during different embryonic behaviors in an effort to understand how these neurons might play a specialized role in gating activation of the somatosensory pathway during self-generated movements in the zebrafish embryo. We show that the synaptic

properties of embryonic CoPAs are highly tuned for gating sensory information in order to ensure the appropriate activation of the touch response. Embryonic CoPAs receive shunting glycinergic depolarization mediated by slowly deactivating glycine receptors during contralateral spinal cord activation. We propose that this corollary discharge prevents inappropriate activation of sensorimotor pathways during a period in which the zebrafish exhibits high levels of spontaneous locomotor activity. In response to touch, fast glutamatergic input from RB sensory neurons arrives prior to glycine-mediated shunting and allows the brief, strong AMPAergic activation of CoPAs necessary to propagate and amplify excitation in the touch reflex pathway. These results further our understanding of how sensory processing is modulated by motor patterns in the vertebrate spinal cord.

III.5.1. Shunting of embryonic CoPA interneurons prevents inappropriate activation of the touch reflex during spontaneous or ongoing evoked behaviors

The mechanosensitive neurites of RB somatosensory neurons form an extensive network of coverage along the surface of the zebrafish trunk to mediate responses to touch or noxious stimuli. A single action potential in a single RB is sufficient to activate an escape behavior at 24 hpf (Douglass et al., 2008), which poses a challenge for the sensorimotor circuit to balance the need for a low rate of false activation under baseline conditions with robust activation when a real stimulus is present. As RBs may be activated and fire during ongoing behaviors such as coiling and swimming, there must be safety measures in place to inhibit ongoing pathway activation. Mechanisms such as presynaptic inhibition of sensory afferents have been observed in the vertebrate spinal cord that could contribute to inactivating RBs during ongoing mechanosensation (reviewed by Rudomin & Schmidt, 1999), although this remains to be examined in zebrafish RBs. Regardless of presynaptic RB firing, our results show that the inhibition of CoPA sensory interneurons provides a sufficiently strong gate to prevent inappropriate activation of the touch reflex.

Embryonic CoPAs show spontaneous patterns of activity in the form of one to two second-long depolarizations that outlast those seen in other spinal neurons at this age (Knogler et al., 2014). We have now shown that this is due to a large, glycine receptor-mediated chloride conductance that effectively shunts the membrane resistance and raises the

threshold for action potential firing. In other cells such as CoSAs and motoneurons, similar glycinergic inputs excite cells and often lead to action potential firing. The dual nature of depolarizing glycinergic (or GABAergic) inputs in the developing nervous system has been widely reported and is known to depend on cellular properties such as resting membrane potential, intracellular chloride concentration, as well as the location of the inhibitory synapses on the neuron (Ben-Ari, 2002; Jean-Xavier et al., 2007). In our study, the efficacy of glycinergic PSCs in shunting activity in CoPAs more than in other cells, even given similar presynaptic inputs, appears to be due in large part to the presence of glycine receptors with slow kinetics in CoPAs. Our results suggest that the long decay phase of glycinergic currents in CoPAs results in effective and long-lasting shunting during spontaneous activity as well as during the ongoing activity of evoked behaviors such as swimming. It should be noted however that these electrophysiological recordings were performed in paralyzed animals, therefore we cannot exclude the possibility that the activity of spinal sensory neurons (such as RBs) and interneurons could be different when the muscles are physically contracting.

The embryonic mammalian α2 glycine receptor subunit imparts slow decay time constants on homomeric α2 and heteromeric α2β glycine receptors (for reviews see Legendre, 2001; Lynch, 2004, 2009). We observed that the glycinergic mPSCs of CoPAs exhibit similarly slow kinetics, suggesting that glycine receptors contain α2 or similar (α4a) subunits. Teleost reticulospinal Mauthner cells exhibit glycine-mediated synaptic and single channel currents with similarly slow kinetics (Ali et al., 2000b; Hatta et al., 2001), an interesting comparison given that these cells are known to be specialized for touch-evoked behaviors (Eaton et al., 1977). The slow kinetics of these currents, particularly early in development when glycine is depolarizing, could ensure that Mauthner cells and CoPAs are adequately shunted during ongoing activity despite relatively few inputs at early stages (Ali et al., 2000b). Motoneurons and CoSAs, in contrast, showed fast glycinergic mPSCs that likely reflect the activation glycine receptors with faster α1 subunits. In addition to this difference in kinetics, a higher concentration of strychnine was required to block glycinergic currents in CoPAs in our experiments compared to other embryonic spinal neurons including Mauthner cells (Ali et al., 2000b; Saint-Amant & Drapeau, 2000). One glycine receptor subunit found to date only in neonatal mammalian neurons, α2*, shows a significantly reduced affinity for

strychnine as a ligand that has been linked to a difference in one amino acid residue from the more common embryonic α2 subunit (Becker et al., 1988; Kushe et al., 1990). As a result, homomeric α2* receptors have a 500-fold lower sensitivity to strychnine than α2 receptors and show only a very small reduction in current in the presence of 1 μM strychnine (Han et al., 2004; Kuhse et al., 1990). Our results raise the possibility that CoPAs express α2*-containing glycine receptors whereas other embryonic spinal neurons are more likely to express the common α2 or α1 subunit. Interestingly, a subset of slow glycinergic currents in adult Mauthner cells was also shown to be less sensitive to strychnine (Hatta et al., 2001). It will be interesting to determine if these slow subunits in CoPAs undergo developmental speeding by replacement with faster subunits or if slow currents persist throughout adulthood.

The identity of the presynaptic glycinergic neurons in zebrafish that provide corollary discharge onto CoPAs is not currently known. In *xenopus*, paired recordings have identified ascending interneurons (aINs) as the source of glycinergic inhibition to dlc interneurons during swimming (Li et al., 2002). The zebrafish homologues of aINs, identified by the common expression of the transcription factor engrailed, are the circumferential ascending (CiA) interneurons (Higashijima et al., 2004b; Li et al., 2004). However, recordings from CiAs in the 20 - 29 hpf embryo do not show spontaneous action potential firing despite the high frequency of glycinergic activity seen in spinal neurons at this age (Saint-Amant & Drapeau, 2001; and our unpublished data). Furthermore, lesion experiments in the 24 hpf embryo have shown that glycinergic inputs to caudal CoPAs as well as to motoneurons are lost following a transection of the spinal cord at the eighth to tenth rostral spinal segment (Pietri et al., 2009), suggesting that rostral spinal cord or hindbrain neurons with descending axons and not CiAs, are the source of glycine. By this same logic, it is unlikely that the glycinergic commissural local (CoLo) interneurons responsible for providing reflex inhibition to Mauthner cells during larval escape behaviors are the source of glycinergic inhibition to CoPAs since their axons span only one somite in length (Satou et al., 2009). A recent study by Moly et al., (2014) showed that a small number of glycine immunoreactive neurons are present in the hindbrain and rostral somites of the spinal cord at 20 hpf, coinciding with the arrival of glycinergic inputs to spinal neurons (Saint-Amant & Drapeau, 2000). One class of spinal neurons, the pacemaker IC cells, is located exclusively in the rostral spinal cord

(Mendelson, 1986), suggesting that this region may contain specialized neurons not present in more caudal regions. Finding the corollary discharge neurons that provide glycinergic input to CoPAs and other neuronal classes will contribute greatly to our understanding of the developing spinal locomotor network.

III.5.2. CoPAs and other neurons in the sensory pathway are excluded from the electrically coupled network

Our recordings from CoPAs in the 24 - 29 hpf embryo showed no evidence of electrical depolarizations, suggesting that these cells are not connected to the electrically coupled ipsilateral network driven by periodically depolarizing pacemaker neurons. In contrast, we have shown that the morphologically similar CoSAs show robust electrical depolarizations resembling those seen in motoneurons that can drive sustained action potential firing at this age. These findings appear inconsistent with a previous study in 20 - 24 hpf zebrafish embryos that reported the presence of electrical depolarizations in the majority of CoPAs but only a small minority of CoSAs (Saint-Amant & Drapeau, 2001). It is unlikely that these two cells types change their coupling to the network at 24 hpf, therefore we believe that CoPAs, having a very similar morphology at early ages to CoSAs, were misidentified. We are confident in our identification of CoPAs and CoSAs in this report because at these later stages, the lateral dendrites and large, triangular soma of CoPAs are obvious and easily distinguishable from the smaller soma of CoSAs that have no dendrites (Fig. 1B).

It has been suggested that the dorsoventral localization of cell types may correlate with their inclusion in the electrically coupled network (Carlisle & Ribera, 2014). Unambiguously identifiable, dorsally located RBs and dorsal lateral ascending (DoLA) interneurons never show electrical depolarizations during the period of 20 hpf - 29 hpf (Saint-Amant & Drapeau, 2001; Douglass et al., 2008; our unpublished observations), which is a predictable result for cells in the sensory pathway that should mediate evoked and not spontaneous, pacemaker-driven behaviors. We believe that CoPAs are not electrically coupled for these same reasons: their lack of observed spontaneous electrical depolarizations, their dorsal soma position and their proposed role in sensory gating.

III.5.3. Strong AMPAergic excitation allows brief activation of CoPA interneurons in response to external touch stimuli prior to the onset of shunting glycinergic inhibition

Despite the evidence that CoPAs are not excited by the spontaneously active electrical network and in fact spend much of their time in a shunted mode due to the effects of their slow glycine receptors, CoPAs can nonetheless mediate a robust touch response prior to shunting *via* glutamatergic signaling. It has been established in *xenopus* that the glutamatergic currents from RBs onto dlc interneurons are mediated mostly by AMPARs, while the glutamatergic currents from dlc interneurons onto downstream motor and premotor interneurons are mediated mostly by NMDARs (Li et al., 2003). Furthermore, a single RB may synapse onto several if not all sensory interneurons of the ipsilateral spinal cord (Pietri et al., 2009; Roberts et al., 2010). The functional significance of these findings is that a few sensory neurons can strongly excite many sensory interneurons, but the relatively weak NMDAR-mediated responses in downstream neurons will not lead to activation of the network unless convergent inputs from sensory interneurons summate and reach threshold (Li et al., 2003).

Our results support these findings in several ways. First, we have shown that following a touch response, CoPAs receive strong, brief glutamatergic inputs with short latencies indicative of monosynaptic connections from RBs that lead to the robust firing of a single overshooting action potential. Secondly, RBs appear to be capable of producing only a single spike at this age (unpublished observations) therefore their synapses onto the CoPA must be strong to ensure that this single spike can activates the touch reflex pathway before shunting glycinergic inputs arrive. Finally, this activation appears to be mediated by AMPARs since we saw neither a reversal of glutamatergic currents at positive potentials nor any change in mEPSC kinetics in the presence of APV.

In neurons such as CoPAs which appear to lack a significant population of NMDARs, calcium-permeable AMPARs are likely to play a key role in raising cytosolic calcium levels needed for neuronal maturation and plasticity (Bowie, 2012). Calcium-permeable AMPARs are highly expressed at early developmental stages but are mostly replaced by AMPARs containing one or more GluR2 subunits later in development (Aizenman et al., 2002; Brill & Huguenard, 2008; Migues et al., 2007; Patten & Ali, 2007). Our results present new evidence

showing that CoPAs express strongly inwardly rectifying AMPARs indicating calcium-permeability (Iino et al., 1990). Additionally, many of these AMPARs were insensitive to polyamine blockade by philanthotoxin, suggesting that they may belong to a recently described, functionally distinct category of AMPARs that are both calcium-permeable and philanthotoxin-resistant (Bowie, 2012). Previous studies have identified the presence of PhTX-insensitive, calcium-permeable AMPARs in the mammalian retina and hippocampus (Mattison et al., 2014; Osswald et al., 2007). In the developing retina the expression of these receptors coincided with the onset of activity in the visual system, suggesting that these novel AMPARs could play a role in synapse maturation. It will be interesting to determine whether the expression of PhTX-insensitive AMPARs in CoPAs coincides with the appearance of early spontaneous and touch–evoked behaviors and if expression is absent in animals in which sensory inputs have been blocked, as has been shown in the retina under conditions of dark-rearing (Osswald et al., 2007).

III.5.4. Sensory gating in other spinal networks

Many predictions regarding the function of different neuronal classes in spinal locomotor systems are based on our knowledge from invertebrates (reviewed by Marder et al., 2005) as well as other simple vertebrates such as lamprey (reviewed by Grillner, 2003) and *xenopus* (reviewed by Roberts et al., 2010). In *C. elegans*, an activated touch reflex circuit driving forward movement provides inhibition to command neurons in the reflex circuit that would otherwise drive backward movement and *vice versa* in order to prevent activation of both circuits at once (Chalfie et al., 1985). During touch-evoked swimming in the *xenopus* tadpole, the dlc sensory interneuron receives postsynaptic inhibition from ascending glycinergic interneurons that suppresses sensory transmission and prevents ongoing activation of the touch reflex (Sillar & Roberts, 1988). Our results reveal that the embryonic zebrafish spinal circuit uses a similar corollary discharge mechanism to inhibit touch reflexes during coiling and swimming. The synaptic properties of CoPAs are likewise tuned to neuronal function as demonstrated by the presence of fast AMPA receptors that drive strong activation following a touch stimulus and slow glycine receptors that mediate lost-lasting shunting. We find physiological evidence that CoPAs express rare glycine receptors with very slow kinetics

and decreased strychnine sensitivity that may correspond to a unique subunit found in neonatal mammalian spinal cord. These findings suggest that both inhibitory corollary discharge and the specialization of postsynaptic receptors are common features of sensory gating in vertebrates. There remains a much greater complexity in dissecting these mechanisms in the mammalian spinal cord, but the recent description of transcription factors defining nine different types of mechanosensory interneurons in the rodent spinal cord (Del Barrio et al., 2013) may provide a tool with which to assess the functional roles and synaptic properties of common sensory interneurons classes across vertebrate species (Jessell, 2000; Goulding, 2009).

III.6. REFERENCES

Aizenman, C. D., Muñoz-Elías, G. and Cline, H. T. (2002). Visually driven modulation of glutamatergic synaptic transmission is mediated by the regulation of intracellular polyamines. *Neuron* 34, 623–34.

Ali, D. W., Buss, R. R. and Drapeau, P. (2000a). Properties of Miniature Glutamatergic EPSCs in Neurons of the Locomotor Regions of the Developing Zebrafish. 181–191.

Ali, D. W., Drapeau, P. and Legendre, P. (2000b). Development of Spontaneous Glycinergic Currents in the Mauthner Neuron of the Zebrafish Embryo. *J. Neurophysiol.* 84, 1726–1736.

Becker, C. M., Hoch, W. and Betz, H. (1988). Glycine receptor heterogeneity in rat spinal cord during postnatal development. *EMBO J.* 7, 3717–26.

Ben-Ari, Y. (2002). Excitatory actions of GABA during development: the nature of the nurture. *Nat. Rev. Neurosci.* 3, 728–739.

Bernhardt, R. R., Chitnis, A. B., Lindamer, L. and Kuwada, J. Y. (1990). Identification of spinal neurons in the embryonic and larval zebrafish. *J. Comp. Neurol.* 302, 603–616.

Bowie, D. (2012). Redefining the classification of AMPA-selective ionotropic glutamate receptors. *J. Physiol.* 590, 49–61.

Brill, J. and Huguenard, J. R. (2008). Sequential changes in AMPA receptor targeting in the developing neocortical excitatory circuit. *J. Neurosci.* 28, 13918–28.

Burzomato, V., Beato, M., Groot-Kormelink, P. J., Colquhoun, D. and Sivilotti, L. G. (2004). Single-channel behavior of heteromeric alpha1beta glycine receptors: an attempt to detect a conformational change before the channel opens. *J. Neurosci.* 24, 10924–40.

Buss, R. R. and Drapeau, P. (2001). Synaptic drive to motoneurons during fictive swimming in the developing zebrafish. *J. Neurophysiol.* 86, 197–210.

Carlisle, T. C. and Ribera, A. B. (2014). Connexin 35b expression in the spinal cord of *Danio rerio* embryos and larvae. *J. Comp. Neurol.* 522, 861–75.

Chalfie, M., Sulston, J. E., White, J. G., Southgate, E., Thomson, J. N. and Brenner, S. (1985). The neural circuit for touch sensitivity in *Caenorhabditis elegans*. *J. Neurosci.* 5, 956–64.

Crapse, T. B. and Sommer, M. A. (2008). Corollary discharge across the animal kingdom. *Nat. Rev. Neurosci.* 9, 587–600.

Del Barrio, M. G., Bourane, S., Grossmann, K., Schüle, R., Britsch, S., O'Leary, D. D. M. and Goulding, M. (2013). A transcription factor code defines nine sensory interneuron subtypes in the mechanosensory area of the spinal cord. *PLoS One* 8, e77928.

Douglass, A. D., Kraves, S., Deisseroth, K., Schier, A. F. and Engert, F. (2008). Escape behavior elicited by single, channelrhodopsin-2-evoked spikes in zebrafish somatosensory neurons. *Curr. Biol.* 18, 1133–7.

Drapeau, P., Ali, D. W., Buss, R. R. and Saint-Amant, L. (1999). In vivo recording from identifiable neurons of the locomotor network in the developing zebrafish. *J. Neurosci. Methods* 88, 1–13.

Easley-Neal, C., Fierro, J., Buchanan, J. and Washbourne, P. (2013). Late recruitment of synapsin to nascent synapses is regulated by Cdk5. *Cell Rep.* 3, 1199–212.

Eaton, R. C., Farley, R. D., Kimmel, C. B. and Schabtach, E. (1977). Functional development in the Mauthner cell system of embryos and larvae of the zebra fish. *J. Neurobiol.* 8, 151–72.

Goulding, M. (2009). Circuits controlling vertebrate locomotion: moving in a new direction. *Nat. Rev. Neurosci.* 10, 507–518.

Grillner, S. (2003). The motor infrastructure: from ion channels to neuronal networks. *Nat. Rev. Neurosci.* 4, 573–86.

Hale, M. E., Ritter, D. A. and Fetcho, J. R. (2001). A confocal study of spinal interneurons in living larval zebrafish. *J. Comp. Neurol.* 437, 1–16.

Han, Y., Li, P. and Slaughter, M. M. (2004). Selective antagonism of rat inhibitory glycine receptor subunits. *J. Physiol.* 554, 649–58.

Hatta, K., Ankri, N., Faber, D. S. and Korn, H. (2001). Slow inhibitory potentials in the teleost Mauthner cell. *Neuroscience* 103, 561–79.

Higashijima, S.-I., Mandel, G. and Fetcho, J. R. (2004a). Distribution of prospective glutamatergic, glycinergic and GABAergic neurons in embryonic and larval zebrafish. *J. Comp. Neurol.* 480, 1–18.

Higashijima, S.-I., Masino, M. A., Mandel, G. and Fetcho, J. R. (2004b). Engrailed-1 expression marks a primitive class of inhibitory spinal interneuron. *J. Neurosci.* 24, 5827–5839.

Iino, B. Y. M., Ozawa, S. and Tsuzuki, K. (1990). Permeation of calcium through excitatory amino acid receptor channels in cultured rat hippocampal neurones. *J. Physiol.* 424, 151-65.

Jean-Xavier, C., Mentis, G. Z., O'Donovan, M. J., Cattaert, D. and Vinay, L. (2007). Dual personality of GABA/glycine-mediated depolarizations in immature spinal cord. *Proc. Natl. Acad. Sci. U. S. A.* 104, 11477–82.

Jessell, T. M. (2000). Neuronal specification in the spinal cord: inductive signals and transcriptional codes. *Nat. Rev. Genet.* 1, 20–9.

Kimmel, C.B., Ballard, W.W., Kimmel, S.R., Ullmann, B. and Schilling, T.F. (1995). Stages of embryonic development of the zebrafish. *Dev. Dyn.* 203, 253–310.

Knogler, L.D., Ryan, J., Saint-Amant, L. and Drapeau, P. (2014). A hybrid electrical/chemical circuit in the spinal cord generates a transient embryonic motor behavior. *J. Neurosci.* 34, 9644–9655.

Kuhse, J., Schmieden, V. and Betz, H. (1990). A single amino acid exchange alters the pharmacology of neonatal rat glycine receptor subunit. *Neuron* 5, 867—873.

Legendre, P. (2001). The glycinergic inhibitory synapse. *Cell. Mol. Life Sci. C.* 58, 760–793.

Li, W.-C., Higashijima, S., Parry, D. M., Roberts, A. and Soffe, S. R. (2004). Primitive roles for inhibitory interneurons in developing frog spinal cord. *J. Neurosci.* 24, 5840–8.

Li, W.-C., Soffe, S. R. and Roberts, A. (2002). Spinal inhibitory neurons that modulate cutaneous sensory pathways during locomotion in a simple vertebrate. *J. Neurosci.* 22, 10924–34.

Li, W.-C., Soffe, S. R. and Roberts, A. (2003). The spinal interneurons and properties of glutamatergic synapses in a primitive vertebrate cutaneous flexion reflex. *J. Neurosci.* 23, 9068–77.

Liao, J. C. and Fetcho, J. R. (2008). Shared versus specialized glycinergic spinal interneurons in axial motor circuits of larval zebrafish. *J. Neurosci.* 28, 12982–12992.

Lynch, J. W. (2004). Molecular structure and function of the glycine receptor chloride channel. *Physiol. Rev.* 84, 1051–95.

Lynch, J. W. (2009). Native glycine receptor subtypes and their physiological roles. *Neuropharmacology* 56, 303–9.

Man, H.-Y. (2011). GluA2-lacking, calcium-permeable AMPA receptors--inducers of plasticity? *Curr. Opin. Neurobiol.* 21, 291–8.

Marder, E., Bucher, D., Schulz, D. J. and Taylor, A. L. (2005). Invertebrate central pattern generation moves along. *Curr. Biol.* 15, R685–99.

Mangin, J.M., Baloul, M., Prado de Carvalho, L., Rogister, B., Rigo, J.M. and Legendre, P. (2003). Kinetic properties of the α2 homo-oligomeric glycine receptor impairs a proper synaptic functioning. *J. Physiol.* 553, 369–386.

Masino, M. A. and Fetcho, J. R. (2005). Fictive swimming motor patterns in wild type and mutant larval zebrafish. *J. Neurophysiol.* 93, 3177–88.

Mattison, H. A., Bagal, A. A., Mohammadi, M., Pulimood, N. S., Reich, C. G., Alger, B. E., Kao, J. P. Y. and Thompson, S. M. (2014). Evidence of calcium-permeable AMPA receptors in dendritic spines of CA1 pyramidal neurons. *J. Neurophysiol.* Apr 2014,DOI: 10.1152/jn.00578.2013.

McDearmid, J. R. and Drapeau, P. (2006). Rhythmic motor activity evoked by NMDA in the spinal zebrafish larva. *J. Neurophysiol.* 95, 401–417.

Mendelson, B. (1986). Development of reticulospinal neurons of the zebrafish. II. Early axonal outgrowth and cell body position. *J. Comp. Neurol.* 251, 172–184.

Migues, P. V, Cammarota, M., Kavanagh, J., Atkinson, R., Powis, D. A. and Rostas, J. A. P. (2007). Maturational Changes in the Subunit Composition of AMPA Receptors and the Functional Consequences of Their Activation in Chicken Forebrain. *Dev. Neurosci.* 29, 232–240.

Moly, P. K., Ikenaga, T., Kamihagi, C. and Islam, A. F. M. T. (2014). Identification of initially appearing glycine-immunoreactive neurons in the embryonic zebrafish brain. *Dev. Neurobiol.* 74, 616-32.

Osswald, I. K., Galan, A. and Bowie, D. (2007). Light triggers expression of philanthotoxin-insensitive Ca2+-permeable AMPA receptors in the developing rat retina. *J. Physiol.* 582, 95–111.

Patten, S. A. and Ali, D. W. (2007). AMPA receptors associated with zebrafish Mauthner cells switch subunits during development. *J. Physiol.* 581, 1043–56.

Pietri, T., Manalo, E., Ryan, J., Saint-Amant, L. and Washbourne, P. (2009). Glutamate drives the touch response through a rostral loop in the spinal cord of zebrafish embryos. *Dev. Neurobiol.* 69, 780–795.

Roberts, A., Li, W.-C. and Soffe, S. R. (2010). How neurons generate behavior in a hatchling amphibian tadpole: an outline. *Front. Behav. Neurosci.* 4, 16.

Rudomin, P. and Schmidt, R. F. (1999). Presynaptic inhibition in the vertebrate spinal cord revisited. *Exp. Brain Res.*, 129, 1–37.

Saint-Amant, L. and Drapeau, P. (2000). Motoneuron activity patterns related to the earliest behavior of the zebrafish embryo. *J. Neurosci.* 20, 3964–3972.

Saint-Amant, L. and Drapeau, P. (2001). Synchronization of an embryonic network of identified spinal interneurons solely by electrical coupling. *Neuron* 31, 1035–1046.

Saint-Amant, L. and Drapeau, P. (1998). Time course of the development of motor behaviors in the zebrafish embryo. *J. Neurobiol.* 37, 622–632.

Satou, C., Kimura, Y., Kohashi, T., Horikawa, K., Takeda, H., Oda, Y. and Higashijima, S.-I. (2009). Functional role of a specialized class of spinal commissural inhibitory neurons during fast escapes in zebrafish. *J. Neurosci.*, 29, 6780–93.

Satou, C., Kimura, Y. and Higashijima, S.-I. (2012). Generation of Multiple Classes of V0 Neurons in Zebrafish Spinal Cord: Progenitor Heterogeneity and Temporal Control of Neuronal Diversity. *J. Neurosci.* 32, 1771–1783.

Sillar, K. T. and Roberts, A. (1988). A neuronal mechanism for sensory gating during locomotion in a vertebrate. *Nature* 331, 262–265.

Singer, J. H., Talley, E. M., Bayliss, D. A., Berger, A. J., Martin, L. S., Cerda, F., Jimenez, V., Fuentealba, J., Muñoz, B., Luis, G., et al., (1998). Development of Glycinergic Synaptic Transmission to Rat Brain Stem Motoneurons. *J. Neurophysiol.* 80, 2608–2620.

Soffe, S. R. (1993). Two distinct rhythmic motor patterns are driven by common premotor and motor neurons in a simple vertebrate spinal cord. *J. Neurosci.* 13, 4456–69.

Takahashi, T. (2005). Postsynaptic receptor mechanisms underlying developmental speeding of synaptic transmission. *Neurosci. Res.* 53, 229–40.

Tong, H. and McDearmid, J. R. (2012). Pacemaker and plateau potentials shape output of a developing locomotor network. *Curr. Biol.* 22, 2285–93.

III.7. FIGURES

FIGURE 1

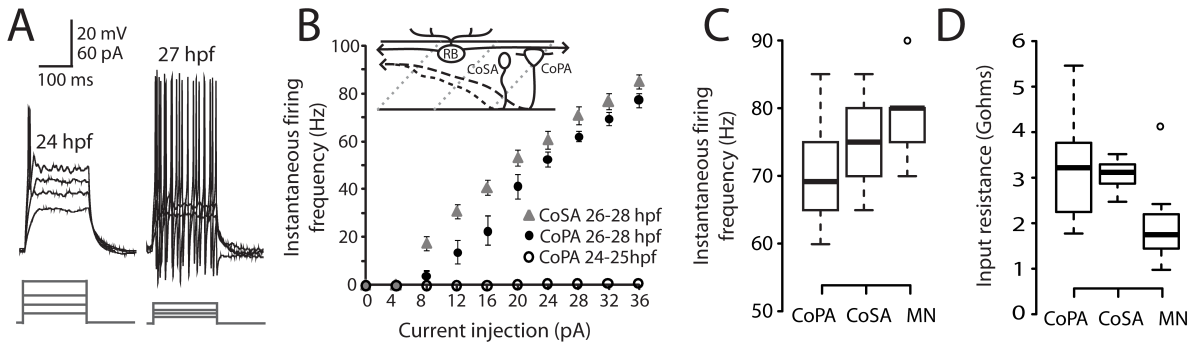

Figure 1. Intrinsic properties of embryonic CoPA interneurons are similar to other spinal neurons. (A) Representative current injections showing single versus burst firing of action potentials in CoPAs at 24 hpf and 27 hpf, respectively. Upper traces, current-clamp recording, lower traces, current steps. Note the reduction in action potential threshold at 27 hpf. **(B)** Quantification of instantaneous firing frequency (Hz) versus current injection (pA) for CoPA and CoSA neurons in 26 – 28 hpf embryos (N = 9, 9) and CoPA neurons in 24 – 25 hpf embryos (N = 5). Inset shows the general morphology of these spinal neurons and the sensory RB neuron that contacts CoPAs. In the drawing, rostral is to the left, dorsal is up, dotted grey lines indicate somite boundaries and dashed black lines indicate commissural axonal projections. **(C)** Box plot showing the similarity of firing frequencies between CoPAs, CoSAs and MNs in 26 – 28 hpf embryos in response to a 32 pA step of depolarizing current (N = 9, 5, 9; $p > 0.05$ for all pairwise comparisons). **(D)** Box plot showing the input resistances for the same classes of neurons as in (C). (N = 9, 7, 9; $p > 0.05$ for all pairwise comparisons).

FIGURE 2

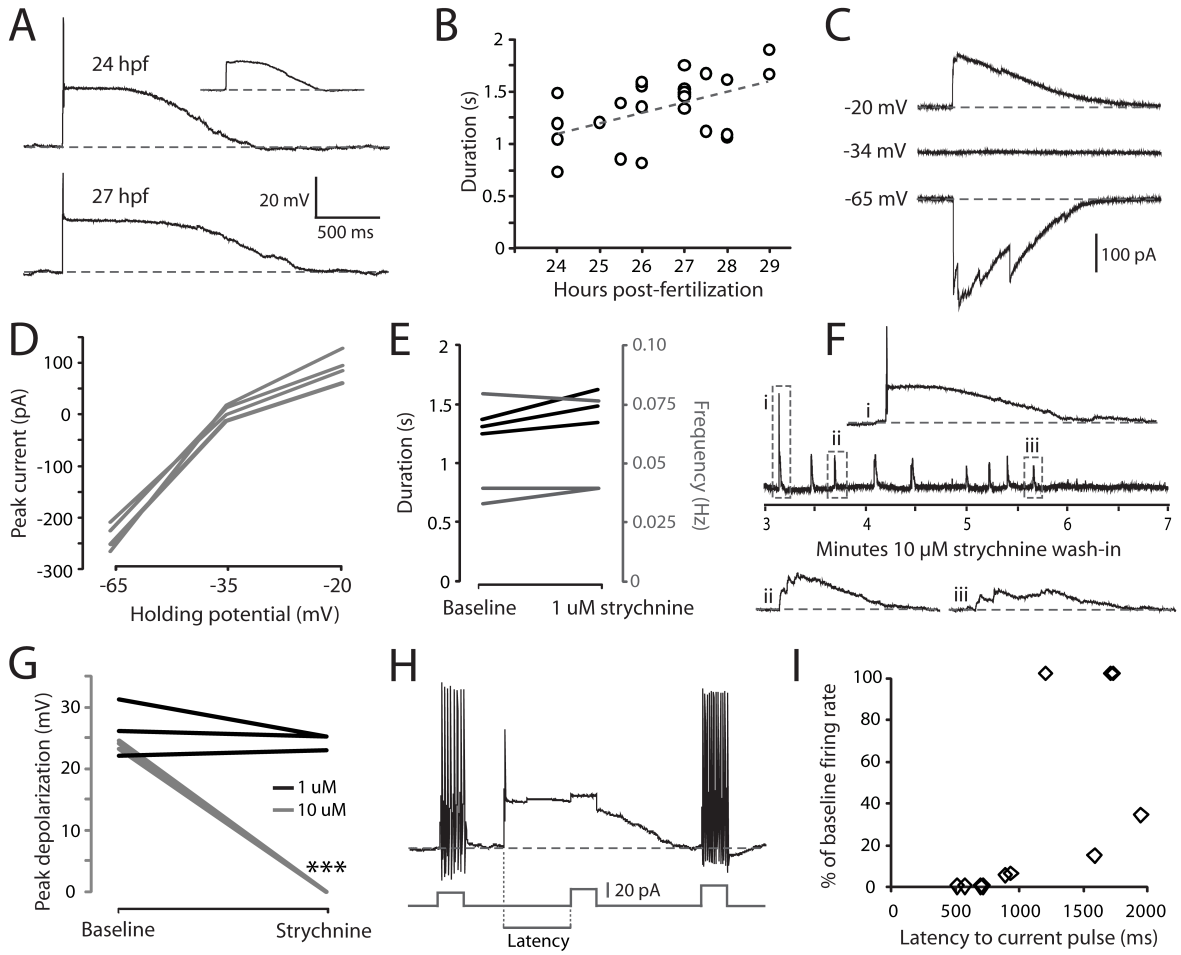

Figure 2. Embryonic CoPAs show spontaneous activity in the form of a long-lasting depolarization that has low strychnine sensitivity and shunts excitation. (A) Large upper trace, representative example of a whole-cell current-clamp recording of a spontaneous depolarizing event in a CoPA interneuron from a 24 hpf embryo that often triggered a small action potential at the onset. Baseline is shown as a dashed grey line for reference and resting membrane potential is -60 ± 5 mV in this and all subsequent current-clamp recordings. Inset upper right, example of a spontaneous depolarizing event in the same neuron that does not produce an action potential (scaled to 50%). Lower trace, a spontaneous depolarizing event recorded from an older 27 hpf embryo. **(B)** A significant positive correlation was found between embryonic age and the duration of depolarizing events in CoPAs. Pearson's correlation coefficient r = 0.49 ($p < 0.05$; N = 25). The best linear fit is shown as a grey

dashed line. **(C)** Representative whole-cell voltage-clamp recording from a CoPA neuron showing that the spontaneous currents are reversed at less negative holding potentials (-20 mV) compared to baseline (-65 mV) and that the net current is zero at -34 mV, the approximate chloride reversal potential. Timescale same as in (A). **(D)** Average peak currents (not including initial spike) for CoPAs at three different holding potentials (N = 4). **(E)** Line graph showing that spontaneous depolarizing events do not change in duration (black lines) or frequency (grey lines) following addition of 1 μM strychnine ($p > 0.05$; N = 3). **(F)** Middle trace, a four-minute excerpt of a current-clamp recording of spontaneous CoPA activity in a 27.5 hpf embryo showing how 10 μM strychnine washing into the extracellular solution eliminates all spontaneous depolarizations over the course of several minutes. Events in dashed boxes i – iii are shown on an expanded timescale for clarity. Scale for i – iii same as in (A). **(G)** Line graph showing that spontaneous depolarizing events are maintained in 1 μM strychnine (black lines; $p > 0.05$; N = 3) but completely lost in 10 μM strychnine (grey lines; $p < 0.001$; N = 3). **(H)** An example of an injection of positive current in a CoPA from a 27 hpf embryo that normally results in sustained action potential firing at baseline (beginning and end of trace) but fails to elicit any action potentials during a spontaneous depolarizing event (middle of trace). Scale for upper trace same as in (A), scale for current injection is shown. The measure of latency used for the subsequent panel is indicated. **(I)** Scatterplot of the reduction in firing frequency as a percentage of baseline when a positive current injection arrives during a spontaneous depolarizing event at various delays. N = 11 events from 5 embryos.

FIGURE 3

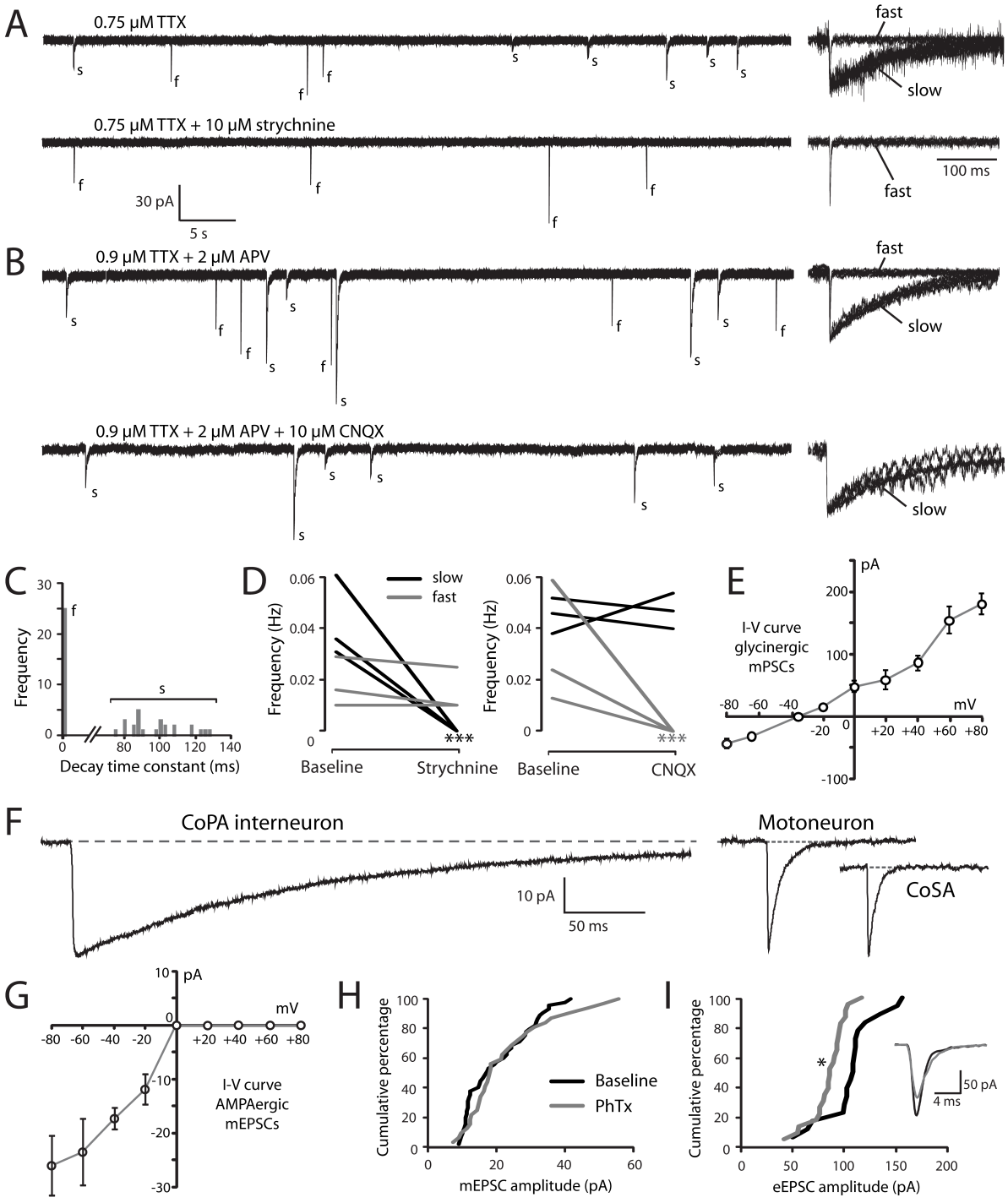
A
0.75 µM TTX
fast
slow
0.75 µM TTX + 10 µM strychnine
30 pA
5 s
100 ms
fast
B
0.9 µM TTX + 2 µM APV
fast
slow
0.9 µM TTX + 2 µM APV + 10 µM CNQX
slow
C
Frequency
Decay time constant (ms)
D
Frequency (Hz)
slow
fast
Baseline
Strychnine
Baseline
CNQX
E
pA
I-V curve
glycinergic
mPSCs
mV
F
CoPA interneuron
10 pA
50 ms
Motoneuron
CoSA
G
pA
mV
I-V curve
AMPAergic
mEPSCs
H
Cumulative percentage
Baseline
PhTx
mEPSC amplitude (pA)
I
Cumulative percentage
50 pA
4 ms
eEPSC amplitude (pA)

Figure 3. Embryonic CoPAs have slow glycinergic mPSCs. (A) Representative excerpt of a whole-cell voltage-clamp recording from a CoPA interneuron in a 29 hpf embryo showing the presence of two distinct categories of mPSCs in the presence of 0.75 μM TTX alone (upper trace, left) labeled "s" and "f" to denote slow and fast events, respectively. Following the additional wash-in of 10 μM strychnine (lower trace, left), slow events are lost but fast events remain, indicating that slow events are glycinergic. Insets at the right show the vertically scaled overlay of all events from the recording excerpt at the left on an expanded timescale. **(B)** Representative excerpt of a whole-cell voltage-clamp recording of mPSCs from a CoPA interneuron in a 28 hpf embryo in the presence of 0.9 μM TTX and 2 μM APV (upper trace) with events labeled as in (A). Following the additional wash-in of 10 μM CNQX (lower trace), fast events are lost but slow events remain, indicating that fast events are glutamatergic. Scale for traces and inset same as for (A). **(C)** Frequency histogram of the first 50 events from the recording in TTX only in (A) showing a clear bimodal distribution of the decay time constants for mPSCs. **(D)** Left, line graph showing that the frequency of slow glycinergic mPSCs (black lines) is abolished with 10 μM strychnine ($p < 0.001$) while fast glutamatergic mPSCs (grey lines) are unaffected ($p > 0.20$; $N = 3$). Right, line graph showing that fast mPSCs are abolished with 10 μM CNQX ($p < 0.001$) while slow mPSC frequency is unaffected ($p > 0.20$; $N = 3$). **(E)** I-V curve of the average peak amplitude for glycinergic mPSCs as a function of membrane holding potential. **(F)** Representative example of an averaged glycinergic mPSC from a recording in a CoPA (left trace, N = 19 events), a motoneuron (middle trace, N = 30 events) and a CoSA neuron (right trace, N = 13 events) in a 29 hpf embryo in the presence of 1 μM TTX and 0.7 μM CNQX. See Table 1 for quantification of mPSC properties. **(G)** I-V curve of the average peak amplitude for AMPAergic mPSCs as a function of membrane holding potential. See Table 2 for quantification of mEPSC properties. **(H)** Cumulative histogram of AMPAergic mEPSC amplitudes at baseline (black trace) and following 10 μM PhTX treatment (grey trace; $p > 0.05$; $N = 3$). **(I)** Cumulative histogram of evoked AMPAergic EPSC amplitudes at baseline (black trace) and following 20 μM PhTX treatment (grey trace; $p < 0.05$; $N = 3$). Inset, overlay of averaged evoked AMPAergic EPSCs from one recording.

FIGURE 4

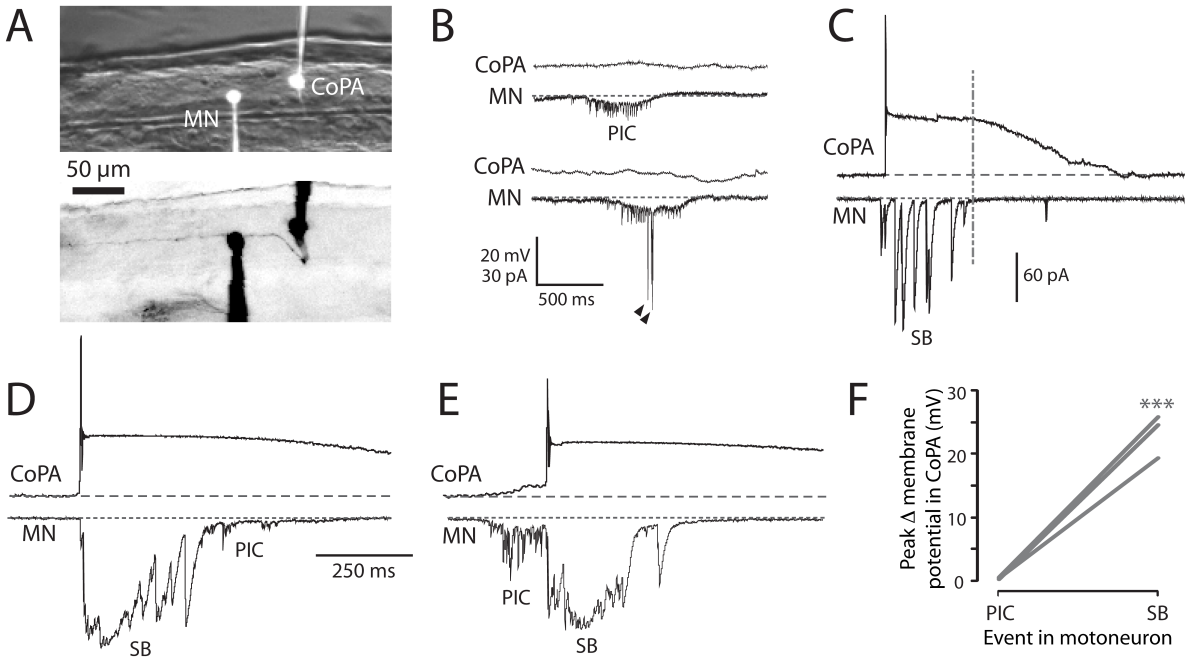

Figure 4. Embryonic CoPAs are inactive during fictive ipsilateral coils and are depolarized by glycinergic inputs during fictive contralateral coils. (A) Image of filled neurons from a simultaneous whole-cell recording of a CoPA and ipsilateral MN. The upper image shows the filled cell bodies in fluorescence against the spinal cord in brightfield. The lower image shows the inverted fluorescent image of rhodamine-filled ipsilateral cell bodies with the ascending contralateral CoPA axon in focus spanning several somites (the ventral MN axon is obscured by the recording electrode). Rostral is to the left and dorsal is to the top. **(B)** Simultaneous whole-cell recordings from a 26 hpf embryo of activity in a CoPA (current clamp, top trace in all pairs) and a MN (voltage-clamp, bottom trace in all pairs) during a spontaneous fictive ipsilateral single coil. The CoPA is inactive during a gap junction-driven current (periodic inward current, PIC) in the ipsilateral MN. Holding potential of MN was -65 mV and baseline is shown as a dotted grey line. Arrowheads in MN trace denote large glutamatergic peaks. **(C)** Depolarizing glycinergic events in CoPAs coincide with glycinergic synaptic bursts (SBs) in ipsilateral MNs during a spontaneous fictive contralateral single coil. Scale same as in (B) but note different vertical scale for MN trace. A vertical dashed line marks the end of the SB in the MN trace. **(D)** A depolarizing glycinergic event in a CoPA

during a spontaneous fictive double coil (synaptic burst, SB, followed by PIC) in a MN resembles the activity seen during a single coil and coincides with the glycinergic portion of the mixed event in the MN. Scale same as in (C) but note different time scale. **(E)** Same conditions as (D) but here for a fictive double coil beginning on the ipsilateral side (PIC preceding SB). All recordings are from the same pair of neurons pictured in (A). **(F)** Comparison of the average change in membrane potential for CoPAs during each type of activity in the MN ($p < 0.001$).

FIGURE 5

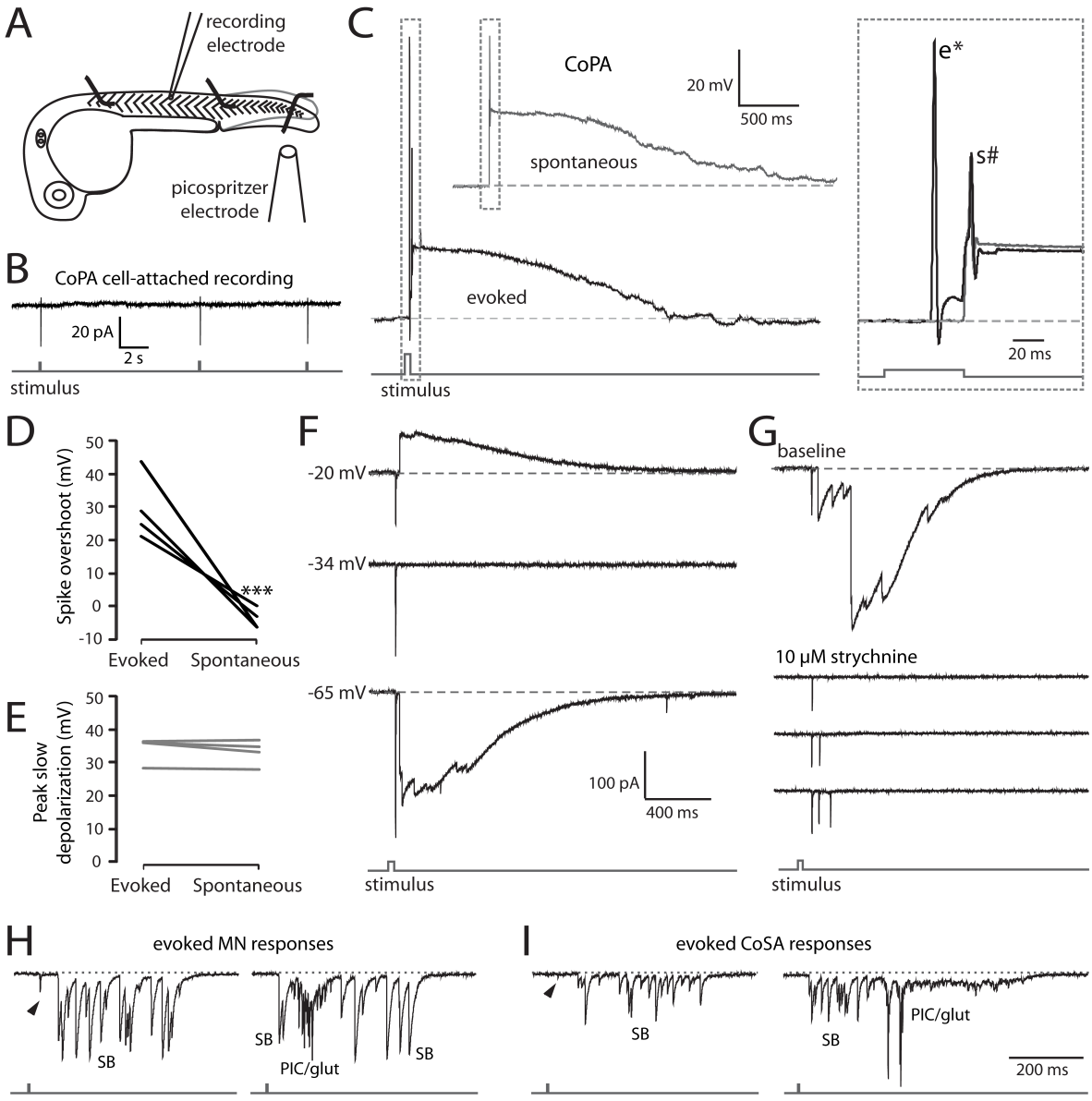

Figure 5. Embryonic CoPAs receive brief glutamatergic excitation then long lasting, shunting glycinergic inputs in response to touch. (A) Cartoon depicting the experimental set-up for recording touch-evoked responses. **(B)** Representative cell-attached recording of single spikes consistently elicited in CoPAs (upper trace) in response to touch stimuli (lower trace). No spontaneous spikes were seen in the absence of stimuli. N = 3. **(C)** Representative

current-clamp recordings of a spontaneous event (upper trace, grey) and an evoked event (middle trace, black and lower stimulus trace, grey) in a 26.5 hpf embryo. Inset, expanded view of the overlapping traces to show the presence of a large amplitude action potential (e*) occurring in the evoked event only and a second smaller action potential (s#) occurring in both events. **(D)** Comparison of the average overshoot reached by the first spike in an evoked *vs* spontaneous event ($p < 0.001$). **(E)** Comparison of the average peak slow depolarization during an evoked *vs* spontaneous event ($p > 0.20$). **(F)** Voltage-clamp recording from the same neuron as in C showing that the evoked response is mediated by two different synaptic inputs: a short-latency glutamatergic EPSP that decreases in amplitude at less negative holding potentials (-20 mV) but does not reverse and a later, long duration glycinergic input that reverses beyond -34 mV. **(G)** Voltage-clamp CoPA recording from a 26 hpf embryo showing that the wash-in in 10 μM strychnine selectively blocks the glycinergic currents but leaves the short latency, fast glutamatergic currents unaffected. Scale same as for (F). **(H, I)** Voltage-clamp recordings of synaptic currents in a motoneuron (H) and a CoSA (I) evoked by an ipsilateral touch stimuli in a 27.5 hpf embryo. Scale same as in (F). Glycinergic synaptic bursts are labeled SB and coincident electrical periodic inward currents and glutamatergic currents are labeled PIC/glut.

FIGURE 6

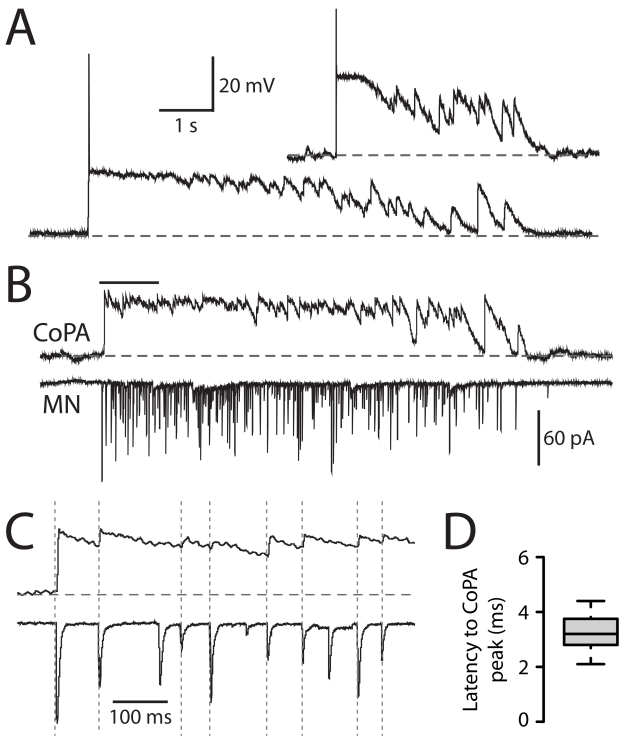

Figure 6. CoPAs receive rhythmic inhibition in phase with excitation to ipsilateral MNs during burst swimming episodes. (A) Two examples of activity patterns in CoPAs from embryos at 27 - 29 hpf that have longer durations than fictive coiling events and whose durations resemble those of bouts of immature swimming at this age. **(B)** Example of a simultaneous whole-cell recording from a 29 hpf embryo of activity in a CoPA (in current clamp) and an ipsilateral motoneuron (in voltage-clamp) during a spontaneous bout of fictive burst swimming. Scale for CoPA trace same as for (A), vertical scale shown for MN trace. **(C)** Ten times horizontally expanded view of the burst from the indicated region in (B). Dotted vertical lines indicate local maxima (peaks) in the CoPA trace that correlate with MN peaks. **(D)** Quantification of the latency between peaks in the CoPA trace relative to peaks in the MN trace. N = 20 peaks from 1 event.

CHAPTER 4

IV. ARTICLE: "SYNAPTIC SCALING AND THE DEVELOPMENT OF A MOTOR NETWORK"

The Journal of Neuroscience (2010) 30(26): 8871– 81.

LINKER STATEMENT

The following study was based on work begun during my masters and completed during my doctorate that aimed to show how developing spinal circuits adapt to changes in network activity. This work was inspired by *in vitro* studies that had revealed a homeostatic mechanism, synaptic scaling, that counteracted decreased neuronal activity with increased synaptic strength. Here, I perturbed network activity with pharmacological manipulations and measured chronic changes in properties at the synapse, neuron, muscle and intact animal using whole-cell electrophysiology and behavioral analyses. This study was one of the first to examine homeostatic synaptic responses in a behavioral context and to reveal the physiological contribution of these plasticity mechanisms to a developing locomotor network.

Section: Behavioral/Systems/Cognitive

Synaptic Scaling and the Development of a Motor Network

Knogler, Laura D.[1,2], Liao, Meijiang[1] and Drapeau, Pierre[1*]

[1]Department of Pathology and Cell Biology and Le Groupe de Recherche sur le Système Nerveux Central, Université de Montréal, Montréal, Québec, Canada H3T 1J4, [2]Graduate program in Neurological Sciences, Department of Neurology and Neurosurgery, McGill University, Montréal, Québec, Canada H3A 2B4

Abbreviated title: Synaptic Scaling during Motor Network Development

*Corresponding author: Pierre Drapeau, Ph.D.
Department of Pathology and Cell Biology
Université de Montréal
C.P. 6128, Succ. Centre-ville
Montréal, Québec H3C 3J7 Canada

Acknowledgements: This work was funded by a grant (PD) from the Canadian Institutes of Health Research and the Groupe de Recherche sur le Système Nerveux Central and a studentship (LK) from the Natural Sciences and Engineering Research Council of Canada. We thank H. Okamoto for the Isl1-GFP transgenic line, L. Saint-Amant for suggesting the bungarotoxin experiment and to him, G. Armstrong and E. Brustein for critiques of the manuscript.

IV.1. ABSTRACT

Neurons respond homeostatically to chronic changes in network activity with compensatory changes such as a uniform alteration in the size of miniature post-synaptic current (mPSC) amplitudes termed synaptic scaling. However, little is known about the impact of synaptic scaling on the function of neural networks *in vivo*. We used the embryonic zebrafish to address the effect of synaptic scaling on the neural network underlying locomotion. Activity was decreased during development by TTX injection to block action potentials or CNQX injection to block glutamatergic transmission. Alternatively TNFα was chronically applied. Recordings from spinal neurons showed that glutamatergic mPSCs scaled up ~25% after activity reduction and fortuitously scaled down ~20% after TNFα treatment and were unchanged following blockade of neuromuscular activity alone with α-bungarotoxin. Regardless of the direction of scaling, immediately following reversal of treatment no chronic effect was distinguishable in motoneuron activity patterns or in swimming behavior. We also acutely induced a similar increase of glutamatergic mPSC amplitudes using cyclothiazide to reduce AMPA receptor desensitization or decrease of glutamatergic mPSC amplitudes using a low concentration of CNQX to partially block AMPA receptors. Though the strength of the motor output was altered, neither chronic nor acute treatments disrupted the patterning of synaptic activity or swimming. Our results show, for the first time, that scaling of glutamatergic synapses can be induced *in vivo* in the zebrafish and that synaptic patterning is less plastic than synaptic strength during development.

Keywords: homeostatic plasticity, activity blockade, development, spinal neurons, synaptic activity, zebrafish

IV.2. INTRODUCTION

A key feature of synapses is their ability to undergo pre- and/or post-synaptic modifications during development and in response to experience and environmental changes. While Hebbian plasticity is known to act rapidly at individual synapses to alter the efficiency of specific neuronal connections (reviewed by Malenka & Bear, 2004), other plasticity mechanisms must integrate these changes over a longer time scale so that synapses onto a given cell are changed accordingly to allow for the net input to remain constant (Miller, 1996). Several forms of homeostatic synaptic plasticity have been described, the best-characterized example of which is synaptic scaling where the strength of all synapses onto a neuron are multiplicatively scaled in a direction that opposes chronic changes in activity (Turrigiano et al., 1998). Most investigations into synaptic scaling have been done *in vitro* or by computational modeling, leaving unanswered the significance of these changes in biologically relevant processes such as development, learning, or disease (Horn et al., 1996; Rabinowitch & Segev, 2008; Turrigiano, 2008; Savioz et al., 2009). Furthermore, of the investigations of glutamatergic synaptic scaling *in vivo* (Desai et al., 2002; Gozales-Islas et al., 2006; Echegoyen et al., 2007; Kaneko et al., 2009; Pawlak et al., 2005), there are very few (Mongeon et al., 2009; Whiting et al., 2009) that also looked at synaptic scaling at glycinergic synapses despite their known role in learning and memory processes (Gaiarsa et al., 2002) and proper patterning of the motor central pattern generator (CPG) of the spinal cord (reviewed by Roberts et al., 2008).

To better understand the characteristics of synaptic scaling and how this affects functional network activity and behavior *in vivo*, we focused on measuring changes at synaptic, network and behavioral levels using the developing zebrafish (*Danio rerio*) motor network as an experimentally accessible model. Development of the zebrafish motor network is rapid as at 18 hours post-fertilization (hpf) the embryo shows spontaneous coiling, at 27hpf a robust touch response can induce swimming events and by 52hpf the embryo has hatched and exhibits swimming behavior (Drapeau et al., 2002; Saint-Amant & Drapeau, 1998). If synaptic scaling is truly a homeostatic process during development, then the changes in synaptic strength following activity perturbation should serve to stabilize this behaviorally relevant network activity.

We tested this hypothesis *in vivo* by examining miniature spontaneous synaptic activity, integrated motoneuron inputs, their output to muscle fibers and the consequent swimming behavior following induction of synaptic scaling. Despite a significant scaling up or down of glutamatergic (but not glycinergic) synapses in spinal neurons following chronic activity blockade or TNFα exposure, respectively, the strength of the motor output was altered but network activity patterns and overall motor behavior did not differ from controls. Furthermore, acute pharmacological manipulations to increase or decrease synaptic amplitudes and the strength of the motor output to a similar extent as observed during chronic synaptic scaling failed to disrupt the pattern of network activity. We conclude that the spinal network can manifest synaptic scaling but the network nonetheless develops a robust activity pattern.

IV.3. MATERIALS AND METHODS

IV.3.1. Zebrafish maintenance

Zebrafish (*Danio rerio*) were bred and maintained at 28.5°C according to standard procedures (Westerfield, 1995). All experiments were performed in compliance with the guidelines of the Canadian Council for Animal Care and conducted at the University of Montreal.

IV.3.2. Pharmacological injections

Wild-type or transgenic embryos (Isl1::GFP transgenic line, gift of H. Okamoto) were anaesthetized in 0.04% tricaine (MS-222; Sigma) dissolved in modified Evans (see later), dechorionated and embedded in a 1% solution of low melting point agarose. Embryos were injected at 17, 24, 48, or 72hpf with either vehicle or the following concentrated doses of drugs to allow for subsequent dilution in the embryo; 250µM 6-cyano-7-nitroquinoxaline-2,3-dione (CNQX; Sigma); 250µM tetrodotoxin (TTX; Tocris); 600µM (2R)-amino-5-phosphonovaleric acid (AP-5; Sigma); or 200 µM α-bungarotoxin (α-BgTx; Sigma). Solutions were injected as a bolus into the brain (up to 30hpf) or heart (after 30hpf) using a fine glass electrode connected to a Picospritzer III (General Valve, Fairfield, NJ). Injection

solutions contained 1% Fast Green for visual control. Embryos were then removed from the agarose and raised as usual. To verify the efficacy of the injections, touch response was assessed over time following injections. Control-injected fish recovered within minutes whereas fish injected with drugs did not recover for several hours if at all. Thus fish responding to touch within minutes following pharmacological injection were excluded (<5%), as well as any fish displaying unusual morphology (<5%).

IV.3.3. Neural recordings

Zebrafish were anaesthetized in 0.04% tricaine dissolved in modified Evans solution containing, in mM: 134 NaCl, 2.9 KCl, 2.1 CaCl2, 1.2 MgCl2, 10 HEPES, 10 glucose, adjusted to 290 mOsm and pH 7.8 and dissected according to previously described procedures (Drapeau et al., 1999). Briefly, spinal neurons in somites 10-15 were selected for recording based on soma size and position as visualized by oblique illumination (Olympus BX61W1). All experiments and manipulations were performed at room temperature.

To record mPSCs, 15µM d-tubocurarine (Sigma) was added to the Evans solution to fully block neuromuscular transmission. Electrophysiological recordings were done in the presence of 0.5µM TTX and 1µM strychnine to isolate glutamatergic mPSCs, or in 0.5µM TTX, 10µM CNQX and 50µM AP-5 to isolate glycinergic mPSCs. Patch-clamp electrodes for spinal neurons (5–12MΩ) pulled from thin-walled Kimax-51 borosilicate glass and were filled with the following intracellular solution, in mM: 105 d-gluconic acid; 16 KCl; 2 MgCl2; 10 HEPES; 10 EGTA adjusted to pH 7.2, 290 mOsm. 0.1% sulforhodamine B (Sigma) was also included in the patch solution to label the cells and confirm their identity after a recording. Standard whole-cell recordings from 3-4dpf larvae were obtained using an Axopatch 200B and an Axon Instruments CV 203BU headstage amplifier (Molecular Devices, Union City, CA). Data were acquired at 40kHz and low-pass filtered at 5kHz. Cells were held near their resting potential at -65mV under voltage-clamp unless otherwise specified. A maximum of three neural recordings were obtained from each larva.

IV.3.4. Intrinsic excitability

Measurements of intrinsic cellular excitability were made with whole-cell current-clamp recordings performed in a TTX-free recording solution. Current was injected into the cell as a continuously increasing ramp (0-500pA, 100ms duration) to measure the minimum required (rheobasic) current to produce an action potential. Spike threshold was also calculated with these data by finding the difference between the voltage threshold for firing and the resting membrane voltage. A plot of action potential firing frequency *versus* current was made by injecting current into the cell in steps (25pA steps up to 375pA, 100ms duration).

IV.3.5. NMDA-induced slow oscillations

Measurements of the frequency of neuronal slow oscillations (related to episodes of swimming) were made by perfusing 200μM NMDA into the extracellular solution, which causes gradual membrane depolarizations of up to 20mV and induces persistent rhythmic activity (McDearmid & Drapeau, 2006). To compensate for the depolarization, up to 60pA of negative current was injected to maintain the troughs of oscillation at -65mV and amplify this part of the activity. Data were analyzed by quantifying the number of complete episodes in a 40s period, yielding a measure of the slow oscillation frequency.

IV.3.6. Muscle recordings

Standard whole-cell recordings using 2-5MΩ electrodes were obtained from slow twitch (embryonic red; ER) muscle fibers identified visually by their proximity to the surface and longitudinal orientation (Buss & Drapeau, 2000). In these recordings the concentration of d-tubocurarine was reduced to approximately 2-3μM to prevent muscle contractions while only partially blocking neuromuscular transmission. The ryanodine receptor antagonist 20μM N-benzyl-p-toluenefonamide (N-BTS; Sigma) in 0.1% DMSO was also added to muscle recordings at 4dpf to prevent muscle contractions. This treatment did not appear to alter neural activity. Fictive swimming patterns in the muscle were either spontaneous or evoked by turning a light on and off. Recordings were analyzed for episode duration, burst duration,

burst frequency, synaptic peaks related to the number of contractions per burst, their frequency, maximum amplitude and percent time active.

IV.3.7. Acute pharmacological treatment

CNQX (1.2-2.4μM) or cyclothiazide (CTZ; 7-10μM; Sigma) was dissolved in Evans and perfused into the recording bath after collecting 5 min of baseline whole-cell neuron or muscle recordings. Data representing the acute CNQX and CTZ treatments were collected from 5 min following the start of the drug application onward.

IV.3.8. Analysis

Electrophysiological analyses were performed offline using Clampex 10.2 and Clampfit 10.2 software (Axon Instruments). mPSCs recordings (lasting 10 minutes) were analyzed using a template to collect the first consecutive 50-200 mPSCs starting 100s into the recording to allow the patch to stabilize. All mPSCs were verified visually before inclusion and mPSCs from each cell were averaged for comparison of amplitudes and frequencies. Measurements of intrinsic excitability, slow oscillation frequency and muscle fiber parameters were measured by hand using program cursors.

SigmaStat 3.5 (Systat Software Inc.) was used to assess data for statistical significance. Statistical analyses used one-way or two-way ANOVA grouped by day and experimental treatment to ensure that there was no interaction effect and thus data could be pooled across days. For paired data sets, the paired Student's t-test was used. For nonparametric statistical testing, we used the Mann-Whitney rank sum test. Significance was assessed at $p<0.05$, as indicated by one asterisk. Two asterisks indicate $p<0.01$ and three asterisks indicate $p<0.001$. All data are represented as mean ± standard error of the mean. All individual mPSCs from each condition were also plotted on a cumulative histograms using Kaleidagraph 3.1 software

IV.3.9. Tnfα expression

RT-PCR from cDNA pools reverse transcribed from RNA isolated from 18, 24, 48, 72, 96 and 120hpf wild-type zebrafish was performed to examine the endogenous expression

of tnfα (GenBank accession: AY427649) during development using the primer pair :(5') ACGTCTGAACTGACTGAGGAACA and (3') GCCAAGAGTGTATGATAGAGGTCA (Invitrogen). tnfb (as a control for cDNA quality) was also amplified using the primer pair: (5') GTACCTGAGCCACACCATCAATC and (3') AGTGCCCTTGTTATAGTGCTCTTG. Fragments were cloned into pGEM-T Easy cloning vector (Promega) and sequenced to confirm identity.

Recombinant zebrafish TNFα was produced from tnfα mRNA synthesized *in vitro*. Briefly, mRNA from zebrafish embryos was isolated and reverse transcribed to make cDNA that was subcloned into the pCS2 vector at the BamH I and Xho I sites and the mRNA was synthesized by the mMESSAGE mMACHINE high yield capped RNA transcription kit (Ambion). tnfα cDNA was inserted into a pQE30 vector by BamH I and pstI fusion with 6his tag. Purification of TNFα protein under native conditions was done by protocols 9 and 12 of QIAexpressionist (Qiagen). Dose-response experiments showed high survival rates and lower concentrations proved just as effective as higher concentrations in preliminary experiments, therefore we chose to inject 1μM of TNFα at 1-2dpf as described above for a final concentration of approximately 50nM after dilution in the embryos, a concentration shown to acutely induce synaptic scaling *in vitro* (Stellwagen et al., 2005).

IV.3.10. Confocal microscopy

To investigate changes in number of neurons across treatments, fixed Isl1-GFP transgenic embryos were imaged using a Quorum WaveFX spinning disk system (Quorum Technologies Inc, Guelph, ON) based on a modified Yokogawa CSU-10 head (Yokogawa Electric) mounted on an upright Olympus BX61W1 fluorescence microscope and connected to a Hamamatsu ORCA-ER camera. Briefly, a set of stacked Z-series images were collected using Volocity software (Improvision) and the number of GFP+ neurons per somite was counted per embryo using Image J.

IV.3.11. Behavioral recordings

Responses to touch at 24hpf were evoked by tapping the fish lightly on the tail with forceps and quantified as either responding or not. These measurements were repeated at

regular intervals to determine the time course of recovery of touch response following injection. Swimming was measured at either 3 or 4dpf to parallel different experimental paradigms that elicited synaptic scaling. Swimming behavior in larval zebrafish transitions rapidly from sustained burst swimming at 2-3dpf to a more mature beat-and-glide pattern by 4dpf (Buss & Drapeau, 2001). Therefore it was most informative to measure tail contraction frequency and free-swimming velocity at 3dpf, when burst swimming is still observed and to measure tail contraction frequency and beat duration at 4dpf, when discrete "beat" periods are present (Buss & Drapeau, 2001).

To measure tail contraction frequency (Buss & Drapeau, 2001), larvae were embedded in 1% low melting-point agarose (Gibco BRL) dorsal side up with the tail free to move. Episodes of tail alternations representative of swimming were elicited by a light tap on the tail with forceps. Movements were filmed at 60Hz with a Point Grey Research (PGR; Vancouver, BC) Grasshopper 2 camera mounted on a Zeiss dissection microscope. A minimum of three episodes of swimming were obtained from each fish to be averaged. Frequency of tail contractions was measured offline by counting the number of full tail contractions per distinct bout of swimming, thus accounting for differences in contraction frequency at the beginning versus end of a swimming bout. Duration of individual swimming beat periods at 4dpf was also measured and averaged across fish in each condition before statistical analysis.

To measure swimming velocity, free-swimming 3dpf larvae were individually placed in a large dish filled with egg water at room temperature and filmed at 15Hz with a PGR Flea 2 camera. The larva was touched lightly on the tail to initiate swimming. Swimming velocity was calculated from the change in position of the larva's head in each frame divided by the duration of swimming using the "manual tracking" plug-in for ImageJ software. Velocity calculations did not include periods of swimming in which the larva was touching or alongside of the wall of the dish.

All video recordings were made using PGR FlyCap software and all video analyses were done using ImageJ software. Data were averaged across all embryos in each experimental group to obtain means for comparison between conditions and statistically analyzed as described for neural and muscle recordings.

IV.4. RESULTS

As synaptic scaling has not been previously studied in zebrafish, we first sought to determine whether and under what conditions it could be induced in living embryos and post-hatching larvae. Electrophysiological and behavioral experiments were performed mostly on 3 or 4dpf zebrafish larvae that were injected with drugs as early as 17hpf, allowing a few days for chronic changes to occur. We started by testing the effects of TTX or CNQX treatment, which reduced activity and caused upward scaling and later those of TNFα treatment, which caused downward scaling.

IV.4.1. Scaling up occurs at glutamatergic synapses upon activity blockade in the zebrafish embryo

The first report of synaptic scaling used chronic TTX treatment of cultured cortical neurons to block action potentials globally and this paradigm has since proved to be a robust way to elicit synaptic scaling in other systems (Turrigiano et al., 1998). We therefore sought to test the effects of TTX on synaptic activity in zebrafish motoneurons. To investigate the *in vivo* effects of drug treatment on developing zebrafish, drugs had to be injected directly into the embryo, as described in the Methods. In order to confirm the efficacy of this method, touch response (Saint-Amant & Drapeau, 1998) was measured post-injection. Injections of TTX 250μM, diluted ~20-fold in the 24hpf embryo, resulted in complete paralysis that never recovered up to 6dpf, thus confirming an effective block of motor activity as previously reported for neural activity (Saint-Amant & Drapeau, 2001). Additionally, while control embryos recovered from their sham injection within 10 minutes to show a touch response, only 50% of CNQX-injected (250 or 500μM) embryos showed a touch response after 2 hours and 100% only after 5-6 hours post-injection. Therefore CNQX significantly reduced activity in comparison to control, though not as persistently as for TTX, possibly indicating a developmental window for its effect. None of these injections resulted in gross morphological abnormalities.

Zebrafish embryos and larvae show two types of swim-related spinal cord synaptic activity: glutamatergic and glycinergic (Buss & Drapeau, 2001; Saint-Amant & Drapeau, 2001) and we therefore examined each type. Electrophysiological recordings of isolated

glutamatergic mPSCs (in the presence of acutely applied TTX and strychnine) were obtained from spinal neurons (N = 132) in 4dpf larvae following various time intervals of chronic TTX treatment. Interestingly, we were able to consistently induce synaptic scaling only after a minimum of 48hrs of TTX treatment when embryos were treated at 2dpf (control, n = 13; TTX, n = 7; amplitudes for control and TTX were 17.5 ± 3 and 20.9 ± 0.9 pA, respectively; $p < 0.05$), or a minimum of 72hrs when embryos were treated at 1dpf (control, n = 17; TTX, n = 17; amplitudes for control and TTX were 18.0 ± 1 and 24.2 ± 2 pA, respectively; $p < 0.05$) (summarized in Fig. 1) . Synaptic scaling induced by these two treatments were comparable, thus data from these conditions were grouped. No synaptic scaling was seen following 48hrs of TTX treatment between 1 and 3dpf (control, n = 20; TTX, n = 23; amplitudes for control and TTX were 22.4 ± 1 and 21.0 ± 0.7 pA, respectively; $p = 0.31$), or after only 24hrs of TTX treatment at any age tested (control, N = 23; TTX, N = 22; $p > 0.80$ for all time intervals) (Fig. 1).

Recordings following TTX treatment from 1 or 2dpf to 4dpf showed that synapses were significantly scaled up by an average ~30% in comparison to amplitudes from vehicle-injected controls (Fig. 2A) (control, n = 24; TTX, n = 30; amplitudes for control and TTX were 18.0 ± 1.4 and 23.4 ± 1.3 pA, respectively; $p < 0.01$). This change in amplitude was not accompanied by any changes in glutamatergic mPSC frequency ($p = 0.33$) or time course (Fig. 2A). Furthermore, a cumulative histogram showed that when a scaling factor was applied, the TTX distribution was almost perfectly superimposable on the control distribution (Fig. 2A), indicating that every synapse was scaled multiplicatively in proportion to its original strength, a hallmark of synaptic scaling.

Furthermore, significantly increased glutamatergic mPSC amplitudes were also seen following CNQX treatment using the same timing of injections (1 or 2 to 4dpf) as was used to induce synaptic scaling with TTX treatment (Fig. 2B). These amplitudes were on average ~20% larger than vehicle-injected controls (control, n = 17; CNQX, n = 22; amplitudes for control and CNQX were 21.0 ± 1.2 and 25.6 ± 1.3 pA, respectively; $p < 0.05$) and also showed evidence of multiplicative scaling (Fig. 2B). Glutamatergic mPSC frequency after CNQX treatment was unchanged from control values ($p = 0.90$) as was the time course (Fig. 2B). Pooled data from TTX and CNQX experiments showed that the degree of scaling

induced was comparable between identified MNs and INs (MNs, n = 18; INs, n = 15; p = 0.50). In contrast to the effects of TTX and CNQX, embryos injected with AP-5 showed no significant differences from vehicle-injected controls in glutamatergic mPSC amplitude (control, n = 9; AP-5, n = 13; p = 0.37) (Fig. 2C), time course, or frequency (p = 0.82). This was in accord with previous literature that showed no effect of chronic AP-5 exposure on glutamatergic mPSC amplitudes (Turrigiano et al., 1998). These experiments thus support the role of bona fide synaptic scaling *in vivo* in the embryonic zebrafish spinal cord in response to activity perturbation, either completely with TTX, or transiently with CNQX.

To determine whether the increase in glutamatergic mPSC amplitudes following TTX or CNQX treatment was due to a reduction in electrical activity within the CNS rather than as a generalized consequence of altered muscle activity, embryos were injected at 1dpf with a high dose of α –BgTx to selectively block muscle nicotinic acetylcholine receptors, resulting in total muscle paralysis but an otherwise normal CNS level of activity. Whole-cell patch-clamp recordings of glutamatergic mPSC amplitudes at 4dpf from α-BgTx treated larvae were not significantly different from vehicle-injected controls (control, n = 5; α-BgTx, n = 4; control and α-BgTx amplitudes were 21.2 ± 2.2 and 20.5 ± 0.9 pA, respectively; p = 0.77), showing that the synaptic scaling seen with TTX and CNQX treatment was dependent on electrical activity within the CNS and not the absence of movement.

IV.4.2. Absence of synaptic scaling at glycinergic synapses

As discussed previously, despite the prevalence of glycinergic synapses in the spinal cord, synaptic scaling has been predominantly investigated at glutamatergic synapses. Interestingly, the same timing of TTX and CNQX treatments (1 or 2 to 4dpf) that elicited synaptic scaling in glutamatergic mPSCs described above was unable to induce significant scaling of glycinergic mPSC amplitudes (Fig. 3A,B) (TTX treatment, p = 0.24; CNQX treatment, p = 0.60). While there was a trend towards smaller glycinergic mPSC amplitudes, which was particularly significant in the presence of CNQX, the amplitudes varied considerably and cumulative histograms showed an uneven decrease that was not indicative of multiplicative synaptic scaling and therefore not similar to the effects seen with glutamatergic mPSCs (Fig. 3A,B). Furthermore, these treatments with TTX or CNQX

resulted in no significant differences in glycinergic mPSC time course (Fig. 3A,B) or frequency (TTX treatment, $p = 0.82$; CNQX treatment, $p = 0.36$). Following AP-5 treatment, there was significant variation in mPSC amplitudes and frequencies between different experimental days (Fig. 3C) (control, $n = 9$; AP-5, $n = 10$; interaction effect between day and condition $p < 0.001$ for amplitude and frequency).

To summarize, our experimental manipulations with TTX and CNQX caused a significant, multiplicative increase in glutamatergic but not in glycinergic mPSC amplitudes or frequency. Our results suggest that the properties of glycinergic and glutamatergic mPSCs are regulated via different mechanisms under these conditions.

IV.4.3. TNFα induces synaptic scaling down

As TNFα plays a significant and biologically relevant role in promoting synaptic scaling (Kaneko et al., 2008; Stellwagen et al., 2005, 2006), we sought to test its effects in the zebrafish embryo. Before testing the effect of manipulating TNFα levels, we first investigated the expression of endogenous TNFα in the embryonic zebrafish with RT-PCR at 18, 24, 48, 72, 96 and 120hpf. Bands corresponding to the amplified sequence were clearly seen at all time points tested, with the exception of low or absent expression at 22hpf (Fig. 4A; $n = 3$) and these bands were confirmed to be TNFα upon sequencing.

We produced recombinant zebrafish TNFα protein (see methods) and injected it into 24hpf embryos at high concentrations (1-5μM) and the injected embryos showed an excellent survival rate (>90%). We timed our injections of TNFα to follow the same parameters as used to induce synaptic scaling with TTX and CNQX treatment (2dpf to 4dpf), but electrophysiological recordings of glutamatergic mPSCs failed to show any significant changes in amplitude that would be indicative of synaptic scaling (control, $n = 6$; TNFα, $n = 7$; amplitudes for control and TNFα were 19.6 ± 2 and 19.0 ± 2 pA, respectively; $p = 0.79$). However, varying the time points of injection and recording revealed that glutamatergic mPSCs were significantly and surprisingly scaled down by ~20% following treatment with TNFα protein from 1 or 2dpf to 3dpf (Fig. 4B,C) (control, $n = 27$; TNFα, $n = 32$; amplitudes for control and TNFα were 22.6 ± 0.9 and 18.0 ± 0.5 pA, respectively; $p < 0.001$). A

cumulative histogram showed that this scaling was indeed a multiplicative phenomenon (Fig. 4B). As before, the time course of the glutamatergic mPSCs did not change (Fig. 4C).

However, the frequency of glutamatergic mPSCs was significantly reduced by approximately 20% following TNFα treatment (Fig. 4D) (frequencies for control and TNFα were 0.11 ± 0.01 and 0.09 ± 0.01 Hz, respectively; $p < 0.05$), perhaps a a result of smaller events being lost in the baseline noise.. A reduction in glutamatergic mPSC frequency could also be representative of a loss of synapses, or even of neurons. Isl1::GFP transgenic zebrafish injected with TNFα at 2dpf were imaged by confocal microscopy at 3dpf to investigate possible changes in the number of spinal neurons. Cell counts showed no significant difference in GFP-positive cells per somite, with an average of 42-45 per somite (Fig. 4D) (control, n = 7; TNFα, n = 6; $p = 0.69$), suggesting that neuronal numbers remained the same but leaving the possibility that synapse number had decreased, though we have no measure of synaptic numbers that would be of sufficient sensitivity to detect such a small (20%) change.

Using the same TNFα treatment protocol that elicited synaptic scaling in glutamatergic mPSCs (injection at 1-2dpf, recording at 3dpf), we investigated glycinergic mPSC characteristics but we found no significant differences between the amplitude of glycinergic mPSCs from TNFα-treated embryos and controls (control, n = 5; TNFα, n = 5; $p = 0.79$). A cumulative histogram showed no clear shift of the amplitude distribution in either direction neither were there any changes in mPSC time course (Fig. 4E). Additionally, the frequency of glycinergic mPSCs under this experimental condition was comparable to control ($p = 0.79$).

To summarize, while we could robustly elicit synaptic scaling in glutamatergic mPSCs with TTX, CNQX, or TNFα treatment, no changes were seen in glycinergic mPSC amplitude or time course or in the frequency of either type of mPSC following any of these treatments.

IV.4.4. No changes in intrinsic cellular excitability

Although the spinal network underlying locomotion in the zebrafish embryo appears to be synaptically driven (Buss and Drapeau, 2000) rather than due to intrinsic rhythmic neural firing properties (Buss et al., 2003), studies in the chick embryo have shown that intrinsic changes in cellular excitability can accompany, or precede, changes in synaptic

strength (Wilhelm et al., 2009). We therefore examined intrinsic excitability in 3dpf larvae treated with TNFα and in 4dpf larvae treated with CNQX, the different stages at which scaling down and scaling up, respectively, of mPSCs were observed.

Electrophysiological recordings of spinal neurons under current clamp from TNFα-treated larvae showed that no significant changes in intrinsic cellular excitability from control larvae at 3dpf as measured by average rheobase current (Fig. 5A) ($p = 0.08$), spike threshold (Fig. 5B) ($p = 0.79$) and frequency versus current (f-I) plot (Fig. 4D) (control, $n = 11$; TNFα, $n = 10$; $p > 0.05$ for all frequency data pairs at a given current step). Likewise, no significant differences were found at 4dpf between CNQX-treated and control larvae for average rheobase current (Fig. 5A) ($p = 0.32$), spike threshold (Fig. 5B) ($p = 0.77$), or frequency versus current (f-I) plot (Fig. 5C,D) (control, $n = 6$; CNQX, $n = 8$; $p > 0.05$ for all frequency data pairs at a given current step). These results suggest that synaptic rather than intrinsic modes of homeostatic plasticity dominated under these experimental conditions.

IV.4.5. Homeostatic plasticity of network activity and motor behavior

Beyond synaptic scaling and intrinsic excitability, homeostatic plasticity may be measurable as changes in network activity that arise from the integration of cellular and synaptic properties. Because CNQX and TNFα exhibit their effects at different stages in our protocols, we measured neural, muscular and behavioral activity in 3dpf larvae treated with TNFα or in 4dpf larvae treated with CNQX, the different stages at which glutamatergic mEPSCs scaled down and scaled up, respectively.

We examined the rhythmic input to MNs to investigate if components of 'fictive' swimming (in partially paralyzed embryos; Drapeau et al., 1999) were disrupted at the spinal network level following perturbation of network activity. We found that the frequency of slow, swim episode-related oscillations in spinal neurons evoked by the application of 200μM NMDA (McDearmid & Drapeau, 2006) appeared to not be significantly different following chronic TNFα (control, $n = 4$; TNFα, $n = 3$; $p = 0.19$) or CNQX (control, $n = 3$; CNQX, $n = 3$; $p = 0.71$) treatment (Fig. 6). Thus, slow oscillation frequencies at 3dpf were within the range of 0.7-1.1Hz for control and TNFα-treated larvae and in the range of 0.7-0.9Hz at 4dpf for CNQX-treated and control larvae.

Following this, we investigated the neuromuscular output of the spinal MNs onto muscle fibers in partially paralyzed embryos (see methods). The recordings were performed under the same conditions where synaptic scaling of glutamatergic mPSCs was seen in MNs. At 3dpf, recordings of synaptic activity representing fictive bursts of swimming in slow twitch (red) muscle were quantitatively compared between TNFα-treated and control larvae (Fig. 7A,B). These bursts consist of a steady synaptic depolarization on which is superimposed a regular oscillation in synaptic intensity, with peaks that correspond to ipsilateral muscle contractions (Buss & Drapeau, 2001). The maximum synaptic amplitude of bursts was significantly reduced from control values by ~40% in TNFα- treated larvae (amplitudes of control and TNFα were 5.1 ± 1.0 and 8. 5 ± 1.0 mV, respectively; $p < 0.05$) but no significant changes were seen from control values in burst duration or synaptic peak frequency (control, n = 11; TNFα, n = 9; $p = 0.90$ and 0.17, respectively). At 4dpf, recordings of synaptic activity representing episodes of fictive beat and glide swimming from slow twitch muscle in CNQX-treated and control larvae were not significantly different from control in any parameter, including episode duration, beat duration, beat frequency, synaptic peaks per beat, synaptic peak frequency, maximum synaptic amplitude, or percent time active (Fig. 7C,D) (control, n = 6; CNQX, n = 8; $p > 0.05$ for all parameters).

Finally, under the same conditions where synaptic scaling of glutamatergic mPSCs was seen in MNs, we examined plasticity in the intact organism by looking at behavioral changes following activity perturbations in parameters of burst swimming at 3dpf and beat-and-glide swimming at 4dpf using high-speed video recordings (Fig. 8A). Quantitative analysis of burst swimming behavior of TNFα- treated larvae at 3dpf revealed that their motor activity was not measurably different from controls in terms of tail contraction frequency (control, n = 3; TNFα, n = 5; $p = 0.33$) or free-swimming velocity (Fig. 8B; control, n = 11; TNFα, n = 13; $p = 0.95$). Contraction frequency was within the range of 36-40Hz and average velocity was approximately 28mm/s for both conditions at 3dpf. Likewise, analysis of beat and glide swimming at 4dpf in CNQX-treated larvae revealed that their swimming behavior was not measurably different from controls in terms of tail contraction frequency (control, n = 8; CNQX, n = 9; $p = 0.51$) or beat duration (Fig. 8C; control, n = 8; CNQX, n = 9; $p = 0.11$).

Contraction frequency was close to 20Hz at 4dpf while beat duration was approximately 300-400ms for both conditions at 4dpf.

Together, these results indicate that normal levels of neural, muscular and behavioral activity were maintained under conditions of upwards or downwards synaptic scaling.

IV.4.6. Comparable acute changes in synaptic amplitudes do not disrupt network activity patterns

While the results presented above indicate that synaptic scaling may help stabilize motor activity patterns, it is possible if not likely that an intrinsic developmental program is equally important for motor development. To examine this latter possibility, we attempted to induce an increase or decrease in synaptic strength by acute pharmacological treatments and determine its impact on patterned motor network function. The treatments consisted of either immediately reducing synaptic strength with a low concentration of CNQX, or increasing synaptic amplitude by reducing AMPA receptor desensitization with CTZ (Trussell et al., 1993).

Preliminary electrophysiological experiments measuring the effect of acute CNQX treatment on glutamatergic mPSC amplitudes (n = 9) indicated that a concentration of 1μM CNQX reduced glutamatergic mPSC amplitudes by ~15% (n = 5; average amplitude at baseline and following CNQX was 20.7 ± 1.2 and 17.6 ± 0.7 pA, respectively; $p < 0.05$), as seen during scaling down following chronic TNFα treatment. Another set of preliminary experiments investigating the effects of acute CTZ treatment on glutamatergic mPSC amplitudes showed that 10μM CTZ acutely and significantly increased amplitudes by ~25% (n = 5; average amplitude at baseline and following CTZ was 24.8 ± 2.3 and 30.2 ± 1.9 pA, respectively; $p < 0.05$).

In order to rapidly introduce these agents, we recorded patterned motor input to muscle cells in exposed preparations during acute perfusion with either 1μM CNQX or 10μM CTZ. At 3dpf, recordings from slow twitch muscle showed that acute application of CNQX was sufficient to significantly reduce maximum synaptic amplitude during episodes of fictive swimming by ~25% (n = 3; amplitudes at baseline and following CNQX were 10.3 ± 1.7 and 7.5 ± 1.1 pA, respectively; $p < 0.05$) but failed to affect burst length and synaptic peak

frequency (Fig. 9A,B) ($p = 0.33$ and 0.42, respectively). At 4dpf, recordings from slow twitch muscle showed that acute application of 10μM CTZ significantly increased the maximum synaptic amplitude during fictive swimming by ~50% (Fig. 9C,D) ($n = 10$; amplitudes at baseline and following CTZ were 2.3 ± 0.4 and 3.5 ± 0.6 pA, respectively; $p < 0.01$) and slightly but significantly increased the synaptic peak frequency as well (Fig. 9D) (average frequency at baseline and following CTZ was 22.2 ± 0.6 and 23.4 ± 0.6 pA, respectively; $p < 0.01$). However, episode duration, beat duration, beat frequency, number of synaptic peaks per beat and percent time active remained unchanged (Fig. 9D) ($p > 0.05$ for all parameters). Together, these results indicate that the proper patterning of motor output can be maintained under conditions of altered synaptic amplitudes equivalent to those achieved by synaptic scaling.

IV.5. DISCUSSION

Previous studies have shown that neurons can respond homeostatically to reductions in network activity in a variety of ways, one of which is synaptic scaling. We have shown here that glutamatergic synaptic scaling occurs in the developing zebrafish and the behavioral implications are described for the first time in any preparation. In agreement with the literature, chronically reducing activity with either CNQX or TTX *in vivo* resulted in a significant and multiplicative scaling up (by approximately 30%) of glutamatergic mPSCs. However, in contrast to the scaling up observed following acute treatment with TNFα (Stellwagen et al., 2005, 2006), we observed that chronic TNFα treatment caused a significant and multiplicative scaling down (by approximately 20%) of glutamatergic mPSCs. Peripheral blockade of NMJs was insufficient to induce scaling, indicating a requirement for alteration of central network activity. No effect was seen with AP-5 treatment or of TTX treatment on the amplitudes of glycinergic mPSCs, on the frequency of either type of mPSCs, or on intrinsic excitability of spinal neurons, although CNQX treatment caused an un-scaled reduction in mPSC amplitudes. Proper patterning of motor activity, as recorded in neurons, muscle cells and in behavioral analyses, was maintained upon chronic synaptic scaling, either up or down, though the total synaptic amplitude may have changed. During comparable acute

pharmacological alterations in synaptic strength, motor activity showed reduced total synaptic amplitude but normal patterning persisted.

IV.5.1. Neuronal activity

Our results and those published previously for other preparations (Gozales-Islas et al., 2006; Echegoyen et al., 2007; O'Brien et al., 1998; Sutton et al., 2006; Thiagarajan et al., 2005; Turrigiano et al., 1998) showed an increase in synaptic strength at glutamatergic synapses following TTX or CNQX treatment. As TTX blocked all activity whereas CNQX blocked only transiently, this indicates that a reduction of activity is sufficient to induce the maximal scaling up observed upon complete block of activity. We observed a striking difference in the response of glutamatergic synapses to chronic TNFα treatment in our experiments. In cultured hippocampal neurons, acute exposure to TNFα rapidly scales synapses up by approximately 125% within 15 minutes (Stellwagen et al., 2005, 2006), while in our experiments they were significantly and multiplicatively scaled down after 24 hours to approximately 80% of control values. Interestingly, chronic TNFα treatment did result in a small but significant decrease in glutamatergic mPSC frequency of approximately 20% from control values, but this may simply reflect an inability to detect some smaller amplitude events as they become obscured by background noise. Perhaps the differences in homeostatic responses to TNFα are due to differences in dose- or time-dependence in different preparations. Although the research to date has not shown that the same molecule is capable of mediating synaptic scaling bidirectionally, it is nonetheless possible that the concentration or timing of TNFα action could change the direction of synaptic scaling.

Although no significant scaling up or down of glycinergic mPSCs was seen following any of our treatments, other studies have provided evidence of activity-dependent synaptic scaling of glycinergic synapses in a homeostatic manner. Mongeon et al., (2009) demonstrated *in vivo* that evoked glycinergic IPSC amplitudes from spinal motor neurons in zebrafish shocked glial glycine transporter mutants scale down as the fish recover their ability to swim. Also, Whiting et al., (2009) showed that glycine receptor subunit expression in the rat cochlear nucleus was downregulated *in vivo* following monaural deprivation. Further

investigations will be required to better elucidate the role of glycinergic synapses in mechanisms of homeostatic plasticity.

In addition to changes in synaptic properties, we also looked for possible changes in intrinsic cellular excitability following perturbations in network activity. However, the minimum current threshold required to produce an action potential, the spike voltage threshold and the input-output relationship for current-induced firing were not significantly different in CNQX or TNFα treated larvae. The CNQX treatment results are in agreement with a recent study by Wilhelm et al., (2009) that showed no changes in cellular excitability in spinal neurons regardless of the duration of glutamatergic receptor blockade. In contrast, they found a significant increase in cellular excitability 12 hours into chronic GABA receptor blockade as measured by rheobase current and spike threshold and these changes decreased with time so that by 48hrs post-injection excitability was comparable to controls.

IV.5.2. Behavioral consequences

Network activity is hypothesized to be maintained in the face of activity perturbation if synaptic scaling is a homeostatic process. Recordings of mature swimming behavior (at 3dpf following TNFα treatment and 4dpf following CNQX treatment) showed that no parameters of patterned swimming behavior were different from control at these stages. Similarly, our recordings from muscle fibers in TNFα- or CNQX-treated preparations showed no change from control in any temporal parameter of fictive swimming such as frequency or duration of swimming bursts and no changes were measured in the slow oscillation component of rhythmic MN activity that are related to fictive swimming, consistent with a homeostatic maintenance of swimming activity. Acute pharmacological treatments that induced similar changes in synaptic strength and in the synaptic amplitude of motor output had no effect on the patterning of motor output. These latter results indicate that while synaptic scaling can be induced in the zebrafish spinal cord, synaptic patterning is more robust than synaptic strength during development and patterning can occur in the absence of homeostasis.

Certain caveats apply to the interpretation of our results in zebrafish spinal cord. We may have underestimated the extent of synaptic scaling up as we observed partial reversal of

inhibition by CNQX. Nonetheless, Wilhelm and Wenner (2008) used a similar technique of a bolus injection of activity-reducing drugs in the *in ovo* chick spinal cord and measured the recovery of spontaneous network activity by mechanisms that include synaptic scaling. They showed that injection of a single receptor antagonist such as CNQX resulted in a temporary reduction in spontaneous network activity (as measured by immature limb movements) that recovered to control levels within hours. Nonetheless, we were surprised at the robustness of the patterned motor activity in muscle since near complete blockade by CNQX was required to suppress it, reflecting the resilience of the motor circuitry. However, in the absence of a behavioral measure of the consequences of acute changes in synaptic strength, we cannot exclude the possibility that these changes have significant behavioral consequences. Alternatively, it could be that global changes in excitatory transmission reset the entire system up or down and therefore leave the original balance intact and that they would have seen an impact had they induced a targeted change in excitability.

Activity-dependent scaling of glutamatergic synapses appears to be a ubiquitous neural phenomenon and helped compensate for changes in synaptic strength in the zebrafish motor network. However, synaptic scaling did not appear to be required to maintain the patterning of motor activity *in vivo*, which likely forms as a consequence of an intrinsic developmental program. It is interesting to note that complete blockade of glycinergic activity in zebrafish embryos has a drastic effect on neurogenesis, resulting in the loss of half the spinal neurons and indicating that there is a minimal activity-dependence for these early steps of differentiation in development (McDearmid et al., 2006; Reynolds et al., 2008). The milder disruptions in glycinergic function observed in a glycine transporter mutant indicate that glycinergic strength is also susceptible to a form of synaptic homeostasis over a period of several days (Mongeon et al., 2009). Perhaps synaptic scaling may be required for maintaining a strong motor output and for motor development once the circuits become more dependent on feedback from the environment and descending control mechanisms.

IV.6. REFERENCES

Buss RR, Drapeau P (2000) Physiological properties of zebrafish embryonic red and white muscle fibers during early development. J Neurophysiol 84:1545-1557.

Buss RR, Drapeau P (2001) Synaptic drive to motoneurons during fictive swimming in the developing zebrafish. J Neurophysiol 86:197-210.

Buss RR, Bourque CW, Drapeau P (2003) Membrane properties related to the firing behavior of zebrafish motoneurons. J Neurophysiol 89:657-664.

Desai NS, Cudmore RH, Nelson SB, Turrigiano GG (2002) Critical periods for experience-dependent synaptic scaling in visual cortex. Nat Neurosci 5:783-789.

Drapeau P, Ali DW, Buss RR, Saint-Amant L (1999) *In vivo* recording from identifiable neurons of the locomotor network in the developing zebrafish. J Neurosci Methods 88:1-13.

Drapeau P, Saint-Amant L, Buss RR, Chong M, McDearmid JR, Brustein E (2002) Development of the locomotor network in zebrafish. Prog Neurobiol 68:85-111.

Echegoyen J, Neu A, Graber KD, Soltesz I (2007) Homeostatic plasticity studied using *in vivo* hippocampal activity-blockade: Synaptic scaling, intrinsic plasticity and age-dependence. PLoS ONE 2:e700.

Gaiarsa J-L, Caillard O, Ben-Ari Y (2002) Long-term plasticity at GABAergic and glycinergic synapses: Mechanisms and functional significance. Trends Neurosci 25:564-570.

Gonzalez-Islas C, Wenner P (2006) Spontaneous network activity in the embryonic spinal cord regulates AMPAergic and GABAergic synaptic strength. Neuron 49:563-575.

Horn D, Levy N, Ruppin E (1996) Neuronal-based synaptic compensation: A computational study in Alzheimer's disease. Neural Comput 8:1227-1243.

Kaneko M, Stellwagen D, Malenka RC, Stryker MP (2008) Tumor necrosis factor-[alpha] mediates one component of competitive, experience-dependent plasticity in developing visual cortex. Neuron 58:673-680.

Malenka RC, Bear MF (2004) LTP and LTD: An embarrassment of riches. Neuron 44:5-21.

McDearmid JR, Drapeau P (2006) Rhythmic motor activity evoked by NMDA in the spinal zebrafish larva. J Neurophysiol 95:401-417.

McDearmid JR, Liao M, Drapeau P (2006) Glycine receptors regulate interneuron differentiation during spinal network development. Proc Natl Acad Sci USA 103:9679-9684.

Miller KD (1996) Synaptic economics: Competition and cooperation in synaptic plasticity. Neuron 17:371-374.

Mongeon R, Gleason MR, Masino MA, Fetcho JR, Mandel G, Brehm P, Dallman JE (2008) Synaptic homeostasis in a zebrafish glial glycine transporter mutant. J Neurophysiol 100:1716-1723.

O'Brien RJ, Kamboj S, Ehlers MD, Rosen KR, Fischbach GD, Huganir RL (1998) Activity-dependent modulation of synaptic AMPA receptor accumulation. Neuron 21:1067-1078.

Pawlak V, Schupp BJ, Single FN, Seeburg PH, Kohr G (2005) Impaired synaptic scaling in mouse hippocampal neurones expressing NMDA receptors with reduced calcium permeability. The Journal of Physiology 562:771-783.

Rabinowitch I, Segev I (2008) Two opposing plasticity mechanisms pulling a single synapse. Trends Neurosci 31:377-383.

Reynolds A, Brustein E, Liao M, Mercado A, Babilonia E, Mount DB, Drapeau P (2008) Neurogenic role of the depolarizing chloride gradient revealed by global overexpression of kcc2 from the onset of development. J Neurosci 28:1588-1597.

Roberts A, Li W-C, Soffe S (2008) Roles for inhibition: Studies on networks controlling swimming in young frog tadpoles. J Comp Physiol A 194:185-193.

Saint-Amant L, Drapeau P (1998) Time course of the development of motor behaviors in the zebrafish embryo. J Neurobiol 37:622-632.

Saint-Amant L, Drapeau P (2001) Synchronization of an embryonic network of identified spinal interneurons solely by electrical coupling. Neuron 31:1035-1046.

Savioz A, Leuba G, Vallet PG, Walzer C (2009) Contribution of neural networks to Alzheimer disease's progression. Brain Res Bull 80:309-314.

Stellwagen D, Beattie EC, Seo JY, Malenka RC (2005) Differential regulation of AMPA receptor and GABA receptor trafficking by tumor necrosis factor-{alpha}. J Neurosci 25:3219-3228.

Stellwagen D, Malenka RC (2006) Synaptic scaling mediated by glial TNF-[alpha]. Nature 440:1054-1059.

Sutton MA, Ito HT, Cressy P, Kempf C, Woo JC, Schuman EM (2006) Miniature neurotransmission stabilizes synaptic function via tonic suppression of local dendritic protein synthesis. 125:785-799.

Thiagarajan TC, Lindskog M, Tsien RW (2005) Adaptation to synaptic inactivity in hippocampal neurons. Neuron 47:725-737.

Trussell LO, Zhang S, Ramant IM (1993) Desensitization of AMPA receptors upon multiquantal neurotransmitter release. Neuron 10:1185-1196.

Turrigiano GG (2008) The self-tuning neuron: Synaptic scaling of excitatory synapses. Cell 135:422-435.

Turrigiano GG, Leslie KR, Desai NS, Rutherford LC, Nelson SB (1998) Activity-dependent scaling of quantal amplitude in neocortical neurons. Nature 391:892-896.

Westerfield M (1995) The zebrafish book: A guide for laboratory use of zebrafish (*brachydanio rerio*). Eugene, OR: University of Oregon.

Whiting B, Moiseff A, Rubio ME (2009) Cochlear nucleus neurons redistribute synaptic AMPA and glycine receptors in response to monaural conductive hearing loss. Neuroscience 163:1264-1276.

Wilhelm JC, Rich MM, Wenner P (2009) Compensatory changes in cellular excitability, not synaptic scaling, contribute to homeostatic recovery of embryonic network activity. Proc Natl Acad Sci USA 106:6760-6765.

Wilhelm JC, Wenner P (2008) GABAA transmission is a critical step in the process of triggering homeostatic increases in quantal amplitude. Proc Natl Acad Sci USA 105:11412-11417.

IV.7. FIGURES

FIGURE 1

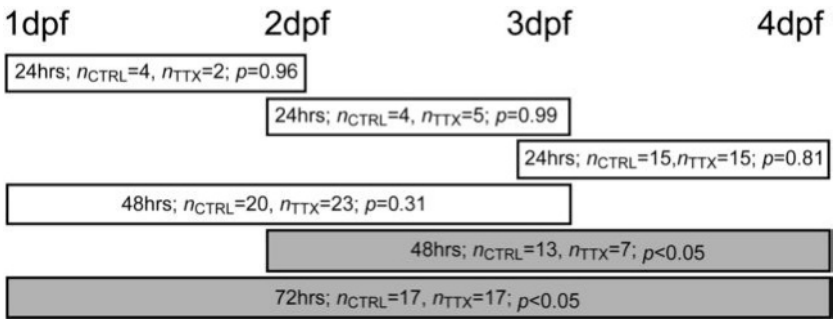

Figure 1. A significant increase in glutamatergic mPSC amplitude was only seen following chronic blockade of network activity with TTX from 1 or 2dpf to 4dpf. Boxed text refers to TTX treatment duration starting at time of injection and ending at time of recording, number of recordings in control and treated larvae and significance of mPSC amplitude change.

FIGURE 2

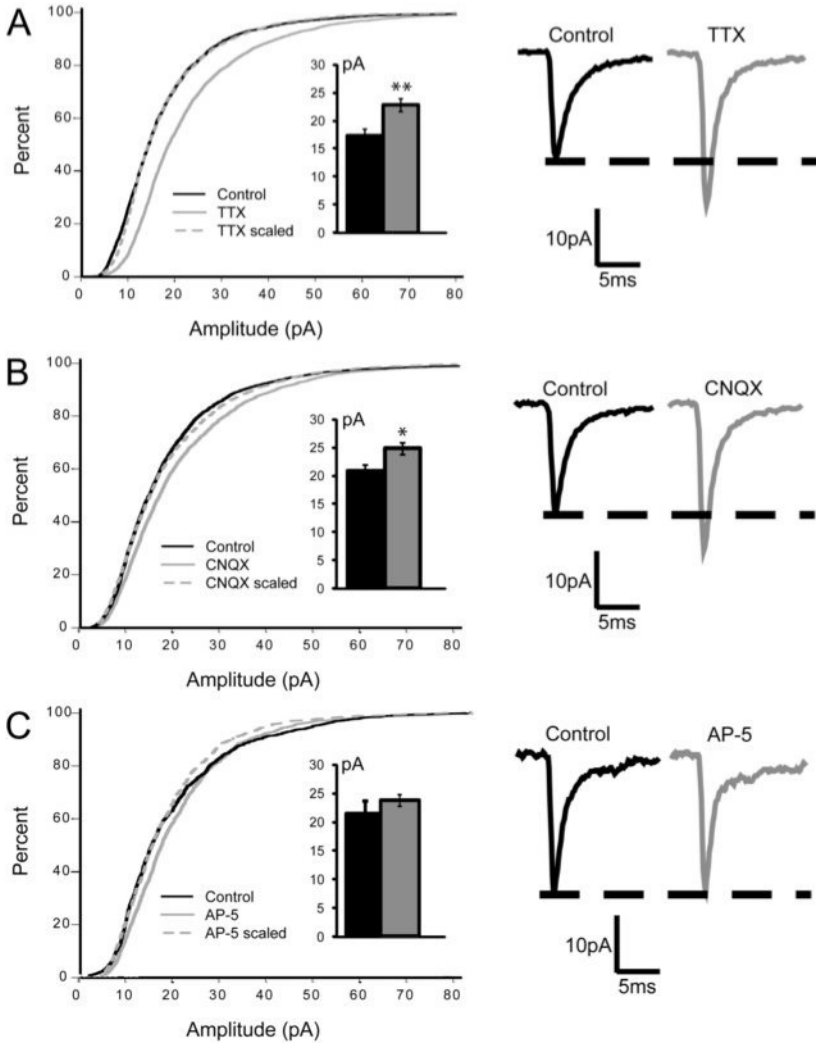

Figure 2. Chronic TTX or CNQX treatment results in a scaling up of glutamatergic mEPSC amplitudes at 4dpf. A. Left, cumulative histograms of glutamatergic mEPSC amplitudes from control (n = 24) and TTX-treated (n = 30) embryos (≥ 50 events per neuron). Inset, average mEPSC amplitude for the same conditions. Right, average mEPSC waveforms of one neuron for the same conditions. B. Left, cumulative histograms of glutamatergic mEPSC amplitudes from control (n = 17) and CNQX-treated (n = 22) embryos. Inset, average mEPSC amplitude for the same conditions. Right, average mEPSC waveforms of one neuron for the same conditions. C. Left, cumulative histograms of glutamatergic mEPSC amplitudes from control (n = 9) and AP-5-treated (n = 13) embryos. Inset, average mEPSC amplitude for the same conditions. Right, average mEPSC waveforms of one neuron for the same conditions. All data here and below are reported as mean ± SEM for the number of neurons indicated; 2-way ANOVA, *$p<0.05$, **$p<0.01$.

FIGURE 3

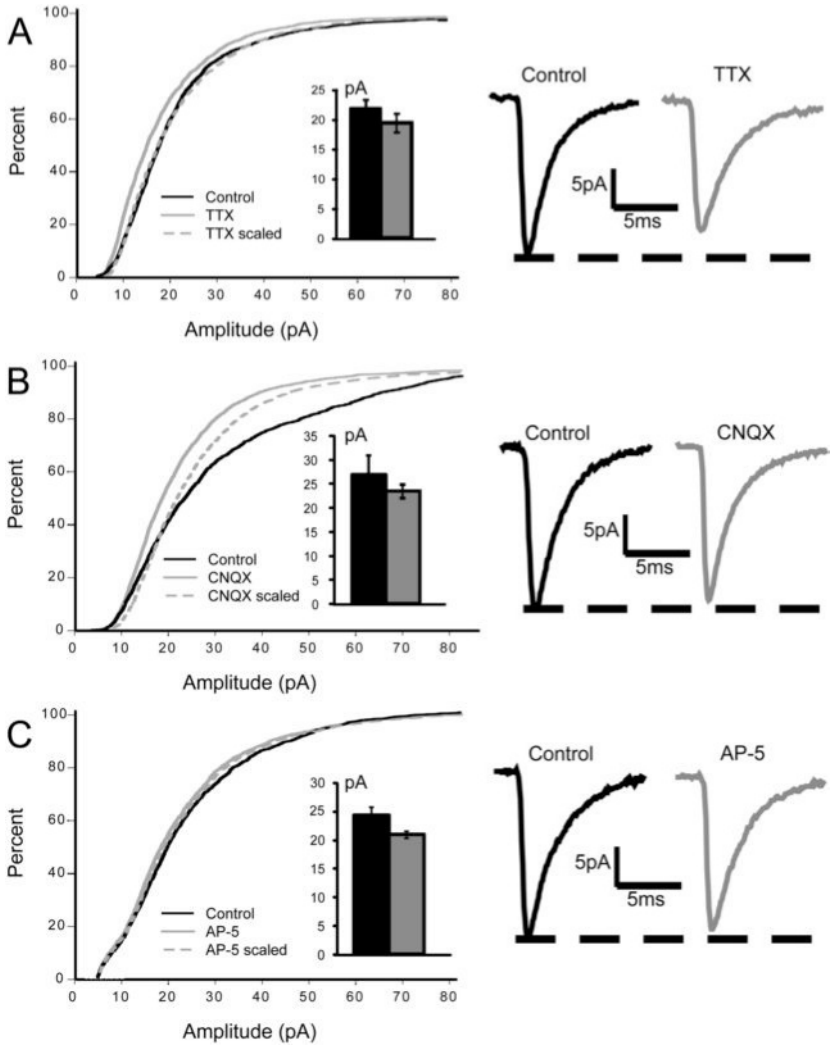

Figure 3. Chronic TTX, CNQX, or AP-5 treatment has no effect on glycinergic mIPSC amplitudes at 4dpf. A. Left, cumulative histograms of glycinergic mIPSC amplitudes from control (n = 11) and TTX-treated (n = 12) embryos. Inset, average mIPSC amplitude for the same conditions. Right, average mIPSC waveforms of one neuron for the same conditions. B. Left, cumulative histograms of glycinergic mIPSC amplitudes from control (n = 11) and CNQX-treated (n = 16) embryos. Inset, average mIPSC amplitude for the same conditions. Right, average mIPSC waveforms of one neuron for the same conditions. C. Left, cumulative histograms of glycinergic mIPSC amplitudes from control (n = 9) and AP-5-treated (n = 10) embryos. Inset, average mIPSC amplitude for the same conditions. Right, average mIPSC waveforms of one neuron for the same conditions.

FIGURE 4

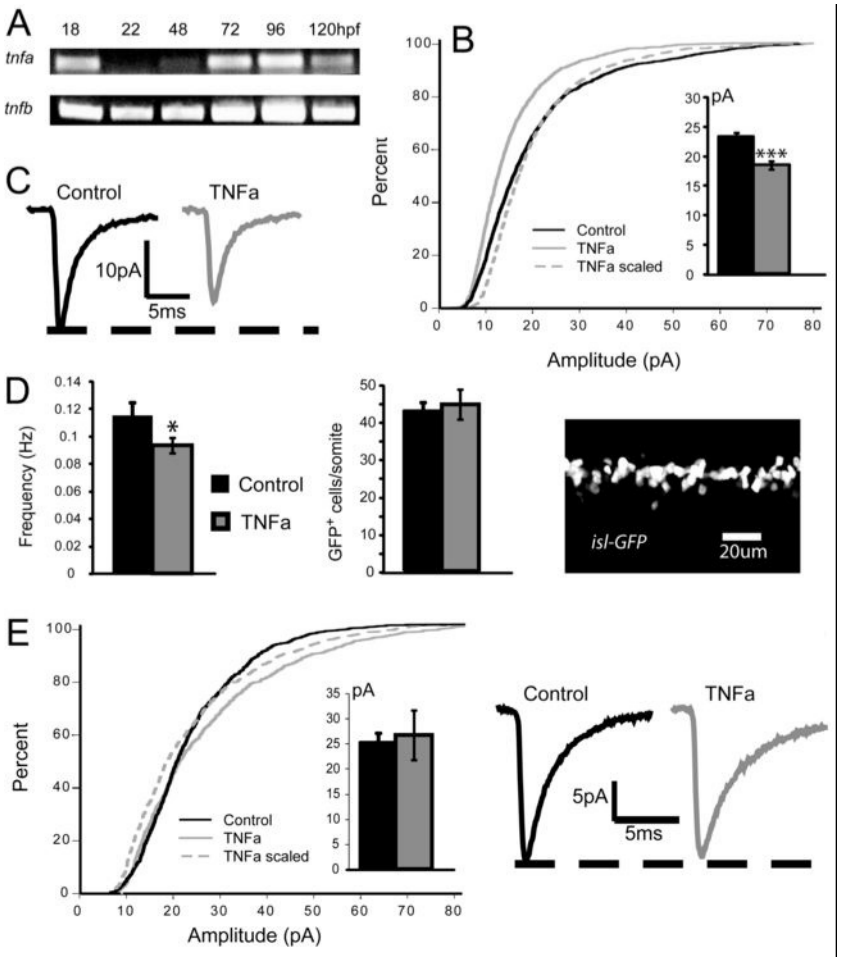

Figure 4. Chronic TNFα treatment results in a scaling down of glutamatergic mEPSC amplitudes at 3dpf. A. RT-PCR for zebrafish tnfα at 18, 24, 48, 72, 96 and 120hpf. tnfα is clearly expressed at 18hpf and from 72-120hpf, but expression may be reduced or absent from 24-48hpf. Band identity was confirmed by sequencing. Primers for the ubiquitously expressed tnfb serve as a control. B. Cumulative histogram of glutamatergic mEPSC amplitudes from control (n = 27) and TNFα-treated (n = 32) embryos. Inset, average mEPSC amplitude for the same conditions. C. Average mEPSC waveforms for the same conditions as B. D. Left, average frequency of glutamatergic mEPSCs from same conditions as B. Center, average number of GFP+ cells per somite from control (n = 7) and TNFα-treated (n = 6) embryos. Right, example confocal image of one somite from an Isl-GFP transgenic fish spinal cord. E. Left, cumulative histograms of glycinergic mIPSC amplitudes from control (n = 5) and TNFα-treated (n = 5) embryos. Inset, average mIPSC amplitude for the same conditions. Right, average mIPSC waveforms for the same conditions.

FIGURE 5

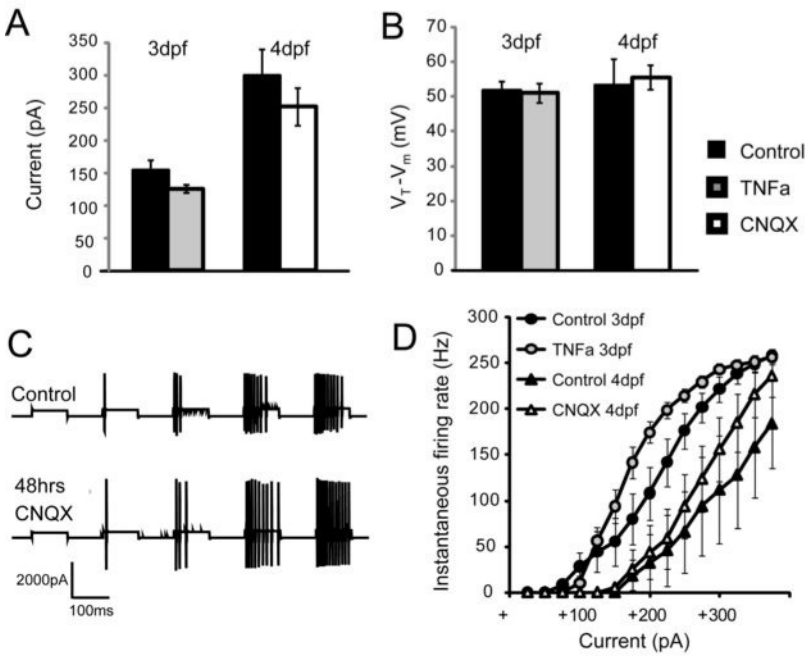

Figure 5. Chronic CNQX or TNFα treatment does not alter cellular excitability. A. Rheobase current was not significantly different at 3dpf between control (n = 11) and TNFα-treated (n = 10) larvae, at 4dpf between control (n = 6) and CNQX-treated (n = 8) larvae. B. The average spike threshold (VT -Vm) was also unchanged after chronic TNFα or CNQX treatment under same conditions as B. C. Representative spike trains evoked by somatic current injection steps (step = 25pA, 100ms duration, 15 steps total) in control and treated motoneurons at 4dpf. D. Average f-I curves were also unchanged after chronic TNFα or CNQX treatment under same conditions as B.

FIGURE 6

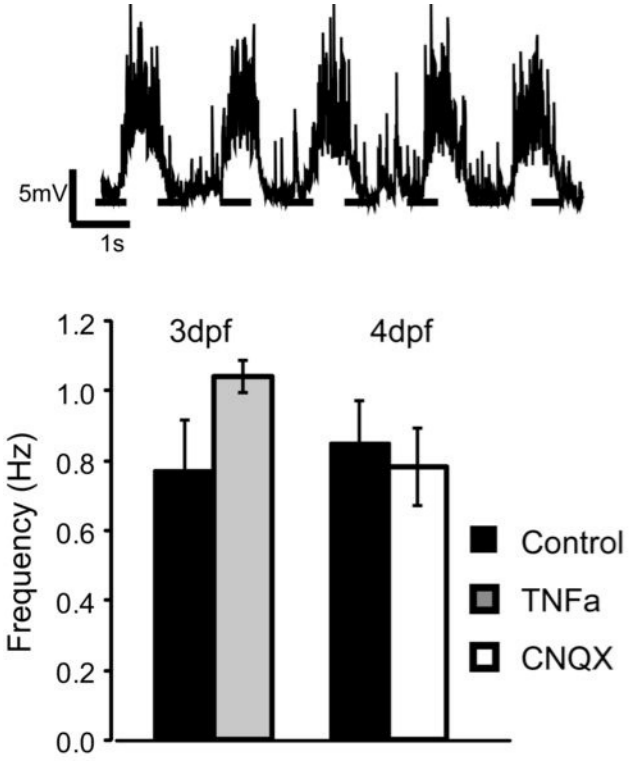

Figure 6. Slow oscillation frequency underlying fictive swimming in motoneurons is unchanged following chronic CNQX or TNFα treatment. Top, an example whole-cell current-clamp trace showing the slow oscillations elicited in a motoneuron by the extracellular application of 200μM NMDA. Bottom, average frequency of NMDA-induced slow oscillations in motoneurons are not significantly different between control (n=4) and TNFα-treated (n=3) larvae at 3dpf and control (n=3) and CNQX-treated (n=3) larvae at 4dpf.

FIGURE 7

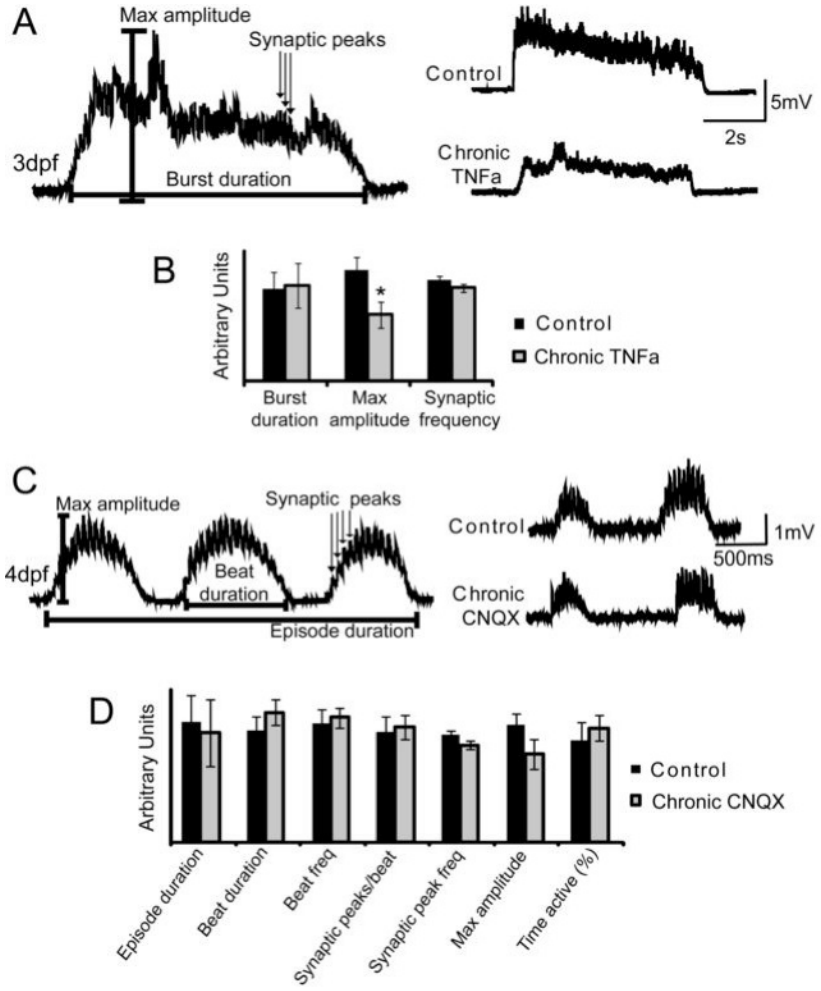

Figure 7. Chronic TNFα or CNQX treatment does not significantly alter the patterning of motor input to muscle cells at 3dpf or 4dpf, respectively. A. Left, example whole-cell current-clamp recording from a slow-twitch muscle fiber of a fictive swimming burst at 3dpf. Analysis parameters are indicated. Right, sample burst recordings from a control or TNFα-treated larvae at 3dpf. B. Average burst duration, maximum synaptic amplitude and synaptic frequency for slow-twitch muscle fibers at 3dpf for control (n = 11) and TNFα-treated (n = 9) larvae *$p<0.05$. C. Left, example whole-cell current-clamp recording from a slow-twitch muscle fiber of fictive beat-and-glide swimming at 4dpf. Analysis parameters are indicated. Right, sample beat-and-glide recordings from a control or CNQX-treated larvae at 4dpf. D. Episode duration, burst duration, beat frequency, synaptic peaks per beat, synaptic peak frequency, maximum synaptic amplitude and percent time active for slow-twitch muscle fibers at 4dpf for control (n = 6) and CNQX-treated (n = 8) larvae. None of the differences between conditions were significant ($p>0.05$).

FIGURE 8

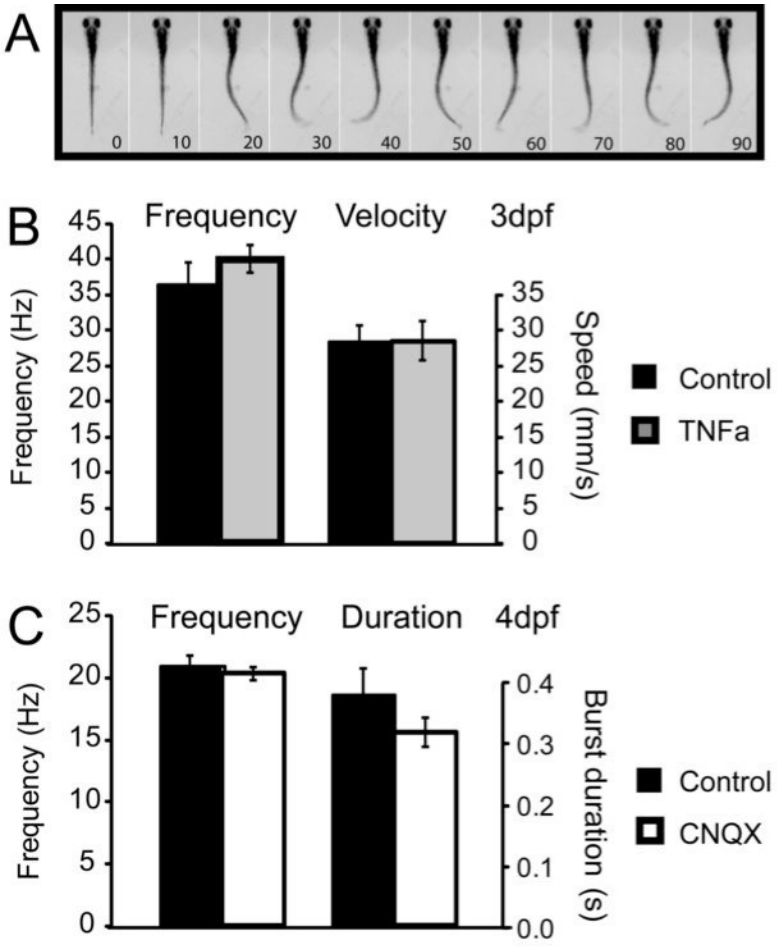

Figure 8. Larval swimming behavior is not altered following chronic TNFα or CNQX treatment. A. Swimming activity at 3-4dpf is composed of high frequency (20-30Hz), low-amplitude tail contractions. In this example, one full cycle of swimming is observed from 50 to 80 ms. The larva is immobilized in agarose, dorsal side up and anterior to the top of the image. Time of each frame is shown in the bottom right corner. B. Left, average swimming frequency of control (n = 3) and TNFα-treated (n = 5) larvae at 3dpf. Right, average free-swimming velocity under same conditions (control n = 11, TNFα-treated n = 13). C. Left, average swimming frequency of control (n = 8) and CNQX-treated (n = 9) larvae at 4dpf. Right, average duration of swimming bursts under same conditions (control n = 8, TNFα-treated n = 9).

FIGURE 9

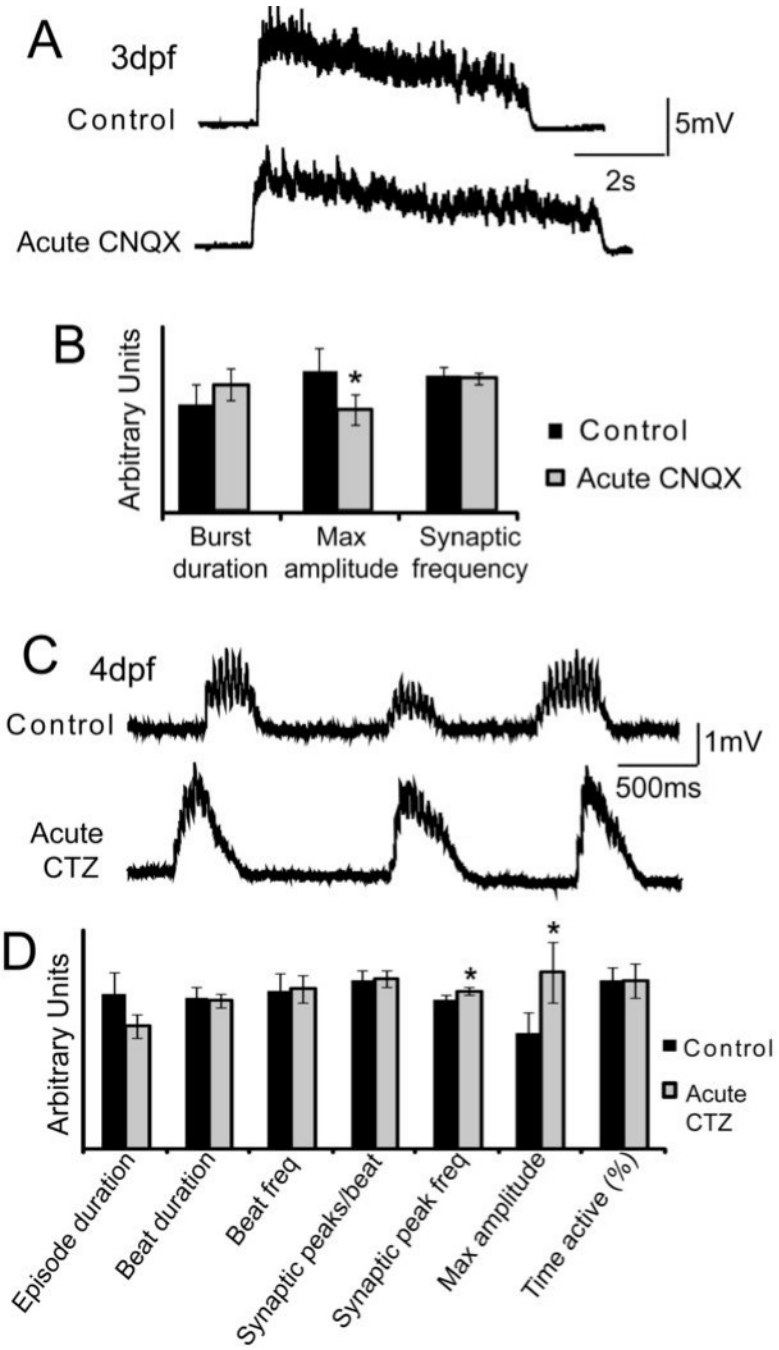

Figure 9. Acute CNQX or CTZ treatment significantly altered maximum synaptic amplitude (and contraction frequency of motor input - only in the second case) to muscle cells at 3dpf or 4dpf, respectively. A. Sample fictive swimming burst recordings at 3dpf from a muscle fiber at baseline (control) and again 5 minutes after start of CNQX application.

B. Average burst duration, maximum synaptic amplitude and synaptic peak frequency at 3dpf for slow-twitch muscle fibers at baseline and following CNQX application (n = 3). Paired Student's t test, *$p < 0.05$. C. Sample fictive beat-and-glide swimming recordings at 3dpf from a muscle fiber at baseline (control) and again 5 minutes after start of CTZ application. D. Episode duration, burst duration, beat frequency, synaptic peaks per beat, synaptic peak frequency, maximum synaptic amplitude and percent time active at 4dpf for slow-twitch muscle fibers at baseline and following CNQX application (n = 10). Paired Student's t test, **$p < 0.01$.

CHAPTER 5

V. GENERAL DISCUSSION

V.1. GENERAL SIGNIFICANCE

Here we have used the zebrafish, *Danio rerio*, as a vertebrate model system to understand the neural circuits that control locomotion. The work presented in this thesis addressed three aims related to understanding the development, function and plasticity of spinal circuits and motor behaviors in the intact animal. From these studies of the developing zebrafish spinal cord we have published several novel findings that are relevant to understanding the organization of vertebrate locomotor networks and behavior. The following section will discuss these results in the context of emerging principles regarding the organization of spinal circuits and will describe future directions for this research.

V.2. SPONTANEOUS ACTIVITY IN DEVELOPING LOCOMOTOR NETWORKS

Spontaneous network activity is a highly stereotyped feature of the developing spinal cord as well as other areas of the nervous system including the hippocampus, retina and cerebellum (Feller, 1999; Blankenship and Feller, 2010). Despite the diversity of these structures, the features of spontaneous network events are very similar and consist of slow depolarizations that produce bursts of action potentials at their peak (Blankenship and Feller, 2010). Spontaneous activity in the retina, hippocampus and other cortical areas is best measured with techniques such as electrophysiology and calcium imaging since there is otherwise no observable effect of this network activity. In the spinal cord however, these spontaneous bursts occur in several classes of neurons including motoneurons (Saint-Amant & Drapeau, 2000, 2001) which innervate muscles and thus produce an observable motor output. Spontaneous network activity in the spinal cord is thus directly linked to and can be measured by, spontaneous motor movements.

V.2.1. Transient, spontaneous motor behaviors appear as the locomotor network matures

In vertebrates such as zebrafish that are fertilized externally and develop within a transparent membrane, researchers can directly quantify behavior in the intact embryo in its natural state. In Chapter 2 of this thesis, we used this method to describe a novel spontaneous behavior, double coiling, that we observed in the zebrafish embryo. Although the

development of the earliest motor behaviors (including single coiling) had been previously characterized (Saint-Amant & Drapeau, 1998), our use of high-speed video recordings to follow the precise timing and maturation of coiling revealed a transformation of single coils to alternating double coils to swimming over the course of just six hours. Double coils resembled previously described spontaneous "S-bends" in the salamander (Coghill, 1929), chick (Hamburger, 1963) and rat (Narayanan et al., 1971). Like in these other species, double coiling was a developmental intermediate following slow, single flexures and preceding more mature, coordinated behaviors such as swimming. Our results indicate that zebrafish embryos follow a conserved and stereotyped vertebrate behavioral development.

In zebrafish larvae, studies of locomotion have carefully quantified different types of spontaneous movements including routine turns (Budick & O'Malley, 2000; Danos & Lauder, 2007) and swim bouts (Budick & O'Malley, 2000; Granato et al., 1996). Spontaneous motor patterns may be combined to enable more complex and sensory-evoked locomotor behavior such as prey capture (Patterson et al., 2013; Trivedi & Bollmann, 2013; Westphal & O'Malley, 2013). Much like in our studies of double coiling, the categorization of individual motor components or patterns in larval locomotion will allow researchers to determine the effect of manipulating circuit activity on behavioral performance. For example, recent studies have used calcium imaging, stimulations, ablations and electrophysiology to identify populations of hindbrain neurons that control spontaneous and visually-evoked turning (Huang et al., 2013) and swimming (Sankrithi & O'Malley, 2010; Severi et al., 2014) in the zebrafish larva. Careful quantitative analyses of motor behaviors in parallel with anatomical and functional analyses at the cellular level will no doubt continue to reveal important aspects of the organization and function of vertebrate locomotor circuits.

V.2.2. CPG circuits driving spontaneous double coiling in the zebrafish

A variety of experimental techniques are available that can be used to probe the underlying neural circuitry that produces motor behaviors in the zebrafish. As described in Chapter 2, an acute pharmacological blockade of glutamatergic signalling caused double coils to revert to single coils. These findings suggested that during development glutamatergic signalling becomes integrated within the original electrical circuit in zebrafish that drives

single coils (Saint-Amant & Drapeau, 2001). We used a multidisciplinary approach to show that the onset of double coiling coincided with the appearance of anatomical synapses from glutamatergic CiD interneurons onto primary motoneurons as well as the appearance of AMPA receptor-dependent activity patterns in these cells. Double coiling also required intact supraspinal connections, although the isolated spinal cord could recover this behavior by increasing background depolarization. Electrical pacemaker activity at this age is still strong (Tong & McDearmid, 2012) therefore these results suggest that a "hybrid" electrical and chemical circuit drives double coiling. The appearance of double coiling likely marks the point at which chemical (glutamatergic) neurotransmission becomes a major driving force for locomotor behavior and the influence of gap junctions begins to decline.

Although CiDs appear to be in the right place and active at the right time for double coiling, we initially hypothesizd that a commissural glutamatergic interneuron would be important for providing coordinated but delayed excitation to the opposite side of the spinal cord to produce a double coil. However, our results (Chapter 3) clearly showed that commissural glutamatergic CoPAs were not playing this role and in fact several studies have suggested that bilateral drive can actually produce alternating activity in the locomotor CPG. In the lamprey, forward swimming is correlated with the symmetrical bilateral activation of a large group of reticulospinal neurons (Brocard et al., 2010; Deligiana et al., 2002). In the zebrafish embryo, the direct simultaneous bilateral optogenetic stimulation (*via* rebound excitation) of groups of spinal neurons produced a wave of neuronal activity that alternated between sides of the spinal cord with a delay typically seen during spontaneous motor activity (Warp et al., 2012). The similarity between spontaneous and optogenetic-evoked alternation suggests that a bilateral, spinal and/or supraspinal drive may be responsible for triggering the earliest alternating behavior (double coiling) in the embryonic zebrafish.

V.2.3. The contribution of gap junctions to spontaneous coiling and swimming

Our findings suggest that as development proceeds in the zebrafish embryo, electrical coupling initiates a coiling event during which glutamatergic signaling recruits a second, alternating activation of the spinal cord to produce a double coil. We unfortunately could not assess the effect of specifically blocking gap junctions at this point in development as

pharmacological antagonists of these channels are not selective and have many off-target effects on other ion channels. Gap junctions are likely still present through larval stages and may also contribute to locomotor circuits in the adult, as has been shown in the adult goldfish (Fetcho & Faber, 1988) and mosquitofish (Serrano-Velez et al., 2014). It has been previously shown that monosynaptic glutamatergic connections between CiDs and MNs are present at 2 dpf, when the larva is capable of swimming (Kimura et al., 2006). There is also evidence for electrical coupling between CiDs and MNs at this age, though the coupling is low (< 10%), not found in all cells and in the majority of cases is combined with a glutamatergic synapse between the neurons (Kimura et al., 2006), suggesting that by 2 dpf electrical coupling is diminishing as chemical neurotransmission takes over. Blockade of glutamatergic signaling at 3 dpf abolishes fictive swimming patterns in MNs (Buss & Drapeau, 2001) and can also prevent the touch response and swimming behavior (Knogler et al., 2010), therefore electrical neurotransmission does not appear to be sufficient to drive behavior at larval stages.

The changing biophysical properties of cells may account for much of the decrease in gap junction control during development. Although the number of ions that flow through the gap junction channel (the conductance) contributes to the amplitude of the change in the membrane potential, so too do passive properties of the coupled neuron such as its resistance and capacitance (Bennett, 1966). Most spinal neurons in the < 24 hpf embryo have very high input resistances of more than one gigaohm (Ali et al., 2000b; Saint-Amant & Drapeau, 2000; Tong & McDearmid, 2012). This is because at early stages cells do not have many proteins such as ion channels in their cell membranes that make them “leaky” and their small size also contributes to a higher resistance. From 24 hpf onwards, chemical synaptogenesis increases rapidly and the input resistances of spinal neurons drop to several hundred megaohms by 2 - 3 dpf in the zebrafish (Ali et al., 2000b; Drapeau et al., 1999). As Ohm’s law dictates, voltage is equal to the product of current and resistance (V=IR) therefore as the membrane resistance decreases the same amount of current coming through gap junctions will produce a proportionally smaller change in voltage in the cell. Electric coupling is affected to a greater degree by changes in the membrane resistance and capacitance of the postsynaptic neuron than chemical neurotransmission because gap junctions have no mechanisms to amplify the presynaptic signal (Pereda et al., 2013).

Despite the reduced contribution of electrical coupling to driving neuronal firing at later developmental stages, an increasing number of studies show that electrical coupling is present in many areas of the developing and adult nervous system and in most organisms including mammals, thus suggesting an ongoing contribution to circuit function (reviewed by Pereda, 2014). Although gap junction proteins are expressed in nearly all tissues of the body, only a few of these proteins, known as connexins, are present in vertebrate neurons (Pereda, 2014). As studies continue to reveal the identity of specific connexin proteins in different cell types of the zebrafish nervous system (Carlisle & Ribera, 2014; Jabeen & Thirumalai, 2014) we may be able to manipulate the function of gap junctions with genetic techniques in order to better define their role in motor behaviors. Many synapses in the nervous system are now thought to use both electrical and chemical components to communicate therefore it is of widespread interest to understand how these hybrid circuits function.

V.2.4. Double coiling as an indicator of locomotor CPG function

In addition to furthering our understanding of spinal cord circuits during development, our characterization of double coiling behavior could have interesting applications for studies of human health. Our study revealed that double coil events were very sensitive to the appropriate balance of excitation and inhibition. Too little glutamatergic activity resulted in a loss of double coils and a reversion to single coils, whereas a reduction in glycinergic signaling led to the production of multiple coils and unusually long quiescent periods in the embryo. These discrete categories of coiling represent simple, quantifiable behaviors that may serve as a readout by which to identify perturbations of early chemical synapse development or to assess the relative balance between excitation and inhibition in the motor network. Coiling events are considerably easier to observe and quantify than more complex motor behaviors such as swimming, therefore analysis of this new behavior may be well suited for gene function studies and disease modeling.

In support of this idea, a recent zebrafish model of Rett syndrome carrying a mecp2-null mutation was shown to have a significantly increased frequency of multiple-coil events as compared to wild-type embryos (Pietri et al., 2013). These findings suggested an imbalance in excitation and inhibition and further experimentation revealed a decreased efficacy of

glycinergic signaling in the mutant. Coiling is a slow and simple behavior therefore automated analysis is feasible and could be applicable to high-throughput genetic or pharmacological screens. ZebraZoom is an example of a recently developed program that successfully used supervised machine learning to detect and quantify larval movements in order to identify abnormal motor behaviors in mutants or zebrafish treated with a glycine receptor antagonist (Mirat et al., 2013). Coiling is a straightforward behavior to analyze because it has discrete categories (single coil, double coil, triple coil, etc) and occurs spontaneously, requiring no intervention on the part of the researcher.

V.2.5. Future work

An important follow-up to our work on double coiling would be to determine the neccessity and sufficiency of spinal and/or hindbrain CiDs for this behavior. Our study suggested that descending supraspinal glutamatergic inputs might provide important additional glutamate, in a tonic or phasic form, that allows the double coil circuit to reach threshold. Given the putative role of spinal CiD interneurons in double coiling, their hindbrain counterparts (Kimura et al., 2013) might act as additional means of signal amplification and have much the same phasic activity patterns. It will thus be informative to extend our study of CiD neurons to the hindbrain population. Both spinal and hindbrain CiDs can be genetically targeted by their expression of the transcription factor chx10 to express transgenes that will specifically alter the function of these cells. Tetanus toxin can be used to prevent the release of neurotransmitter from CiDs while leaving their firing properties (and electrical coupling) intact (Asakawa et al., 2008). This should reveal the necessity of glutamate release from these cells for double coiling.

Optogenetic switches (Portugues et al., 2013) to either excite (e.g. channelrhodopsin) or silence (e.g. halorhodopsin) neurons could also be expressed to confirm the sufficiency and necessity, respectively, of activity in CiDs for double coiling. However, transgene promoters can be leaky or the site of insertion can have positional effects resulting in ectopic expression in other neuronal populations. Indeed, when crossed with UAS reporter lines, our experiments showed that the chx10:gal4 line (Kimura et al., 2013) shows expression in many primary motoneurons and thus this transgenic line cannot be used in functional experiments. Care

must therefore be taken to ensure that there is specific expression in the targeted population of interest because any experiments assessing the role of interneurons in producing a motor behavior will be severely confounded by ectopic expression in motoneurons or other spinal neurons.

Ectopic expression is less problematic if we wish to observe rather than manipulate activity. We used this method successfully to fluorescently label neuronal morphology and synaptophysin puncta in several embryonic CiDs in order to investigate the formation of putative glutmatergic synapses. Recently, others have expressed the fluorescent calcium indicator GCaMP fused to synaptophysin to reveal both anatomical and functional features of developing synapses (Nikolaou et al., 2012; Menelaou et al., 2014). Furthermore, an intensity-based glutamate-sensing fluorescent reporter (iGluSnFR) was recently developed for *in vivo* imaging that could allow us to observe the earliest sites and patterning of spontaneous postsynaptic glutamate binding throughout the spinal cord (Marvin et al., 2013). This is particularly useful in a hybrid circuit because calcium indicators alone would not be able to distinguish between calcium influx due to electrical or chemical neurotransmission. Mapping the relatively sparse glutamatergic connectivity driving spontaneous double coiling could provide a blueprint for the increasingly elaborate spinal cord circuits that underlie more complex motor behaviors such as swimming.

V.3. SENSORIMOTOR CIRCUITS IN THE EMBRYONIC SPINAL CORD

Touch reflexes are the first sensory-evoked motor behavior to appear in the vertebrate embryo. In the zebrafish embryo, a light touch stimulus initially elicits coiling movements and later produces swimming as the locomotor CPG matures. At both stages, touch-evoked and spontaneous behaviors are nearly identical, suggesting that the majority of the underlying neural circuitry is the same. The components of a touch-evoked circuit typically include a sensory neuron and one or more sensory interneurons that mediate activation of the locomotor CPG through feed-forward excitation. It is also clear that feedback pathways exist from elements of the motor network onto sensory neurons or interneurons that play an important role in sensory gating. Here we will discuss our current understanding of these sensorimotor circuits in the embryonic zebrafish.

V.3.1. Sensory interneurons gate activation of the locomotor CPG during fictive embryonic motor behaviors

Like in other lower vertebrates, spontaneous activity precedes the onset of the response to touch in the zebrafish, in this case by four hours (Saint-Amant & Drapeau, 1998). Sensory RB neurons synapse onto CoPA interneurons, which project across the spinal cord to excite neurons in the motor pathway including CiDs (Pietri et al., 2009). In Chapter 3 of this thesis, I showed that embryonic CoPAs are highly specialized for gating the somatosensory pathway and thus the touch response. Using whole-cell electrophysiology, I revealed that CoPAs are strongly (and briefly) activated at the onset of a touch stimulus but specifically silenced during spontaneous and ongoing fictive movements. This silencing is achieved by the combination of a generic glycinergic corollary discharge signal activating a unique long-lasting chloride conductance through a glycine receptor in the CoPA and this inhibition is maintained during the transition from primitive coiling to early swimming behaviors. To our knowledge, this is the earliest embryonic corollary discharge pathway that has been elucidated thus far. The corollary discharge signal must be initially activated by a neuron in the locomotor CPG because the signal is produced during centrally generated (spontaneous) fictive behaviors in addition to ongoing touch-evoked fictive behaviors. Thus, not only do local somatosensory pathways activate the locomotor CPG to elicit motor behaviors, so too does the activity of the CPG influence sensory feedback through gating inhibition.

These findings may also explain why spontaneous multiple coiling occurred in the zebrafish embryo following the blockade of glycine receptors as described in our spontaneous double coiling study in Chapter 2. RB sensory neurons have mechanosensitive neurites that do not distinguish between self-generated and external touch activation and are likely to fire an action potential during both spontaneous and sensory-evoked movement. It may be possible to confirm the firing activity of RBs in the freely moving embryo using bioluminescent signals from these sensory neurons (Naumann et al., 2010; C. Wyart personal communication). A single action potential in a single RB is sufficient to activate an escape behavior at 24 hpf (Douglass et al., 2008), therefore if the CoPAs are not inhibited by glycinergic corollary discharge signals then a spontaneous coil event could drive RB firing

and keep triggering additional touch-evoked coils until the network is no longer capable of sustaining the activity. We observed much longer periods of inactivity following multiple coiling than following single or double coils that we hypothesized were due to activity-dependent network depression. The mechanisms responsible for this depression may include a buildup of adenosine from ATP release that depresses presynaptic neurotransmitter release, a depletion of glutamate itself, or a hyperpolarization of neuronal membrane potentials (Chub & O'Donovan, 2001; O'Donovan et al., 1998). Regardless, spontaneous activity appears to remain somewhat "self-regulating" even in the absence of proper sensory gating, suggesting that network activation may be constrained by other means (Tabak et al., 2001).

It is worthwhile to consider that under physiological conditions sensory feedback typically modulates ongoing locomotor activity in a "closed-loop" process. In our electrophysiological recordings of fictive behaviors such as coiling and swimming in the paralyzed embryo, this loop is broken and normal sensory feedback from RBs is absent. Studies using closed-loop virtual-reality environments (where visual feedback is updated in real time to reflect the fictive movements of the larval zebrafish as measured *via* ventral root recordings) show that patterned locomotor output is much more similar to free-swimming behavior in the closed-loop than in the open-loop condition (Portugues & Engert, 2011). There may therefore be a differential recruitment of neurons during fictive behaviors in the zebrafish that does not entirely recapitulate real motor behaviors. This has recently been observed in the larva in a class of cerebrospinal fluid-contacting ventral interneurons that fire during active but not fictive swimming (C. Wyart, personal communication). At early embryonic stages zebrafish are not yet responsive to sensory modalities other than touch therefore the gating inhibition of the somatosensory pathway by corollary discharge is likely to block out any potential sensory feedback that would be initiated by RB neurons in the freely moving embryo. It will nonetheless be important to study sensorimotor circuit function whenever possible in both closed-loop (virtual-reality or freely moving) and open-loop (paralyzed) conditions, particularly at later stages when other modalities such as vision and the lateral line system have developed.

V.3.2. Motor pathways send corollary discharge to sensory pathways

Corollary discharge is used in a number of invertebrate and vertebrate species for reflex inhibition and sensory filtration (reviewed by Crapse & Sommer, 2008). Essentially, corollary discharge is a motor-related signal coming from some level of the motor output and targeting part of a sensory pathway in an effort to filter out reafferent (self-generated) sensory stimuli that is the result of body movements. This is a very common strategy in the animal kingdom although the organization of the corollary discharge circuits themselves may be different between species. In zebrafish we show that embryonic sensory interneurons are selectively silenced to gate the touch reflex, however many corollary discharge circuits often target sensory neurons themselves for silencing through mechanisms of presynaptic inhibition (Crapse & Sommer, 2008). For example, in the crayfish, mechanosensitive hair cells are contacted by interneurons that produce presynaptic inhibition of the afferent terminals when the animal is moving (Kirk & Wine, 1984). It is also possible that the organization of the corollary discharge circuits in the zebrafish spinal cord changes during development (see below).

Higher order cognition such as perception may also be dependent on corollary discharge pathways (Crapse & Sommer, 2008). Although this is difficult to assess experimentally, some psychophysical studies in primates have shown that experimentally induced defects in corollary discharge result in altered perception (Logothetis, 1998; Parker & Newsome, 1998). Furthermore, several researchers have proposed models that implicate abnormal or unsynchronized corollary discharge pathways in producing the stereotypical symptoms of schizophrenia including delusions and hallucinations (reviewed by Lisman, 2012). One study has found that patients with schizophrenia have poor communication between their frontal and temporal lobes, where speech or a verbal thought is generated and perceived, respectively (Ford et al., 2002). This suggests that patients with schizophrenia might fail to recognize inner speech as self-generated and thus misattribute this to an external stimulus. Defining the pathways that carry corollary discharge between motor and sensory pathways is difficult and in general are not well-defined, therefore it is advantageous to study these types of pathways in a simple system such as we have done in Chapter 3.

V.3.3. Developmental reorganization of sensorimotor circuits

Our work in the zebrafish embryo found that at pre-swimming stages, CoPAs appeared to receive glycinergic inputs at the same time as other ipsilateral spinal CPG neurons including motorneurons but that CoPAs were preferentially silenced due to their uniquely slow glycine receptor. However, during the onset of swimming just hours later, we saw that the CoPA and ipsilateral motoneuron no longer received glycinergic inputs in phase but rather CoPAs received glycine in phase with excitation (glutamate) to the motoneuron. We know from previous work in zebrafish that motoneurons receive glycinergic inputs out of phase with excitation during larval swimming (Buss & Drapeau, 2001). There may therefore be a point in development where these glycinergic interneurons split into two groups that either selectively inhibit sensory pathways with on-cycle corollary discharge or inhibit motor pathways with mid-cycle inhibition.

One hypothesis is that a single class of inhibitory interneurons can initially be multifunctional and involved in many pathways whereas later in development separate classes of interneurons carry out each specialized function (Li et al., 2004). In *xenopus* tapdoles, RBs activated by a touch stimulus excite commissural dlc interneurons and these in turn drive the activity of contralateral spinal neurons including motoneurons to produce a simple flexion (Roberts et al., 2010). In order to prevent restarting the touch response during evoked swimming, RBs also excite ipsilateral glycinergic ascending interneurons (aINs) that directly synapse onto and inhibit dlcs just after activation and in phase with excitation to motoneurons during swimming (Li et al., 2002). These aINs synapse onto dlc interneurons as well as other spinal neurons including motoneurons to provide early-cycle inhibition to synchronize CPG neurons during swimming, suggesting that they might be a multifunctional glycinergic interneuron in *xenopus* that initially provides glycine to many pathways (Li et al., 2004). The main source of mid-cycle inhibition comes from commissural glycinergic interneurons (cINs) that inhibit neurons in the CPG to maintain left-right phase coordination (Dale, 1985) but all studies in the *xenopus* embryo have been carried out at the time of hatching (stage 37/38, 53 - 55 hpf) when tadpoles are capable of swimming, therefore by this stage some important development transitions may have already occurred.

A homologue of aINs exists in zebrafish, the circumferential ascending (CiA) interneurons (Higashijima et al., 2004a; Bernhardt et al., 1990). Our unpublished observations show that this cell is not active during coiling but anatomical and physiological evidence shows that CiAs contact ipsilateral CoPAs at 4 -5 dpf (Higashijima et al., 2004a), consistent for a role of CiAs to provide rhythmic, shunting glycinergic input to CoPAs during swimming at this stage. Furthermore, other classes of glycinergic commissural interneurons (CoBLs and CoSAs) are not active during coiling behavior in the embryonic zebrafish but become important for larval swimming, escape and struggling (Liao & Fetcho, 2008). Even in the absence of distinct morphological classes of spinal neurons some degree of specialization might be achieved simply by dorsoventral specializations within a single class, as has been demonstrated with the dorsoventral gradient of spinal CiD interneurons and motoneurons that determines their recruitment for different locomotor speeds (Ampatzis et al., 2014; McLean et al., 2007, 2008). It is possible that similar mechanisms could enable dorsal interneurons to inhibit sensory pathways and perform corollary discharge while ventral interneurons inhibit motor pathways and regulate motor activity (Li et al., 2004).

It will also be of great interest to follow the target of corollary discharge interneurons, the CoPA, throughout development because many questions remain regarding their role in the zebrafish larva. RBs undergo developmental apoptosis (programmed cell death) beginning at approximately 1.5 dpf and in the majority of larvae these cells have completely disappeared by 3.5 dpf (Williams et al., 2000). Dorsal root ganglion (DRG) neurons appear around 2 dpf and although they do not influence RB death they take over functionally to mediate mechanosensation in the larva and adult (Reyes et al., 2004). Although their axons run longitudinally along the dorsal spinal cord similar to the RB axonal projections (Bernhardt et al., 1990), it has not been determined if DRGs become the new presynaptic partners of CoPAs. It is possible that CoPAs, like RBs, disappear during the larval stage or that a different class of interneurons takes their place in the somatosensory pathway.

A transgenic zebrafish line now exists where embryonic CoPAs are fortuitously labeled with GFP (Wells et al., 2011) but this expression is downregulated at larval stages as is expression of the transcript mafba/valentino that specifically label CoPAs in the embryo (S. Wells, personal communication). This does not in itself mean that CoPAs are absent in the

larvae since CoPA neurons have been visualized with intracellular dye filling at 4 - 5 dpf and revealed to have a similar pattern of activity as we have now shown during immature embryonic swimming (Higashijima et al., 2004a). By 4 dpf, a population of ascending spinal commissural cells provides direct spinal input to the forebrain of zebrafish (Bernhardt et al., 1990). If these neurons are CoPAs then these excitatory projections could recruit additional neurons for descending control of spinal motor circuits in response to touch-evoked stimuli and thus continue to play an important role in the activation of sensorimotor circuits. Very few investigations have been made of CoPAs in the zebrafish larva (or of the homologous dlc interneurons of *xenopus* beyond the tadpole stage) but these results underline the potential importance of these sensory interneurons in larval and adult somatosensory circuits.

V.3.4. Future work

In order to better understand how the motor and sensory pathways connect it is of foremost importance to identify the embryonic corollary discharge interneuron in the zebrafish. The population of neurons responsible for the earliest glycinergic activity in the zebrafish spinal cord is currently unknown but evidence points to them being located in the rostral spinal cord and sending descending inputs to several spinal neurons including CoPAs (Pietri et al., 2009; Saint-Amant & Drapeau 2000, 2001). Retrograde rabies virus tracing is currently being adapted for use in the zebrafish nervous system and could be used to visualize the direct presynaptic partners of CoPAs. Single-cell labeling can be achieved by electroporating a CoPA with the viral genes necessary to cross the synapse (Wickersham et al., 2007), thus defining the microcircuit of this sensory interneuron. This technique should label many (if not all) ipsilateral RB sensory neurons (Easley-Neal et al., 2013) as well as the unidentified glycinergic interneurons that provide inhibitory corollary discharge that we predict are located in the rostral spinal cord (Moly et al., 2014).

Finally, our findings from Chapter 3 suggest that CoPAs express a unique α2* glycine receptor subunit but this remains to be confirmed molecularly. The transgenic CoPA-GFP line (Wells et al., 2011) would permit the use of fluorescence-activated cell sorting (FACS) to enrich for CoPAs for genomic and proteomic studies. It is otherwise difficult to show with *in situ* hybridization or by PCR the presence of the α2* glycine subunit since only five base pairs

differ from the more standard α2 subunit in this variant. The α2* subunit has previously only been found in the neonatal rat spinal cord but the identity of the cells in which it is found is unknown (Kuhse et al., 1990). Our findings suggest that the expression of this particular glycine receptor with its slow kinetics provides a post-synaptic specialization that allows a generic glycinergic corollary discharge signal to specifically gate the somatosensory pathway. It would be worthwhile to search for a parallel in the rat by finding the spinal neurons that express this particular glycine receptor. Performing comparative studies of spinal circuits across vertebrates is an invaluable way to dissect the complexity of interactions between sensory and motor networks of the nervous system.

V.4. STABILITY AND PLASTICITY OF SPINAL LOCOMOTOR CIRCUITS

In addition to defining the connectivity of locomotor circuits it is important to consider the different kinds of plasticity in the nervous system that can act over different spatial and temporal scales to modify the properties of cells within neural circuits. Although one generally thinks of cortical circuits as being the most "plastic" area of the nervous system, in Chapter 4 we explored how homeostatic plasticity might be important for the maintenance of locomotor circuits. Spinal locomotor circuits produce robust and highly stereotyped patterns of activity that underlie motor behaviors and remain remarkably consistent despite developmental growth and environmental changes. Here we will discuss the mechanisms that appear to contribute to the stability of locomotor networks during development and explore the role of spontaneous activity in network maintenance.

V.4.1. Synaptic scaling

Over the last two decades, a great number of studies have sought to study homeostatic synaptic plasticity in a variety of brain regions and animal models (for excellent reviews see Davis, 2013; Turrigiano, 2011, 2012). Although much of the initial work was carried out *in vitro*, many investigations are now being made into homeostatic synaptic plasticity *in vivo* and with a focus on understanding how changes at the cellular level translate to network and/or behavioral stability.

In our work described in Chapter 4, we attempted to describe the link between changes in synaptic strength and behavior in the developing zebrafish through chronic manipulations of network activity that we hypothesized would induce homeostatic compensation. Our study found that excitatory (AMPAergic) but not glycinergic synaptic strength was increased approximately 25% following a chronic reduction in network activity *in vivo*, showing for the first time that synaptic scaling could be elicited in the zebrafish nervous system. However, when we mimicked an acute 25% increase in synaptic strength by using an AMPA receptor agonist this increase in excitatory synaptic strength failed to produce a noticeable effect on larval swimming behavior. This and other investigations of homeostatic plasticity from the embryonic chick spinal cord show that although excitatory synapses onto spinal motoneurons scale up following a chronic reduction in network activity the physiological role of synaptic scaling at this age remains unclear because it does not appear to be responsible for restoring normal activity levels (Wilhelm & Wenner, 2008; Wilhelm et al., 2009).

Our results suggest that in the developing zebrafish spinal cord, synaptic scaling does not maintain the patterning of locomotor activity. Instead, we propose that the zebrafish locomotor CPG network remains stable because it follows an intrinsic developmental program that is not very susceptible to homeostatic plasticity mechanisms at this age. It has been proposed that homeostatic signaling might be restricted during development in order to allow major activity-dependent modulation of neural function to take effect (Davis, 2006) and several studies have shown that homeostatic mechanisms may be up- or down-regulated in different areas of the nervous system during activity-dependent critical periods (reviewed by Turrigiano & Nelson, 2004). Perhaps synaptic scaling plays a larger role later in motor development once stable connectivity has been established and the locomotor CPG becomes more dependent on sensory feedback and descending inputs.

We also investigated potential changes in glycinergic synaptic strength that might parallel changes at excitatory synapses because the balance between excitation and inhibition can have a major impact on ongoing activity and thus glycinergic and glutamatergic synapses might be regulated in parallel following chronic changes in network activity. Our results showed no synaptic scaling at glycinergic synapses however changes in glycinergic signaling (or lack thereof) are difficult to interpret because glycine is depolarizing in immature neurons

and can be functionally excitatory or inhibitory depending on different cellular parameters (Ben-Ari, 2002). Studies from the chick embryo show that GABAergic synapse strength scales up following $GABA_A$ receptor blockade and this result is believed to be homeostatic and compensatory because GABA is depolarizing and excitatory at this stage (Wenner, 2014). In the zebrafish, the role of depolarizing glycine on motoneuron activity is not well understood but it does not appear to drive action potential firing in motoneurons (Saint-Amant & Drapeau, 2000, 2001). Excitatory glutamatergic synapses may therefore be the primary locus of homeostatic plasticity at this developmental stage.

V.4.2. Intrinsic plasticity

Rhythmic behaviors such as swimming are generated by locomotor circuits whose output is determined not only by the synaptic strength of connections between CPG neurons but also by their intrinsic firing properties. The combination of ionic currents expressed by each neuron determines its intrinsic properties but is subject to ongoing modifications that can alter cellular excitability much like changes in the number of post-synaptic receptors can alter synaptic strength. However, intrinsic plasticity mechanisms (reviewed by Zhang & Linden, 2003) have been far less studied than mechanisms relating to changes in synaptic plasticity such as homeostatic synaptic scaling.

Our work in Chapter 4 identified a non-significant trend towards increased excitability of spinal motoneurons following chronic activity reduction but we did not investigate short-term (< 2 day) changes in their intrinsic properties. In the chick locomotor CPG, embryonic motoneurons show compensatory changes in cellular excitability that occur in parallel with the recovery of embryonic motor activity and precede changes in synaptic strength (Wilhelm & Wenner, 2008; Wilhelm et al., 2009). These studies found that intrinsic homeostatic changes were evident after just 12 hours of chronic activity reduction by $GABA_A$ blockade but were returning to baseline levels by 48 hours of treatment, at which point synaptic scaling of both GABAergic and AMPAergic synapses had occurred. It is possible that homeostatic intrinsic and synaptic plasticity mechanisms are dynamic processes that follow different time courses and thus require more frequent observations from the onset of activity perturbations. The pathway that mediates these changes in excitability remains unknown.

There are many possible combinations of intrinsic and synaptic properties of neurons in a circuit that can give rise to a certain motor pattern (Prinz et al., 2004; Goaillard et al., 2009; Grashow et al., 2010) therefore neural networks including motor CPGs may maximize this flexibility of neurons by changing several parameters to keep overall activity consistent (Marder & Goaillard, 2006). In the invertebrate motor CPG, neuromodulators such as dopamine and serotonin play a key role in the recovery of rhythmic activity following network perturbation by signaling through metabotropic receptors to control the homeostatic transcription of ion channels (Khorkova and Golowasch, 2007; Temporal et al., 2011). In the developing embryo, synaptic rather than intrinsic plasticity mechanisms might dominate due to a developmental delay in the appearance of neuromodulatory circuits. For example, serotonergic neurons begin appearing in the zebrafish hindbrain and spinal cord around 2 dpf but do not appear to play a functional role in modulating network activity until 4 dpf (Brustein et al., 2003). Further research describing the development and function of neuromodulation in vertebrate locomotor circuits will help us understand how these pathways might be employed for homeostatic changes in intrinsic properties to maximize the stability of patterned output.

V.4.3. Developmental role of spontaneous activity in locomotor circuits

Our results in Chapter 4 suggest that the patterning of the zebrafish locomotor CPG is largely hard-wired early in development. In support of this idea, others have observed that zebrafish and *xenopus* larvae raised in anaesthetic are able to swim upon washout of the drug although certain defects were apparent in this behavior (Haverkamp and Oppenheim, 1986; Saint-Amant & Drapeau, 1998). Genetic cues appear to be sufficient to establish a rough locomotor circuit during development but it seems that activity is nonetheless important for fine-tuning this circuit. Spontaneous activity may therefore provide important signals for activity-dependent developmental processes.

Several studies have shown that spontaneous movements are important for the proper development of muscles and joints and there is extensive evidence to suggest that spontaneous neuronal activity is important for fundamental features of network development, including the survival, proliferation and differentation of neurons as well as axonal pathfinding, synaptogenesis, dendritic branching and other fine-tuning of circuits (reviewed by O'Donovan

et al., 1998; Kirkby et al., 2013) including the change in intracellular chloride concentration that mediates a shift from post-synaptic depolarization to hyperpolarization (Fiumelli & Woodin, 2007).

Compensatory homeostatic mechanisms may not be able to fully recapitulate endogenous patterns of spontaneous activity. A study in which *Drosophila* motoneurons were driven to fire synchronously rather than following their natural spontaneous activity patterns caused developmental delays in the onset of motor behaviors, suggesting that precise patterns of activity are required for network development (Crisp et al., 2011). This is supported by findings in the chick embryo where innervation of muscles by motorneurons was disrupted following spontaneous activity blockade but rescued by mimicking endogenous patterns of motoneuron activation in the chick embryo with optogenetics (Hanson & Landmesser, 2004; Kastanenka & Landmesser, 2010). Recent work in the zebrafish embryo showed that chronically inhibiting spinal motoneuron activity from 18 - 19 hpf caused significant delays in the development of coordinated activity patterns important for motor behaviors (Warp et al., 2012). These results suggest that endogenous patterns of spontaneous activity play an essential role in guiding the formation and maturation of motor networks. The extent to which homeostatic mechanisms can compensate for changes in spontaneous activity during development is likely to vary considerably depending on the type of activity perturbation and the compensatory mechanisms available at that developmental stage.

V.4.4. Future work

Perturbing network activity globally may activate a number of synaptic, cellular and/or network-wide compensatory mechanisms and thus it becomes difficult to interpret these experimental results. In contrast to global pharmacological perturbations of activity, a more experimentally tractable and developmentally relevant situation would be a selective reduction in synaptic activity in a subset of neurons. We have shown the zebrafish to be a useful model for investigating homeostatic plasticity at the cellular and organismal level and many genetic techniques are now available with which to selectively target and manipulate the activity of neural subpopulations. Optogenetic tools can be used over short timescales (e.g. minutes to hours) to produce patterned activation or silencing of populations of neurons

(Warp et al., 2012) while the expression of neural toxins such as tetanus toxin can produce an irreversible blockade of chemical neurotransmission throughout development (Asakawa et al., 2008) or starting at later time points under the control of an inducible promoter (Gerety et al., 2013).

Our results from Chapters 2 and 3 have described the roles of CiD and CoPA interneurons in embryonic locomotor behaviors. Understanding their function in the network under physiological conditions allows us to make better predictions about the type of homeostatic plasticity mechanisms that might be used to recover their activity. For example, if the firing of CiDs is chronically reduced in the embryo, we would predict that the strength of their synapses onto motoneurons would increase (scale up) in order to counteract this reduction in activity. Knowing that electrical networks are also present at this time we might also predict that the strength of electrical synapses between these neurons might increase, for example by adding more connexin proteins to form gap junctions. This type of response has been observed in the circuits that mediate spontaneous retinal waves mammalian embryos. Retinal waves are initially driven by gap junctions then taken over by cholinergic neurotransmission during the first postnatal week, but if cholinergic signaling is blocked genetically or pharmacologically gap junctions continue to drive retinal waves postnatally (Stacy et al., 2005; Sun et al., 2008). The mechanisms underlying this compensation are not yet known but may be well suited to investigation in the developing zebrafish spinal cord.

V.5. OUTLOOKS FOR THE STUDY OF LOCOMOTOR CIRCUITS

A long and fruitful history of work in model organisms has paved the way for much of our current understanding of spinal locomotor circuits. Systematic anatomical and electrophysiological surveys of spinal neuronal classes, whether by dye-filled patch clamp recordings or targeted genetic approaches, have laid an important foundation for understanding the development and organization of the spinal cord. In the field of systems neuroscience, however, the goal is to understand the integrated activity of neural circuits and this is the driving force for modern research in locomotion. This section will discuss some of the most recently developed approaches to dissect vertebrate locomotor circuits, in particular in the zebrafish, and consider where this field of research is headed in the future.

V.5.1. Genetic tools for visualizing and manipulating network activity

The ever-improving genetic toolbox has been a major part of recent advances in understanding locomotor circuits. Functional calcium imaging of neuronal activity has been around for decades but the development of genetically-encoded calcium indicators such as GCaMP in the nervous system has revolutionized neuroscience because this tool allows for the non-invasive observation of the activity of entire populations of genetically-defined neurons (Portugues et al., 2013). Functional imaging techniques can complement detailed but low-throughput electrophysiological studies with larger-scale activity maps and have been employed in countless studies and model organisms. Recently, researchers have developed techniques to perform whole-brain calcium imaging with single cell resolution in the behaving larval zebrafish to dissect the neural circuits mediating motor control and learning (Ahrens et al., 2012). Fluorescent reporters of glutamate binding (iGluSnFr; Marvin et al., 2013) and of intracellular chloride concentration (Clomeleon; Kuner & Augustine, 2000) can also be used to visualize the activity of excitatory and inhibitory neurotransmission, respectively. The expression of Clomeleon in spinal motoneurons and interneurons in the chick embryo was recently used to show that the homeostatic synaptic scaling induced by chronic $GABA_A$ receptor blockade was due to an increase in intracellular chloride levels (Lindsly et al., 2014).

Optogenetic switches make it possible to turn neuron activity either on or off and can be used to assess the sufficiency and necessity of certain neural populations for behavior (Portugues et al., 2013). The activation of hindbrain CiD interneurons with channelrhodopsin, a light-gated cation channel, triggers swimming behavior in zebrafish larvae (Eklöf-Ljunggren et al., 2014; Kimura et al., 2013), providing strong evidence that this cell is a key excitatory interneuron in the zebrafish locomotor CPG. A light-gated iontotropic glutamate receptor, LiGluR (Svobota et al., 2007; Volgraf et al., 2005), can also be used to activate neurons and was used to identify a novel role of the Kolmer-Agduhr spinal neuron for triggering slow swimming in the zebrafish larvae (Wyart et al., 2009). Both light-gated chloride (halorhodopsin) and proton (archaeorhodopsin) pumps can be use to reversibly silence neuronal firing and the former has been used to identify hindbrain neurons in the larval

zebrafish that are necessary for initiating swimming (Arrenberg et al., 2009; Kimura et al., 2013) or for generating eye saccades (Schoonheim et al., 2010).

The expression of transgenes coding for neuronal toxins such as tetanus toxin can also be used to block neurotransmitter release albeit without the fine temporal resolution and reversibility of optogenetic techniques (Asakawa et al., 2008). Efficient genetic strategies such as CRISPRS for targeted gene editing have made it possible to induce a gene knockout, mutation, or overexpression in a targeted neuronal type in order to investigate changes in circuit function (Kimura et al., 2014). These latter genetic techniques may be particularly useful for examining the developmental role of neuronal activity whereas optogenetics tools have fine spatiotemporal control and can be adapted for a wide variety of experiments.

V.5.2. Anatomical studies of the "connectome"

A diagram of connectivity of the entire nervous system, referred to as a "connectome," is a goal currently being pursued by many neuroscientists (Kleinfeld et al., 2011). The synaptic connectivity of local circuits is being investigated at extremely high resolution using serial section or block-face electron microscopy techniques to reconstruct the anatomy of small but complex pieces of nervous system tissues, for example the *Drosophila* brain and a mouse cortical column (reviewed by Plaza et al., 2014). The field of connectomics is growing tremendously but is hindered by time- and labor-intensive data analysis, therefore the small size of model organisms such as *Drosophila* and zebrafish provide an advantage. As data collection and analysis improves, mapping the connectome may become a standardized tool for investigating neural circuits including those of the spinal cord. However, many researchers view the field of connectomics as useful but far from sufficient to understand circuit function - in other words " a necessary beginning, but not in itself an answer" (Marder, 2012). The complete connectome of adult *C. elegans* has been reconstructed from serial-section electron microscopy (Varshney et al., 2011; White et al., 1986) yet even this "simple" nervous system diagram containing just 302 neurons has not greatly advanced our understanding of circuit function (Bargmann, 2012).

The anatomical labeling of microcircuits using rabies virus techniques is likely of greater value for the current study of neural circuits. With this technique, monosynaptically

restricted presynaptic partners of a single neuron of interest can be labeled with fluorescent proteins (Wickersham et al., 2007) or even made to express useful optogenetic tools for observing or controlling activity or constructs to manipulate gene expression (Osakada et al., 2011), thus allowing researchers to study both structure and function. This transsynaptic rabies virus technique has been used in several studies to characterize the interneurons that contact the motoneurons of defined muscles in the mammalian spinal cord (Dougherty et al., 2013; Stepien et al., 2010; Tripodi et al., 2011). An intersectional approach to label neurons presynaptic to both motoneurons and the cerebellum revealed interneurons that are likely to provide an efferent copy of the motor command (corollary discharge) to higher brain centers and therefore play a key role in motor control in the mouse (Pivetta et al., 2014). It is also possible to label the postsynaptic partners of sensory neurons using a similar rabies virus technique (Zampieri et al., 2014). The study of microcircuits using these techniques is currently being adapted for use in other model organisms including the zebrafish and will no doubt be a powerful tool for future studies of the anatomy and function of locomotor circuits across species.

V.5.3. Computer modeling and bioengineering of integrated circuits

Finally, it is important to consider the work being done to create an integrated model of locomotor function within the field of computational neuroscience. By feeding experimental data from neurobiology into biophysical models, testable predictions arise that can be addressed with further experimentation, creating a feedback loop that serves to validate and refine a model (Prinz, 2006). Anatomical and physiological data from experimental studies have been used to generate realistic models of many locomotor CPGs (reviewed by Ijspeert, 2008) including the larval zebrafish (Hill et al., 2005; Kuo & Eliasmith, 2005; Knudsen et al., 2006). This approach can help reveal how network patterns emerge from the properties of individual elements (neurons), for example that motor patterning appears to be extremely stable across a large range of synaptic strengths in the locomotor CPG (Kuo & Eliasmith, 2005). Computer modeling is also crucial for linking the activity of neural networks to behavior, making it possible to compare the conceptual model of a locomotor

circuit against recorded locomotor patterns from an animal and to change model parameters to better fit the biological data (Ijspeert, 2008).

Modern robotics engineering is a fast growing field that has made much practical use of locomotor CPG research but like computer modeling has also revealed major gaps in our understanding of these circuits. For example, it is relatively straightforward to have prosthetic limbs that are controlled by a patient's motor cortex but it remains difficult to send somatosensory feedback from the limb to the nervous system (Bensmaia & Miller, 2014). A field known as biorobotics aims to construct biomimetic robots that recapitulate the known locomotor patterns of animals and their corresponding sensorimotor skills. These biorobots can be used to test hypotheses about circuit function under different environmental conditions similar to computer modeling while also informing biomechanical design, thus benefitting both fundamental biology and bioengineering (Ijspeert, 2014). Biorobots will be an important step towards understanding human locomotion much in the same way that experimental research in model organisms has greatly advanced our understanding of the mammalian nervous system.

V.5.4. Final thoughts

In this thesis I have outlined how model organisms have advanced the study of the neural control of locomotion and presented novel findings from the zebrafish embryo that contribute to our understanding of developing locomotor networks. Despite the knowledge and experimental tools we have with which to dissect neural circuits in the zebrafish it is clear that even these relatively "simple" embryonic circuits are still very complex and difficult to understand. Furthermore, different species are likely to use both shared and specialized strategies for locomotor control that reflect their ecological niche. Multidisciplinary approaches in a wide variety of model organisms will be needed to reach even our modest goal of understanding the developing spinal locomotor network.

Our work here has been presented primarily in the context of spinal circuits and motor behaviors but may nonetheless shed light on the mechanisms and strategies of developing neural circuits for higher-order cognition. In his excellent essay in which he poses the question "shall we even understand the fly's brain?" the neuroscientist G. Laurent laments that

"when it comes to computation, integrative principles or to 'cognitive' issues such as perception, ...most neuroscientists act as if King Cortex appeared one bright morning out of nowhere, leaving in the mud a zoo of robotic critters, prisoners of their flawed designs and obviously incapable of perception, feeling, pain, sleep, emotions, to name but a few of their deficiencies. How nineteenth century!" (van Hemmen & Sejnowski, 2006). Many researchers have identified significant parallels between vertebrate spinal cord and brainstem CPG circuits and neocortical circuits that suggest a highly similar underlying organization and function (Llinás, 2002; Yuste et al., 2005). Our investigations of embryonic zebrafish locomotor networks may therefore provide unexpected insights into the nature of neural circuits beyond the spinal cord.

REFERENCES

Ahrens MB, Li JM, Orger MB, Robson DN, Schier AF, Engert F, Portugues R (2012) Brain-wide neuronal dynamics during motor adaptation in zebrafish. Nature 485:471–477.

Ali DW, Buss RR, Drapeau P (2000a) Properties of miniature glutamatergic EPSCs in neurons of the locomotor regions of the developing zebrafish. 83:181–191.

Ali DW, Drapeau P, Legendre P (2000b) Development of spontaneous glycinergic currents in the mauthner neuron of the zebrafish embryo. 84:1726–1736.

Ampatzis K, Song J, Ausborn J, El Manira A (2014) Separate microcircuit modules of distinct V2a interneurons and motoneurons control the speed of locomotion. Neuron 83:934–943.

Arrenberg AB, Bene F Del, Baier H (2009) Optical control of zebrafish behavior with halorhodopsin. Proc Natl Acad Sci 106:17968–17973.

Asakawa K, Suster ML, Mizusawa K, Nagayoshi S, Kotani T, Urasaki A, Kishimoto Y, Hibi M, Kawakami K (2008) Genetic dissection of neural circuits by Tol2 transposon-mediated Gal4 gene and enhancer trapping in zebrafish. Proc Natl Acad Sci 105:1255–1260.

Bargmann CI (2012) Beyond the connectome: how neuromodulators shape neural circuits. Bioessays 34:458–465.

Ben-Ari Y (2002) Excitatory actions of GABA during development: the nature of the nurture. Nat Rev Neurosci 3:728–739.

Bennett MV (1966) Physiology of electrotonic junctions. Ann N Y Acad Sci 137:509–539.

Bensmaia SJ, Miller LE (2014) Restoring sensorimotor function through intracortical interfaces: progress and looming challenges. Nat Rev Neurosci 15:313–325.

Bernhardt RR, Chitnis a B, Lindamer L, Kuwada JY (1990) Identification of spinal neurons in the embryonic and larval zebrafish. J Comp Neurol 302:603–616.

Blackburn PR, Campbell JM, Clark KJ, Ekker SC (2013) The CRISPR system—keeping zebrafish gene targeting fresh. Zebrafish 10:116–118.

Blankenship AG, Feller MB (2010) Mechanisms underlying spontaneous patterned activity in developing neural circuits. Nat Rev Neurosci 11:18–29.

Brocard F, Ryczko D, Fénelon K, Hatem R, Gonzales D, Auclair F, Dubuc R (2010) The transformation of a unilateral locomotor command into a symmetrical bilateral activation in the brainstem. J Neurosci 30:523–533.

Broch L, Morales RD, Sandoval AV, Hedrick MS (2002) Regulation of the respiratory central pattern generator by chloride-dependent inhibition during development in the bullfrog (*Rana catesbeiana*). J Exp Biol 205:1161–1169.

Brodin L, Grillner S, Rovainen CM (1985) N-Methyl-D-aspartate (NMDA), kainate and quisqualate receptors and the generation of fictive locomotion in the lamprey spinal cord. Brain Res 325:302–306.

Brown TG (1911) The intrinsic factors in the act of progression in the mammal. Proc R Soc London Ser B:308–319.

Brown TG (1914) On the nature of the fundamental activity of the nervous centres; together with an analysis of the conditioning of rhythmic activity in progression, and a theory of the evolution of function in the nervous system. J Physiol 48:18–46.

Brustein E, Chong M, Holmqvist B, Drapeau P (2003) Serotonin patterns locomotor network activity in the developing zebrafish by modulating quiescent periods. J Neurobiol 57:303–322.
Buchanan JT (1982) Identification of interneurons with contralateral, caudal axons in the lamprey spinal cord: synaptic interactions and morphology. J Neurophysiol 47:961–975.
Buchanan JT, Grillner S (1987) Newly identified'glutamate interneurons' and their role in locomotion in the lamprey spinal cord. Science 236:312–314.
Buchanan JT, Grillner S, Cullheim S, Risling M (1989) Identification of excitatory interneurons contributing to generation of locomotion in lamprey: structure, pharmacology, and function. J Neurophysiol 62:59–69.
Budick SA, O'Malley DM (2000) Locomotor repertoire of the larval zebrafish: swimming, turning and prey capture. J Exp Biol 203:2565–2579.
Bullock TH (1961) The origins of patterned nervous discharge. Behaviour:48–59.
Buss RR, Drapeau P (2001) Synaptic drive to motoneurons during fictive swimming in the developing zebrafish. J Neurophysiol 86:197–210.
Carlisle TC, Ribera AB (2014) *Connexin 35b* expression in the spinal cord of *Danio rerio* embryos and larvae. J Comp Neurol 522:861–875.
Chong M, Drapeau P (2007) Interaction between hindbrain and spinal networks during the development of locomotion in zebrafish. Dev Neurobiol 67:933–947.
Chub N, O'Donovan MJ (1998) Blockade and recovery of spontaneous rhythmic activity after application of neurotransmitter antagonists to spinal networks of the chick embryo. J Neurosci 18:294–306.
Chub N, O'Donovan MJ (2001) Post-episode depression of GABAergic transmission in spinal neurons of the chick embryo. J Neurophysiol 85:2166–2176.
Clarac F (2008) Some historical reflections on the neural control of locomotion. Brain Res Rev 57:13–21.
Coghill GE (1929) Anatomy and the problem of behavior. Cambridge Univ Press, Cambridge, England.
Cohen AH, Wallén P (1980) The neuronal correlate of locomotion in fish. Exp Brain Res 41:11–18.
Crapse TB, Sommer MA (2008) Corollary discharge across the animal kingdom. Nat Rev Neurosci 9:587–600.
Crisp SJ, Evers JF, Bate M (2011) Endogenous patterns of activity are required for the maturation of a motor network. J Neurosci 31:10445–10450.
Dale N (1985) Reciprocal inhibitory interneurones in the *Xenopus* embryo spinal cord. J Physiol 363:61–70.
Dale N (1995) Experimentally derived model for the locomotor pattern generator in the *Xenopus* embryo. J Physiol 489:489–510.
Dale N, Grillner S (1986) Dual-component synaptic potentials in the lamprey mediated by excitatory amino acid receptors. J Neurosci 6:2653–2661.
Danos N, Lauder G V (2007) The ontogeny of fin function during routine turns in zebrafish *Danio rerio*. J Exp Biol 210:3374–3386.
Davis GW (2006) Homeostatic control of neural activity: from phenomenology to molecular design. Annu Rev Neurosci 29:307–323.

Davis GW (2013) Homeostatic signaling and the stabilization of neural function. Neuron 80:718–728.
Deeg KE, Aizenman CD (2011) Sensory modality-specific homeostatic plasticity in the developing optic tectum. Nat Neurosci 14:548–550.
Deliagina TG, Zelenin P V, Orlovsky GN (2002) Encoding and decoding of reticulospinal commands. 40:166–177.
Desai NS, Cudmore RH, Nelson SB, Turrigiano GG (2002) Critical periods for experience-dependent synaptic scaling in visual cortex. Nat Neurosci 5:783–789.
Dougherty KJ, Kiehn O (2010) Functional organization of V2a-related locomotor circuits in the rodent spinal cord. Ann N Y Acad Sci 1198:85–93.
Dougherty KJ, Zagoraiou L, Satoh D, Rozani I, Doobar S, Arber S, Jessell TM, Kiehn O (2013) Locomotor rhythm generation linked to the output of spinal shox2 excitatory interneurons. Neuron 80:920–933.
Douglass AD, Kraves S, Deisseroth K, Schier AF, Engert F (2008) Escape behavior elicited by single, channelrhodopsin-2-evoked spikes in zebrafish somatosensory neurons. Curr Biol 18:1133–1137.
Downes GB, Granato M (2006) Supraspinal input is dispensable to generate glycine-mediated locomotive behaviors in the zebrafish embryo. J Neurobiol 66:437–451.
Downes GB, Waterbury JA, Granato M (2002) Rapid *in vivo* labeling of identified zebrafish neurons. Genesis 34:196–202.
Drapeau P, Saint-Amant L, Buss RR, Chong M, McDearmid JR, Brustein E (2002) Development of the locomotor network in zebrafish. Prog Neurobiol 68:85–111.
Easley-Neal C, Fierro J, Buchanan J, Washbourne P (2013) Late recruitment of synapsin to nascent synapses is regulated by Cdk5. Cell Rep 3:1199–1212.
Eklof-Ljunggren E, Haupt S, Ausborn J, Dehnisch I, Uhlen P, Higashijima S-I., El Manira A. (2012) Origin of excitation underlying locomotion in the spinal circuit of zebrafish. Proc Natl Acad Sci 109:5511–5516.
El Manira A, Grillner S (2014) Motion with direction and balance. Neuron 83:515–517.
Feller MB (1999) Spontaneous correlated activity in developing neural circuits. Neuron 22:653-656.
Felt RHM, Mulder EJH, Lüchinger AB, van Kan CM, Taverne MA, de Vries JI (2012) Spontaneous cyclic embryonic movements in humans and guinea pigs. Dev Neurobiol 72:1133–1139.
Fetcho JR (1992) The spinal motor system in early vertebrates and some of its evolutionary changes. Brain Behav Evol 40:82–97.
Fetcho JR, Faber DS (1988) Identification of motoneurons and interneurons in the spinal network for escapes initiated by the mauthner cell in goldfish. J Neurosci 8:4192–4213.
Fiumelli H, Woodin MA (2007) Role of activity-dependent regulation of neuronal chloride homeostasis in development. Curr Opin Neurobiol 17:81–86.
Ford JM, Mathalon DH, Whitfield S, Faustman WO, Roth WT (2002) Reduced communication between frontal and temporal lobes during talking in schizophrenia. Biol Psychiatry 51:485–492.
Friedrich RW, Jacobson GA, Zhu P (2010) Circuit neuroscience in zebrafish. Curr Biol 20:R371–R381.

Gallace A, Spence C (2010) The science of interpersonal touch: an overview. Neurosci Biobehav Rev 34:246–259.
Gallego R, Kuno M, Nunez R, Snider WD (1979) Disuse enhances synaptic efficacy in spinal mononeurones. J Physiol 291:191–205.
Gerety SS, Breau M a, Sasai N, Xu Q, Briscoe J, Wilkinson DG (2013) An inducible transgene expression system for zebrafish and chick. Development 140:2235–2243.
Goaillard J-M, Taylor AL, Schulz DJ, Marder E (2009) Functional consequences of animal-to-animal variation in circuit parameters. Nat Neurosci 12:1424–1430.
Gonzalez-Islas C, Wenner P (2006) Spontaneous network activity in the embryonic spinal cord regulates AMPAergic and GABAergic synaptic strength. Neuron 49:563–575.
Gosgnach S, Lanuza GM, Butt SJB, Saueressig H, Zhang Y, Velasquez T, Riethmacher D, Callaway EM, Kiehn O, Goulding M (2006) V1 spinal neurons regulate the speed of vertebrate locomotor outputs. Nature 440:215–219.
Goulding M (2009) Circuits controlling vertebrate locomotion: moving in a new direction. Nat Rev Neurosci 10:507–518.
Goulding M, Lanuza G, Sapir T, Narayan S (2002) The formation of sensorimotor circuits. Curr Opin Neurobiol 12:508–515.
Goulding M, Pfaff SL (2005) Development of circuits that generate simple rhythmic behaviors in vertebrates. Curr Opin Neurobiol 15:14–20.
Granato M, van Eeden FJ, Schach U, Trowe T, Brand M, Furutani-Seiki M, Haffter P, Hammerschmidt M, Heisenberg CP, Jiang YJ, Kane DA, Kelsh RN, Mullins MC, Odenthal J, Nüsslein-Volhard C (1996) Genes controlling and mediating locomotion behavior of the zebrafish embryo and larva. Development 123:399–413.
Grashow R, Brookings T, Marder E (2010) Compensation for variable intrinsic neuronal excitability by circuit-synaptic interactions. J Neurosci 30:9145–9156.
Grillner S (2003) The motor infrastructure: from ion channels to neuronal networks. Nat Rev Neurosci 4:573–586.
Grillner S (2006) Biological pattern generation: the cellular and computational logic of networks in motion. Neuron 52:751–766.
Grillner S, Robertson B, Stephenson-Jones M (2013) The evolutionary origin of the vertebrate basal ganglia and its role in action selection. J Physiol 591:5425.
Grillner S, Wallen P, Brodin L, Lansner A (1991) Neuronal network generating locomotor behavior in lamprey: circuitry, transmitters, membrane properties, and simulation. Annu Rev Neurosci 14:169–199.
Guertin PA (2009) The mammalian central pattern generator for locomotion. Brain Res Rev 62:45–56.
Hale ME, Ritter DA, Fetcho JR (2001) A confocal study of spinal interneurons in living larval zebrafish. J Comp Neurol 437:1–16.
Hamburger V (1963) Some aspects of the embryology of behavior. Q Rev Biol 38:342–365.
Hamburger V (1989) The journey of a neuroembryologist. Annu Rev Neurosci 12:1–13.
Hamburger V, Balaban M (1963) Observations and experiments on spontaneous rhythmical behavior in the chick embryo. Dev Biol 7:533–545.
Hamburger V, Balaban M, Oppenheim R, Wenger E (1965) Periodic motility of normal and spinal chick embryos between 8 and 17 days of incubation. J Exp Zool 159:1–13.

Hamburger, V and Hamilton H (1951) A series of normal stages in the development of the chick embryo. J Morphol 88:49–92.
Hanson MG, Landmesser LT (2004) Normal patterns of spontaneous activity are required for correct motor axon guidance and the expression of specific guidance molecules. Neuron 43:687–701.
Harris-Warrick RM (2011) Neuromodulation and flexibility in Central Pattern Generator networks. Curr Opin Neurobiol 21:685–692.
Harvey W (1651) Exercitationes de generatione animalium. Du-Gardianis, London, England.
Haverkamp LJ, Oppenheim RW (1986) Behavioral development in the absence of neural activity: effects of chronic immobilization on amphibian embryos. J Neurosci 6:1332–1337.
Higashijima S, Masino MA, Mandel G, Fetcho JR (2004a) Engrailed-1 expression marks a primitive class of inhibitory spinal interneuron. J Neurosci 24:5827–5839.
Higashijima S-I, Schaefer M, Fetcho JR (2004b) Neurotransmitter properties of spinal interneurons in embryonic and larval zebrafish. J Comp Neurol 480:19–37.
Hill SA, Liu X-P, Borla MA, José JV, O'Malley DM (2005) Neurokinematic modeling of complex swimming patterns of the larval zebrafish. Neurocomputing 65:61–68.
Hooker D (1952) The prenatal origin of behavior. Univ Kansas Press Lawrence, Kansas.
Horn KG, Memelli H, Solomon IC (2012) Emergent central pattern generator behavior in gap-junction-coupled Hodgkin-Huxley style neuron model. Comput Intell Neurosci 2012:11.
Huang K-H, Ahrens MB, Dunn TW, Engert F (2013) Spinal projection neurons control turning behaviors in zebrafish. Curr Biol 23:1566–1573.
Ijspeert AJ (2014) Biorobotics: Using robots to emulate and investigate agile locomotion. Science 346:196–203.
Ijspeert AJ (2008) Central pattern generators for locomotion control in animals and robots: a review. Neural Netw 21:642–653.
Jabeen S, Thirumalai V (2013) Distribution of the gap junction protein connexin 35 in the central nervous system of developing zebrafish larvae. Front Neural Circuits 7:91.
Jean-Xavier C, Mentis GZ, O'Donovan MJ, Cattaert D, Vinay L (2007) Dual personality of GABA/glycine-mediated depolarizations in immature spinal cord. Proc Natl Acad Sci 104:11477–11482.
Jessell TM (2000) Neuronal specification in the spinal cord: inductive signals and transcriptional codes. Nat Rev Genet 1:20–29.
Jordan LM (1998) Initiation of locomotion in mammals. Ann N Y Acad Sci 860:83–93.
Kaneko M, Stellwagen D, Malenka RC, Stryker MP (2008) Tumor necrosis factor-α mediates one component of competitive, experience-dependent plasticity in developing visual cortex. Neuron 58:673–680.
Kastanenka K V, Landmesser LT (2010) *In vivo* activation of channelrhodopsin-2 reveals that normal patterns of spontaneous activity are required for motoneuron guidance and maintenance of guidance molecules. J Neurosci 30:10575–10585.
Katz PS (1995) Intrinsic and extrinsic neuromodulation of motor circuits. Curr Opin Neurobiol 5:799–808.
Kepler TB, Marder E, Abbott LF (1990) The effect of electrical coupling on the frequency of model neuronal oscillators. Science 248:83–85.

Khorkova O, Golowasch J (2007) Neuromodulators, not activity, control coordinated expression of ionic currents. J Neurosci 27:8709–8718.
Kiehn O (2006) Locomotor circuits in the mammalian spinal cord. Annu Rev Neurosci 29:279–306.
Kiehn O, Tresch MC (2002) Gap junctions and motor behavior. Trends Neurosci 25:108–115.
Kimmel CB, Ballard WW, Kimmel SR, Ullmann B, Schilling TF (1995) Stages of embryonic development of the zebrafish. Dev Dyn 203:253–310.
Kimura Y, Okamura Y, Higashijima S-I (2006) *alx*, a zebrafish homolog of *Chx10*, marks ipsilateral descending excitatory interneurons that participate in the regulation of spinal locomotor circuits. J Neurosci 26:5684–5697.
Kimura Y, Satou C, Fujioka S, Shoji W, Umeda K, Ishizuka T, Yawo H, Higashijima S-I (2013) Hindbrain V2a neurons in the excitation of spinal locomotor circuits during zebrafish swimming. Curr Biol 23:843–849.
Kirk MD, Wine JJ (1984) Identified interneurons produce both primary afferent depolarization and presynaptic inhibition. Science 225:854–856.
Kirkby LA, Sack GS, Firl A, Feller MB (2013) A role for correlated spontaneous activity in the assembly of neural circuits. Neuron 80:1129–1144.
Kleinfeld D, Bharioke A, Blinder P, Bock DD, Briggman KL, Chklovskii DB, Denk W, Helmstaedter M, Kaufhold JP, Lee W-CA (2011) Large-scale automated histology in the pursuit of connectomes. J Neurosci 31:16125–16138.
Knudsen DP, Arsenault JT, Hill SA, O'Malley DM, José JV (2006) Locomotor network modeling based on identified zebrafish neurons. Neurocomputing 69:1169–1174.
Korn H, Faber DS (2005) The Mauthner cell half a century later: a neurobiological model for decision-making? Neuron 47:13–28.
Kuhse J, Schmieden V, Betz H (1990) A single amino acid exchange alters the pharmacology of neonatal rat glycine receptor subunit. Neuron 5:867—873.
Kuner T, Augustine GJ, Carolina N (2000) Neurotechnique indicator for chloride: capturing chloride transients in cultured hippocampal neurons. 27:447–459.
Kuo PD, Eliasmith C (2005) Integrating behavioral and neural data in a model of zebrafish network interaction. Biol Cybern 93:178–187.
Lacquaniti F, Ivanenko YP, Zago M (2012) Development of human locomotion. Curr Opin Neurobiol 22:822–828.
Li W-C (2011) Generation of locomotion rhythms without inhibition in vertebrates: the search for pacemaker neurons. Integr Comp Biol 51:879–889.
Li W-C, Higashijima S-I, Parry DM, Roberts A, Soffe SR (2004) Primitive roles for inhibitory interneurons in developing frog spinal cord. J Neurosci 24:5840–5848.
Li W-C, Soffe SR, Roberts A (2002) Spinal inhibitory neurons that modulate cutaneous sensory pathways during locomotion in a simple vertebrate. J Neurosci 22:10924–10934.
Li W-C, Soffe SR, Roberts A (2003) The spinal interneurons and properties of glutamatergic synapses in a primitive vertebrate cutaneous flexion reflex. J Neurosci 23:9068–9077.
Li W-C, Soffe SR, Wolf E, Roberts A (2006) Persistent responses to brief stimuli: feedback excitation among brainstem neurons. J Neurosci 26:4026–4035.
Liao JC, Fetcho JR (2008) Shared versus specialized glycinergic spinal interneurons in axial motor circuits of larval zebrafish. J Neurosci 28:12982–12992.

Lindsly C, Gonzalez-Islas C, Wenner P (2014) Activity blockade and GABAA receptor blockade produce synaptic scaling through chloride accumulation in embryonic spinal motoneurons and interneurons. PLoS One 9:e94559.
Lisman J (2012) Excitation, inhibition, local oscillations, or large-scale loops: what causes the symptoms of schizophrenia? Curr Opin Neurobiol 22:537–544.
Llinás RR (2002) I of the vortex: From neurons to self. MIT press.
Loewenstein Y, Yarom Y, Sompolinsky H (2001) The generation of oscillations in networks of electrically coupled cells. Proc Natl Acad Sci 98:8095–8100.
Logothetis NK (1998) Single units and conscious vision. Philos Trans R Soc London Ser B Biol Sci 353:1801–1818.
Low SE, Ryan J, Sprague SM, Hirata H, Cui WW, Zhou W, Hume RI, Kuwada JY, Saint-Amant L (2010) *touché* is required for touch-evoked generator potentials within vertebrate sensory neurons. J Neurosci 30:9359–9367.
Low SE, Woods IG, Lachance M, Ryan J, Schier AF, Saint-Amant L (2012) Touch responsiveness in zebrafish requires voltage-gated calcium channel 2.1b. J Neurophysiol 108:148–159.
Malenka RC, Bear MF (2004) LTP and LTD: an embarrassment of riches. Neuron 44:5–21.
Manabe T, Kaneko S, Kuno M (1989) Disuse-induced enhancement of Ia synaptic transmission in spinal motoneurons of the rat. J Neurosci 9:2455–2461.
Marder E (2012) Neuromodulation of neuronal circuits: back to the future. Neuron 76:1–11.
Marder E, Goaillard J-M (2006) Variability, compensation and homeostasis in neuron and network function. Nat Rev Neurosci 7:563–574.
Marvin JS, Borghuis BG, Tian L, Cichon J, Harnett MT, Akerboom J, Gordus A, Renninger SL, Chen T, Bargmann CI, Orger MB, Schreiter ER, Demb JB, Gan W, Hires SA, Looger LL (2013) An optimized fluorescent probe for visualizing glutamate neurotransmission. Nat Methods 10:162–170.
McLean DL, Fan J, Higashijima S, Hale ME, Fetcho JR (2007) A topographic map of recruitment in spinal cord. Nature 446:71–75.
McLean DL, Fetcho JR (2008) Using imaging and genetics in zebrafish to study developing spinal circuits *in vivo*. Dev Neurobiol 68:817–834.
McLean DL, Masino MA, Koh IY, Lindquist WB, Fetcho JR (2008) Continuous shifts in the active set of spinal interneurons during changes in locomotor speed. Nat Neurosci 11:1419–1429.
Mendelson B (1986) Development of reticulospinal neurons of the zebrafish. II. Early axonal outgrowth and cell body position. J Comp Neurol 251:172–184.
Menelaou E, VanDunk C, McLean DL (2014) Differences in the morphology of spinal V2a neurons reflect their recruitment order during swimming in larval zebrafish. J Comp Neurol 522:1232–1248.
Mirat O, Sternberg JR, Severi KE, Wyart C (2013) ZebraZoom: an automated program for high-throughput behavioral analysis and categorization. Front Neural Circuits 7.
Moly PK, Ikenaga T, Kamihagi C, Islam AFM, Hatta K (2014) Identification of initially appearing glycine-immunoreactive neurons in the embryonic zebrafish brain. Dev Neurobiol 74:616–632.
Myers PZ, Eisen JS, Westerfield M (1986) Development and axonal outgrowth of identified motoneurons in the zebrafish. J Neurosci 6:2278–2289.

Narayanan CH, Fox MW, Hamburger V (1971) Prenatal development of spontaneous and evoked activity in the rat (*Rattus norvegicus albinus*). Behaviour 40:100–134.
Naumann EA, Kampff AR, Prober DA, Schier AF, Engert F (2010) Monitoring neural activity with bioluminescence during natural behavior. Nat Neurosci 13:513–520.
Nelson SB, Turrigiano GG (2008) Strength through diversity. Neuron 60:477–482.
Nguyen PV, Aniksztejn L, Catarsi S, Drapeau P (1999) Maturation of neuromuscular transmission during early development in zebrafish. J Neurophysiol 81:2852–2861.
Nikolaou N, Lowe AS, Walker AS, Abbas F, Hunter PR, Thompson ID, Meyer MP (2012) Parametric functional maps of visual inputs to the tectum. Neuron 76:317–324.
O'Donovan MJ, Chub N, Wenner P (1998) Mechanisms of spontaneous activity in developing spinal networks. J Neurobiol 37:131–145.
Osakada F, Mori T, Cetin AH, Marshel JH, Virgen B, Callaway EM (2011) New rabies virus variants for monitoring and manipulating activity and gene expression in defined neural circuits. Neuron 71:617–631.
Parker AJ, Newsome WT (1998) Sense and the single neuron: probing the physiology of perception. Annu Rev Neurosci 21:227–277.
Patterson BW, Abraham AO, MacIver MA, McLean DL (2013) Visually guided gradation of prey capture movements in larval zebrafish. J Exp Biol 216:3071–3083.
Pereda AE (2014) Electrical synapses and their functional interactions with chemical synapses. Nat Rev Neurosci 15:250–263.
Pereda AE, Curti S, Hoge G, Cachope R, Flores CE, Rash JE (2013) Gap junction-mediated electrical transmission: regulatory mechanisms and plasticity. Biochim Biophys Acta 1828:134–146.
Pietri T, Manalo E, Ryan J, Saint-Amant L, Washbourne P (2009) Glutamate drives the touch response through a rostral loop in the spinal cord of zebrafish embryos. Dev Neurobiol 69:780–795.
Pietri T, Roman A-C, Guyon N, Romano SA, Washbourne P, Moens CB, de Polavieja GG, Sumbre G (2013) The first mecp2-null zebrafish model shows altered motor behaviors. Front Neural Circuits 7:118.
Pivetta C, Esposito MS, Sigrist M, Arber S (2014) Motor-circuit communication matrix from spinal cord to brainstem neurons revealed by developmental origin. Cell 156:537–548.
Plaza SM, Scheffer LK, Chklovskii DB (2014) Toward large-scale connectome reconstructions. Curr Opin Neurobiol 25:201–210.
Portugues R, Engert F (2011) Adaptive locomotor behavior in larval zebrafish. Front Syst Neurosci 5:72.
Portugues R, Severi KE, Wyart C, Ahrens MB (2013) Optogenetics in a transparent animal: circuit function in the larval zebrafish. Curr Opin Neurobiol 23:119–126.
Preyer WT (1885) Specielle physiologie des embryo. Grieben, Leipzig, Germany.
Prinz AA (2006) Insights from models of rhythmic motor systems. Curr Opin Neurobiol 16:615–620.
Prinz AA, Bucher D, Marder E (2004) Similar network activity from disparate circuit parameters. Nat Neurosci 7:1345–1352.
Reyes R, Haendel M, Grant D, Melancon E, Eisen JS (2004) Slow degeneration of zebrafish Rohon-Beard neurons during programmed cell death. Dev Dyn 229:30–41.

Roberts A, Li W-C, Soffe SR (2010) How neurons generate behavior in a hatchling amphibian tadpole: an outline. Front Behav Neurosci 4:16.
Roberts A, Soffe SR, Wolf ES, Yoshida M, Zhao F (1998) Central circuits controlling locomotion in young frog tadpoles. Ann N Y Acad Sci 860:19–34.
Rossignol S, Dubuc R, Gossard J-P (2006) Dynamic sensorimotor interactions in locomotion. Physiol Rev 86:89–154.
Rovainen CM (1974) Synaptic interactions of reticulospinal neurons and nerve cells in the spinal cord of the sea lamprey. J Comp Neurol 154:207–223.
Rovainen CM (1982) Neurophysiology. Biol Lampreys 4:1–136.
Saint-Amant L (2006) Development of motor networks in zebrafish embryos. Zebrafish 3:173–190.
Saint-Amant L (2010) Development of motor rhythms in zebrafish embryos. Prog Brain Res 187:47–61.
Saint-Amant L, Drapeau P (1998) Time course of the development of motor behaviors in the zebrafish embryo. J Neurobiol 37:622–632.
Saint-Amant L, Drapeau P (2000) Motoneuron activity patterns related to the earliest behavior of the zebrafish embryo. J Neurosci 20:3964–3972.
Saint-Amant L, Drapeau P (2001) Synchronization of an embryonic network of identified spinal interneurons solely by electrical coupling. Neuron 31:1035–1046.
Sakurai A, Katz PS (2009) Functional recovery after lesion of a central pattern generator. J Neurosci 29:13115–13125.
Sankrithi NS, O'Malley DM (2010) Activation of a multisensory, multifunctional nucleus in the zebrafish midbrain during diverse locomotor behaviors. Neuroscience 166:970–993.
Sapir T, Geiman EJ, Wang Z, Velasquez T, Mitsui S, Yoshihara Y, Frank E, Alvarez FJ, Goulding M (2004) *Pax6* and *Engrailed 1* regulate two distinct aspects of Renshaw cell development. J Neurosci 24:1255–1264.
Satou C, Kimura Y, Higashijima S-I (2012) Generation of multiple classes of V0 neurons in zebrafish spinal cord: progenitor heterogeneity and temporal control of neuronal diversity. J Neurosci 32:1771–1783.
Schoonheim PJ, Arrenberg AB, Del Bene F, Baier H (2010) Optogenetic localization and genetic perturbation of saccade-generating neurons in zebrafish. J Neurosci 30:7111–7120.
Seredick SD, Van Ryswyk L, Hutchinson SA, Eisen JS (2012) Zebrafish Mnx proteins specify one motoneuron subtype and suppress acquisition of interneuron characteristics. Neural Dev 7:35.
Serrano-Velez JL, Rodriguez-Alvarado M, Torres-Vazquez II, Fraser SE, Yasumura T, Vanderpool KG, Rash JE, Rosa-Molinar E (2014) Abundance of gap junctions at glutamatergic mixed synapses in adult Mosquitofish spinal cord neurons. Front Neural Circuits 8:66.
Severi KE, Portugues R, Marques JC, O'Malley DM, Orger MB, Engert F (2014) Neural control and modulation of swimming speed in the larval zebrafish. Neuron 83:692-707.
Sherrington CS (1910) Flexion-reflex of the limb, crossed extension-reflex, and reflex stepping and standing. J Physiol 40:28.

Smith JC, Butera RJ, Koshiya N, Del C, Wilson CG, Johnson SM (2000) Respiratory rhythm generation in neonatal and adult mammals: the hybrid pacemaker – network model. Resp Physiol 122:131–147.
Soffe SR, Roberts A, Li W-C (2009) Defining the excitatory neurons that drive the locomotor rhythm in a simple vertebrate: insights into the origin of reticulospinal control. J Physiol 587:4829–4844.
Stacy RC, Demas J, Burgess RW, Sanes JR, Wong RO (2005) Disruption and recovery of patterned retinal activity in the absence of acetylcholine. J Neurosci 25:9347–9357.
Stepien AE, Tripodi M, Arber S (2010) Monosynaptic rabies virus reveals premotor network organization and synaptic specificity of cholinergic partition cells. Neuron 68:456–472.
Sun C, Warland DK, Ballesteros JM, van der List D, Chalupa LM (2008) Retinal waves in mice lacking the β2 subunit of the nicotinic acetylcholine receptor. Proc Natl Acad Sci 105:13638–13643.
Suster ML, Kania A, Liao M, Asakawa K, Charron F, Kawakami K, Drapeau P (2009) A novel conserved *evx1* enhancer links spinal interneuron morphology and cis-regulation from fish to mammals. Dev Biol 325:422–433.
Szobota S, Gorostiza P, Del Bene F, Wyart C, Fortin DL, Kolstad KD, Tulyathan O, Volgraf M, Numano R, Aaron HL (2007) Remote control of neuronal activity with a light-gated glutamate receptor. Neuron 54:535–545.
Tabak J, Rinzel J, O'Donovan MJ (2001) The role of activity-dependent network depression in the expression and self-regulation of spontaneous activity in the developing spinal cord. J Neurosci 21:8966–8978.
Temporal S, Desai M, Khorkova O, Varghese G, Dai A, Schulz DJ, Golowasch J (2011) Neuromodulation independently determines correlated channel expression and conductance levels in motor neurons of the stomatogastric ganglion. J Neurophysiol 21:3443-3456.
Thaler J, Harrison K, Sharma K, Lettieri K, Kehrl J, Pfaff SL (1999) Active suppression of interneuron programs within developing motor neurons revealed by analysis of homeodomain factor HB9. Neuron 23:675–687.
Tong H, McDearmid JR (2012) Pacemaker and plateau potentials shape output of a developing locomotor network. Curr Biol 22:2285–2293.
Tracy HC (1926) The development of motility and behavior reactions in the toadfish (*Opsanus tau*). J Comp Neurol 40:253–369.
Tripodi M, Stepien AE, Arber S (2011) Motor antagonism exposed by spatial segregation and timing of neurogenesis. Nature 479:61–66.
Trivedi CA, Bollmann JH (2013) Visually driven chaining of elementary swim patterns into a goal-directed motor sequence: a virtual reality study of zebrafish prey capture. Front Neural Circuits 7.
Turrigiano GG (2008) The self-tuning neuron: synaptic scaling of excitatory synapses. Cell 135:422–435.
Turrigiano GG (2011) Too many cooks? Intrinsic and synaptic homeostatic mechanisms in cortical circuit refinement. Annu Rev Neurosci 34:89–103.
Turrigiano GG (2012) Homeostatic synaptic plasticity: local and global mechanisms for stabilizing neuronal function. Cold Spring Harb Perspect Biol 4:a005736.

Turrigiano GG, Nelson SB (2004) Homeostatic plasticity in the developing nervous system. Nat Rev Neurosci 5:97–107.
Van Hemmen JL, Sejnowski TJ (2006) 23 problems in systems neuroscience. Oxford University Press, New York, USA.
Van Leeuwenhoek A, Palm LC (1989) Collected Letters of Antoni Van Leeuwenhoek. CRC Press.
Varshney LR, Chen BL, Paniagua E, Hall DH, Chklovskii DB (2011) Structural properties of the *Caenorhabditis elegans* neuronal network. PLoS Comput Biol 7:e1001066.
Visintini F, Levi-Montalcini R (1939) Relazione tra differenziazione strutturale e funzionale dei centri e delle vie nervose nell'embrione di pollo. Schweiz Arch Neurol Psychiat 43:150.
Volgraf M, Gorostiza P, Numano R, Kramer RH, Isacoff EY, Trauner D (2005) Allosteric control of an ionotropic glutamate receptor with an optical switch. Nat Chem Biol 2:47–52.
Warp E, Agarwal G, Wyart C, Friedmann D, Oldfield CS, Conner A, Del Bene F, Arrenberg AB, Baier H, Isacoff EY (2012) Emergence of patterned activity in the developing zebrafish spinal cord. Curr Biol 22:93–102.
Webb CB, Cope TC (1992) Modulation of la EPSP amplitude: the effects of chronic synaptic inactivity. J Neurosci 12:338–344.
Wells S, Nornes S, Lardelli M (2011) Transgenic zebrafish recapitulating *tbx16* gene early developmental expression. PLoS One 6:e21559.
Wenner P (2014) Homeostatic synaptic plasticity in developing spinal networks driven by excitatory GABAergic currents. Neuropharmacology 78:55–62.
Westphal RE, O'Malley DM (2013) Fusion of locomotor maneuvers, and improving sensory capabilities, give rise to the flexible homing strikes of juvenile zebrafish. Front Neural Circuits 7.
White JG, Southgate E, Thomson JN, Brenner S (1986) The structure of the nervous system of the nematode *Caenorhabditis elegans*. Philos Trans R Soc London B, Biol Sci 314:1–340.
Whiting B, Moiseff A, Rubio ME (2009) Cochlear nucleus neurons redistribute synaptic AMPA and glycine receptors in response to monaural conductive hearing loss. Neuroscience 163:1264–1276.
Wickersham IR, Lyon DC, Barnard RJ, Mori T, Finke S, Conzelmann K-K, Young JAT, Callaway EM (2007) Monosynaptic restriction of transsynaptic tracing from single, genetically targeted neurons. Neuron 53:639–647.
Wiersma CAG, Ikeda K (1964) Interneurons commanding swimmeret movements in the crayfish, *Procambarus clarkii* (girard). Comp Biochem Physiol 12:509–525.
Wiggin TD, Anderson TM, Eian J, Peck JH, Masino MA (2012) Episodic swimming in the larval zebrafish is generated by a spatially distributed spinal network with modular functional organization. J Neurophysiol 108:925–934.
Wilhelm JC, Rich MM, Wenner P (2009) Compensatory changes in cellular excitability, not synaptic scaling, contribute to homeostatic recovery of embryonic network activity. Proc Natl Acad Sci 106:6760–6765.

Wilhelm JC, Wenner P (2008) GABAA transmission is a critical step in the process of triggering homeostatic increases in quantal amplitude. Proc Natl Acad Sci 105:11412–11417.
Williams JA, Barrios A, Gatchalian C, Rubin L, Wilson SW, Holder N (2000) Programmed cell death in zebrafish rohon beard neurons is influenced by TrkC1/NT-3 signaling. Dev Biol 226:220–230.
Wilson DM (1961) The central nervous control of flight in a locust. J Exp Biol 38:l–490.
Windle WF, Griffin AM (1931) Observations on embryonic and fetal movements of the cat. J Comp Neurol 52:149–188.
Windle WF, O'Donnell JE, Glasshagle EE (1933) The early development of spontaneous and reflex behavior in cat embryos and fetuses. Physiol Zool 6:521–541.
Wyart C, Del Bene F, Warp E, Scott EK, Trauner D, Baier H, Isacoff EY (2009) Optogenetic dissection of a behavioural module in the vertebrate spinal cord. Nature 461:407–410.
Yuste R, Maclean JN, Smith J, Lansner A (2005) The cortex as a central pattern generator. Nat Rev Neurosci 6:477–483.
Zampieri N, Jessell TM, Murray AJ (2014) Mapping sensory circuits by anterograde transsynaptic transfer of recombinant rabies virus. Neuron 81:766–778.
Zhang W, Linden DJ (2003) The other side of the engram: experience-driven changes in neuronal intrinsic excitability. Nat Rev Neurosci 4:885–900.
Zhong G, Droho S, Crone SA, Dietz S, Kwan AC, Webb WW, Sharma K, Harris-Warrick RM (2010) Electrophysiological characterization of V2a interneurons and their locomotor-related activity in the neonatal mouse spinal cord. J Neurosci 30:170–182.

APPENDIX A

CONTRIBUTION TO THE ARTICLES

For the article "**A Hybrid Electrical/Chemical Circuit in the Spinal Cord Generates a Transient Embryonic Motor Behavior**" (Chapter 2 in this thesis), I played a key role in the design, acquisition, analysis and interpretation of the data. This project was initially conceived as a behavioral study by Joel Ryan, a Master's student in the laboratory of Dr. Louis Saint-Amant. Mr. Ryan contributed to designing experiments and collecting data for figures 1-3 including taking videos of spontaneous coiling in wild-type, mutant and lesioned zebrafish as well as some analysis. In total his independent work provided the data for 4 of 41 panels and work that he and I did together provided the data for 6 of 41 panels. I designed the experiments and collected data for the electrophysiological, anatomical and remaining behavioral data that accounted for figures 4-8 (31 of 41 panels). I performed all of the statistical analyses and prepared the final figures. I wrote the article together with my supervisor.

For the article "**Sensory gating of an embryonic zebrafish interneuron during spontaneous motor behaviors**" (Chapter 3 in this thesis), I played a key role in the design, acquisition, analysis and interpretation of the data. I conceived the idea for this project with my supervisor and I carried out all of the experiments including the embryo injections, electrophysiology, behavior and confocal microscopy. I performed all statistical analyses. I prepared the final figures and drafted the manuscript with final editing by my supervisor.

For the article "**Synaptic Scaling and the Development of a Motor Network**" (Chapter 4 in this thesis), I played a key role in the acquisition, analysis and interpretation of the data. My supervisor was responsible for the conception of this study. I carried out all of the experiments including the embryo injections, electrophysiology, behavior and confocal microscopy. My supervisor and I analyzed the results and wrote the paper together. My colleague Meijiang Liao developed a recombinant zebrafish protein for this study that was used in several experiments.